

INSTANTANEOUS KINEMATICS AND JOINT DISPLACEMENT  
ANALYSIS OF FULLY-PARALLEL ROBOTIC DEVICES

BY

MAHER GABER MOHAMED

A DISSERTATION PRESENTED TO THE GRADUATE SCHOOL  
OF THE UNIVERSITY OF FLORIDA IN  
PARTIAL FULFILLMENT OF THE REQUIREMENTS  
FOR THE DEGREE OF DOCTOR OF PHILOSOPHY

UNIVERSITY OF FLORIDA

1983

#### ACKNOWLEDGEMENTS

The author wishes to express his sincere appreciation to his committee chairman, Professor Joseph Duffy, for his invaluable guidance, counseling, and encouragement throughout the preparation of this work. He would like to acknowledge the stimulation and instruction provided by Professor Delbert Tesar, director of the Center of Intelligent Machines and Robotics (CIMAR), who created a very conducive atmosphere for creative work.

In addition, the author would like to thank Dr. Gary K. Matthew for his guidance and computational assistance, Professors John Staudhammer and George N. Sandor for their encouragement, his colleagues in CIMAR for sharing their knowledge, especially Gilbert Lovell and Harvey Lipkin, and his family for their encouragement, spirit, and patience.

Lastly, the author is deeply indebted to the Egyptian people and government for sponsoring his education.

The financial assistance of the National Science Foundation Grant No. MEA83-24725 is also appreciated.

# TABLE OF CONTENTS

	PAGE
ACKNOWLEDGEMENTS .....	ii
LIST OF TABLES .....	vii
LIST OF FIGURES .....	viii
ABSTRACT .....	xiii
CHAPTER	
1 INTRODUCTION .....	1
1.1 Dissertation Overview .....	1
1.2 Serial and Parallel Kinematic Chains .	3
1.2.1 Definitions .....	3
1.2.2 Comparison Between Serial and Parallel Devices .....	7
2 INTRODUCTORY DISCUSSION OF THE THEORY OF SCREWS .....	12
2.1 Line Geometry .....	12
2.1.1 Plücker or Line Coordinates ..	12
2.1.2 Mutual Moments of Two Lines ..	17
2.1.3 Line Systems .....	19
2.2 The Theory of Screws .....	21
2.2.1 Historical Remarks on Screws .	21
2.2.2 Screws and Screw Coordinates .	22
2.2.3 Screw Systems .....	24
2.2.4 Instantaneous Kinematics of a Rigid Body .....	25
2.2.5 Statics of a Rigid Body .....	29
2.3 Introduction to the Instantaneous Kine- matics of Kinematic Chains .....	30
2.3.1 The Series and Parallel Laws of Instantaneous Kinematics ..	31
2.3.2 Instantaneous Kinematics of Serial Manipulators .....	36
2.3.3 Reciprocity of Screws .....	39
2.3.4 Linear Algebra of Screw Sys- tems .....	42
3 TYPE SYNTHESIS OF MECHANISMS .....	46

CHAPTER		PAGE
	3.1 Definitions and Basic Procedures .....	46
	3.2 Type Synthesis of Planar Robotic De- vices .....	53
	3.3 Type Synthesis of Spatial Robotic De- vices .....	62
	3.4 Discussion and Future Robotic Applica- tions of Parallel Devices .....	75
4	INSTANTANEOUS KINEMATICS OF FULLY-PARALLEL DEVICES .....	95
	4.1 Introduction .....	95
	4.2 Instantaneous Kinematics of the End- Effector of Fully-Parallel Symmetrical Devices Using Loop Velocity Equations .	104
	4.2.1 Basic Equations .....	104
	4.2.2 Forward Solution .....	107
	4.2.3 The Concept of Partial Screws .	113
	4.2.4 Reverse Solution .....	115
	4.2.5 Instantaneous Kinematics of the End-Effector of a Six-Degree of Freedom Fully-Parallel Symmet- rical Device with Three Connect- ing Subchains to Platform .....	117
	4.3 A Direct Determination of the Instan- taneous Kinematics of the End-Effector of Fully-Parallel Symmetrical Devices .	124
	4.3.1 Basic Equations .....	124
	4.3.2 Forward Solution .....	125
	4.3.3 The Concept of Partial Screws .	128
	4.3.4 Reverse Solution .....	131
	4.3.5 Instantaneous Kinematics of the End-Effector of Six-Degree of Freedom Fully-Parallel Symmet- rical Devices .....	131
	4.3.6 Instantaneous Kinematics of the End-Effector of a Planar Fully- Parallel Symmetrical Device ...	150
	4.4 Instantaneous Kinematics of the End- Effector of Asymmetrical Fully-Parallel Devices .....	155
5	SPECIAL CONFIGURATIONS .....	162
	5.1 Special Configurations of Single- and Multi-Loop Devices .....	162



CHAPTER	PAGE
5.1.1 Introduction .....	162
5.1.2 Stationary Configurations .....	163
5.1.3 Uncertainty Configurations .....	169
5.2 Special Configurations of Fully-Parallel Devices .....	174
5.2.1 Introduction .....	174
5.2.2 Case I .....	176
5.2.3 Case II .....	177
5.2.4 Case III .....	178
5.2.5 Case IV .....	180
5.2.6 Case V .....	181
5.2.7 Case VI .....	182
5.2.8 Special Configurations of the Planar Version of the Florida Shoulder .....	184
6 DISPLACEMENT ANALYSIS OF THE THREE-DOF PLANAR FLORIDA SHOULDER .....	209
6.1 Introduction .....	209
6.2 Forward Analysis .....	213
6.3 Reverse Analysis .....	229
6.4 Numerical Examples .....	234
7 THE REVERSE JOINT DISPLACEMENT ANALYSIS OF SPATIAL FULLY-PARALLEL DEVICES .....	248
7.1 Introduction .....	248
7.2 The Reverse Analysis of the R-P-SP Device with Three Subchains (Fig. 3.27) .....	249
7.3 The Reverse Analysis of Stewart Platform (Fig. 3.29) .....	264
7.3.1 Case I--The Sliding Joint is Actuated .....	268
7.3.2 Case II--A Revolute Joint is Actuated .....	268
7.3.3 Numerical Examples .....	272
8 SUGGESTIONS FOR FUTURE WORK .....	278
APPENDIX	
A ASSEMBLY CONFIGURATIONS OF THE STRUCTURE ILLUS- TRATED IN FIGURE 6.3 .....	280
B REDUCTION OF COEFFICIENTS 'a' AND 'b' OF EQUATION (6.27) .....	285
C COMPUTER PROGRAMS AND RESULTS OF CHAPTER 6 ....	290

APPENDIX	PAGE
D    COMPUTER PROGRAMS OF CHAPTER 7 .....	300
REFERENCES .....	305
BIOGRAPHICAL SKETCH .....	309

# LIST OF TABLES

TABLE		PAGE
3.1	Screw Systems Applicable to Practical Parallel Robotic Devices .....	52
3.2	Structural Analysis of M=3 Planar Kinematic Chains .....	55
3.3	Franke's Molecule Notation .....	57
3.4	Structural Analysis of M=6 Spatial Kinematic Chains .....	76
5.1	Types of Special Configurations of Fully-Parallel Devices .....	183
6.1	The Coordinates of the End-Effector Lamina and the Corresponding $\theta_{2,2}$ .....	237
6.2	The Required Sets of Joint Displacements ....	241

# LIST OF FIGURES

FIGURE	PAGE
1.1 Industrial Serial Manipulator .....	4
1.2 Three-Degree of Freedom Planar Shoulder .....	5
1.3 Six-Degree of Freedom Stewart Platform .....	6
1.4 Six-Degree of Freedom Spatial Shoulder .....	8
1.5 Partially-Parallel Devices .....	9
1.6 Performance Chart .....	11
2.1 Plücker Line Coordinates .....	15
2.2 Pair of Skew Lines .....	18
2.3 Pure Rotation .....	26
2.4 Pure Translation .....	27
2.5 Twist about a Screw .....	28
2.6 Two Joints in Series .....	32
2.7 Two Joints in Parallel .....	34
2.8 Coupling Graph "G" Representing Bodies Connect- ed in Series .....	35
2.9 Coupling Graphs $G_1, G_2, \dots$ Connected in Par- allel .....	37
2.10 Serial Manipulator with Revolute Joints .....	38
2.11 Wrench Applied on a Body Constrained to Twist .	40
3.1 Types of Kinematic Pairs (Joints) .....	49
3.2 Types of Links .....	51
3.3 Planar Mechanisms with Three-Dof, (a) and (b) Total Mobility $M=3$ , (c) Partial Mobility $M=3$ ..	58
3.4 Structures which Must Be Avoided .....	60

FIGURE	PAGE
3.5 Mechanisms Having (a) Fractionated Mobility, (b) Immobility .....	61
3.6 Group I, Open Chain, $N=4$ , $n_2=4$ , $j=3$ .....	63
3.7 Group II, Single-Loop Closed Chain, $N=6$ , $n_2=6$ , $j=6$ .....	64
3.8 Group III, $N=8$ , $n_2=6$ , $n_3=2$ , $j=9$ .....	65
3.9 Group IV-a, $N=10$ , $n_2=6$ , $n_3=4$ , $j=12$ .....	66
3.10 Group IV-b, $N=10$ , $n_2=7$ , $n_3=2$ , $n_4=1$ , $j=12$ .....	67
3.11 Group IV-c, $N=10$ , $n_2=8$ , $n_4=2$ , $j=12$ .....	68
3.12 Group V-b, $N=12$ , $n_2=7$ , $n_3=4$ , $n_4=1$ , $j=15$ .....	69
3.13 Group V-c, $N=12$ , $n_2=8$ , $n_3=3$ , $n_5=1$ , $j=15$ .....	70
3.14 Group V-d, $N=12$ , $n_2=8$ , $n_3=2$ , $n_4=2$ , $j=15$ .....	71
3.15 Group V-f, $N=12$ , $n_2=9$ , $n_4=3$ , $j=15$ .....	72
3.16 Group V-g, $N=12$ , $n_2=10$ , $n_5=2$ , $j=15$ .....	73
3.17 Group I, Spatial Open Chain, $N=7$ , $n_2=7$ , $j=6$ ..	77
3.18 Group II, Single-loop Closed Chain, $N=12$ , $n_2=$ $12$ , $j=12$ .....	78
3.19 Group III-a, $N=17$ , $n_2=15$ , $n_3=2$ , $j=18$ .....	79
3.20 Group IV-c, $N=22$ , $n_2=20$ , $n_4=2$ , $j=24$ .....	80
3.21 Group V-g, $N=27$ , $n_2=25$ , $n_5=2$ , $j=30$ .....	81
3.22 Group VI, $N=32$ , $n_2=30$ , $n_6=2$ , $j=36$ .....	82
3.23 Seven Possible Connecting Subchains .....	83
3.24 Alternative Form of Figure 3.8-(a) .....	85
3.25 Planar Earth Moving Machinery .....	86
3.26 Three-Degree of Freedom Shoulder .....	87
3.27 R-P-SP Fully-Parallel Device .....	89
3.28 University of Florida Concept for Fully-Paral- lel Robot Device .....	90

FIGURE	PAGE
3.29 Stewart Platform .....	91
3.30 Six-Degree of Freedom Robot Arm .....	92
3.31 Kinematic Representation of Walking Machine ...	94
4.1 Six-Bar Planar Mechanism with Cross-Jointing ..	97
4.2 Directed Graph and Its Circuit Matrix .....	102
4.3 General Fully-Parallel Symmetrical Device .....	105
4.4 Six-Degree of Freedom Fully-Parallel Symmetrical Device with Three Connecting Subchains to Platform .....	118
4.5 Spatial Six-Dof Fully-Parallel Symmetrical Device with Six Connecting Subchains to Platform	132
4.6 Six-Dof Fully-Parallel Symmetrical Device with Two Connecting Subchains to Platform .....	143
4.7 Planar Version of the Spherical Florida Shoulder .....	151
4.8 Six-Degree of Freedom Fully-Parallel Asymmetrical Device with Three Connecting Subchains to Platform .....	156
5.1 Special Configurations and Immovable Structure of a Planar Four-Bar .....	164
5.2 R-S-C-R Spatial Mechanism in a Double Stationary Configuration .....	166
5.3 Some Planar Arrangements with the Same Topology .....	170
5.4 R-S-C-R Spatial Mechanism in a Single-Fold Uncertainty Configuration .....	173
5.5 Example of Case I-(a) .....	185
5.6 Example of Case I-(a) with Folded Subchain .....	188
5.7 Example of Case I-(b) .....	189
5.8 Example of Case II .....	191
5.9 Example of Case III-(a) .....	192

FIGURE	PAGE
5.10 Example of Case III-(a) in Simple Singularity	195
5.11 Example of Case III-(b) .....	196
5.12 Example of Case III-(c) .....	198
5.13 Example of Case IV .....	201
5.14 Example of Case IV .....	204
5.15 Example of Case VI-(a) .....	206
5.16 Example of Case VI-(b) .....	208
6.1 Lamina $\Sigma$ in a General Planar Motion .....	210
6.2 Planar Version of the Florida Shoulder .....	212
6.3 Six-Bar Structure .....	214
6.4 Two Independent Quadrilaterals .....	216
6.5 Determination of Angle $\alpha_2$ .....	227
6.6 Determination of Angle $\phi_{2,i}$ .....	228
6.7 Two-Degree of Freedom Serial Arm .....	230
6.8 Closure Configurations .....	233
6.9 Six Real Points of Intersections of Coupler Curve and Circle, Example 6.1 .....	235
6.10 Configurations 1 and 2 .....	238
6.11 Configurations 3 and 4 .....	239
6.12 Configurations 5 and 6 .....	240
6.13 Six Assembly Configurations, Example 6.1 .....	242
6.14 Planar Florida Shoulder, Example 6.2 .....	243
6.15 Input Angular Displacement $\phi_{1,1}$ , Example 6.2 .	244
6.16 Input Angular Displacement $\phi_{1,2}$ , Example 6.2 .	245
6.17 Input Angular Displacement $\phi_{1,3}$ , Example 6.2 .	246
7.1 Coordinate Systems for the R-P-SP Device .....	250
7.2 The $i$ th Subchain of the R-P-SP Spatial Device	253

FIGURE	PAGE
7.3 Input Angular Displacement $\phi_{1,1}$ for the R-P-SP Device .....	257
7.4 Input Angular Displacement $\phi_{1,2}$ for the R-P-SP Device .....	258
7.5 Input Angular Displacement $\phi_{1,3}$ for the R-P-SP Device .....	259
7.6 Input Sliding Displacement $s_{2,1}$ for the R-P-SP Device .....	260
7.7 Input Sliding Displacement $s_{2,2}$ for the R-P-SP Device .....	261
7.8 Input Sliding Displacement $s_{2,3}$ for the R-P-SP Device .....	262
7.9 Sliding Displacement $s_{6,i}$ for the R-P-SP Device .....	263
7.10 Coordinate Systems for Stewart Platform .....	265
7.11 The $i$ th Subchain of Stewart Platform with Actuated Sliding Joint .....	269
7.12 The $i$ th Subchain of Stewart Platform with Actuated Revolute Joint .....	271
7.13 Input Sliding Displacement $s_{4,i}$ for Stewart Platform .....	273
7.14 Input Angular Displacement $\phi_{1,i}$ of the First Closure for Stewart Platform .....	275
7.15 Input Angular Displacement $\phi_{1,i}$ of the Second Closure for Stewart Platform .....	276
7.16 Input Angular Displacement $\phi_{1,1}$ of the First and the Second Closures for Stewart Platform .	277
A.1 Intersection of Coupler Curve with Circle ....	282



Abstract of Dissertation Presented to the Graduate School  
of the University of Florida in Partial Fulfillment of the  
Requirements for the Degree of Doctor of Philosophy

INSTANTANEOUS KINEMATICS AND JOINT DISPLACEMENT  
ANALYSIS OF FULLY-PARALLEL ROBOTIC DEVICES

By

MAHER GABER MOHAMED

December 1983

Chairman: Dr. Joseph Duffy  
Major Department: Mechanical Engineering

State of the art industrial robot manipulators typically feature a serial sequence of simple joints. Serial robotic devices have been the subject of much study. The same cannot be said for parallel devices where two or more serially connected subchains join an end-effector platform to ground. Such devices do exist and are beginning to be studied in industry as potential robot manipulators. This dissertation presents a fundamental study of these alternative devices to provide a basic understanding and to assess some of the practical aspects.

A type synthesis of parallel robotic devices is performed using an algorithm based on Franke's condensed notation. This is followed by a discussion of potential robotic applications.

This dissertation essentially covers two major topics: instantaneous kinematics and joint displacement analysis of fully-parallel devices. Firstly, two novel procedures for determining the instantaneous motion of the end-effector platform of fully-parallel devices using the theory of screws are presented and an important theorem is derived--for any parallel device, the twist representing the instantaneous motion of the end-effector platform is equal to the sum of its partial twists. Equally important, a characteristic matrix equation is derived and used to describe and categorize various geometrical phenomena called "special configurations" which are by no means fully understood. Six different types of special configurations are tabulated. By the way of example special configurations of the planar Florida Shoulder are studied in detail and numerical results are provided. Secondly, the joint displacement analysis of the planar Florida Shoulder is presented. This is followed by presenting the reverse joint displacement analysis of the well known Stewart Platform and also of the R-P- $\overline{SP}$  spatial robotic device with three subchains connecting the end-effector platform. Numerical examples are presented for each device. Computer programs for the displacement analysis are listed in the appendices.

## CHAPTER 1 INTRODUCTION

### 1.1 Dissertation Overview

Almost all existing industrial robot manipulators are serial devices and have been the subject of much study. Their joint displacement analysis and instantaneous kinematics are fairly well understood. The same cannot be said for parallel devices where two or more serially connected chains join a platform or end-effector to ground. Such devices do exist. For instance, the Stewart Platform which has six serial connecting chains in parallel is used for flight simulation. The Florida Shoulder, which is essentially a spherical parallel device, can be used as a module device in robot systems. These types of devices are beginning to be studied in industry as potential robot manipulators. In this dissertation a fundamental study of parallel devices is presented in order to provide a basic understanding, and to assess some of the practical aspects of these devices.

As suggested by the title, this dissertation essentially covers two major topics. First, the instantaneous kinematics of general fully-parallel devices is investigated using the theory of screws. Second, the joint displacement analysis of a number of fully-parallel devices is presented.

In Chapter 2 line geometry is summarized and then extended to the theory of screws which constitutes a proper foundation for the study of instantaneous kinematics.

In Chapter 3 a type synthesis of parallel robotic devices is performed using an algorithm based on Franke's condensed notation. This yields the structure of all planar and spatial robotic devices for which the end-effector platform has three and six degrees of freedom. This is followed by a discussion of potential robotic applications.

In Chapter 4 two novel procedures are presented for determining the instantaneous motion of the end-effector platform of fully-parallel devices and an important theorem is derived: For any parallel device, the twist representing the instantaneous motion of the platform is equal to the sum of its partial twists. Equally important, a characteristic matrix equation which completely describes the instantaneous kinematics of parallel devices is also derived.

In Chapter 5 the characteristic matrix equation is used to describe and categorize special configurations of fully-parallel devices. Six different types of special configurations are tabulated. By the way of example, special configurations of the planar three-degree of freedom Florida Shoulder are studied in detail and numerical results are provided.

In Chapter 6 the forward and reverse displacement analysis of the planar Florida Shoulder is presented.

In Chapter 7 the reverse displacement analysis of a number of practical six-degree of freedom spatial robotic devices is presented.

Chapter 8 gives suggestions for future work.

By way of introduction in the remainder of this chapter, fully- and partially-parallel devices are defined and examples of each are presented. The performance characteristics of serial and parallel robotic devices are summarized and compared.

## 1.2. Serial and Parallel Kinematic Chains

### 1.2.1. Definitions

A serial kinematic chain is a single open-loop kinematic chain of rigid bodies (or links) connected by a series of joints [1]. Almost all existing industrial robot manipulators are serial chains, and in most cases simple lower pairs (revolute or prismatic pairs) are used. Figure 1.1 illustrates an industrial serial robot manipulator with six controllable rotational freedoms in series.

Hunt in [2] defined "in-parallel-actuated kinematic chains." Examples are the planar device (Fig. 1.2) where the platform is connected to ground by three subchains, the spherical version of which is the Florida Shoulder, and the spatial Stewart Platform (Fig. 1.3) which is connected to ground by six subchains. Each of these devices can be controlled by a single actuator in each of the subchains.

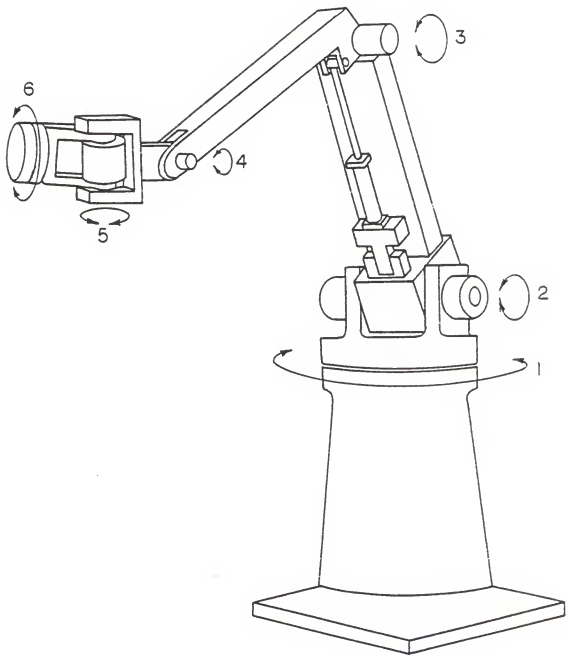


Figure 1.1. Industrial Serial Manipulator

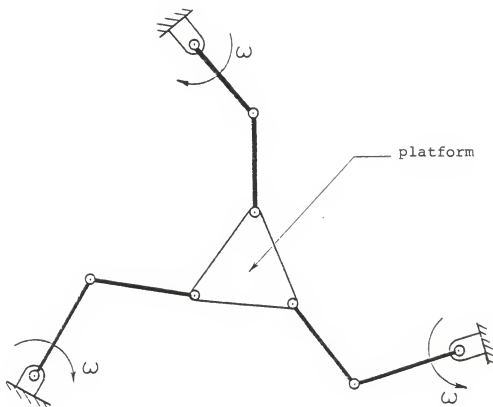


Figure 1.2. Three-Degree of Freedom Planar Shoulder

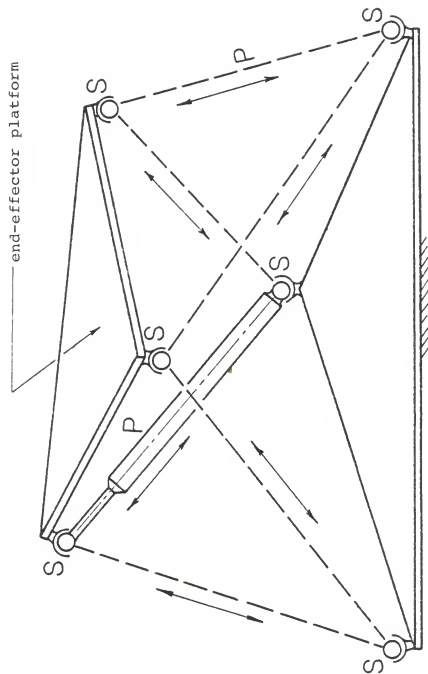


Figure 1.3. Six-Degree of Freedom Stewart Platform



The actuators are therefore in-parallel to one another and this is the basis for Hunt's definition. However, Fig. 1.4 illustrates a spatial platform connected to ground by three subchains. Although as in the previous device the subchains are fully in-parallel, the actuators are not fully in-parallel. All of these three devices will be defined in this text as fully-parallel devices. A fully-parallel device is defined as a platform-type kinematic chain in which the actuated connected subchains are fully in-parallel with one another.

It is necessary to introduce the term fully-parallel device here in order to distinguish between devices such as those illustrated in Fig. 1.5 which will be defined as partially-parallel devices (the actuators are not in-parallel with one another). Hunt himself pointed out that there are many intermediate possibilities between fully-parallel and serial devices [3]. The authors of [4-7] also discussed these intermediate possibilities and they are sometimes referred to as hybrid serial-parallel devices. However, they will be called partially-parallel devices in this text.

### 1.2.2 Comparison between Serial and Parallel Devices

A comparison between general serial and parallel devices in terms of some necessary and desirable performance and control characteristics was presented in great detail in [4]. Some of these characteristics were also proposed in [2,6-8].

Eight of these performance characteristics were discussed in [4]. These characteristics are:

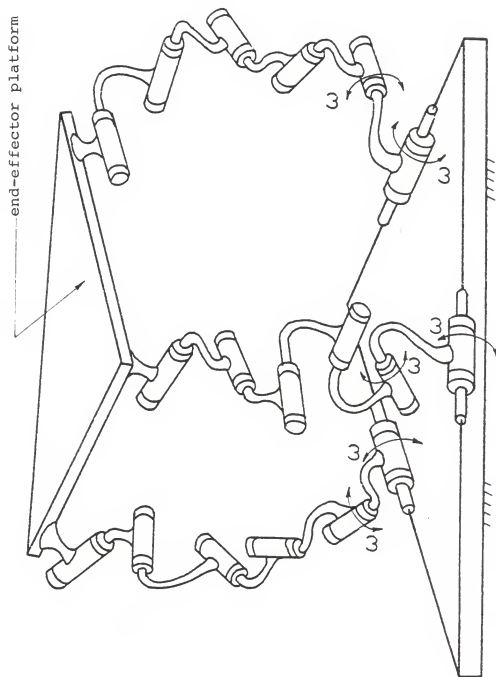
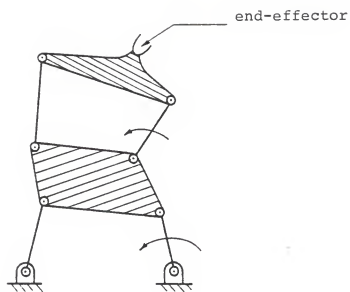
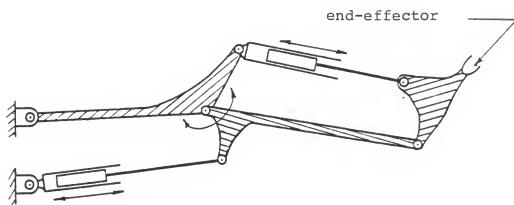


Figure 1.4. Six-Degree of Freedom Spatial Shoulder



(a)



(b)

Figure 1.5. Partially-Parallel Devices

- Range of motion or workspace
- Rigidity or stiffness and strength
- Complexity of end-effector positioning formulation
- Complexity of system dynamics
- Precision positioning
- Load carrying distribution through system
- Fabrication (economics)
- Compactness

Further, Fig. 1.6 illustrates a performance chart which indicates, in a relative manner, which characteristics or criteria tend to be favorable for serial and parallel devices. This chart is a modified-version of the performance chart presented in [4].

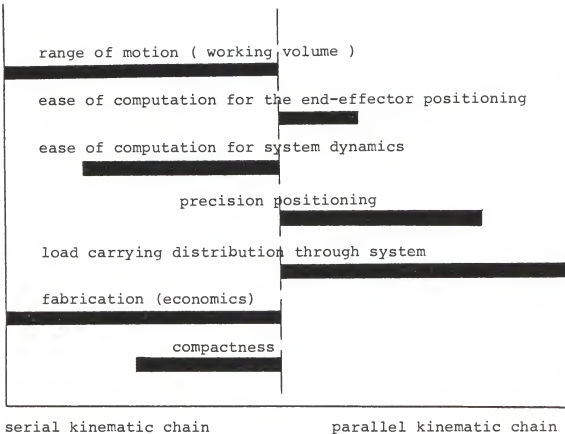


Figure 1.6. Performance Chart

## CHAPTER 2

### INTRODUCTORY DISCUSSION OF THE THEORY OF SCREWS

The major objective of this chapter is to give a summary of the theory of screws and its application in investigating the instantaneous kinematics of serial manipulators. First, line geometry is summarized and then extended to the theory of screws. A brief historical remark which outlines the development of the theory of screws is presented. Following this, the dual concepts of instantaneous kinematics and statics of rigid bodies are investigated using the theory of screws. The so-called "Series" and "Parallel" laws of instantaneous kinematics are presented, and then the series law is applied to investigate the instantaneous kinematics of an open chain of rigid bodies connected by a series of joints. This system models the robot manipulator.

#### 2.1 Line Geometry

##### 2.1.1 Plücker or Line Coordinates

A line in space can be determined by two intersecting planes\* or by two distinct (independent) points.

---

\*In three dimensions a plane is said to be the dual of a point. For every theorem involving points, there exists a corresponding dual theorem which can be obtained simply by interchanging the words point and plane, and of course by modifying phrases to make the statement sensible.

The equation\* (nonparametric) of the unique line joining point  $\underline{r}_1 (x_1, y_1, z_1)$  and point  $\underline{r}_2 (x_2, y_2, z_2)$  is

$$\frac{x-x_1}{x_2-x_1} = \frac{y-y_1}{y_2-y_1} = \frac{z-z_1}{z_2-z_1} \quad (2.1)$$

where  $(x_2-x_1)$ ,  $(y_2-y_1)$ , and  $(z_2-z_1)$  are the direction ratios of a vector

$$\underline{S} = (x_2-x_1)\underline{i} + (y_2-y_1)\underline{j} + (z_2-z_1)\underline{k} \quad (2.2)$$

parallel to the line, and they are related to the distance  $|\underline{S}|$  between the two points by

$$\underline{S} \cdot \underline{S} = |\underline{S}|^2 = (x_2-x_1)^2 + (y_2-y_1)^2 + (z_2-z_1)^2 \quad (2.3)$$

It is usual to write

$$\begin{aligned} L &= (x_2-x_1)/|\underline{S}| \\ M &= (y_2-y_1)/|\underline{S}| \\ N &= (z_2-z_1)/|\underline{S}| \end{aligned} \quad (2.4)$$

where L, M, and N are the direction cosines (unit direction

---

\*The Plücker coordinates  $(\underline{S} ; \underline{S}_0)$  of the line of intersection of two planes (see [9] for more details),

$$\begin{aligned} \underline{r} \cdot \underline{S}_1 &= s_1 \\ \text{and} \quad \underline{r} \cdot \underline{S}_2 &= s_2 \end{aligned}$$

are

$$\begin{aligned} \underline{S} &= \underline{S}_1 \times \underline{S}_2 \\ \underline{S}_0 &= s_2 \underline{S}_1 - s_1 \underline{S}_2 \end{aligned}$$

When  $\underline{S}_1 \times \underline{S}_2 = 0$ , the planes are parallel and they intersect at a line with coordinates  $(0 ; \underline{S}_0)$  in the plane at infinity.

ratios) of the line, or of any other parallel line. Only two of these are independent since they are related by

$$1 = L^2 + M^2 + N^2 \quad (2.5)$$

The vector equation of the line can be expressed in the form

$$\underline{r} \times \underline{S} = \underline{S}_0 \quad (2.6)$$

where

$$\underline{S}_0 = \underline{r}_1 \times \underline{S} \quad (2.7)$$

is the moment of the line about the origin.  $\underline{S}_0$  is origin dependent while  $\underline{S}$  is not. The components of the moment  $\underline{S}_0$  along the x, y, and z axes are, respectively,

$$\begin{aligned} P &= y_1 N - z_1 M \\ Q &= z_1 L - x_1 N \\ R &= x_1 M - y_1 L \end{aligned} \quad (2.8)$$

The quantities L, M, N, P, Q and R must satisfy the quadratic condition of orthogonality

$$\underline{S} \cdot \underline{S}_0 = 0 \quad (2.9)$$

i.e.,

$$LP + MQ + NR = 0 \quad (2.10)$$

Thus the six coordinates (L,M,N ; P,Q,R) can therefore be used to specify a unique line in space (see Fig. 2.1). These six coordinates are often referred to as Plücker's line coordinates or simply Plücker or line coordinates ( $\underline{S}$  ;  $\underline{S}_0$ ). The coordinates ( $\underline{S}$  ;  $\underline{S}_0$ ) are homogeneous coordinates since from (2.6) the coordinates ( $\lambda \underline{S}$  ;  $\lambda \underline{S}_0$ ), where  $\lambda$  is a scalar,



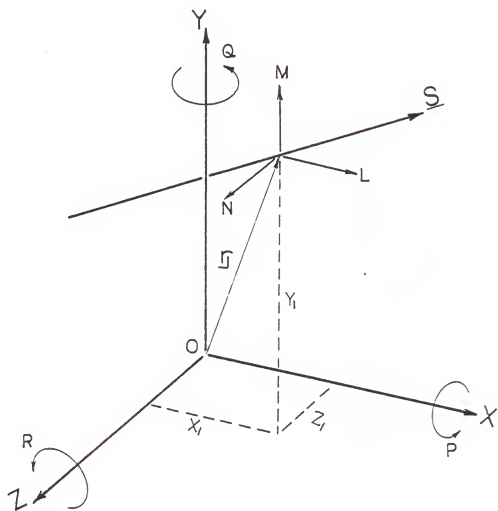


Figure 2.1. Plücker Line Coordinates

determine the same line. Only four of these six coordinates are independent since they are related by (2.5) and (2.10), and hence it can be concluded that there are  $\infty^4$  lines in space.

The vectors  $\underline{S}$  and  $\underline{S}_0$  can be combined into a dual vectors\*  $\underline{\$}$ ,

$$\underline{\$} = \underline{S} + \epsilon \underline{S}_0 \quad (2.11)$$

where  $\epsilon^2 = \epsilon^3 = \dots = 0$ . The vector  $\underline{S}$  is called a line vector [10] and when  $|\underline{S}| = 1$ ,  $\underline{\$}$  is called a unit line vector.

If P, Q, and R are all zero, then the line passes through the origin; while if L, M, and N are all zero, the line lies in the plane at infinity. The line is then perpendicular to a finite line whose direction cosines are P, Q, and R. For instance, the line at infinity (0,0,0 ; 0,0,1) is perpendicular to the Z-axis. Such lines whose rotation axes are infinitely distant from the origin require the modified set of coordinates ( $\underline{0}$  ;  $\underline{S}$ ) and are recognized as unit free vectors.

A line in three-dimensional space can be represented as a point in five-space, the homogeneous coordinates of the point being (L,M,N ; P,Q,R). But the quadratic identity (2.10) has to be satisfied, and this is the equation of a quadric surface in five-space. Hence we conclude that a

---

\*Dual numbers and dual vectors provide a useful means of manipulating Plucker coordinates - and indeed screw coordinates, see section 2.2. Briefly, a dual number has a real part a and dual part b, and is written as  $a + \epsilon b$  where  $\epsilon^2 = \epsilon^3 = \dots = 0$ . a can be identified with  $|\underline{S}| = (L^2 + M^2 + N^2)^{1/2}$  and b with  $|\underline{S}_0| = (P^2 + Q^2 + R^2)^{1/2}$ . Then it is often useful to consider a and b as vectors  $\underline{a}$  and  $\underline{b}$  (or  $\underline{S}$  and  $\underline{S}_0$ ).

line in three-space can be represented as a point on the quadric surface,  $LP + MQ + NR = 0$ , in five-space.

### 2.1.2 Mutual Moment of Two Lines

Figure 2.2 illustrates two skew lines with a mutual perpendicular distance  $a_{12}$  and twist angle  $\alpha_{12}$ . The vector equations of those two lines are, respectively

$$\underline{r}_1 \times \underline{S}_1 = \underline{S}_{o1} \quad (2.12)$$

and

$$\underline{r}_2 \times \underline{S}_2 = \underline{S}_{o2} \quad (2.13)$$

The projection of the moment vector  $a_{12}\underline{a}_{12} \times \underline{S}_2$  on the line  $\underline{S}_1$  is given by  $a_{12}\underline{a}_{12} \times \underline{S}_2 \cdot \underline{S}_1$  and is called the moment of  $\underline{S}_2$  about the line  $\underline{S}_1$ . This scalar quantity is usually called the mutual moment of the two lines. Expanding the triple scalar product, the mutual moment can be expressed in the form

$$\begin{aligned} -a_{12} \sin \alpha_{12} &= \underline{S}_1 \cdot \underline{S}_{o2} + \underline{S}_2 \cdot \underline{S}_{o1} \\ &= L_1P_2 + M_1Q_2 + N_1R_2 + P_1L_2 + Q_1M_2 + R_1N_2 \end{aligned} \quad (2.14)$$

where  $(L_1, M_1, N_1 ; P_1, Q_1, R_1)$  and  $(L_2, M_2, N_2 ; P_2, Q_2, R_2)$  are the Plücker coordinates of the two lines.

Two lines will intersect at a finite point ( $a_{12}=0$ ), or at a point at infinity ( $\sin \alpha_{12}=0$ ) if and only if their mutual moment is zero. Hence the condition for the intersection of two lines is

$$\underline{S}_1 \cdot \underline{S}_{o2} + \underline{S}_2 \cdot \underline{S}_{o1} = 0 \quad (2.15)$$

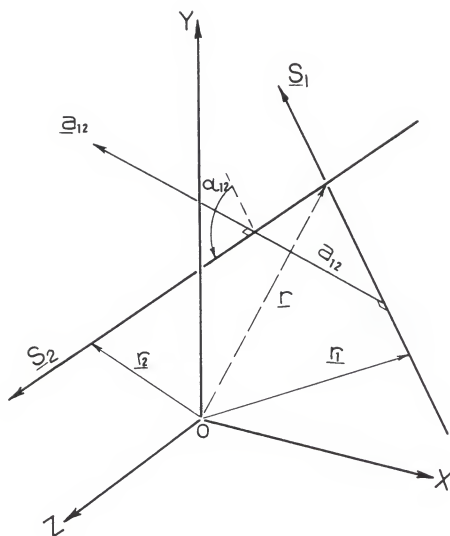


Figure 2.2. Pair of Skew Lines

The point of intersection  $\underline{r}$  of a pair of two skew lines (2.12) and (2.13) can be expressed in the form [9]

$$\underline{r} = \frac{\underline{S}_{o1} \times \underline{S}_{o2}}{\underline{S}_2 \cdot \underline{S}_{o1}} \quad (2.16)$$

If  $\underline{S}_2 \cdot \underline{S}_{o1} = 0$  then the two lines intersect at a point at infinity, and if in addition  $\underline{S}_{o1} \times \underline{S}_{o2} = 0$  then  $\underline{r}$  is indeterminate and the two lines are identical or opposite.

### 2.1.3 Line Systems\*

It has been shown earlier that there are  $\infty^4$  lines in space. However, every condition, relation, or equation in the coordinates of the lines reduces the freedom of the space by one, i.e., reduces the number of lines in the space from  $\infty^4$  to  $\infty^3$ .

Since only two of the equations (2.8) of the moment components of a line passing through a point are independent, therefore the condition that a line should pass through a point imposes two constraints on the line. Thus only two parameters are left to be determined. Hence there are  $\infty^2$  lines passing through a point and they form a line congruence.

If  $L_1, M_1, \text{ and } N_1$  are the direction cosines of a given line, and  $L, M, \text{ and } N$  are the direction cosines of a parallel line, then

$$L_1 : M_1 : N_1 = L : M : N \quad (2.17)$$

---

\*Line systems and their properties are described by Hunt [3] which contains an extensive bibliography on the subject.

which implies

$$\begin{aligned} ML_1 &= LM_1 \\ NL_1 &= LN_1 \end{aligned} \quad (2.18)$$

Equation set (2.18) represents two independent conditions and therefore it is concluded that there are  $\infty^2$  lines parallel to a given line. They also form a line congruence.

Line (S ; S<sub>0</sub>) will lie on the plane (a ; s), if and only if,

$$(\underline{a} \cdot \underline{S}) = 0$$

and

$$\underline{S} \cdot (\underline{a} \times \underline{S}_0) = -s \quad (2.19)$$

Therefore it is concluded that there are  $\infty^2$  lines on a given plane. However, the line and the plane will be just parallel if only

$$(\underline{a} \cdot \underline{S}) = 0 \quad (2.20)$$

Since equation (2.20) is the only constraint, it is concluded that there are  $\infty^3$  lines parallel to a given plane. Such lines form a line complex.

Similarly, it can be concluded that there are  $\infty^1$  lines on a given plane that pass through a point in that plain. Such lines form a planar pencil. In general, there will be  $\infty^1$  lines forming a line series (ruled surface) that satisfies three conditions. Four conditions leave just  $\infty^0$  lines; i.e., a finite number of lines. Ordinarily, no line satisfies five conditions.

## 2.2 The Theory of Screws

The theory of screws is analogous to vector analysis in that both consist of an algebra with a geometric entity as a fundamental element. The vector is the fundamental element for vector analysis, and the screw is the fundamental element for the theory of screws. All operations in the vector domain are formally preserved for the screws. A screw is essentially a vector in six-space and a screw equation is equivalent to six scalar equations.

The concepts of screws, twists, and wrenches are introduced in this section. It is shown how the previously encountered line coordinates can be extended to screw, twist, and wrench coordinates.

### 2.2.1 Historical Remarks on Screws

Since the discovery (attributed to Mozzi, in the early part of the last century) that any three-dimensional rigid body displacement can be accomplished by means of a translation about a unique axis and a rotation about the same axis, the concepts of screws and screw displacements have emerged as some of the most convenient means of describing spatial displacement. In 1900, R.S. Ball published his monumental "Theory of Screws" [11]. The theory as developed by Ball is concerned principally with the instantaneous kinematics and the impulsive dynamics of a rigid body subject to complex constraints. There have arisen, however, different mathematical methods of representing the spatial motion of a

rigid body. Rooney, for example, compared eight of these descriptions in [12], and Lipkin and Duffy gave a brief introduction to some of these methods in [13].

After the first decade of the 20th century, the theory of screws received little attention. It was not until 1948 that Dimentberg [14] applied the algebra of the theory of screws to the analysis of spatial mechanisms. However, it was Phillips and Hunt [15] in the 1960's who applied the theory of screws to the study of instantaneous kinematics of three bodies in relative motion. They rediscovered some of the earlier results of Ball, and subsequently applied the theory of screws to spatial mechanisms. In addition, the works of Waldron [16], Bottema and Roth [17] provided a modern mathematical understanding of the theory of screws. In [18], Woo and Freudenstein developed screw coordinates which are a direct extension of the Plücker coordinates of a line. These are different from the screw coordinates originally introduced by Ball [11]. Ball's approach was to choose six independent screws as reference screws; other screws could then be determined by finding the respective magnitudes of their components along the reference screws.

### 2.2.2 Screws and Screw Coordinates

A screw was defined by Ball [11] as a straight line in space with which a definite scalar called the pitch,  $h$ , is associated. The straight line is called the screw axis.



The six Plücker line coordinates can be extended to a set of screw coordinates. If  $(L, M, N; P, Q, R)$  are the Plücker coordinates of the screw axis, then the screw coordinates are  $(\underline{S}; \underline{S}_0)$  where

$$\begin{aligned}\underline{S} &= \underline{L}_1^* + \underline{M}_2^* + \underline{N}_3^* \\ \underline{S}_0 &= \underline{P}_1^* + \underline{Q}_2^* + \underline{R}_3^*\end{aligned}\quad (2.21)$$

and

$$\begin{aligned}L^* &= L \\ M^* &= M \\ N^* &= N \\ P^* &= P + hL \\ Q^* &= Q + hM \\ R^* &= R + hN\end{aligned}\quad (2.22)$$

A unit screw  $\underline{\$}$ ,  $\underline{S} \cdot \underline{S} = 1$ , can also be expressed as a dual vector

$$\underline{\$} = \underline{S} + \underline{S}_0 \quad (2.23)$$

where

$$\underline{S}_0 = \underline{r} \times \underline{S} + h\underline{S} \quad (2.24)$$

The six screw coordinates (2.22) do not satisfy the quadratic condition of orthogonality,  $\underline{S} \cdot \underline{S}_0 \neq 0$ . Therefore, it can be concluded that a screw can be uniquely specified by five independent quantities (coordinates), four for the axis and one for the pitch.

If the pitch,  $(h = \frac{\underline{S}_0 \cdot \underline{S}}{\underline{S} \cdot \underline{S}})$ , is zero, then the screw coordinates are identical with the line coordinates. For

a screw with infinite pitch,  $L^*$ ,  $M^*$ , and  $N^*$  will all be zero, and the screw coordinates are identical with the free line vector coordinates.

Since there are  $\infty^5$  screws in three-space, a screw can be regarded as a point in five-space [19], and now the totality of all screws of all pitches account for all points in five-space. However, by virtue of the quadratic identity (2.10), all screws of zero pitch in five-space can be represented as the points on a quadric which, when  $h = 0$ , can now be written  $L^*P^* + M^*Q^* + N^*R^* = 0$ . It follows that there is a nesting pattern of  $\infty^1$  quadric surfaces in five-space each quadric having its own characteristic pitch-parameter. The points on one such quadric correspond with those screws in three-space of that particular pitch. It is important to notice that there can be no points common to any two of the nesting quadrics and therefore, no point can represent more than one screw.

### 2.2.3 Screw Systems

A screw system of order  $n$  is defined as a vector space formed by all possible linear combinations of  $n$  independent instantaneous screw axes (ISA's). The order of the screw system of a joint is the connectivity of that joint which is the number of relative degrees of freedom of the bodies connected by the joint. The intersection of two screw systems is itself a screw system.

The screw system of order zero contains no ISA's, that of order one is a single, unique ISA. Screw systems

associated with revolute, prismatic, and screw joints are of order one (Figs. 2.3-2.5). The screw system of order two is a set of ISA's whose axes are the generators of a ruled surface called a "Cylindroid." The pitch of each ISA in this distribution is a unique function of its position on the cylindroid. Finally, the screw system of order six contains the set of all ISA's.

#### 2.2.4 Inatantaneous Kinematics of a Rigid Body

Consider that body 2 in Fig. 2.3 is now rotating about an axis with angular velocity  $\omega \underline{S}$ . The tangential velocity of a point on body 2 which is instantaneously coincident with the origin of the coordinates,  $O$ , is  $\omega(\underline{r} \times \underline{S})$ . Therefore, the instantaneous rotation can be expressed as a scalar multiple of the unit line vector,  $\omega[\underline{S} ; (\underline{r} \times \underline{S})]$ .

If the body translates in direction  $\underline{S}$  (Fig. 2.4) with linear velocity  $v\underline{S}$ , then the instantaneous translation of the body can be expressed as a scalar multiple of a unit free vector,  $v[\underline{O} ; \underline{S}]$ .

The most general instantaneous motion of body 2 relative to body 1 is a combination of an instantaneous rotation (Fig. 2.3) and an instantaneous translation (Fig. 2.4) as illustrated by Fig. 2.5. Since the linear velocity  $\underline{v}$  is parallel to the angular velocity  $\underline{\omega}$ , then  $\underline{v}$  can be expressed as a scalar multiple of  $\underline{\omega}$ ,

$$\underline{v} = h\underline{\omega} \quad (2.25)$$

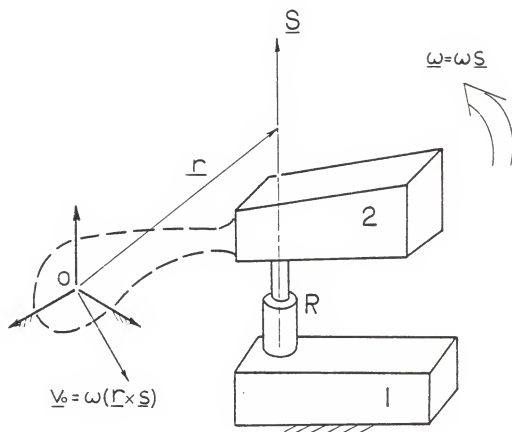


Figure 2.3. Pure Rotation

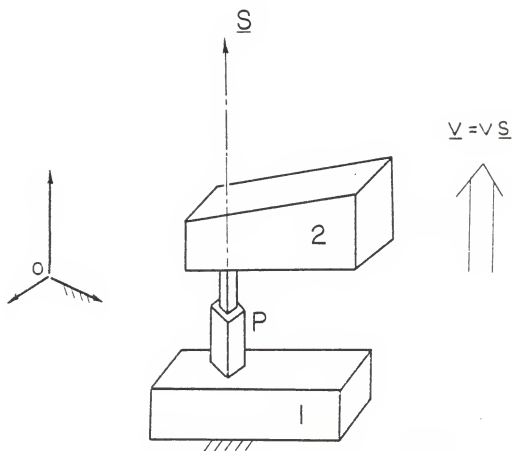


Figure 2.4. Pure Translation

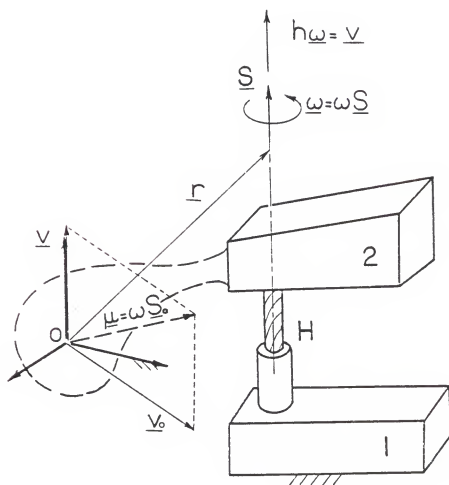


Figure 2.5. Twist about a Screw

The translational velocity of a point on body 2 which is instantaneously coincident with the origin of the coordinates is

$$\underline{u} = \underline{v}_O + \underline{v} \quad (2.26)$$

i.e.,

$$\begin{aligned} \underline{u} &= \omega [(\underline{r} \times \underline{S}) + h\underline{S}] \\ &= \omega \underline{S}_O \end{aligned} \quad (2.27)$$

Therefore, the instantaneous motion can be expressed by the dual vector

$$\begin{aligned} \omega \underline{\$} &= \underline{\omega} + \epsilon \underline{u} \\ &= \omega [\underline{S} + \epsilon \underline{S}_O] \\ &= \hat{\underline{\$}} \end{aligned} \quad (2.28)$$

which is a scalar multiple of a unit screw with a unique pitch,  $h$ , ( $h = \frac{\underline{S}_O \cdot \underline{S}}{\underline{S} \cdot \underline{S}}$ ). Ball called this motion a twist  $\hat{\underline{\$}}$  of amplitude  $\omega$  about a unit screw  $\underline{\$}$ . Generally, the instantaneous relative motion of two bodies connected by a joint of connectivity  $n$  may take place and can be expressed as a twist about any ISA which is a member of the screw system, of order  $n$ , of that joint.

It can be deduced that a pure rotation can be expressed as a twist about a screw with pitch  $h = 0$ , while a pure translation can be expressed as a twist about a screw with pitch  $h = \infty$ .

#### 2.2.5 Statics of a Rigid Body

Analogous to instantaneous kinematics, unit screws can be used to express the action of a force and/or a couple on a rigid body.

The most general system of forces and couples acting on a rigid body can be in general reduced to a force acting through a point and a non-parallel couple. This combination of force and non-parallel couple was called a "Dyname" by Plücker. The dyname can be further reduced to a force and a parallel couple which in turn can be represented as a scalar multiple of unit screw. Therefore, any force system acting on a rigid body can be instantaneously represented as a wrench of intensity  $F$  on a unit screw with pitch  $h$ , ( $h = \frac{\underline{S}_0 \cdot \underline{S}}{\underline{S} \cdot \underline{S}}$ ). Also it can be deduced that a force can be expressed as a wrench on a screw with pitch  $h = 0$ , while a couple can be expressed as a wrench on a screw with pitch  $h = \infty$ .

The remaining discussion about the theory of screws is delayed until the end of the chapter (in 2.3.3 and 2.3.4).

### 2.3 Introduction to the Instantaneous Kinematics of Kinematic Chains

The study of instantaneous kinematics of kinematic chains was pioneered by Waldron [20]. He discussed the concepts of constraint, mobility, and relative degrees of freedom in a kinematic chain. He introduced two laws which are fundamental to the instantaneous kinematics of kinematic chains. These are known as the series and parallel laws, which have direct analogues in the electrical circuit theory.

At the outset, it is important to notice that only instantaneous motions are considered since such motions are commutative. Now it is necessary to distinguish between



two types of joints. A joint in which the bodies joined may or may not be in contact, but all the constraints are not provided by contact between the bodies joined is called a "Complex Joint" by Waldron. The other type is a joint in which all the constraints are provided by the direct physical contact of the two joined bodies alone. This joint is called a "Simple Joint" or simply a joint. Both types of joints will be discussed in the next section.

### 2.3.1 The Series and Parallel Laws of Instantaneous Kinematics

Consider that a body 2 is connected to a body 1 by a joint of connectivity  $m$  and that a body 3 is connected to the body 2 by a joint of connectivity  $n$  (see for example Fig. 2.6 for which  $m = 3$  and  $n = 1$ ). The instantaneous motion of body 3 relative to body 1 is determined by the screw system of the complex joint between these two bodies. This resultant screw system is formed by screws of the two screw systems of both joints simultaneously and it is of order  $m+n-k$  where  $k$  is the order of the intersection of the two screw systems. For the example in Fig. 2.6,  $k = 1$  and thus the order of the resultant screw system is 3. When  $k = 0$  the intersection of the two screw systems contains only the zero vector and therefore the order of the resultant screw system is simply  $m+n$ . In such cases, the bodies are said to be serially connected, and the above law is called the series law.

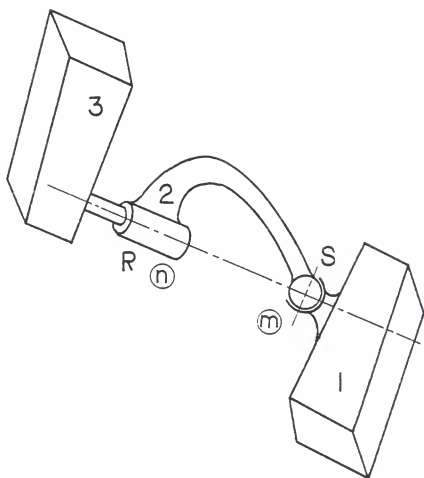


Figure 2.6. Two Joints in Series

Consider now that two bodies are connected by a pair of joints with connectivity  $m$  and  $n$  (see Fig. 2.7). Their relative motion is subjected to the constraints of both joints simultaneously. Clearly, motion can now only occur about the ISA's which are members of the screw systems of both joints. Therefore, if the order of the intersection of the two screw systems is  $k$ , the connectivity of the complex joint between the two bodies is also  $k$ . The two joints are said to be acting in parallel, and the above law is called the parallel law.

Davies and Primrose [21] introduced algebraic expressions for both the series and parallel laws. They employed "Graph Theory" and represented a kinematic chain by a coupling graph. Briefly, any body is represented by a vertex whilst any joint is represented by an edge in the coupling graph. They defined  $J_{ij}^G$  as the Instantaneous Screw System (ISS) of the joint (edge) connecting the two bodies (vertices)  $i$  and  $j$  of the coupling graph  $G$ , Fig. 2.8. They also defined  $S_{in}^G$  as the ISS of the complex joint connecting the two vertices  $i$  and  $n$  of graph  $G$  provided by all vertices and couplings corresponding to  $i$  and  $n$ . Briefly, they expressed the series and parallel laws as follows:

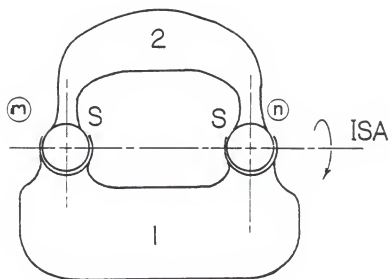


Figure 2.7. Two Joints in Parallel

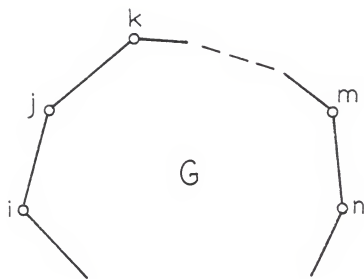


Figure 2.8. Coupling Graph "G" Representing Bodies Connected in Series

### The Series Law (Fig. 2.8)

For any coupling graph  $G$  that consists of bodies (vertices)  $i, j, \dots, n$  connected in series, and joints (edges)  $ij, jk, \dots, mn$  then the ISS that represents the instantaneous relative motion of body  $i$  with respect to body  $n$  can be expressed as

$$S_{in}^G = J_{ij}^G + J_{jk}^G + \dots + J_{mn}^G \quad (2.29)^*$$

### The Parallel Law (Fig. 2.9)

If the coupling graph  $G$  is the union of coupling graphs  $G_1, G_2, \dots$  that have only the vertices  $i$  and  $j$  in common, then

$$S_{ij}^G = S_{ij}^{G_1} \cap S_{ij}^{G_2} \dots \quad (2.30)^*$$

## 2.3.2 Instantaneous Kinematics of Serial Manipulators

The series law (2.29) is now applied to determine the instantaneous motion of body 3 relative to body 1 of the three bodies which are connected serially by turning joints (Fig. 2.10).

The instantaneous motion of body 2 relative to body 1, and of body 3 relative to body 2 are respectively,  $\omega_1 \hat{\underline{s}}_1$ , ( $= \omega_1 [\underline{s}_1 ; \underline{r}_1 \times \underline{s}_1]$ ), and  $\omega_2 \underline{s}_2$ , ( $= \omega_2 [\underline{s}_2 ; \underline{r}_2 \times \underline{s}_2]$ ). The motion of body 3 relative to body 1 is given by the twist  $\hat{\underline{s}} = \omega \hat{\underline{s}}$ , ( $= \omega [\underline{s} ; \underline{s}_0]$ ), where

---

\*The sum, "+", or joining of two subspaces  $W_1$  and  $W_2$  is the space formed by all vectors of the form  $\underline{v}_1 + \underline{v}_2$ , where  $\underline{v}_1$  is a vector of  $W_1$  and  $\underline{v}_2$  is a vector of  $W_2$ .

The intersection " $\cap$ " of two subspaces  $W_1$  and  $W_2$  is the space formed by all vectors that belong to both  $W_1$  and  $W_2$ , and [22]

$$\dim(W_1 + W_2) = \dim(W_1) + \dim(W_2) - \dim(W_1 \cap W_2)$$

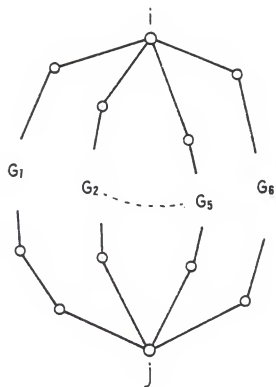


Figure 2.9. Coupling Graphs  $G_1, G_2, \dots$   
Connected in Parallel

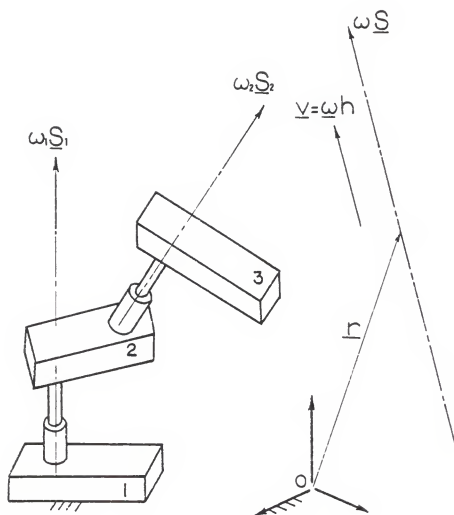


Figure 2.10. Serial Manipulator with Revolute Joints



$$\hat{\underline{\$}} = \omega \underline{\$} = \omega_1 \underline{\$}_1 + \omega_2 \underline{\$}_2 \quad (2.31)$$

and where

$$\begin{aligned} \omega \underline{S} &= \omega_1 \underline{S}_1 + \omega_2 \underline{S}_2 \\ \omega \underline{S}_0 &= \omega_1 (\underline{r}_1 \times \underline{S}_1) + \omega_2 (\underline{r}_2 \times \underline{S}_2) \end{aligned} \quad (2.32)$$

This resultant motion is not a pure rotation, but it is a combination of a pure rotation  $\omega[\underline{S} ; (\underline{S}_0 - h\underline{S})]$ , and a pure translation  $\omega[\underline{0} ; h\underline{S}]$  parallel to the axis of rotation [13].

In general, consider a sequence of  $n$  bodies connected serially with screw pairs. The twist representing the instantaneous motion of body  $n$  (the end-effector of a manipulator) relative to ground can be expressed as the sum of the twists associated with each of these  $n$  screw pairs

$$\hat{\underline{\$}} = \omega \underline{\$} = \sum_{j=1}^n \omega_j \underline{\$}_j \quad (2.33)$$

### 2.3.3 Reciprocity of Screws

A very important concept in the theory of screws due to Ball [11] is the concept of the reciprocity. It establishes the relationship between the motion capabilities and the constraints acting on rigid bodies.

Consider a wrench  $F\underline{\$}_2 = (\underline{F}_2; \underline{C}_2)$  acting on a body constrained to move on a screw  $\underline{\$}_1 = (\underline{S}_1; \underline{S}_{01})$  and it produces a twist  $(\omega_1; \underline{\mu}_1)$  as illustrated in Fig. 2.11. The virtual work produced is given by

$$\begin{aligned} W &= \underline{F}_2 \cdot \underline{\mu}_1 + \omega_1 \cdot \underline{C}_2 \\ &= F\omega(\underline{S}_2 \cdot \underline{S}_{01} + \underline{S}_1 \cdot \underline{S}_{02}) \end{aligned} \quad (2.34)$$

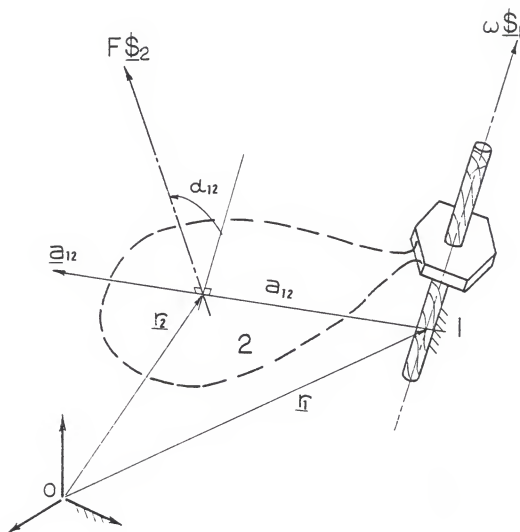


Figure 2.11. Wrench Applied on a Body Constrained to Twist

The above expression of the virtual work can be expressed in the form

$$W = F\omega[(h_1+h_2)\cos \alpha_{12} - a_{12} \sin \alpha_{12}] \quad (2.35)$$

where  $a_{12}$  and  $\alpha_{12}$  are the mutual perpendicular distance and the angle between the two screw axes, respectively, and  $h_1$  and  $h_2$  are the pitches of the two screws.

If the body is in equilibrium, then the applied wrench produces no work on the body,  $\delta W = 0$ , and

$$F\omega[(h_1+h_2)\cos \alpha_{12} - a_{12} \sin \alpha_{12}] = 0 \quad (2.36)$$

For non-zero  $F$  and  $\omega$ , the two screws  $\underline{\$}_1$  and  $\underline{\$}_2$  are reciprocal, and

$$(h_1+h_2)\cos \alpha_{12} - a_{12} \sin \alpha_{12} = 0 \quad (2.37)$$

Equation (2.37) can be expressed in the alternative form

$$\underline{\$}_1 \circ \underline{\$}_2 = \underline{S}_1 \cdot \underline{S}_{02} + \underline{S}_2 \cdot \underline{S}_{01} = 0 \quad (2.38)$$

This type of inner product is usually called the reciprocal product of the two screws. Ball introduced the term reciprocal because the product is symmetrical (a wrench applied about  $\underline{\$}_1$  cannot produce a twist about  $\underline{\$}_2$ ). It is important to recognize that no matter how large the intensity  $F$  of the wrench is, there can be no motion of the body. Some special cases of reciprocal screws are considered in [9].

The subject of reciprocal screw systems and the corresponding degrees of freedom have been studied in great detail by Ball [11], Dimentberg [14], Hunt [3], Waldron [16], Duffy

[9], and others. The most important result concerning the concept of reciprocity is that a rigid body in space which can twist about  $n$  independent screws ( $1 \leq n \leq 6$ ) has a reciprocal screw system of order  $(6-n)$ ; i.e., it is constrained by  $(6-n)$  independent reciprocal wrenches. It can thus be concluded that a reciprocal screw system elegantly describes and quantifies the nature of the constraints acting upon the body.

### 2.3.4 Linear Algebra of Screw Systems

Recently, Sugimoto and Duffy in [23] made use of the linear algebra characteristics of screw systems, and they defined orthogonal screws. The two screws  $\$1 = \underline{S}_1 + \epsilon \underline{S}_{O1}$  and  $\$2 = \underline{S}_2 + \epsilon \underline{S}_{O2}$  are said to be orthogonal when they satisfy the condition

$$\$1 * \$2 = \underline{S}_1 \cdot \underline{S}_2 + \underline{S}_{O1} \cdot \underline{S}_{O2} = 0 \quad (2.39)$$

The product  $*$  is called the inner or orthogonal product of a pair of screws because it is analogous to the inner-dot product of a pair of vectors. When a pair of screws satisfies (2.39), then they cannot be linearly dependent. Two screws  $\$1$  and  $\$2$  are said to be linearly dependent when

$$a_1 \$1 + a_2 \$2 = 0 \quad (2.40)$$

where  $a_1$  and  $a_2$  are non-zero scalars. When (2.40) can only be satisfied by  $a_1 = a_2 = 0$ , the two screws are said to be linearly independent.

It is important to recognize that there is a one-to-one correspondence between reciprocal and orthogonal screws.

If a screw  $\underline{\$}_r$  is reciprocal to a screw system and there is a corresponding screw  $\underline{\$}_o$  which is orthogonal to the screw system, the two screws  $\underline{\$}_r$  and  $\underline{\$}_o$  are related by

$$\underline{\$}_o = T \underline{\$}_r \quad (2.41)$$

where the matrix T is in the form

$$T = \left[ \begin{array}{ccc|ccc} 0 & 0 & 0 & 1 & 0 & 0 \\ 0 & 0 & 0 & 0 & 1 & 0 \\ 0 & 0 & 0 & 0 & 0 & 1 \\ \hline 1 & 0 & 0 & 0 & 0 & 0 \\ 0 & 1 & 0 & 0 & 0 & 0 \\ 0 & 0 & 1 & 0 & 0 & 0 \end{array} \right] \quad (2.42)$$

For example, a body connected to ground by five screws has five independent freedoms and there is a single screw  $\underline{\$}_r$ ,  $(L_r, M_r, N_r ; P_r, Q_r, R_r)$  which is reciprocal to the five-system. In other words there is a single constraint acting upon the body. It can be stated that the body cannot have motion about the corresponding orthogonal screw  $\underline{\$}_o$ ,  $(P_r, Q_r, R_r ; L_r, M_r, N_r)$ . It can be concluded, in general, that orthogonal screw systems describe the unattainable motion of the body.

The well known Gram-Schmidt orthogonalization process, or the modified Gram-Schmidt process, [22-24] can be applied to determine a set of linearly independent screws orthogonal to a screw system. Some other analytical approaches to

determine orthogonal and reciprocal screws are discussed in detail in [9, 23].

Since there are a maximum of six linearly independent screws in three-dimensional space, then sets of seven or more screws are linearly dependent, and

$$\sum_{j=1}^n \omega_j \underline{s}_j = 0 \quad (2.43)$$

for  $n \geq 7$ . The above equation (with  $n = 7$ ) can be expressed in the following matrix form

$$\begin{bmatrix} L_1 & L_2 & \dots & L_7 \\ M_1 & M_2 & \dots & M_7 \\ N_1 & N_2 & \dots & N_7 \\ P_1 & P_2 & \dots & P_7 \\ Q_1 & Q_2 & \dots & Q_7 \\ R_1 & R_2 & \dots & R_7 \end{bmatrix} \begin{Bmatrix} \omega_1 \\ \omega_2 \\ \omega_3 \\ \omega_4 \\ \omega_5 \\ \omega_6 \\ \omega_7 \end{Bmatrix} = \underline{0} \quad (2.44)$$

where  $(L_i, M_i, N_i ; P_i, Q_i, R_i)$  are the screw coordinates and the  $\omega$ 's are the scalar multipliers associated with the twists. Therefore, forming the orthogonal product of (2.43) with each of the  $n$  screws in turn gives a set of  $n$  homogeneous equations in the scalars  $\omega_1, \omega_2, \dots, \omega_n$ . It follows that, the necessary and sufficient condition that  $n$  screws  $\underline{s}_1, \underline{s}_2, \dots, \underline{s}_n$  are linearly dependent is that the Gramian of these screws vanishes,

$$\begin{bmatrix}
 \varphi_1 & * & \varphi_1 & \varphi_1 & * & \varphi_2 & . & . & . & . & \varphi_1 & * & \varphi_n \\
 \varphi_2 & * & \varphi_1 & \varphi_2 & * & \varphi_2 & . & . & . & . & \varphi_2 & * & \varphi_n \\
 . & . & . & . & . & . & . & . & . & . & . & . & . \\
 . & . & . & . & . & . & . & . & . & . & . & . & . \\
 . & . & . & . & . & . & . & . & . & . & . & . & . \\
 . & . & . & . & . & . & . & . & . & . & . & . & . \\
 \varphi_n & * & \varphi_1 & \varphi_n & * & \varphi_2 & . & . & . & . & \varphi_n & * & \varphi_n
 \end{bmatrix} = 0 \quad (2.45)$$

Equations (2.43) and (2.45) are used in Chapter 5 to describe special configurations of mechanisms.

## CHAPTER 3 TYPE SYNTHESIS OF MECHANISMS

### 3.1 Definitions and Basic Procedures

Type synthesis (or number synthesis) of mechanisms provides an exhaustive and very systematic method of discovering, displaying, and evaluating all mechanisms with a given or specified overall mobility  $M$ .

The complete process of type synthesis is defined to involve the determination of:

- Total number and types of kinematic pairs (joints).
- Total number and types of links.
- Total number of unique kinematic chains that can be structurally synthesized using the total number of links and joints (called "Structural Synthesis").

This is followed by the determination of the location of the actuated kinematic pairs and the fixed link (the frame) to form the corresponding mechanisms or devices (sometimes called the "Motors" mechanisms [25,26]).

A kinematic chain can be defined simply as an assemblage of links and pairs. It may be open (unclosed) or closed. Every joint-element of every link in a closed kinematic chain has to be connected to at least one other joint-element of a neighboring link. A mechanism can be formed



by fixing one link of a corresponding kinematic chain. The mobility of a mechanism<sup>\*</sup> may be defined as the number of independent parameters or coordinates necessary to locate each link relative to one another.

A kinematic chain is said to have total mobility  $M$  (see [27-29]) when it can fulfill the following condition; "If any link of the chain is selected to be the frame, and any  $M$ -links are chosen to be independent driving links, then the position of every remaining (driven) link is dependent on the position of all  $M$ -driving links." This means that in order for a kinematic chain to have a total mobility  $M$ , regardless of which link is fixed and also regardless of which pairs are to be actuated<sup>†</sup>, it must not contain within it any closed kinematic subchain (closed-loop) which has less than  $M$ -degrees of mobility. A kinematic chain which cannot fulfill the above condition for total mobility possesses either a partial or fractionated mobility (see Section 3.2 for more details).

The mobility of any mechanism can be determined from the general mobility equation

---

<sup>\*</sup>The author is aware of a trend to abandon the difference in definition between the term mobility and degrees of freedom, as being of trivial importance and to use the symbol  $M$  for mobility or degrees of freedom of a mechanism.

<sup>†</sup>There may be restrictions on which  $M$ -pairs can be used as actuated pairs (inputs). Davies [26] discussed this concept in some detail for kinematic chains which do not possess total mobility. Also, the concept of motion of the actuators being instantaneously dependent is discussed in Chapter 5 of this text.

$$M = d(N-j-1) + \sum_{i=1}^j f_i \quad (3.1)^*$$

where

- $M$ : the effective degree of freedom of the mechanism,  
 $d$ : the degree of freedom of the space in which the mechanism operates (the order of the corresponding screw system), i.e.,  $d = 3$  for planar and spherical motions and  $d = 6$  for spatial motions, in general,  
 $f_i$ : the degree of freedom of the  $i$ th kinematic joint,  
 $\sum_{i=1}^j f_i$ : the number of effective joint freedoms,  
 $N$ : the number of links,  
 $j$ : the number of kinematic joints.

In order to apply (3.1) correctly, it is necessary to examine the types of kinematic pairs and links. In the first instance only revolute or turning pairs ( $R$ ) will be considered. A  $k$ -nary pair is defined as a pair or joint-element which connects  $k$ -links (see Fig. 3.1) and it should be clear in applying the mobility equation (3.1) that ternary, quaternary, ... pairs counts as two, three, ... pairs. However, mechanisms with ternary, quaternary, ... pairs will be excluded from this text.

---

\*Equation (3.1) could be expressed in the form

$$M = d(N-j-1) + \left( \sum_{i=1}^j f_i \right) - I_d$$

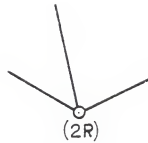
where

- $I_d$ : idle or passive degree of freedom  
 and  $f_i$ : degree of freedom of the  $i$ th kinematic pairs.

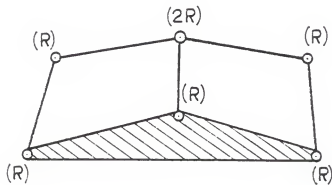
Fig. 3.23 illustrates some connecting chains with idle freedoms. Each idle freedom is represented by a double-headed dotted arrow.



binary pair



ternary (double) pair



double joint version of Watt mechanism

Figure 3.1. Types of Kinematic Pairs (Joints)

Any mechanism (see [27] and [30]) comprised of simple revolute pairs for which  $f_i = 1$  must have a total number of links,  $N$ , and a total number of pairs,  $j$ , given by:

$$N = n_2 + n_3 + \dots = \sum_{p=2} n_p \quad (3.2)$$

$$2j = 2n_2 + 3n_3 + \dots = \sum_{p=2} pn_p \quad (3.3)$$

where  $n_2, n_3, n_4, \dots$  are respectively the number of binary, ternary, quaternary, ..., etc. links (see Fig. 3.2). A  $P$ -nary link is a polygon of  $P$  corners or joint-elements to which  $P$  links are connected.

This text is concerned only with the so-called "Parallel Devices," (see Chapter 1). It has been concluded in [2,3] that no conceivable practical advantage is seen by designing or synthesizing a "mixed- $d$ " device. A "mixed- $d$ " device could be, for instance, a general spatial ( $d=6$ ) loop with planar, spherical and other overconstrained ( $d<6$ ) loops joining to it and moving as it moves. The only parallel robotic devices with practical promise are those with  $d = M = 3$  (three-degree of freedom spherical or planar devices--3/3/second and 3/3/fifth, respectively, see Table 3.1\*) and  $d = M = 6$  (general six-degree of freedom spatial devices).

---

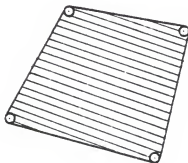
\*This table is adapted from Table 2 [2].



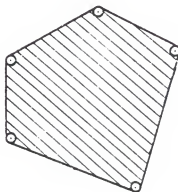
$n_2$  : binary link



$n_3$  : ternary link



$n_4$  : quaternary link



$n_5$  : quinary link

Figure 3.2. Types of Links

Table 3.1  
Screw Systems Applicable to the Practical  
Parallel Robotic Devices

Order of the Screw System (d)	Identification (Classification)	Description of the Screws of the System
3	3/3/second	Screws of zero pitch along all lines throughout a point, namely the system applicable to <u>spherical motion</u>
	3/3/fifth	Screws of infinite pitch along all lines parallel to a given plane together with screws of a specified <u>finite</u> or zero pitch along all lines perpendicular to the plane, this system including that applicable to <u>planar motion</u>
6		ALL screws of all pitches along all lines in all directions

### 3.2 Type Synthesis of Planar Robotic Devices

A type synthesis of planar devices (for which  $d = 3$ ) is now performed. Firstly, it is necessary to determine the links and joints which can be assembled to form a planar kinematic chain with specific mobility  $M$ . This is accomplished using (3.1) which reduces to

$$M = 3(N-1) - 2j \quad (3.4)$$

It can also be rearranged in the form

$$M + 3 = 3N - 2j \quad (3.5)$$

Further substituting for  $N$  and  $j$  using (3.2) and (3.3) gives

$$M + 3 = n_2 - \sum_{p=4} (p-3)n_p \quad (3.6)$$

It is clear from (3.6) that the mobility  $M$  is independent of the number of ternary links  $n_3$  in the chain. Consider that an  $N$ -link kinematic chain is found which contains  $n_3$  ternary links and therefore  $(N-n_3)$  of the other types of links. It follows that there exists other kinematic chains having the same mobility  $M$  and the same number of each link other than ternaries and which contain  $(n_3+2k)$  ternary links where  $k$  is any integer.

At the outset it is most useful to be able to select a minimum number of binary links for a specified value of  $M$ , and it follows from (3.6) that for a closed planar kinematic chain

$$(n_2)_{\min} = M + 3 \quad (\text{or} = 3N - 2j) \quad (3.7)$$

For planar kinematic chains with  $M = 3$ , equation (3.4) can be rearranged in the form

$$j = \frac{3}{2} (N-2) \quad (3.8)$$

Since  $j$  must be an integer, then  $N$  must be even. Using this simple fact, Table 3.2(a) can be constructed. Further, it is possible to change the number of any three successive types of links from  $n_{p-1}$ ,  $n_p$ ,  $n_{p+1}$  to  $(n_{p-1}+1)$ ,  $(n_p-2)$ ,  $(n_{p+1}+1)$  without changing the total number of links or joints, or the mobility. Therefore using equations (3.2), (3.3) and (3.7), and by successive numerical operations of this sort, Table 3.2(b) can be deduced from Table 3.2(a). For instance, group I, with  $n_2 = 4$ , is the simple serial chain. For groups II, III(a), IV(a), . . . , the minimum number of binaries is 6. Since in group IV(a)  $n_2 = 6$  and  $n_3 = 4$ ; therefore group IV(b) will have  $n_2 = 6 + 1 = 7$ ;  $n_3 = 4 - 2 = 2$  and  $n_4 = 0 + 1 = 1$ .

Having determined the number and types of both links and joints, it remains to determine all the possible ways of connecting these links and joints. This process, which is called "Structural Synthesis," is accomplished here by introducing Franke's notation [29,31];

(i) A circle is introduced to represent each polygonal link. The type of each link is designated by placing the so-called valency number within the circle. For instance, a number 3 will indicate that the circle is describing a ternary link.



Table 3.2

Structural Analysis of  $M = 3$  Planar  
Kinematic Chains

(a)

N	4	6	8	10	12	14
J	3	6	9	12	15	18

(b)

Group	j	N	$n_2$	$n_3$	$n_4$	$n_5$	$n_6$	$n_7$	$n_8$
I-a	3	4	4						
II-a	6	6	6	-	-	-	-	-	-
III-a b	9	8	6 7	2 0	1				
IV-a b c d e . . .	12	10	6 7 8 8 9	4 2 0 1 0	- 1 2 0 0	-  1 0 0	-   1	-   	
V-a b c d e f g h i . . .	15	12	6 7 8 8 9 9 10 10 11	6 4 3 2 1 0 0 0 0	- 1 0 2 1 3 0 1 0	-  1 1 0 2 0 0 0	-    1 0	-     0	1
VI-a b c . . .	18	14	6 7 8	8 6 4	- 1 2	-  	-  	-  	

(ii) A straight line is introduced to represent the type of connection of the polygonal links, either by a joint or by one or more binary links in series. Each straight line has also an associated number to indicate the number of binary links in series, or zero to indicate a direct jointing. Table 3.3 illustrates the meaning of the different connections by which two polygonal links may be joined. The associated numbers may be placed adjacent to these lines. Since a ternary link has three joint-elements, three lines should emit from the circle representing a ternary link. Similarly, four and six lines should emit from circles representing quaternary and hexagonal links, respectively.

It remains to convert the molecules obtained above into equivalent kinematic chains and then into the corresponding mechanisms. Because the above method gives combinations that cannot be used, it is necessary to observe the following;

(i) A mechanism has partial mobility  $M$  if the position of some driven links depends on the movements of only a number  $M_p$  of the driving links, where  $M_p > M$ . Figure 3.3 illustrates three planar mechanisms each having mobility  $M = 3$ . In (a) and (b) the lamina A has three degrees of freedom relative to the frame, i.e., its connectivity equals three. However, in (c) the position of the lamina A (as well as the other driven link 3) depends only on the two driving links 2 and 4 in the closed loop a-b-c-d-e which has mobility  $M_p = 2$ . In this case by locking the two driving links 2 and 4, the lamina A and link 3 will

Table 3.3

Franke's Molecule Notation

Number of Connections	Molecules Representation	Some Connections and Their Molecules	
1			
2			
3			

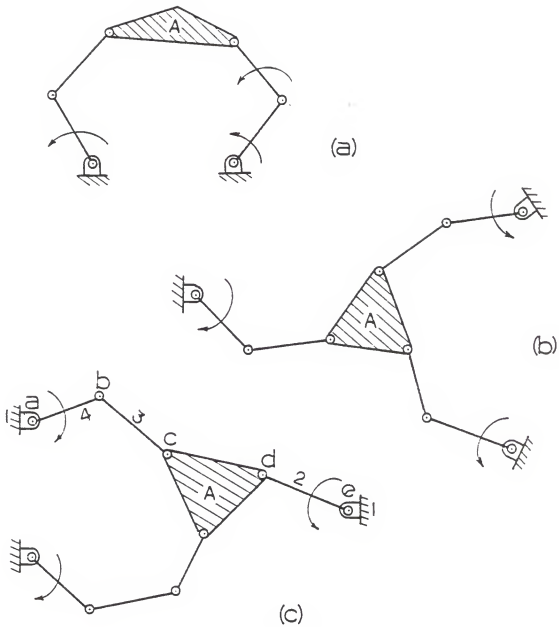


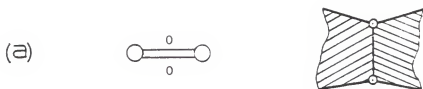
Figure 3.3. Planar Mechanisms with Three-Dof  
 (a) and (b) Total Mobility  $M=3$   
 (c) Partial Mobility  $M=3$

be locked also. Therefore the mechanism in (c) has partial mobility and the lamina A has just two degrees of freedom relative to the frame. Since in the investigation of parallel robotic devices the main concern is the movement of the lamina which has the end-effector, therefore devices with partial mobility will be acceptable as long as the position of the lamina depends on all the M-driving links and as long as the device does not contain within it any closed loops which has mobility  $M_p < 1$ , i.e., structures. Figure 3.4 illustrates some subassembly structures which must be avoided.

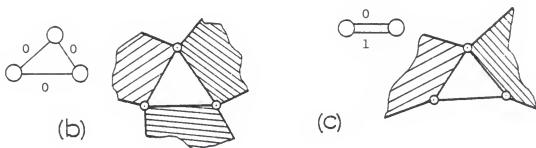
(ii) Rosenauer [32] stated that for mobility  $M = 1$  closed mechanisms, the maximum number of joint-elements attached to a single link must not exceed half the number of links in the chain, ( $P_{\max} \leq \frac{N}{2}$ ). Generally, it could be concluded that the maximum number of joint-elements attached to a single link in a closed mechanism can be expressed in the form

$$P_{\max} \leq \frac{N-M+1}{2} \quad (3.9)$$

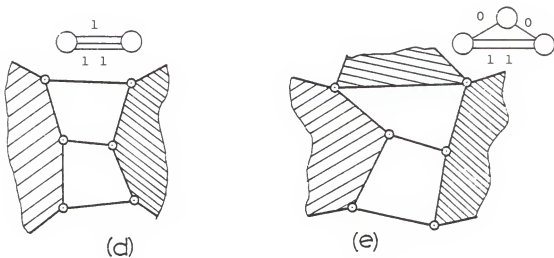
If a mechanism possesses at least one link with  $P_{\max} > \frac{N-M+1}{2}$  then it may be divided into two or more parts, and if that link is selected to be the frame then no driven link is capable of being moved by all the driving links. Such mechanisms possess a fractionated mobility and the sum of the mobilities of all parts is equal to the mobility of the whole mechanism. For instance, for the three-degree of freedom planar mechanism in Fig. 3.5(a),  $P_{\max}$  has to be less than or equal ( $\frac{N-2}{2} = 3$ ). However, because  $P_{\max} = 4$ , this mechanism has two conjoined



(a) (0,0) combination



(b) and (c) structural triangles



(d) and (e) E-quartet structures

Figure 3.4. Structures which Must Be Avoided

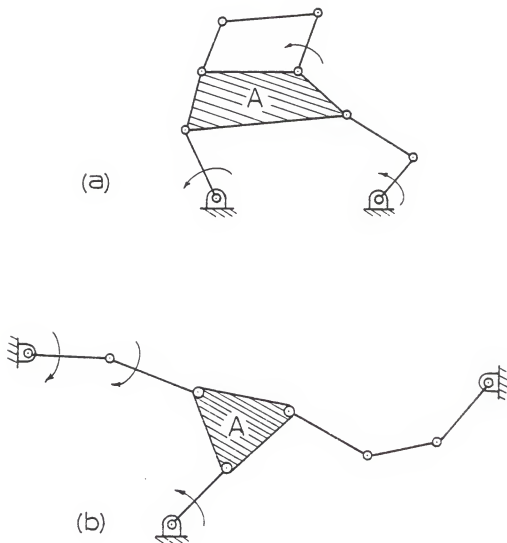


Figure 3.5. Mechanisms Having  
(a) Fractionated Mobility  
(b) Immobility

sub-assemblies of mobilities  $M = 1$  and  $M = 2$ , and the lamina A has two degrees of freedom relative to the frame. In general, mechanisms with fractionated mobility must be avoided.

(iii) If in a mechanism of mobility  $M$ , a closed kinematic subchain exists of mobility less than the number of actuated pairs it contains, then the mechanism is immobile and should be avoided (see Fig. 3.5(b)).

It could be concluded that the kind of mobility is not a notion inherent in any kinematic chain and it is subject to change by the choice of the actuated pairs and of the frame. However, in most parallel robotic devices the actuated pairs are preferred to be close to ground, and the main concern is that the lamina which has the end-effector has to have relative mobility equal to the mobility of the whole device without having structures within the chain. Such devices are now illustrated in Figs. 3.6-3.16.

### 3.3 Type Synthesis of Spatial Robotic Devices

For spatial kinematic chains ( $d = 6$ , in general), the mobility equation (3.1) reduces to

$$M = 6(N-1) - 5j \quad (3.10)$$

where  $f_i = 1$ . Equation (3.10) can be rearranged in the form

$$M + 6 = 6N - 5j \quad (3.11)$$



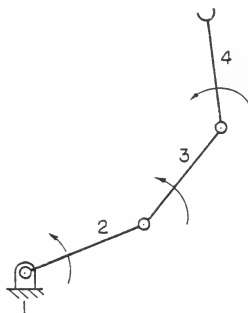


Figure 3.6. Group I, Open Chain  
 $N=4$ ,  $n_2=4$ ,  $j=3$

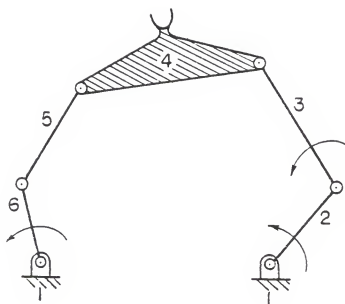
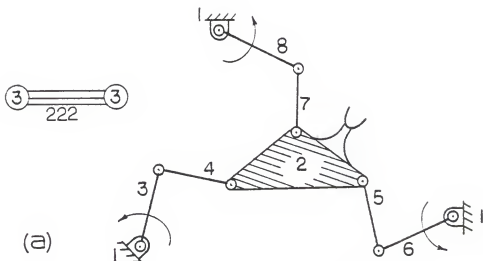
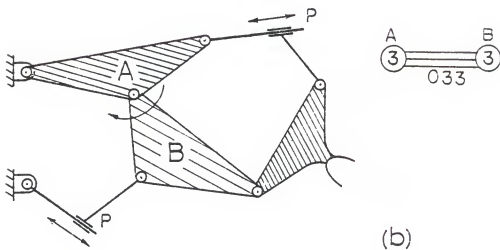


Figure 3.7. Group II, Single-Loop Closed Chain  
 $N=6$ ,  $n_2=6$ ,  $j=6$



(a) fully-parallel device



(b) partially-parallel device

Figure 3.8. Group III  
 $N=8$ ,  $n_2=6$ ,  $n_3=2$ ,  $j=9$

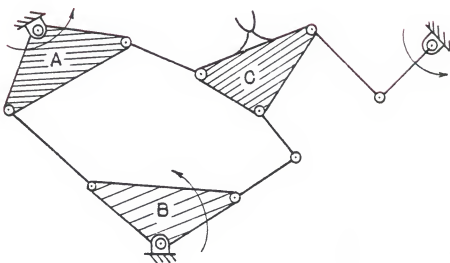
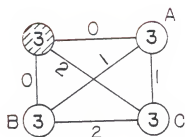


Figure 3.9. Group IV-a  
 $N=10$ ,  $n_2=6$ ,  $n_3=4$ ,  $j=12$

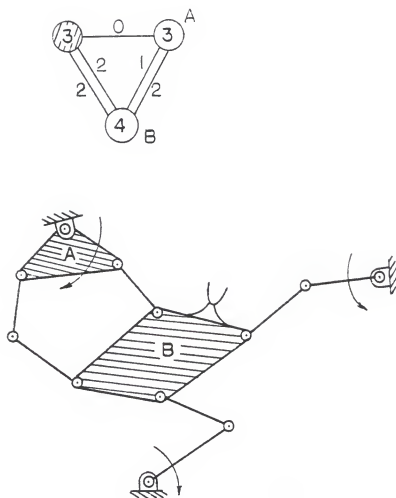
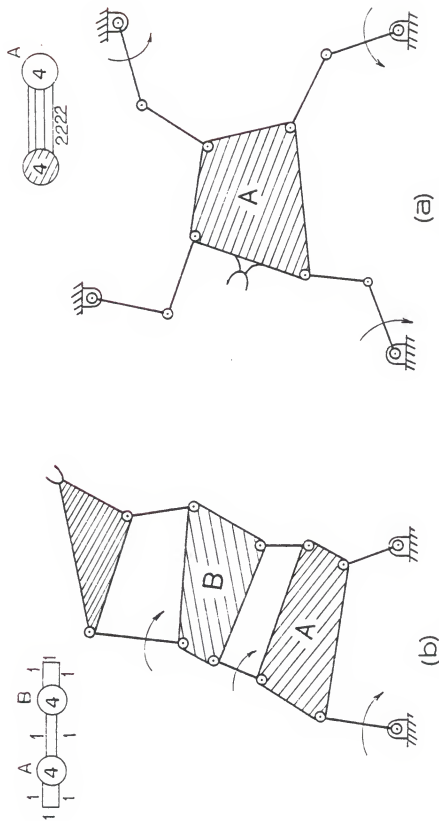


Figure 3.10. Group IV-b  
 $N=10$ ,  $n_2=7$ ,  $n_3=2$ ,  $n_4=1$ ,  $j=12$



fully-parallel device

partially-parallel device

Figure 3.11. Group IV-c,  $N=10$ ,  $n_2=8$ ,  $n_4=2$ ,  $j=12$

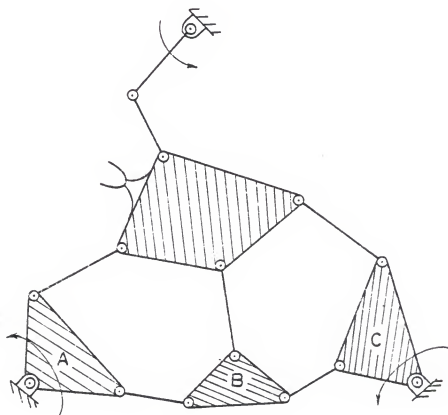
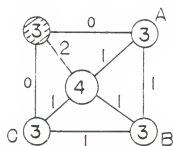


Figure 3.12. Group V-b,  $N=12$ ,  $n_2=7$ ,  
 $n_3=4$ ,  $n_4=1$ ,  $j=15$

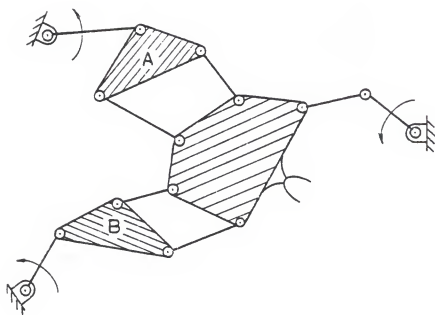
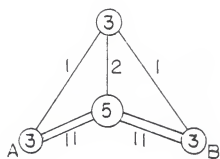


Figure 3.13. Group V-c,  $N=12$ ,  $n_2=8$ ,  
 $n_3=3$ ,  $n_5=1$ ,  $j=15$



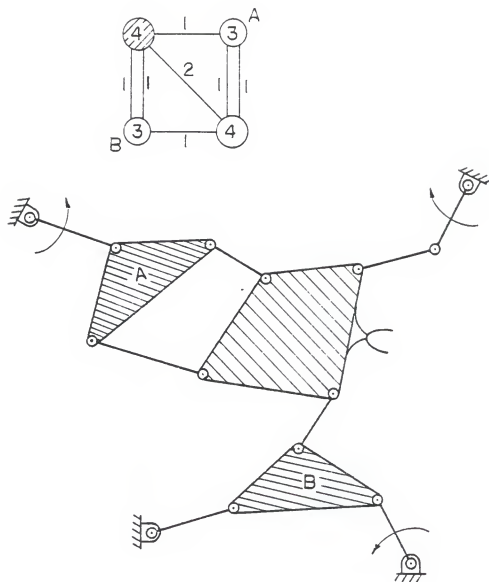


Figure 3.14. Group V-d,  $N=12$ ,  $n_2=8$   
 $n_3=2$ ,  $n_4=2$ ,  $j=15$

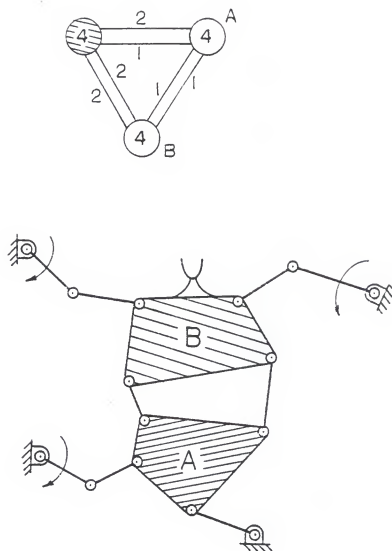


Figure 3.15. Group V-f,  $N=12$ ,  $n_2=9$ ,  
 $n_4=3$ ,  $j=15$

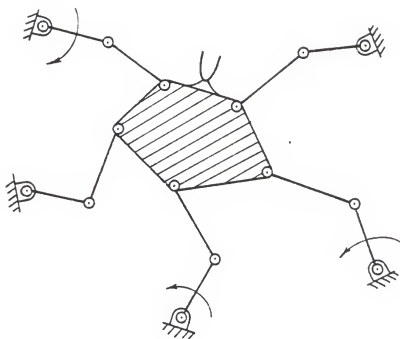
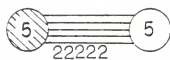


Figure 3.16. Group V-g,  $N=12$ ,  $n_2=10$   
 $n_5=2$ ,  $j=15$

Further substituting for  $N$  and  $j$  using equations (3.2) and (3.3) gives

$$M + 6 = n_2 - \sum_{p=3} \left(\frac{5}{2} p - 6\right) n_p \quad (3.12)$$

As it has been mentioned in Section 3.2, it is most useful to be able to select a minimum number of binary links for a specified  $M$ ,  $N$ , and  $j$ . It follows from equation (3.12) that for a single-loop closed kinematic chain; i.e.,  $n_p = 0$  for  $p > 2$ ,

$$(n_2)_{\min} = M + 6 \quad (3.13)$$

However, unlike the planar kinematic chains, the mobility  $M$  of spatial kinematic chains is dependent on the number of ternary links  $n_3$ . Therefore  $(n_2)_{\min}$  does not equal  $(M + 6)$  in general. By inspection, for a specified  $M$ ,  $N$ , and  $j$ , the number of binary links is minimum when the chain contains only binary and ternary links; i.e.,  $n_p = 0$  for  $p > 3$ . Then equations (3.2) and (3.3) become

$$(n_2)_{\min} + n_3 = N \quad (3.14)$$

and

$$2(n_2)_{\min} + 3n_3 = 2j \quad (3.15)$$

Solving the above equations simultaneously gives

$$(n_2)_{\min} = 3N - 2j \quad (3.16)$$

which agrees with equation (3.7) for the planar devices, and also

$$(n_3)_{\max} = 2(j - N) \quad (3.17)$$

For spatial kinematic chains with mobility  $M = 6$ , equation (3.11) can be rearranged in the form

$$j = \frac{6}{5} (N-2) \quad (3.18)$$

Since  $j$  must be an integer, then  $N$  must be 7, 12, 17, . . . . Using equation (3.18), Table 3.4(a) is constructed and then using equations (3.2), (3.3), (3.16-3.18) and by successive numerical operations (see Section 3.2), Table 3.4(b) can be constructed. It is interesting to note that Table 3.4(b) could be derived from Table 3.2(b) simply by changing the values of  $(n_2)$  starting with  $(n_2)_{\min} = 3N - 2j$  for the values of  $N$  and  $j$  from Table 3.4(a). All other types of links are identical to those in Table 3.2(b).

Following the procedure described in Section 3.2, some molecules and their equivalent devices which have practical promise are illustrated in Figs. 3.17-3.22.

### 3.4 Discussion and Future Robotic Applications of Parallel Devices

The above synthesis has been performed using only revolute or turning pairs with  $f_i = 1$  (or in general screw pairs with  $f_i = 1$ ), however all other pairs could be considered as combinations of screw pairs with certain pitches. The argument for coalescing the pairs can be applied easily. For instance, [RP] and [RRR] joint combinations could be used to simulate [C] and [S] pairs respectively. Figure 3.23 illustrates seven possible connecting subchains and their equivalent R-P representations. Connecting subchains (c), (d), and

Table 3.4

Structural Analysis of  $M = 6$  Spatial  
Kinematic Chains

(a)

N	7	12	17	22	27	32
J	6	12	18	24	30	36

(b)

Group	j	N	$n_2$	$n_3$	$n_4$	$n_5$	$n_6$	$n_7$	$n_8$
I	6	7	7						
II	12	12	12						
III-a b	18	17	15 16	2 0	1				
IV-a b c d e . . .	24	22	18 19 20 20 21	4 2 0 1 0	1 2 0 0	1 0	1		
V-a b c d e f g h i . . .	30	27	21 22 23 23 24 24 25 25 26	6 4 3 2 1 0 0 0 0	1 0 2 1 3 0 1 0	1 1 0 2 0 0	1 0	1	
VI-a b c . . .	36	32	24 25 26 . . . 30	8 6 4 . . . 0	1 2 0	0 0	2		

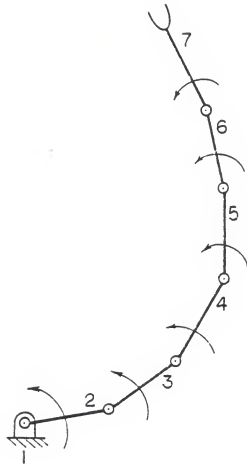


Figure 3.17. Group I, Spatial Open Chain  
 $N=7$ ,  $n_2=7$ ,  $j=6$

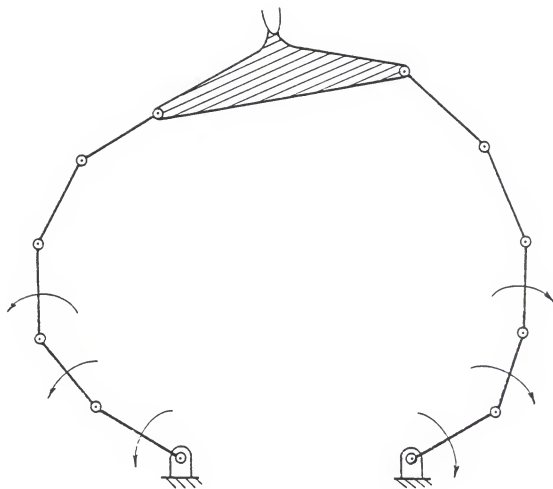


Figure 3.18. Group II, Single-Loop Closed Chain  
 $N=12$ ,  $n_2=12$ ,  $j=12$



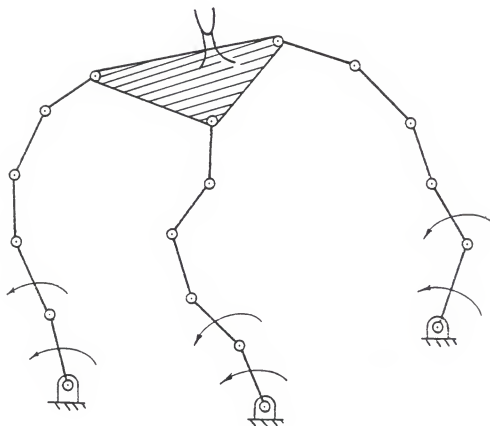
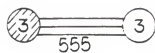


Figure 3.19. Group III-a,  $N=17$ ,  $n_2=15$ ,  
 $n_3=2$ ,  $j=18$

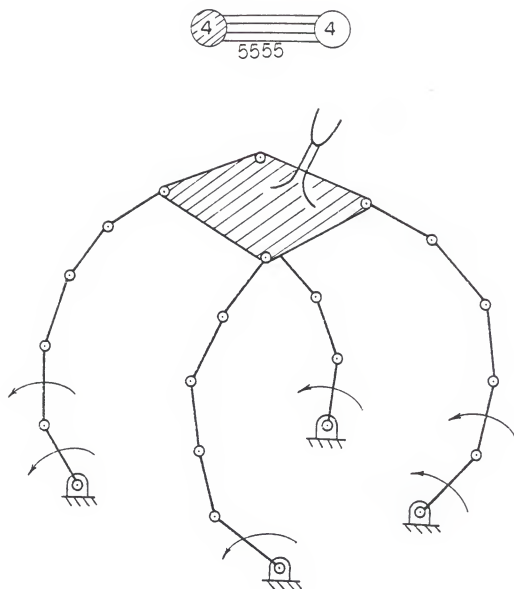


Figure 3.20. Group IV-c,  $N=22$ ,  $n_2=20$ ,  
 $n_4=2$ ,  $j=24$

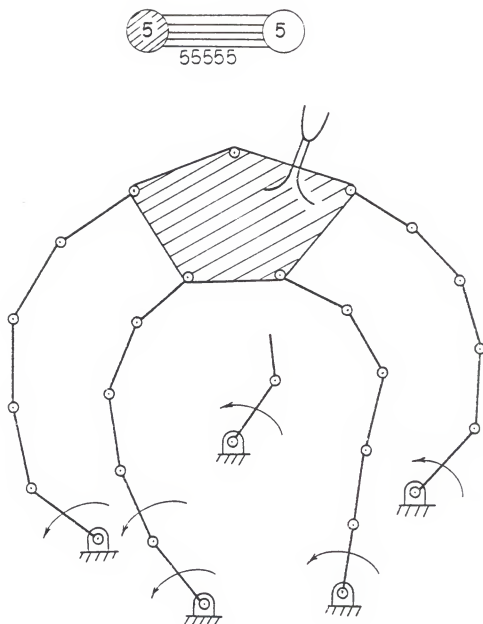


Figure 3.21. Group V-g,  $N=27$ ,  $n_2=25$ ,  
 $n_5=2$ ,  $j=30$

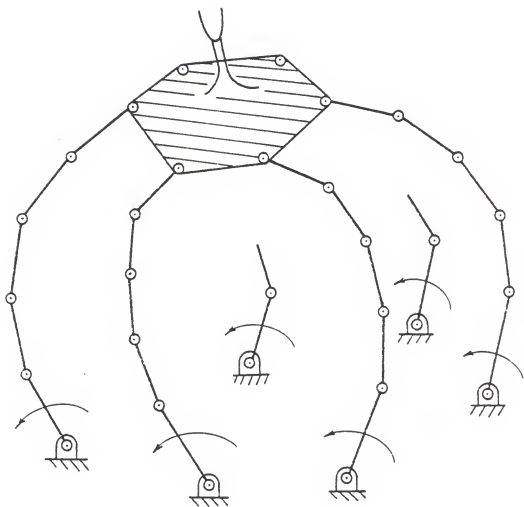
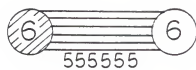


Figure 3.22. Group VI,  $N=32$ ,  $n_2=30$ ,  
 $n_6=2$ ,  $j=36$

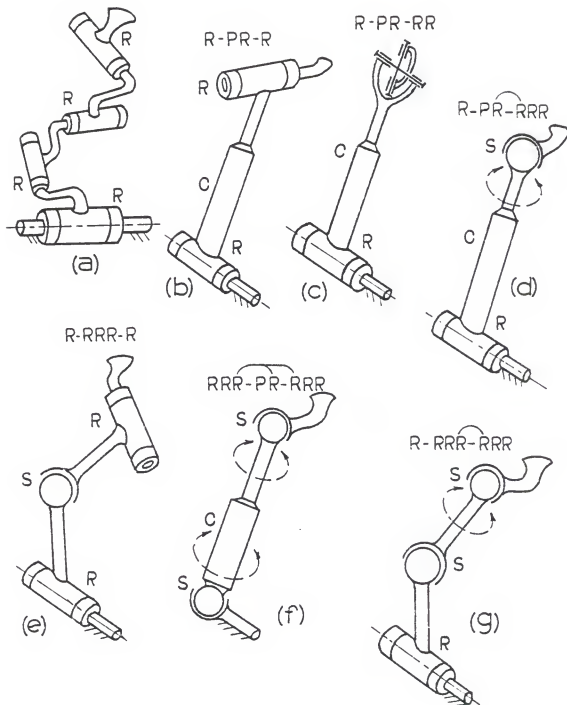


Figure 3.23. Seven Possible Connecting Subchains

(e) have five freedoms while (f) and (g) have six freedoms. Spin-freedoms (idle-freedoms) are denoted by double-headed dotted arrows.

The simplest parallel devices, closed single loop devices illustrated in Figs. 3.7 and 3.18, have a slight advantage of greater rigidity over open loop serial devices such as those illustrated in Figs. 3.6 and 3.17. However, because of the symmetry, high rigidity, and high precision positioning of the device illustrated in Fig. 3.8(a), this device is considered to be one of the most practical planar devices. This particular device has been developed by the "Center of Intelligent Machines and Robotics--CIMAR" at the University of Florida [4]. As discussed in Chapter 1, the three actuated connecting subchains of this device are fully in-parallel with one another, and the device is considered to be a fully-parallel planar device. Three actuated prismatic pairs could be considered instead of the three revolute pairs  $R_2$ ,  $R_5$ , and  $R_8$  (see Fig. 3.24 and [2]).

Figures 3.8(b) and 3.11(b) illustrate two examples of the so-called "partially-parallel" devices (see Chapter 1) in which the actuated connecting subchains are connected partially in-parallel. These type of devices are sometimes incorporated in earth-moving machinery (Fig. 3.25), and may also have been adapted in some specialized robotic devices. Also, as proposed by Hunt [3], a six-degree of freedom robotic device could comprise two three-degree of freedom parallel devices connected in series. Figure 3.26

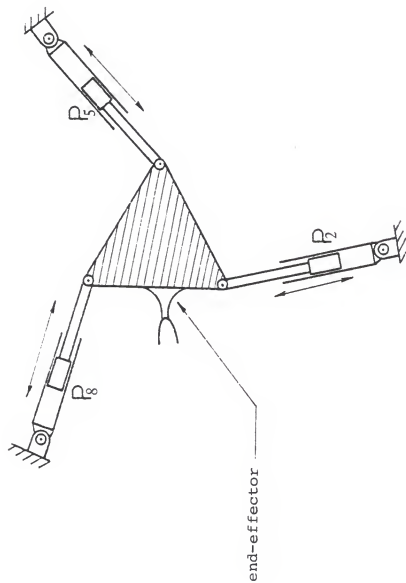


Figure 3.24. Alternative Form of Figure 3.8-(a)

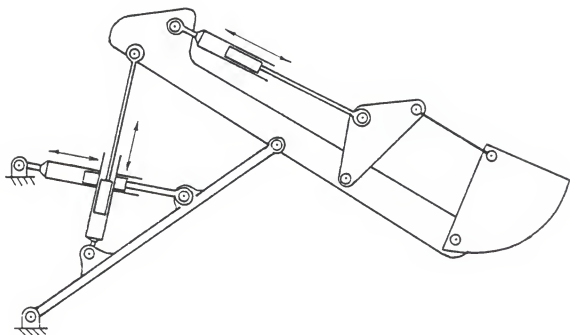


Figure 3.25. Planar Earth Moving Machinery



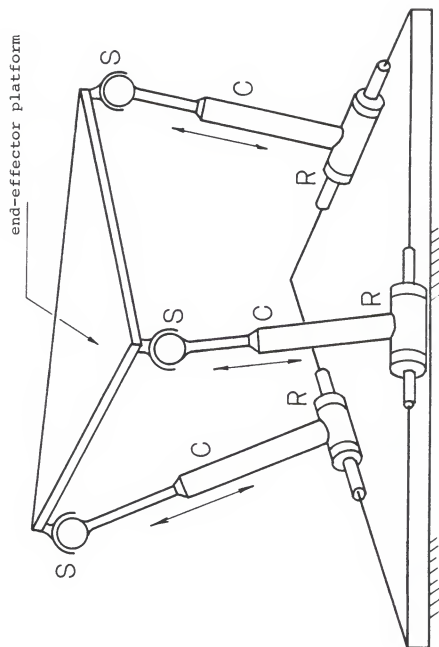


Figure 3.26. Three-Degree of Freedom Shoulder

illustrates a possible three-degree of freedom shoulder with three linear actuators.

Most observers agree that symmetrical fully-parallel devices can be made much stronger and can manipulate heavier loads more precisely within their working volumes than their corresponding serial devices. It is concluded that the devices illustrated in Figs. 3.19 and 3.22 are the two spatial devices with the most practical promise. Figure 3.27 illustrates a practical design based on Fig. 3.19. It has three turning actuated pairs at the base followed by three linear actuators. Figure 3.28 [7] illustrates a practical design developed by the CIMAR research group at the University of Florida which was based on Fig. 3.22. The well known "Stewart Platform" which stems from Fig. 3.22 is illustrated in Fig. 3.29. It is constructed by connecting two hexagonal links, frame and platform, to six adjustable subchains (legs). However, Hunt [2] indicated that an arrangement close to the variable-edge-length octahedron has important merits. This arrangement is another version of the "Stewart Platform." The six adjustable subchains (only one is shown in full in Fig. 3.30) are distributed in a triangular pattern around two ternary links using double-spherical joints. Further, the R-pair in series gives the arm an extra rotary freedom relative to the base. The "Stewart Platform" type of device was originally designed as an aircraft simulator, and was also suggested for the application of machine tool, space vehicle

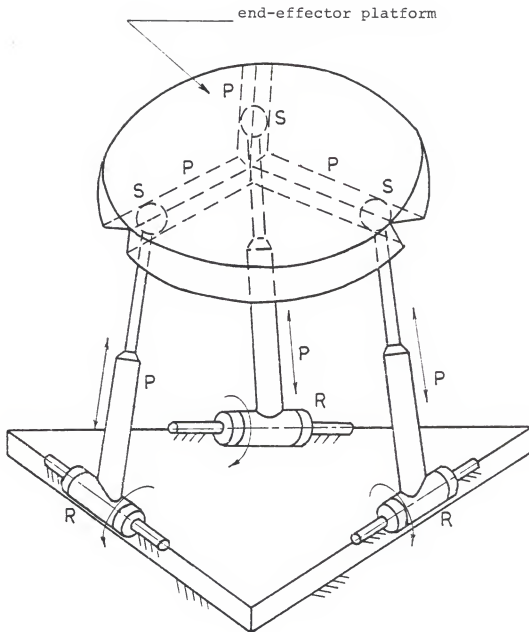


Figure 3.27. R-P-SP Fully-Parallel Device

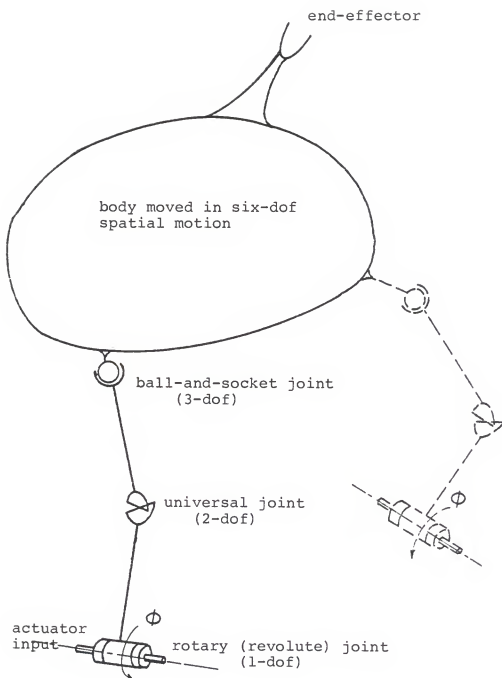


Figure 3.28. University of Florida Concept for Fully-Parallel Robot Device

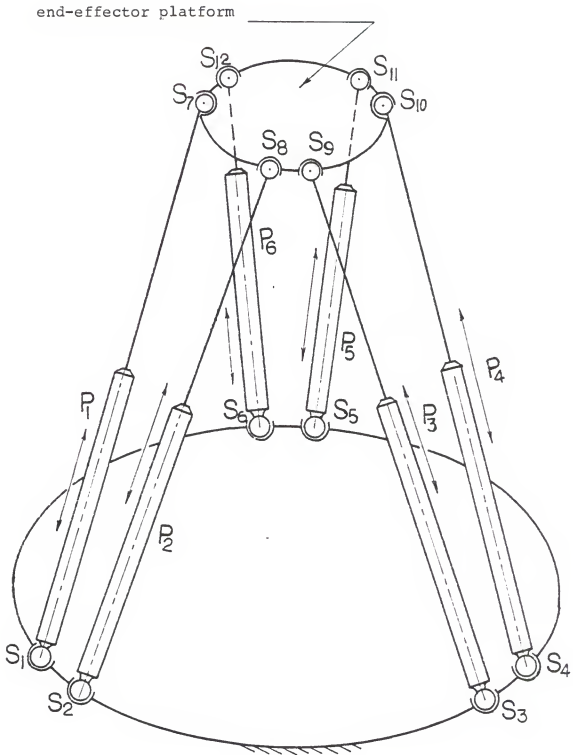


Figure 3.29. Stewart Platform

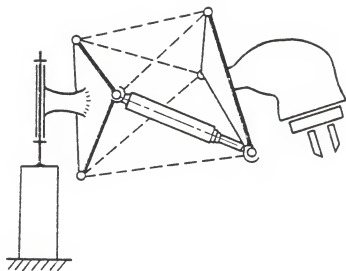


Figure 3.30. Six-Degree of Freedom Robot Arm

simulator, transfer machine, etc. However, recently it has been adapted as a mechanism for robotic uses [2,3,33]. Another application of the concept of Fig.3.22 is the so-called "Pedipulators" or "Walking Machines" [34]. These devices usually form a six-degree of freedom spatial device with six-connecting subchains as they achieve locomotion. As the pedipulator walks the serial open-loop kinematic subchains form closed subchains with the earth (see Fig. 3.31). Some other applications are discussed in [4,6,35-37].

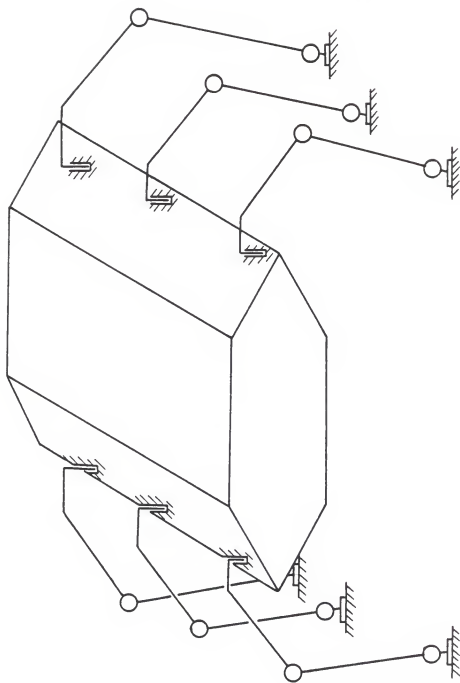


Figure 3.31. Kinematic Representation of Walking Machine



## CHAPTER 4 INSTANTANEOUS KINEMATICS OF FULLY-PARALLEL DEVICES

### 4.1 Introduction

The instantaneous kinematics of serial kinematic chains which model the vast majority of existing industrial robots has been studied widely using a variety of techniques.

The instantaneous kinematics of such serial devices has been described elegantly using the theory of screws. However, because of the complexity of the geometry of parallel devices relative to the geometry of serial devices, the analysis of parallel devices has received relatively little or no attention. This chapter together with the subsequent chapter is devoted to establishing analytical procedures for investigating the instantaneous kinematics of fully-parallel devices using the theory of screws.

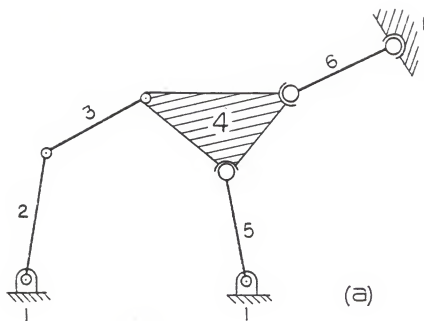
It was concluded in the previous chapter that there is no conceivable practical advantage in using a "mixed-d" device. Therefore, the instantaneous kinematics of only parallel planar devices ( $M=3$ ) and parallel spatial devices ( $M=6$ ) is studied here. It was also concluded in Chapter 3 that parallel devices with practical promise are either fully-, or partially-parallel. Further, fully-parallel devices can be classified according to the distribution of

both actuated and non-actuated joints into "Symmetrical" and satisfy the following conditions:

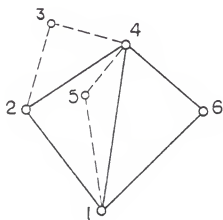
- (i) There is the same number of joints in each subchain.
- (ii) There is the same number of actuated joints in each subchain.
- (iii) The location of the actuators in each subchain is the same.

When at least one of the criteria (i)-(iii) is not satisfied the device will be called "Asymmetrical."

The study of the instantaneous kinematics of kinematic chains was pioneered by Waldron [20] (see also Chapter 2) when he introduced the series and parallel laws of instantaneous kinematics. However, Davies and Primrose [21], and later Baker [37] pointed out that the series and parallel laws were insufficient for determining the relative freedom between any two bodies divided by cross-jointing. Figure 4.1 illustrates an example in which bodies 2 and 6 are divided by cross-jointing. Davies and Primrose [21] and Baker [37] pointed out that the parallel law cannot be applied in this case since there are no coupling graphs (see Fig. 4.1(b)) that have only vertices 2 and 6 in common. It is important to recognize that the graph in Fig. 4.1(b) is analogous to the Wheatstone Bridge which is neither a series nor a parallel electrical circuit and this may well have inspired Davies to apply the well-known Kirchoff's Circulation Law to mechanical networks [38].



(a)



(b)

Figure 4.1. Six-Bar Planar Mechanism with Cross-Jointing

Because Davies and Primrose [21] were not concerned with the magnitude of the twists, they specified a screw by its homogeneous coordinates. This enables them to represent the screw by a point in five-dimensional projective space (see Section 2.2.2). Subsequently, they introduced a new theorem which is a generalized version of the Aronhold-Kennedy theorem of three centers.

Baker [37] made use of motor algebra [10,39]. This enabled him to specify all the six-coordinates of a screw and further enabled him to compute the relative magnitude of the twist. He extended the notation of Davies and Primrose. He defined  $\underline{J}_{12}$  to be the Instantaneous Screw Axis (ISA) vector corresponding to the screw system of order one of the joint between bodies 1 and 2, and  $\underline{S}_{12}$  to be the resultant screw motor (twist) which describes the instantaneous motion of body 2 relative to body 1. He also defined  $\underline{J}_{14}$  (see Fig. 4.1) to be the set of screws governed by the direct jointing of bodies 1 and 4. However, he pointed out that this direct jointing may well place a further constraint on the relative freedom between bodies 2 and 6, and because of this three distinct cases may arise:

Case (i): If

$$\underline{J}_{14} \supseteq (\underline{J}_{12} + \underline{J}_{24}) \cap (\underline{J}_{16} + \underline{J}_{64}) \quad (4.1)$$

then the direct jointing imposes no additional constraints. The series and parallel laws may be used to determine the relative freedom between bodies 2 and 6, and

$$S_{26} = (J_{24} + J_{46}) \cap (J_{21} + J_{16}) \quad (4.2)$$

Case (ii) : If

$$J_{14} \cap (J_{12} + J_{24}) \cap (J_{16} + J_{64}) = \underline{0} \quad (4.3)$$

then the three subchains between bodies 1 and 4 result in the prevention of the relative motion between the two bodies. Therefore, only relative motion between bodies 2 and 6 will be due to part-chain mobility alone. The series and parallel laws can be applied, and

$$S_{26} = (J_{24} \cap J_{21}) + (J_{46} \cap J_{16}) \quad (4.4)$$

Case (iii) :

When neither (4.1) nor (4.3) is satisfied then Baker pointed out that the series and parallel laws were insufficient to determine the relative motion of bodies 2 and 6 but only infer upper and lower bounds for  $S_{26}$ . Subsequently, he introduced an algebraic procedure which is equivalent to the theorem introduced by Davies and Primrose [21]. However, this procedure is complicated. Firstly, he computed  $S_{26}$  using

$$S_{26} = (J_{24} \cap J_{21}) + (J_{46} \cap J_{16}) + S'_{26} \quad (4.5)^*$$

where  $(J_{24} \cap J_{21}) + (J_{46} \cap J_{16})$  is the screw system representing the relative motion of bodies 2 and 6 when bodies 1 and 4

---

\*The author in [37] used the union " $\cup$ " instead of the sum or join "+" in (4.1-4.5) and used " $\phi$ " (empty set) instead of the " $\underline{0}$ " in (4.3) which are not correct. The sum or join of two subspaces is always a subspace but the union is a subspace if and only if one of the subspaces is contained in the other, which is not the case here, in general. The intersection of subspaces is not the empty set but is a subspace which contains at least the zero vector.

are fixed (see case (b) above). Then he defined  $S'_{26}$  to be a restricted\* set of screws which governs the relative motion between bodies 2 and 6 in a way which is compatible with the relative motion between bodies 1 and 4.

In order to determine  $S'_{26}$ , the twist  $S_{14}$  representing the motion of body 4 relative to 1 has to be determined from the following three equations

$$\begin{aligned}\sum_i \omega_{12}^i J_{12}^i + \sum_j \omega_{24}^j J_{24}^j &= S_{14} = \sum_n \Omega_{14}^n \underline{\$}_{14}^n \\ \sum_k \omega_{14}^k J_{14}^k &= S_{14} = \sum_n \Omega_{14}^n \underline{\$}_{14}^n \\ \sum_\ell \omega_{16}^\ell J_{16}^\ell + \sum_m \omega_{64}^m J_{64}^m &= S_{14} = \sum_n \Omega_{14}^n \underline{\$}_{14}^n\end{aligned}\quad (4.6)$$

In (4.6) the superscripts represent in general the order of the screw systems. Using (4.6) the base screw vectors  $\underline{\$}_{14}^1, \dots, \underline{\$}_{14}^n$  can be determined and all the twist magnitudes  $\omega_{12}^i, \omega_{24}^j, \omega_{14}^k, \omega_{16}^\ell$  and  $\omega_{64}^m$  can also be determined in terms of the magnitudes of  $\Omega_{14}^n$ . Once  $\omega_{12}^i, \omega_{24}^j, \dots, \omega_{64}^m$  have been determined then it is possible to determine the base screw vectors  $\underline{\$}_{26}^{'r}$  of  $S'_{26}$  from the following set of equations

$$\begin{aligned}\sum_j \omega_{24}^j J_{24}^j - \sum_m \omega_{64}^m J_{64}^m &= \sum_r \Omega_{26}^{'r} \underline{\$}_{26}^{'r} \\ -\sum_i \omega_{12}^i J_{12}^i + \sum_\ell \omega_{16}^\ell J_{16}^\ell &= \sum_r \Omega_{26}^{'r} \underline{\$}_{26}^{'r}\end{aligned}\quad (4.7)$$

---

\* $S'_{26}$  is not an ordinary screw system because it is spanned by only certain prescribed combinations of individual screws rather than by arbitrary combinations of them.

where the magnitudes of  $\Omega'_{26}$  will be expressible ultimately in terms of the  $\Omega^n_{14}$ .

Summarizing, using Baker's procedure, it is necessary to identify which of the cases (i), (ii), or (iii) a mechanism belongs to.

Recently, Davies [38] avoided this problem by developing a constraint law for a mechanical network which is analogous to Kirchhoff's Circulation Law.

Kirchhoff's voltage law states that

$$[B]\{\underline{v}\} = \underline{0} \quad (4.8)$$

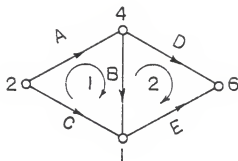
where  $[B]$  is the circuit matrix (see Fig. 4.2) and the voltage  $v_i$  is associated with edge  $i$ . By analogy Davies expressed the constraint law for a kinematic chain in the form

$$B_{v,e} S_{e,6} = O_{v,6} \quad (4.9)$$

where,  $B_{v,e}$  ( $\equiv [B]$ ), is the circuit matrix which has  $v$  rows, (number of independent loops) and  $e$  columns, (number of edges), and  $S_{e,6}$  is a matrix which has  $e$  rows and six columns. Each row is a twist, and the matrix  $S_{e,6}$  can be replaced by the product  $\dot{\psi}_{e,e} \hat{S}_{e,6}$  where  $\dot{\psi}_{e,e}$  is a diagonal matrix containing the  $e$  scalars. Each row of  $\hat{S}_{e,6}$  is a unit screw. The set (4.9) consists of  $6v$  simultaneous linear equations in  $e$  unknowns which can be expressed in the matrix form

$$C_{6v,e} \dot{\psi}_{e,1} = O_{6v,1} \quad (4.10)$$

where  $C_{6v,e}$  is defined as the constraint matrix, and (4.10) is defined as the constraint equation. The constraint



(a)

$$[B] = \begin{matrix} & \begin{matrix} A & B & C & D & E \end{matrix} \\ \begin{bmatrix} 1 & 1 & -1 & 0 & 0 \\ 0 & -1 & 0 & 1 & -1 \end{bmatrix} & \begin{matrix} 1 \\ 2 \end{matrix} \end{matrix}$$

(b)

Figure 4.2. Directed Graph and Its Circuit Matrix



equation (4.10) is transformed into the canonical form

$$\left[ \begin{array}{c|c} \frac{I_{r,r}}{O_{6v-r,r}} & \frac{A_{r,F}}{O_{6v-r,F}} \end{array} \right] \left\{ \begin{array}{c} \dot{\phi}_{r,1} \\ \dot{q}_{F,1} \end{array} \right\} = O_{6v,1} \quad (4.11)$$

The unknowns in the vector  $\dot{\psi}_{e,1}$  in (4.10) are separated in (4.11) into  $r$  secondary (dependent) coordinates  $\dot{\phi}_{r,1}$  that can be expressed in terms of the remaining  $F$  primary (generalized) coordinates  $\dot{q}_{F,1}$ , where  $r$  is the rank of  $C_{6v,e}$ , and  $F$  ( $F=e-r$ ) is the degree of mobility\*. Solving (4.11) in terms of these  $F$  known coordinates gives

$$\dot{\psi}_{e,1} = \left\{ \begin{array}{c} \dot{q}_{F,1} \\ \dot{\phi}_{r,1} \end{array} \right\} = \left[ \begin{array}{c} I_{F,F} \\ -A_{r,F} \end{array} \right] \left\{ \dot{q}_{F,1} \right\} \quad (4.12)$$

Therefore in order to find  $S_{ij}$ , Davies indicated that it is necessary to select any path in the directed graph "G" from  $i$  to  $j$  and sum the screw motors (twists) associated with these joints corresponding to the edge, taking into consideration the orientation of these edges.

In this chapter two novel procedures are presented for determining the instantaneous motion of the end-effector platform of fully-parallel devices. The initial or first procedure was obtained by determining explicit expressions for the unknown scalar multipliers,  $\omega_j^{(i)}$ , of the twists associated with the joints in one of the subchains connecting the end-effector

---

\*Here it is preferable to follow the same notation used in [38]. However, in Chapter 3, the symbol  $M$  rather than  $F$  was used to denote mobility and  $M$  will be used throughout the remainder of this text.

to the base using loop velocity equations. At the outset the objective was to provide an alternative improved procedure to that presented by Davies [38] for analyzing the instantaneous kinematics of platform-type devices. However, further investigation led to yet another procedure for which the instantaneous motion of the end-effector is expressed directly in terms of the known input scalar multipliers (the magnitudes of the twists associated with the input-actuated joints).

Further, both procedures yield a novel and important theorem; "For any parallel device the twist representing the instantaneous motion of the end-effector platform is equal to the sum of its partial twists." A partial twist is defined as the twist representing the instantaneous motion of the end-effector when all but one of the input actuators are locked. The author believes that this result provides, in general, a proper foundation for the investigation of special configurations of fully-parallel devices for which the screw system degenerates and the end-effector loses one or more degrees of freedom (see Chapter 5).

#### 4.2 Instantaneous Kinematics of the End-Effector of Fully-Parallel Symmetrical Devices Using Loop Velocity Equations

##### 4.2.1 Basic Equations

Figure 4.3 illustrates an end-effector platform of a general fully-parallel symmetrical device. The end-effector is connected to the base by  $N$  connecting subchains. Each subchain consists of  $M$  joints, where  $M$  is the mobility of the

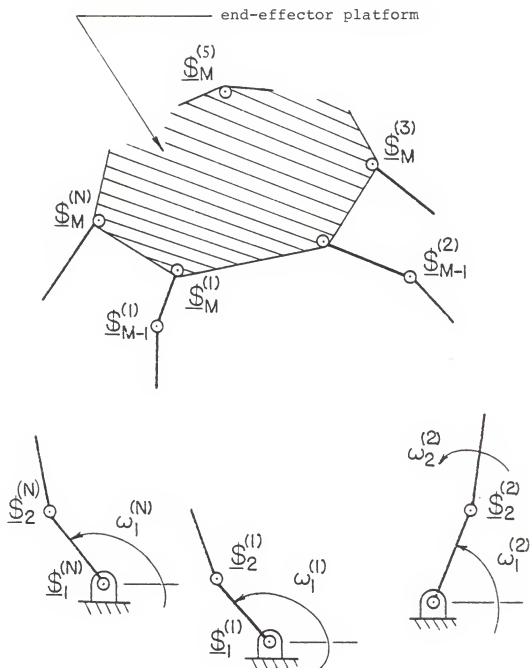


Figure 4.3. General Fully-Parallel Symmetrical Device

end-effector and it is either 3 for planar devices or 6 for spatial devices (see Chapter 3). In order for the end-effector to have mobility  $M$ , the number of input-actuated joints,  $g$ , in each subchain is given by  $g = \frac{M}{N}$ . Therefore, it is obvious that the number of connecting subchains,  $N$ , has to equal 3 for symmetrical planar devices and equal 2, 3, or 6 for symmetrical spatial devices. For example, when  $M = N = 6$  then there is one actuator in each subchain. It has been indicated in the previous chapter that there may be restrictions on which  $M$  joints can be used as actuated joints but for the sake of simplicity and without loss of generality the actuators will be assumed to be located at the base\*.

In what follows it is convenient to choose a single subchain and call it the first subchain. It could, of course, be any subchain in the device. This subchain will be labelled with the superscript (1). The remaining subchains will be labelled with the superscript (i), ( $i=2,3,\dots,N$ ). There are a total of  $(N-1)$  independent closed loops in the device which contain the first subchain, and the set of loop velocity equations for those  $(N-1)$  independent loops can be expressed in the form

$$\begin{aligned}
 & (\omega_1^{(1)} \underline{\dot{x}}_1^{(1)} + \omega_2^{(1)} \underline{\dot{x}}_2^{(1)} + \dots + \omega_M^{(1)} \underline{\dot{x}}_M^{(1)}) \\
 & - (\omega_1^{(i)} \underline{\dot{x}}_1^{(i)} + \omega_2^{(i)} \underline{\dot{x}}_2^{(i)} + \dots + \omega_M^{(i)} \underline{\dot{x}}_M^{(i)}) = 0 \quad (4.13)
 \end{aligned}$$

---

\*Also for practical reasons it is preferable to locate the actuators at the base joints.

The set (4.13) can be expressed in the abbreviated form

$$\sum_{j=1}^M (\omega_j^{(1)} \underline{\dot{x}}_j^{(1)}) - \sum_{j=1}^M \omega_j^{(i)} \underline{\dot{x}}_j^{(i)} = 0 \quad (4.14)$$

where  $i = 2, 3, \dots, N$ . Further, the twist  $\hat{\underline{\dot{x}}}$ , ( $= \omega \underline{\dot{x}}$ ), representing the instantaneous motion of the end-effector can be expressed as a linear combination of the joint velocities in the first subchain.

$$\hat{\underline{\dot{x}}} = \omega \underline{\dot{x}} = \omega_1^{(1)} \underline{\dot{x}}_1^{(1)} + \omega_2^{(1)} \underline{\dot{x}}_2^{(1)} + \dots + \omega_M^{(1)} \underline{\dot{x}}_M^{(1)} \quad (4.15)$$

Two solutions of the loop velocity equations (4.14) and the twist equation (4.15) will be presented. Firstly, it will be assumed that scalar multipliers of the twists of the input joints are known and that it is required to determine the twist  $\hat{\underline{\dot{x}}}$  of the end-effector. This will be called the forward solution. Secondly, it will be assumed that the twist  $\hat{\underline{\dot{x}}}$  of the end-effector is specified and that it is required to compute the scalar multipliers. This will be called the reverse solution.

#### 4.2.2 Forward Solution

For the forward solution let  $\omega_m^{(1)}$  and  $\omega_m^{(i)}$ , where  $m = 1, 2, \dots, g$  and  $i = 2, 3, \dots, N$ , denote the  $M$  known scalar multipliers. For example, when  $M = N = 6$  then  $g = 1$  and the known scalar multipliers will be  $\omega_1^{(1)}$  and  $\omega_1^{(i)}$ , where  $i = 2, 3, \dots, 6$ . When  $M = 6$ ,  $N = 3$  then  $g = 2$  and the known scalar multipliers will be  $\omega_1^{(1)}$ ,  $\omega_2^{(1)}$  and  $\omega_1^{(i)}$ ,  $\omega_2^{(i)}$  where  $i = 2, 3$ . Further, there are  $(M-g)$  unknown

scalar multipliers,  $\omega_j^{(1)}$  where  $j = (g+1), (g+2), \dots, M$  which are common to all the  $(N-1)$  equations in the set (4.14). Also there are  $(M-g)$  unknown scalar multipliers  $\omega_j^{(i)}$ ,  $(i=2, 3, \dots, N)$ , in each equation which are not contained in the remaining equations. It is necessary to eliminate these  $(M-g)$  unknown scalar multipliers  $\omega_j^{(i)}$ . This is accomplished by determining  $g$  screws which are orthogonal (or reciprocal)\* to the  $(M-g)$  screws,  $\$_{\underline{j}}^{(i)}$ , in each one of the independent loops. These  $g$  screws will be denoted by  $\$_{\underline{oL}}^{(i)}$  where  $L = 1, 2, \dots, g$  and  $i = 2, 3, \dots, N$ . Taking the inner product of each orthogonal screw  $\$_{\underline{oL}}^{(i)}$  with the corresponding equation in the set (4.14) gives  $(M-g)$ ,  $(= g(N-1))$ , equations which are linear in the  $(M-g)$  unknown scalar multipliers  $\omega_j^{(1)}$  where  $j = (g+1), (g+2), \dots, M$ . This set of equations can be arranged in the form

$$\begin{aligned} & [\omega_{g+1}^{(1)} (\$_{g+1}^{(1)} * \$_{\underline{oL}}^{(i)}) + \dots + \omega_M^{(1)} (\$_M^{(1)} * \$_{\underline{oL}}^{(i)})] = \\ & - [\omega_1^{(1)} (\$_1^{(1)} * \$_{\underline{oL}}^{(i)}) + \dots + \omega_g^{(1)} (\$_g^{(1)} * \$_{\underline{oL}}^{(i)})] \\ & + [\omega_1^{(i)} (\$_1^{(i)} * \$_{\underline{oL}}^{(i)}) + \dots + \omega_g^{(i)} (\$_g^{(i)} * \$_{\underline{oL}}^{(i)})] \end{aligned} \quad (4.16)$$

where  $i = 2, 3, \dots, N$ , and  $L = 1, 2, \dots, g$ . The set (4.14) can be expressed in the abbreviated form

---

\*As discussed in Chapter 2, there is a one-to-one correspondence between orthogonal and reciprocal screws (see equations (2.41 and 2.42)). Therefore, throughout this chapter along with the subsequent chapter the words orthogonal and reciprocal can simply be interchanged and, of course, with modifying phrases to make the statements sensible.

$$\begin{aligned}
& \sum_{j=g+1}^M \omega_j^{(1)} (\underline{\$}_j^{(1)} * \underline{\$}_{OL}^{(1)}) \\
&= \sum_{m=1}^g [-\omega_m^{(1)} (\underline{\$}_m^{(1)} * \underline{\$}_{OL}^{(1)}) + \omega_m^{(i)} (\underline{\$}_m^{(i)} * \underline{\$}_{OL}^{(i)})] \quad (4.17)
\end{aligned}$$

The left side of (4.17) contains the unknown scalar multipliers  $\omega_j^{(1)}$  where  $j = (g+1), (g+2), \dots, M$  and the right side contains the known scalar multipliers  $\omega_m^{(1)}$  and  $\omega_m^{(i)}$ ,  $m = 1, 2, \dots, g$ . The set (4.17) can be written in the matrix form

$$[A]\{\omega^{(1)}\} = [B]\{\omega^{(i)}\} \quad (4.18)$$

where  $[A]$  is a square  $[(M-g) \times (M-g)]$  matrix which is a function of the inner products (i.e., it is a function only of the configuration of the device),

$$[A] = \begin{bmatrix} \phi_{g+1}^{(1)} * \phi_{o1}^{(2)} & \phi_{g+2}^{(1)} * \phi_{o1}^{(2)} & \dots & \phi_M^{(1)} * \phi_{o1}^{(2)} \\ \phi_{g+1}^{(1)} * \phi_{o2}^{(2)} & \phi_{g+2}^{(1)} * \phi_{o2}^{(2)} & \dots & \phi_M^{(1)} * \phi_{o2}^{(2)} \\ \vdots & \vdots & & \vdots \\ \phi_{g+1}^{(1)} * \phi_{og}^{(2)} & \phi_{g+2}^{(1)} * \phi_{og}^{(2)} & \dots & \phi_M^{(1)} * \phi_{og}^{(2)} \\ \phi_{g+1}^{(1)} * \phi_{o1}^{(3)} & \dots & \dots & \phi_M^{(1)} * \phi_{o1}^{(3)} \\ \vdots & & & \vdots \\ \phi_{g+1}^{(1)} * \phi_{og}^{(3)} & \dots & \dots & \phi_M^{(1)} * \phi_{og}^{(3)} \\ \vdots & & & \vdots \\ \phi_{g+1}^{(1)} * \phi_{o1}^{(N)} & \phi_{g+2}^{(1)} * \phi_{o1}^{(N)} & \dots & \phi_M^{(1)} * \phi_{o1}^{(N)} \\ \vdots & \vdots & & \vdots \\ \phi_{g+1}^{(1)} * \phi_{og}^{(N)} & \phi_{g+2}^{(1)} * \phi_{og}^{(N)} & \dots & \phi_M^{(1)} * \phi_{og}^{(N)} \end{bmatrix} \quad (4.19)$$

$[B]$  is a  $[(M-g) \times (M)]$  matrix which is also a function of position,

$$[B] = \begin{bmatrix} -B_{12} & B_{22} & 0 & 0 & \dots & 0 \\ -B_{13} & 0 & B_{33} & 0 & \dots & 0 \\ -B_{14} & 0 & 0 & B_{44} & & \vdots \\ \vdots & \vdots & & & & \vdots \\ \vdots & \vdots & & & & \vdots \\ \vdots & \vdots & & & & \vdots \\ \vdots & \vdots & & & B_{(N-1)(N-1)} & 0 \\ -B_{1N} & 0 & 0 & \dots & 0 & B_{NN} \end{bmatrix} \quad (4.20)$$



where  $B_{ij}$  is a  $[g \times g]$  matrix such that

$$B_{ij} = \begin{bmatrix} \phi_1^{(i)} * \phi_{o1}^{(j)} & \phi_2^{(i)} * \phi_{o1}^{(j)} & \dots & \phi_g^{(i)} * \phi_{o1}^{(j)} \\ \phi_1^{(i)} * \phi_{o2}^{(j)} & \phi_2^{(i)} * \phi_{o2}^{(j)} & \dots & \phi_g^{(i)} * \phi_{o2}^{(j)} \\ \vdots & \vdots & \ddots & \vdots \\ \phi_1^{(i)} * \phi_{og}^{(j)} & \phi_2^{(i)} * \phi_{og}^{(j)} & \dots & \phi_g^{(i)} * \phi_{og}^{(j)} \end{bmatrix} \quad (4.21)$$

for  $i = 1, 2, \dots, N$  and  $j = 2, 3, \dots, N$ .

$\{\omega^{(1)}\}$  is a  $[(M-g) \times 1]$  column vector representing the unknown scalar multipliers in the first subchain,

$$\{\omega^{(1)}\} = [\omega_{g+1}^{(1)} \quad \omega_{g+2}^{(1)} \quad \dots \quad \omega_M^{(1)}]^T \quad (4.22)$$

and  $\{\omega^{(i)}\}$  is a  $[M \times 1]$  column vector representing the known scalar multipliers,

$$\{\omega^{(i)}\} = [\omega_1^{(1)} \quad \omega_2^{(1)} \dots \omega_g^{(1)} \quad \omega_1^{(2)} \quad \omega_2^{(2)} \dots \omega_g^{(N)}]^T \quad (4.23)$$

Further, since matrix  $[A]$  is nonsingular in general, when the device is not in special configuration (see chapter 5), (4.18) can be expressed in the form

$$\{\omega^{(1)}\} = [K_{j\ell}] \{\omega^{(i)}\} \quad (4.24)$$

where  $\ell = 1, 2, \dots, M$ ,  $j = (g+1), (g+2), \dots, M$ , and  $[K_{j\ell}]$  is a  $[(M-g) \times M]$  matrix which is also a function of position,

$$[K_{j\ell}] = \begin{bmatrix} K_{(g+1)1} & K_{(g+1)2} & \dots & K_{(g+1)M} \\ K_{(g+2)1} & K_{(g+2)2} & \dots & K_{(g+2)M} \\ \vdots & \vdots & & \vdots \\ \vdots & \vdots & & \vdots \\ \vdots & \vdots & & \vdots \\ \vdots & \vdots & & \vdots \\ K_{M1} & K_{M2} & \dots & K_{MM} \end{bmatrix} \quad (4.25)$$

Expanding (4.24), explicit expressions for the unknown scalar multipliers  $\omega_j^{(1)}$  can be expressed in the form

$$\begin{aligned} \omega_j^{(1)} &= [K_{j1}\omega_1^{(1)} + K_{j2}\omega_2^{(1)} + \dots + K_{jg}\omega_g^{(1)}] \\ &\quad + [K_{j(g+1)}\omega_1^{(2)} + K_{j(g+2)}\omega_2^{(2)} + \dots + K_{j(2g)}\omega_g^{(2)}] \\ &\quad + \dots + [K_{j[1+g(N-1)]}\omega_1^{(N)} + \dots + K_{jM}\omega_g^{(N)}] \end{aligned} \quad (4.26)$$

The twist  $\hat{\underline{\$}}$  representing the end-effector can be determined by substituting (4.26) in (4.15) and hence

$$\begin{aligned} \hat{\underline{\$}} = \omega \underline{\$} &= \sum_{m=1}^g \omega_m^{(1)} [\underline{\$}_m^{(1)} + \sum_{j=g+1}^M K_{jm} \underline{\$}_j^{(1)}] \\ &\quad + \sum_{i=2}^N \sum_{m=1}^g \omega_m^{(i)} \sum_{j=g+1}^M K_{j[m+g(i-1)]} \underline{\$}_j^{(1)} \end{aligned} \quad (4.27)$$

Further examination of (4.27) provides an alternative form and an important result is deduced which will now be discussed in detail.

#### 4.2.3 The Concept of Partial Screws

Equation (4.27) can be written in the following form

$$\begin{aligned}
 \hat{\underline{\$}} = \omega \underline{\$} = & \omega_1^{(1)} [\underline{\$}_1^{(1)} + \sum_{j=g+1}^M K_{j1} \underline{\$}_j^{(1)}] \\
 & + \omega_2^{(1)} [\underline{\$}_2^{(1)} + \sum_{j=g+1}^M K_{j2} \underline{\$}_j^{(1)}] \\
 & \dots + \omega_g^{(1)} [\underline{\$}_g^{(1)} + \sum_{j=g+1}^M K_{jg} \underline{\$}_j^{(1)}] \\
 & + \sum_{i=2}^N \{ [\omega_1^{(i)} \sum_{j=g+1}^M K_{j[1+g(i-1)]} \underline{\$}_j^{(1)}] \\
 & \quad + [\omega_2^{(i)} \sum_{j=g+1}^M K_{j[2+g(i-1)]} \underline{\$}_j^{(1)}] \\
 & \quad \dots + [\omega_g^{(i)} \sum_{j=g+1}^M K_{j[ig]} \underline{\$}_j^{(1)}] \} \quad (4.28)
 \end{aligned}$$

Consider now that all the input actuators are locked except the actuator at the first base joint in the first subchain, i.e.,  $\omega_2^{(1)} = \omega_3^{(1)} \dots = \omega_g^{(1)} = 0$ , and  $\omega_1^{(i)} = \omega_2^{(i)} \dots = \omega_g^{(i)} = 0$ . The instantaneous motion of the end-effector is due solely to the twist  $\hat{\underline{\$}}_1^{(1)} = \omega_1^{(1)} \underline{\$}_1^{(1)}$ . The twist representing this instantaneous motion will be labelled  $\hat{\underline{\$}}_{p1}^{(1)}$ , ( $= \omega_{p1}^{(1)} \underline{\$}_{p1}^{(1)}$ ), and will be defined as the partial twist due to the input twist  $\omega_1^{(1)} \underline{\$}_1^{(1)}$ . Equation (4.28) reduces to

$$\hat{\underline{\$}}_{p1}^{(1)} = \omega_{p1}^{(1)} \underline{\$}_{p1}^{(1)} = \omega_1^{(1)} [\underline{\$}_1^{(1)} + \sum_{j=g+1}^M K_{j1} \underline{\$}_j^{(1)}] \quad (4.29)$$

Similarly the partial twist  $\hat{\underline{\$}}_{p2}^{(1)}$ , ( $= \omega_{p2}^{(1)} \underline{\$}_{p2}^{(1)}$ ), representing the instantaneous motion of the end-effector due to the input twist  $\omega_2^{(1)} \underline{\$}_2^{(1)}$  is given by

$$\hat{\$}_{p2}^{(1)} = \omega_{p2}^{(1)} \$_{p2}^{(1)} = \omega_2^{(1)} [\$_2^{(1)} + \sum_{j=g+1}^M K_{j2} \$_j^{(1)}] \quad (4.30)$$

Also, the partial twist  $\hat{\$}_{p1}^{(2)}$  representing the end-effector instantaneous motion due to the input twist  $\omega_1^{(2)} \$_1^{(2)}$  is given by

$$\hat{\$}_{p1}^{(2)} = \omega_{p1}^{(2)} \$_{p1}^{(2)} = \omega_1^{(2)} \sum_{j=g+1}^M K_{j[g+1]} \$_j^{(1)} \quad (4.31)$$

Generally, the partial twist representing the instantaneous motion of the end-effector due to the input twist  $\omega_m^{(1)} \$_m^{(1)}$  can be expressed in the form

$$\hat{\$}_{pm}^{(1)} = \omega_{pm}^{(1)} \$_{pm}^{(1)} = \omega_m^{(1)} [\$_m^{(1)} + \sum_{j=g+1}^M K_{jm} \$_j^{(1)}] \quad (4.32)$$

and the partial twist representing the instantaneous motion of the end-effector due to the input twist  $\omega_m^{(i)} \$_m^{(i)}$ , for  $i = 2, 3, \dots, N$ , can be expressed in the form

$$\hat{\$}_{pm}^{(i)} = \omega_{pm}^{(i)} \$_{pm}^{(i)} = \omega_m^{(i)} \sum_{j=g+1}^M K_{j[m+g(i-1)]} \$_j^{(1)} \quad (4.33)$$

Introducing this notation, equation (4.28) can be expressed in the form

$$\begin{aligned} \hat{\$} = & \omega_{p1}^{(1)} \$_{p1}^{(1)} + \omega_{p2}^{(1)} \$_{p2}^{(1)} + \dots + \omega_{pg}^{(1)} \$_{pg}^{(1)} + \\ & + \omega_{p1}^{(2)} \$_{p1}^{(2)} + \omega_{p2}^{(2)} \$_{p2}^{(2)} + \dots + \omega_{pg}^{(2)} \$_{pg}^{(2)} + \\ & + \dots + \omega_{p1}^{(N)} \$_{p1}^{(N)} + \omega_{p2}^{(N)} \$_{p2}^{(N)} + \dots + \omega_{pg}^{(N)} \$_{pg}^{(N)} \end{aligned} \quad (4.34)$$

Finally, equation (4.34) can be expressed in the abbreviated form

$$\hat{\$} = \omega \$ = \sum_{i=1}^N \sum_{m=1}^g \hat{\$}_{pm}^{(i)} \quad (4.35)$$

The twist representing the instantaneous motion of the end-effector is therefore the sum of all partial twists. A partial twist is defined as the twist representing the instantaneous motion of the end-effector due solely to a single input actuator.

For a six-degree of freedom spatial device ( $d=6$ ), the right side of (4.35) will contain six partial screws. When the right side of (4.35) contains less than six independent partial screws, then the end-effector will belong to a five-system or less. Therefore it appears that equations (4.18) and (4.35) will provide the geometrical conditioning and a proper base for investigating special configurations of fully-parallel devices.

#### 4.2.4 Reverse Solution

The twist representing the instantaneous motion of the end-effector which is now specified was expressed as a linear combination of the joint twists in the first subchain (see (4.15)). Clearly the twist can be expressed as a linear combination of the joint twists in any subchain and thus

$$\hat{\$} = \omega \$ = \omega_1^{(i)} \$_1^{(i)} + \omega_2^{(i)} \$_2^{(i)} + \dots + \omega_M^{(i)} \$_M^{(i)} \quad (4.36)$$

where  $i = 1, 2, \dots, n, \dots$  or  $N$ .

It is required to compute the  $g$  scalar multipliers of the twists of the  $g$  input actuated joints in each subchain. This is accomplished by forming in turn  $g$  screws each of

which is orthogonal to all screws in the subchain except one of the input screws in the subchain. Consider for example that  $g = 2$  in the  $n$ th subchain where  $\underline{\$}_1^{(n)}$  and  $\underline{\$}_2^{(n)}$  are the two input screws. It is possible to determine two screws  $\underline{\$}_{o1}^{(n)}$  and  $\underline{\$}_{o2}^{(n)}$  which are orthogonal to the screws  $\{\underline{\$}_2^{(n)}, \underline{\$}_3^{(n)}, \dots, \underline{\$}_M^{(n)}\}$  and  $\{\underline{\$}_1^{(n)}, \underline{\$}_3^{(n)}, \dots, \underline{\$}_M^{(n)}\}$  respectively. Taking the orthogonal product of the left and right side of (4.36) for  $i = n$  with  $\underline{\$}_{o1}^{(n)}$  and  $\underline{\$}_{o2}^{(n)}$ , and solving for  $\omega_1^{(n)}$  and  $\omega_2^{(n)}$  gives

$$\omega_1^{(n)} = \frac{\hat{\underline{\$}}_{o1}^{(n)} * \underline{\$}_{o1}^{(n)}}{\underline{\$}_1^{(n)} * \underline{\$}_{o1}^{(n)}} \quad (4.37)$$

and

$$\omega_2^{(n)} = \frac{\hat{\underline{\$}}_{o2}^{(n)} * \underline{\$}_{o2}^{(n)}}{\underline{\$}_2^{(n)} * \underline{\$}_{o2}^{(n)}} \quad (4.38)$$

Generally, any unknown scalar multiplier  $\omega_m^{(i)}$  can be computed using the expression

$$\omega_m^{(i)} = \frac{\hat{\underline{\$}}_{om}^{(i)} * \underline{\$}_{om}^{(i)}}{\underline{\$}_m^{(i)} * \underline{\$}_{om}^{(i)}} \quad (4.39)$$

where  $i = 1, 2, \dots, N$ ,  $m = 1, 2, \dots, g$ , and  $\underline{\$}_{om}^{(i)}$  is a screw which is orthogonal to all screws in the  $i$ th subchain except  $\underline{\$}_m^{(i)}$ .

#### 4.2.5 Instantaneous Kinematics of the End-Effector of a Six-Degree of Freedom Fully-Parallel Symmetrical Device with Three Connecting Subchains to Platform

The instantaneous kinematics of the end-effector of a six-dof fully-parallel symmetrical device with three connecting subchains to the platform ( $N=3$  and  $M=6$ ) is now investigated in detail using the loop velocity equations method described in the previous sections. The instantaneous kinematics of the end-effector of six-dof fully-parallel symmetrical devices with six, three, and two connecting subchains are investigated in sections 4.3.5.1 - 4.3.5.3 using the shorter direct method of analysis together with an investigation of the instantaneous kinematics of a fully-parallel planar device which is given in section 4.3.6.

In order for the end-effector in Fig. 4.4 to have mobility  $M = 6$ , there are two input actuators, ( $g = \frac{M}{N} = 2$ ), in each subchain which is assumed to be located at the first two joints from the base of each subchain, i.e.,  $\omega_1^{(1)}$ ,  $\omega_2^{(1)}$ ,  $\omega_1^{(2)}$ ,  $\omega_2^{(2)}$ ,  $\omega_1^{(3)}$ , and  $\omega_2^{(3)}$  are the six known scalar multipliers. There are two independent loops which contain the first subchain. The set of two loop velocity equations for these two independent loops can be expressed in the form

$$\begin{aligned} \sum_{j=1}^6 \omega_j^{(1)} \underline{\$}_j^{(1)} - \sum_{j=1}^6 \omega_j^{(2)} \underline{\$}_j^{(2)} &= 0 \\ \sum_{j=1}^6 \omega_j^{(1)} \underline{\$}_j^{(1)} - \sum_{j=1}^6 \omega_j^{(3)} \underline{\$}_j^{(3)} &= 0 \end{aligned} \quad (4.40)$$

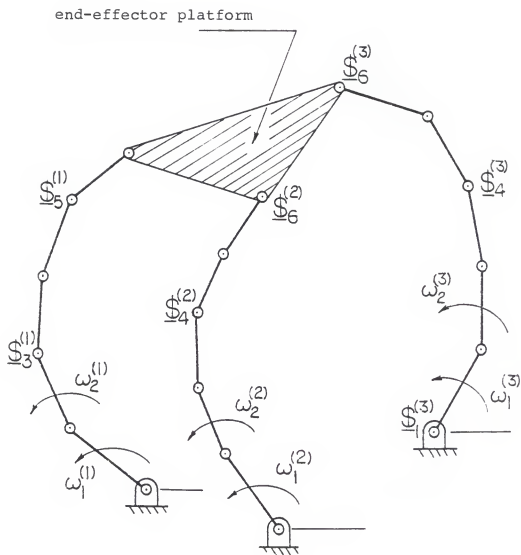


Figure 4.4. Six-Degree of Freedom Fully-Parallel Symmetrical Device with Three Connecting Subchains to Platform



For the forward solution, the six input scalar multipliers are specified. There are four ( $M-g = 6-2 = 4$ ) unknown scalar multipliers  $\omega_3^{(1)}$ ,  $\omega_4^{(1)}$ ,  $\omega_5^{(1)}$ , and  $\omega_6^{(1)}$  which are common to the two equations in (4.40). Also there are four unknown scalar multipliers in each equation which are not contained in the other; i.e.,  $\omega_3^{(3)}$ ,  $\omega_4^{(3)}$ ,  $\omega_5^{(3)}$ , and  $\omega_6^{(3)}$  are contained in the second equation but not contained in the first equation of (4.40). In order to eliminate those four unknowns in each equation, it is necessary to determine screws  $\$_{o1}^{(2)}$  and  $\$_{o2}^{(2)}$  orthogonal to the set  $\{\$_3^{(2)}, \$_4^{(2)}, \$_5^{(2)}, \$_6^{(2)}\}$  and to determine screws  $\$_{o1}^{(3)}$  and  $\$_{o2}^{(3)}$  orthogonal to the set  $\{\$_3^{(3)}, \$_4^{(3)}, \$_5^{(3)}, \$_6^{(3)}\}$ . Taking the orthogonal product of  $\$_{o1}^{(2)}$  and then of  $\$_{o2}^{(2)}$  with the first equation of (4.40), the orthogonal product of  $\$_{o1}^{(3)}$  and then of  $\$_{o2}^{(3)}$  with the second equation, gives four equations which are linear in the four unknowns  $\omega_3^{(1)}$ ,  $\omega_4^{(1)}$ ,  $\omega_5^{(1)}$ , and  $\omega_6^{(1)}$ . This set of four linear equations can be written in the following matrix form:

$$\begin{bmatrix} \underline{\$}_3^{(1)} * \underline{\$}_{o1}^{(2)} & \underline{\$}_4^{(1)} * \underline{\$}_{o1}^{(2)} & \underline{\$}_5^{(1)} * \underline{\$}_{o1}^{(2)} & \underline{\$}_6^{(1)} * \underline{\$}_{o1}^{(2)} \\ \underline{\$}_3^{(1)} * \underline{\$}_{o2}^{(2)} & \underline{\$}_4^{(1)} * \underline{\$}_{o2}^{(2)} & \underline{\$}_5^{(1)} * \underline{\$}_{o2}^{(2)} & \underline{\$}_6^{(1)} * \underline{\$}_{o2}^{(2)} \\ \underline{\$}_3^{(1)} * \underline{\$}_{o1}^{(3)} & \underline{\$}_4^{(1)} * \underline{\$}_{o1}^{(3)} & \underline{\$}_5^{(1)} * \underline{\$}_{o1}^{(3)} & \underline{\$}_6^{(1)} * \underline{\$}_{o1}^{(3)} \\ \underline{\$}_3^{(1)} * \underline{\$}_{o2}^{(3)} & \underline{\$}_4^{(1)} * \underline{\$}_{o2}^{(3)} & \underline{\$}_5^{(1)} * \underline{\$}_{o2}^{(3)} & \underline{\$}_6^{(1)} * \underline{\$}_{o2}^{(3)} \end{bmatrix} \quad \left\{ \begin{matrix} \omega_3^{(1)} \\ \omega_4^{(1)} \\ \omega_5^{(1)} \\ \omega_6^{(1)} \end{matrix} \right\}$$

$$= \begin{bmatrix} -(\underline{\$}_1^{(1)} * \underline{\$}_{o1}^{(2)}) - (\underline{\$}_2^{(1)} * \underline{\$}_{o1}^{(2)}) & \underline{\$}_1^{(2)} * \underline{\$}_{o1}^{(2)} & \underline{\$}_2^{(2)} * \underline{\$}_{o1}^{(2)} & 0 & 0 \\ -(\underline{\$}_1^{(1)} * \underline{\$}_{o2}^{(2)}) - (\underline{\$}_2^{(1)} * \underline{\$}_{o2}^{(2)}) & \underline{\$}_1^{(2)} * \underline{\$}_{o2}^{(2)} & \underline{\$}_2^{(2)} * \underline{\$}_{o2}^{(2)} & 0 & 0 \\ -(\underline{\$}_1^{(1)} * \underline{\$}_{o1}^{(3)}) - (\underline{\$}_2^{(1)} * \underline{\$}_{o1}^{(3)}) & 0 & 0 & \underline{\$}_1^{(3)} * \underline{\$}_{o1}^{(3)} & \underline{\$}_2^{(3)} * \underline{\$}_{o1}^{(3)} \\ -(\underline{\$}_1^{(1)} * \underline{\$}_{o2}^{(3)}) - (\underline{\$}_2^{(1)} * \underline{\$}_{o2}^{(3)}) & 0 & 0 & \underline{\$}_1^{(3)} * \underline{\$}_{o2}^{(3)} & \underline{\$}_2^{(3)} * \underline{\$}_{o2}^{(3)} \end{bmatrix} \quad \left\{ \begin{matrix} \omega_1^{(1)} \\ \omega_2^{(1)} \\ \omega_1^{(2)} \\ \omega_2^{(2)} \\ \omega_1^{(3)} \\ \omega_2^{(3)} \end{matrix} \right\}$$

(4.41)

Further, since the square matrix on the left side of (4.41) is non-singular, in general, then (4.24) reduces to

$$\begin{Bmatrix} \omega_3^{(1)} \\ \omega_4^{(1)} \\ \omega_5^{(1)} \\ \omega_6^{(1)} \end{Bmatrix} = \begin{bmatrix} K_{31} & K_{32} & K_{33} & K_{34} & K_{35} & K_{36} \\ K_{41} & K_{42} & K_{43} & K_{44} & K_{45} & K_{46} \\ K_{51} & K_{52} & K_{53} & K_{54} & K_{55} & K_{56} \\ K_{61} & K_{62} & K_{63} & K_{64} & K_{65} & K_{66} \end{bmatrix} \begin{Bmatrix} \omega_1^{(1)} \\ \omega_2^{(1)} \\ \omega_1^{(2)} \\ \omega_2^{(2)} \\ \omega_1^{(3)} \\ \omega_2^{(3)} \end{Bmatrix} \quad (4.42)$$

Expanding (4.42), explicit expressions for the unknown scalar multipliers  $\omega_j^{(1)}$ , where  $j = 3, 4, 5, 6$ , can be determined.

Equation (4.26) reduces to

$$\begin{aligned} \omega_j^{(1)} = & (K_{j1}\omega_1^{(1)} + K_{j2}\omega_2^{(1)}) + (K_{j3}\omega_1^{(2)} + K_{j4}\omega_2^{(2)}) \\ & + (K_{j5}\omega_1^{(3)} + K_{j6}\omega_2^{(3)}) \end{aligned} \quad (4.43)$$

The twist  $\hat{\underline{\$}}$  representing the instantaneous motion of the end-effector can be expressed in the form

$$\hat{\underline{\$}} = \omega \underline{\$} = \omega_1^{(1)} \underline{\$}_1^{(1)} + \omega_2^{(1)} \underline{\$}_2^{(1)} + \dots + \omega_6^{(1)} \underline{\$}_6^{(1)} \quad (4.44)$$

Finally substituting (4.43) in (4.44),  $\hat{\underline{\$}}$  can be expressed in the form

$$\begin{aligned}\hat{\underline{\$}} = \omega \underline{\$} = & \omega_1^{(1)} [\underline{\$}_1^{(1)} + \sum_{j=3}^6 K_{j1} \underline{\$}_j^{(1)}] + \omega_2^{(1)} [\underline{\$}_2^{(1)} + \sum_{j=3}^6 K_{j2} \underline{\$}_j^{(1)}] \\ & + \sum_{i=2}^3 \{ \omega_1^{(i)} \sum_{j=3}^6 (K_{j(2i-1)} \underline{\$}_j^{(1)}) + \omega_2^{(i)} \sum_{j=3}^6 (K_{j(2i)} \underline{\$}_j^{(1)}) \} \end{aligned} \quad (4.45)$$

Now consider that all actuators are locked except the actuator at the first base joint in the first subchain,  $\omega_2^{(2)} = \omega_2^{(1)} = \omega_1^{(2)} = \omega_1^{(3)} = \omega_2^{(3)} = 0$  and  $\omega_1^{(1)} \neq 0$ . The instantaneous motion of the end-effector is due solely to the input twist  $\omega_1^{(1)} \underline{\$}_1^{(1)}$ . The partial twist  $\hat{\underline{\$}}_{p1}^{(1)}$  representing this instantaneous motion will be expressed as follows:

$$\hat{\underline{\$}}_{p1}^{(1)} = \omega_{p1}^{(1)} \underline{\$}_{p1}^{(1)} = \omega_1^{(1)} [\underline{\$}_1^{(1)} + \sum_{j=3}^6 K_{j1} \underline{\$}_j^{(1)}] \quad (4.46)$$

If all actuators are locked except the actuator at the second joint in the first subchain, i.e., only  $\omega_2^{(1)} \neq 0$ , then the partial twist  $\hat{\underline{\$}}_2^{(1)}$  representing the instantaneous motion of the end-effector can be expressed as follows:

$$\hat{\underline{\$}}_{p2}^{(1)} = \omega_{p2}^{(1)} \underline{\$}_{p2}^{(1)} = \omega_2^{(1)} [\underline{\$}_2^{(1)} + \sum_{j=3}^6 K_{j2} \underline{\$}_j^{(1)}] \quad (4.47)$$

Also the partial twists representing the instantaneous motion of the end-effector due solely to the input twists  $\omega_1^{(2)} \underline{\$}_1^{(2)}$ ,  $\omega_2^{(2)} \underline{\$}_2^{(2)}$ ,  $\omega_1^{(3)} \underline{\$}_1^{(3)}$ , and  $\omega_2^{(3)} \underline{\$}_2^{(3)}$  can be determined using (4.33) respectively as follows:

$$\hat{\underline{\$}}_{p1}^{(2)} = \omega_{p1}^{(2)} \underline{\$}_{p1}^{(2)} = \omega_1^{(2)} \sum_{j=3}^6 K_{j3} \underline{\$}_j^{(1)} \quad (4.48)$$

$$\hat{\underline{\$}}_{p2}^{(2)} = \omega_{p2}^{(2)} \underline{\$}_{p2}^{(2)} = \omega_2^{(2)} \sum_{j=3}^6 K_{j4} \underline{\$}_j^{(1)} \quad (4.49)$$

$$\hat{\underline{\$}}_{p1}^{(3)} = \omega_{p1}^{(3)} \underline{\$}_{p1}^{(3)} = \omega_1^{(3)} \sum_{j=3}^6 K_{j5} \underline{\$}_j^{(1)} \quad (4.50)$$

$$\hat{\underline{\$}}_{p2}^{(3)} = \omega_{p2}^{(3)} \underline{\$}_{p2}^{(3)} = \omega_2^{(3)} \sum_{j=3}^6 K_{j6} \underline{\$}_j^{(1)} \quad (4.51)$$

Introducing this notation, (4.45) can be expressed in the form

$$\hat{\underline{\$}} = \omega \underline{\$} = \sum_{i=1}^3 \sum_{m=1}^2 \hat{\underline{\$}}_{pm}^{(i)} \quad (4.52)$$

Equation (4.52) expresses that the twist  $\hat{\underline{\$}}$  representing the instantaneous motion of the end-effector is the sum of all six partial twists.

For the reverse solution, where the twist  $\hat{\underline{\$}}$  is specified, this twist can be expressed in the form

$$\hat{\underline{\$}} = \omega_1^{(i)} \underline{\$}_1^{(i)} + \omega_2^{(i)} \underline{\$}_2^{(i)} + \dots + \omega_6^{(i)} \underline{\$}_6^{(i)} \quad (4.53)$$

where  $i = 1, 2, 3$ . It is required to compute the input scalar multipliers in each subchain, i.e., to compute  $\omega_1^{(i)}$  and  $\omega_2^{(i)}$  for  $i = 1, 2, 3$ . This is accomplished by determining six screws  $\underline{\$}_{o1}^{(i)}$  and  $\underline{\$}_{o2}^{(i)}$ , for  $i = 1, 2, 3$ , where  $\underline{\$}_{o1}^{(i)}$  is orthogonal to the set of screws  $\{\underline{\$}_2^{(i)}, \underline{\$}_3^{(i)}, \dots, \underline{\$}_6^{(i)}\}$  and  $\underline{\$}_{o2}^{(i)}$  is orthogonal to the set  $\{\underline{\$}_1^{(i)}, \underline{\$}_3^{(i)}, \dots, \underline{\$}_6^{(i)}\}$ . Taking the orthogonal product of the right and the left side of (4.53) with  $\underline{s}_{o1}^{(i)}$  and  $\underline{s}_{o2}^{(i)}$ , for  $i = 1, 2, 3$ , and solving for the six

unknown input scalar multipliers  $\omega_1^{(i)}$  and  $\omega_2^{(i)}$ , then these scalars can be expressed as follows:

$$\omega_1^{(i)} = \frac{\hat{\$} * \$_{o1}^{(i)}}{\$ _1^{(i)} * \$_{o1}^{(i)}} \quad (4.54)$$

and

$$\omega_2^{(i)} = \frac{\hat{\$} * \$_{o2}^{(i)}}{\$ _2^{(i)} * \$_{o2}^{(i)}} \quad (4.55)$$

where  $i = 1, 2, 3$ .

#### 4.3 A Direct Determination of the Instantaneous Kinematics of the End-Effector of Fully-Parallel Symmetrical Devices

##### 4.3.1 Basic Equations

The twist  $\hat{\$}$ , ( $= \omega \$$ ), representing the instantaneous motion of the end-effector of the general  $M$  degree of freedom fully-parallel symmetrical device (Fig. 4.3) can be expressed as a linear combination of the joint twists in any of the  $N$  subchains (see equation (4.15) and section 4.2.4)

$$\hat{\$} = \omega \$ = \omega_1^{(n)} \$ _1^{(n)} + \omega_2^{(n)} \$ _2^{(n)} + \dots + \omega_M^{(n)} \$ _M^{(n)} \quad (4.56)$$

where  $1 \leq n \leq N$ .

Two solutions of the twist equation (4.56) will be presented. Firstly, the forward solution where the input twists are assumed to be known, it is required to determine the twist  $\hat{\$}$  of the end-effector. Secondly, the reverse solution where the twist  $\hat{\$}$  is assumed to be specified, it is required to compute the input twists.

#### 4.3.2 Forward Solution

For the forward solution (see section 4.2.2), let  $\omega_m^{(i)}$  denote the  $M$  known input scalar multipliers, where  $m = 1, 2, \dots, g$ ,  $g = \frac{M}{N}$ , and  $i = 1, 2, \dots, N$ . In each subchain, there are  $(M-g)$  unknown scalar multipliers,  $\omega_j^{(i)}$ , where  $j = (g+1), (g+2), \dots, M$ , and it is necessary to eliminate these  $(M-g)$  unknown scalar multipliers. This is accomplished by forming  $g$  screws each of which is orthogonal to all screws in the subchain except the screw associated with one of the input actuators in this subchain. Consider for example that  $g=2$  and  $\$1^{(1)}$  and  $\$2^{(1)}$  are the two screws associated with the two input actuated joints in the first subchain. It is possible to determine two screws  $\$01^{(1)}$  and  $\$02^{(1)}$  which are orthogonal to the sets of screws  $\{\$2^{(1)}, \$3^{(1)}, \dots, \$M^{(1)}\}$  and  $\{\$1^{(1)}, \$3^{(1)}, \dots, \$M^{(1)}\}$  respectively. Taking the orthogonal product of both sides of (4.56) with the appropriate orthogonal screw  $\$0m^{(i)}$ , (orthogonal to all screws in the  $i$ th subchain except  $\$m^{(i)}$ ), for  $i = 1, 2, \dots, N$ , and  $m = 1, 2, \dots, g$ , gives  $M (= gN)$  linear equations. This set of  $M$  equations can be written in a matrix form as follows:

$$\begin{bmatrix} \frac{1}{2} \frac{f_{o1}}{f_{o1}}^{(1)} \\ \frac{1}{2} \frac{f_{o2}}{f_{o2}}^{(1)} \\ \vdots \\ \frac{1}{2} \frac{f_{og}}{f_{og}}^{(1)} \\ \frac{1}{2} \frac{f_{o1}}{f_{o1}}^{(2)} \\ \frac{1}{2} \frac{f_{o2}}{f_{o2}}^{(2)} \\ \vdots \\ \frac{1}{2} \frac{f_{og}}{f_{og}}^{(2)} \\ \vdots \\ \frac{1}{2} \frac{f_{og}}{f_{og}}^{(N)} \end{bmatrix} = \begin{bmatrix} \frac{1}{2} \frac{f_{o1}}{f_{o1}}^{(1)} & 0 & 0 & 0 & 0 & 0 \\ 0 & \frac{1}{2} \frac{f_{o2}}{f_{o2}}^{(1)} & \dots & 0 & 0 & 0 \\ 0 & 0 & \dots & 0 & 0 & 0 \\ \frac{1}{2} \frac{f_{og}}{f_{og}}^{(1)} & \dots & \dots & \frac{1}{2} \frac{f_{og}}{f_{og}}^{(1)} & 0 & 0 \\ 0 & 0 & \dots & \frac{1}{2} \frac{f_{o1}}{f_{o1}}^{(2)} & \frac{1}{2} \frac{f_{o2}}{f_{o2}}^{(2)} & 0 \\ 0 & \frac{1}{2} \frac{f_{o2}}{f_{o2}}^{(1)} & \dots & 0 & \frac{1}{2} \frac{f_{o2}}{f_{o2}}^{(2)} & \dots \\ \vdots & \vdots & \vdots & \vdots & \vdots & \vdots \\ \frac{1}{2} \frac{f_{og}}{f_{og}}^{(2)} & \vdots & \vdots & 0 & 0 & 0 \\ \vdots & \vdots & \vdots & \vdots & \vdots & \vdots \\ \frac{1}{2} \frac{f_{og}}{f_{og}}^{(N)} & 0 & 0 & 0 & 0 & \frac{1}{2} \frac{f_{og}}{f_{og}}^{(N)} \end{bmatrix} \begin{bmatrix} \omega_1^{(1)} \\ \omega_2^{(1)} \\ \vdots \\ \omega_g^{(1)} \\ \omega_1^{(2)} \\ \omega_2^{(2)} \\ \vdots \\ \omega_g^{(2)} \\ \vdots \\ \omega_g^{(N)} \end{bmatrix}$$

(4.57)



Equation (4.57) will be called the characteristic matrix equation of fully-parallel devices. If the diagonal matrix on the right side of (4.57) is nonsingular, then (4.57) can be rearranged in the form

$$\left\{ \begin{array}{c} \omega_1^{(1)} \\ \omega_2^{(1)} \\ \vdots \\ \omega_g^{(1)} \\ \omega_1^{(2)} \\ \vdots \\ \omega_g^{(2)} \\ \vdots \\ \omega_g^{(N)} \end{array} \right\} = \left[ \begin{array}{c} \frac{1}{\Phi_1^{(1)} * \Phi_{01}^{(1)}} \Phi_{01}^{(1)T} \\ \frac{1}{\Phi_2^{(1)} * \Phi_{02}^{(1)}} \Phi_{02}^{(1)T} \\ \vdots \\ \frac{1}{\Phi_g^{(1)} * \Phi_{0g}^{(1)}} \Phi_{0g}^{(1)T} \\ \frac{1}{\Phi_1^{(2)} * \Phi_{01}^{(2)}} \Phi_{01}^{(2)T} \\ \vdots \\ \frac{1}{\Phi_g^{(2)} * \Phi_{0g}^{(2)}} \Phi_{0g}^{(2)T} \\ \vdots \\ \frac{1}{\Phi_g^{(N)} * \Phi_{0g}^{(N)}} \Phi_{0g}^{(N)T} \end{array} \right] \{\hat{\Phi}\}$$

(4.58)\*

\*For any two column vectors,  $\underline{v}_1$  and  $\underline{v}_2$

$$\underline{v}_1 * \underline{v}_2 \equiv \{\underline{v}_1\}^T \{\underline{v}_2\}$$

Further, since the square matrix on the right side of (4.58) is, in general, nonsingular (if the device is not in a special configuration) then (4.58) can be expressed in the form

$$\hat{\underline{\$}} = [\underline{R}]\{\omega\} \quad (4.59)$$

where  $\{\omega\}$  is an  $[M \times 1]$  column vector representing the known input scalar multipliers,

$$\{\omega\} = [\omega_1^{(1)} \omega_2^{(1)} \dots \omega_g^{(1)} \omega_1^{(2)} \dots \omega_g^{(N)}]^T \quad (4.60)$$

and  $[\underline{R}]$  is an  $[M \times M]$  square matrix which is a function of position only,

$$[\underline{R}] = [\underline{R}_1 \ \underline{R}_2 \ \underline{R}_3 \ \dots \ \underline{R}_M] \quad (4.61)$$

where  $\underline{R}_j$  is an  $[M \times 1]$  column vector.

Expanding (4.59), the twist  $\hat{\underline{\$}}$  representing the instantaneous motion of the end-effector can be expressed in the form

$$\begin{aligned} \hat{\underline{\$}} = \omega \underline{\$} &= (\omega_1^{(1)} \underline{R}_1 + \omega_2^{(1)} \underline{R}_2 + \dots + \omega_g^{(1)} \underline{R}_g) \\ &+ (\omega_1^{(2)} \underline{R}_{g+1} + \dots + \omega_g^{(2)} \underline{R}_{2g}) \\ &\dots + (\omega_1^{(N)} \underline{R}_{[1+g(N-1)]} + \dots + \omega_g^{(N)} \underline{R}_M) \end{aligned} \quad (4.62)$$

Further examination of (4.62) provides an alternative form and an important result is deduced which will now be discussed in detail.

#### 4.3.3 The Concept of Partial Screws

Following the procedure in section 4.2.3, consider now that all actuators are locked except the actuator at the

first base joint in the first subchain, i.e.,  $\omega_2^{(1)} = \omega_3^{(1)} = \dots = \omega_g^{(1)} = 0$  and  $\omega_1^{(i)} = \dots = \omega_g^{(i)} = 0$ , for  $i = 2, 3, \dots, N$ .

The instantaneous motion of the end-effector is due solely to the input twist  $\omega_1^{(1)} \underline{\$}_1^{(1)}$ . The partial twist representing this motion will be labelled  $\hat{\underline{\$}}_{p1}^{(1)}$ , ( $= \omega_{p1}^{(1)} \underline{\$}_{p1}^{(1)}$ ). Equation (4.62) reduces to

$$\hat{\underline{\$}}_{p1}^{(1)} = \omega_{p1}^{(1)} \underline{\$}_{p1}^{(1)} = \omega_1^{(1)} \underline{R}_1 \quad (4.63)$$

Similarly, the partial twist  $\underline{\$}_{p2}^{(1)}$ , ( $= \omega_{p2}^{(1)} \underline{\$}_{p2}^{(1)}$ ), representing the instantaneous motion of the end-effector due to the input twist  $\omega_2^{(1)} \underline{\$}_2^{(1)}$  is given by

$$\hat{\underline{\$}}_{p2}^{(1)} = \omega_{p2}^{(1)} \underline{\$}_{p2}^{(1)} = \omega_2^{(1)} \underline{R}_2 \quad (4.64)$$

Also, the partial twist  $\hat{\underline{\$}}_{p1}^{(2)}$  representing the instantaneous motion of the end-effector due to the input twist  $\omega_1^{(2)} \underline{\$}_1^{(2)}$  is given by

$$\hat{\underline{\$}}_{p1}^{(2)} = \omega_{p1}^{(2)} \underline{\$}_{p1}^{(2)} = \omega_1^{(2)} \underline{R}_{g+1} \quad (4.65)$$

In general, the partial twist representing the instantaneous motion of the end-effector due to the input twist  $\omega_m^{(i)} \underline{\$}_m^{(i)}$ , for  $i = 1, 2, \dots, N$  and  $m = 1, 2, \dots, g$ , can be expressed in the form

$$\hat{\underline{\$}}_{pm}^{(i)} = \omega_{pm}^{(i)} \underline{\$}_{pm}^{(i)} = \omega_m^{(i)} \underline{R}_{[m+g(i-1)]} \quad (4.66)$$

Introducing this notation, (4.62) can be expressed in the form

$$\begin{aligned}\hat{\$} = \omega \$ = & (\hat{\$}_{p1}^{(1)} + \hat{\$}_{p2}^{(1)} + \dots + \hat{\$}_{pg}^{(1)}) \\ & + (\hat{\$}_{p1}^{(2)} + \hat{\$}_{p2}^{(2)} + \dots + \hat{\$}_{pg}^{(2)}) \\ & \dots + (\hat{\$}_{p1}^{(N)} + \hat{\$}_{p2}^{(N)} + \dots + \hat{\$}_{pg}^{(N)})\end{aligned}\quad (4.67)$$

Finally, equation (4.67) can be expressed in the abbreviated form

$$\hat{\$} = \omega \$ = \sum_{i=1}^N \sum_{m=1}^g \hat{\$}_{pm}^{(i)} \quad (4.68)$$

The twist  $\hat{\$}$  representing the instantaneous motion of the end-effector is therefore the sum of all (M) partial twists.

It is evident that the results derived in this section are in exact agreement with those derived in section 4.2. For instance, equations (4.62) and (4.27) are essentially identical as are equations (4.68) and (4.35). Equations (4.18) and (4.35) in section 4.2 as well as equations (4.57) and (4.68) in this section completely describe the screw system of the end-effector and provide the basis for examining the geometrical conditions of special configurations (see Chapter 5). However, the procedure presented in this section is more direct and requires less numerical computations. Also it is easier to explain the singularity in equation (4.57) than in equation (4.18). Therefore, the procedure presented in this section is considered to be superior to the procedure in section 4.2.

#### 4.3.4 Reverse Solution

The twist representing the instantaneous motion of the end-effector which is now specified was expressed as a linear combination of the joint twists in any of the subchains (see equation (4.56)). It is required now to compute the  $g$  input scalar multipliers in each subchain. This is accomplished from equation (4.58) where any unknown input scalar multiplier  $\omega_m^{(i)}$  can be computed as

$$\omega_m^{(i)} = \frac{\hat{\$}_m^{(i)} * \hat{\$}_{om}^{(i)}}{\hat{\$}_m^{(i)} * \hat{\$}_{om}^{(i)}} \quad (\text{or} = \frac{\hat{\$}_{om}^{(i)} o \hat{\$}_{rm}^{(i)}}{\hat{\$}_m^{(i)} o \hat{\$}_{rm}^{(i)}}) \quad (4.69)$$

where  $i = 1, 2, \dots, N$ ,  $m = 1, 2, \dots, g$ , and where  $\hat{\$}_{om}^{(i)}$  is a screw which is orthogonal to every screw in the  $i$ th subchain except  $\hat{\$}_m^{(i)}$ . Equation (4.69) is identical to equation (4.39).

#### 4.3.5 Instantaneous Kinematics of the End-Effector of Six-Degree of Freedom Fully-Parallel Symmetrical Devices

The instantaneous kinematics of the end-effector of fully-parallel symmetrical devices with six, three, and two connecting subchains are now investigated using the shorter direct procedure of analysis described in the previous sections (4.3.1-4.3.4).

##### 4.3.5.1 Six connecting subchains to platform, (N=6)

In Fig. 4.5, the end-effector is connected to the base by six subchains, i.e.,  $N = 6$ . There is one input actuator

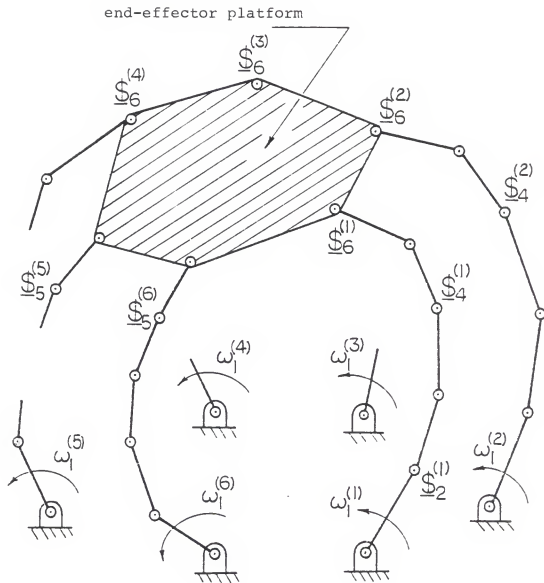


Figure 4.5. Spatial Six-Dof Fully-Parallel Symmetrical Device with Six Connecting Subchains to Platform

( $g=1$ ) in each subchain such that the end-effector has mobility  $M = 6$ . It is assumed that this input actuator is located at the base joint of each subchain; i.e.,  $\omega_1^{(i)} \underline{\$}_1^{(i)}$ , where  $i = 1, 2, \dots, 6$ , are the six known input twists. Further, there are five ( $M-g = 6-1 = 5$ ) unknown scalar multipliers,  $\omega_j^{(i)}$ , in each subchain where  $j = 2, 3, 4, 5, 6$ . The twist  $\hat{\underline{\$}}$ , ( $= \omega \underline{\$}$ ), representing the instantaneous motion of the end-effector could be expressed as follows:

$$\hat{\underline{\$}} = \omega \underline{\$} = \sum_{j=1}^6 \omega_j^{(i)} \underline{\$}_j^{(i)} \quad (4.70)$$

where  $i = 1, 2, \dots$ , or 6.

It is necessary to eliminate the five unknown scalar multipliers  $\omega_j^{(i)}$ , for  $j = 2, 3, 4, 5, 6$ , in each subchain. This is accomplished by determining a screw  $\underline{\$}_{01}^{(i)}$  orthogonal to  $\{\underline{\$}_2^{(i)}, \underline{\$}_3^{(i)}, \dots, \underline{\$}_6^{(i)}\}$  in each subchain. Taking the orthogonal product of both sides of (4.70) with  $\underline{\$}_{01}^{(i)}$  for  $i = 1, 2, \dots, 6$ , gives a total of six linear equations. Therefore, the characteristic matrix equation (4.57) reduces to

$$\begin{bmatrix} \underline{\xi}_1^{(1)} \ast \underline{\xi}_{01}^{(1)} \\ \underline{\xi}_1^{(2)} \ast \underline{\xi}_{01}^{(2)} \\ \underline{\xi}_1^{(3)} \ast \underline{\xi}_{01}^{(3)} \\ \underline{\xi}_1^{(4)} \ast \underline{\xi}_{01}^{(4)} \\ \underline{\xi}_1^{(5)} \ast \underline{\xi}_{01}^{(5)} \\ \underline{\xi}_1^{(6)} \ast \underline{\xi}_{01}^{(6)} \end{bmatrix} = \begin{bmatrix} \underline{\xi}_1^{(1)} \ast \underline{\xi}_{01}^{(1)} & 0 & 0 & 0 & 0 & 0 \\ 0 & \underline{\xi}_1^{(2)} \ast \underline{\xi}_{01}^{(2)} & 0 & 0 & 0 & 0 \\ 0 & 0 & \underline{\xi}_1^{(3)} \ast \underline{\xi}_{01}^{(3)} & 0 & 0 & 0 \\ 0 & 0 & 0 & \underline{\xi}_1^{(4)} \ast \underline{\xi}_{01}^{(4)} & 0 & 0 \\ 0 & 0 & 0 & 0 & \underline{\xi}_1^{(5)} \ast \underline{\xi}_{01}^{(5)} & 0 \\ 0 & 0 & 0 & 0 & 0 & \underline{\xi}_1^{(6)} \ast \underline{\xi}_{01}^{(6)} \end{bmatrix} \begin{Bmatrix} \omega_1^{(1)} \\ \omega_1^{(2)} \\ \omega_1^{(3)} \\ \omega_1^{(4)} \\ \omega_1^{(5)} \\ \omega_1^{(6)} \end{Bmatrix} \quad (4.71)$$



Since, in general, the diagonal matrix in (4.71) is nonsingular, then (4.71) can be rearranged as follows

$$\left\{ \begin{matrix} \omega_1^{(1)} \\ \omega_1^{(2)} \\ \omega_1^{(3)} \\ \omega_1^{(4)} \\ \omega_1^{(5)} \\ \omega_1^{(6)} \end{matrix} \right\} = \left[ \begin{matrix} \frac{1}{\underline{\$}_1^{(1)} * \underline{\$}_{o1}^{(1)}} \underline{\$}_{o1}^{(1)T} \\ \frac{1}{\underline{\$}_1^{(2)} * \underline{\$}_{o1}^{(2)}} \underline{\$}_{o1}^{(2)T} \\ \frac{1}{\underline{\$}_1^{(3)} * \underline{\$}_{o1}^{(3)}} \underline{\$}_{o1}^{(3)T} \\ \frac{1}{\underline{\$}_1^{(4)} * \underline{\$}_{o1}^{(4)}} \underline{\$}_{o1}^{(4)T} \\ \frac{1}{\underline{\$}_1^{(5)} * \underline{\$}_{o1}^{(5)}} \underline{\$}_{o1}^{(5)T} \\ \frac{1}{\underline{\$}_1^{(6)} * \underline{\$}_{o1}^{(6)}} \underline{\$}_{o1}^{(6)T} \end{matrix} \right] \{ \hat{\underline{\$}} \} \quad (4.72)$$

Further, since the square matrix on the right side of (4.72) is also nonsingular, if the device is not in special configuration, then (4.72) can be expressed in the form

$$\hat{\underline{\$}} = \omega \underline{\$} = [\underline{R}_1 \ \underline{R}_2 \ \underline{R}_3 \ \underline{R}_4 \ \underline{R}_5 \ \underline{R}_6] \left\{ \begin{matrix} \omega_1^{(1)} \\ \omega_1^{(2)} \\ \omega_1^{(3)} \\ \omega_1^{(4)} \\ \omega_1^{(5)} \\ \omega_1^{(6)} \end{matrix} \right\} \quad (4.73)$$

Therefore, the twist  $\hat{\underline{\$}}$  can be expressed in the form

$$\hat{\underline{\$}} = \omega \underline{\$} = \omega_1^{(1)} \underline{R}_1 + \omega_1^{(2)} \underline{R}_2 + \dots + \omega_1^{(6)} \underline{R}_6 \quad (4.74)$$

Equation (4.74) could be deduced from (4.63), for  $M = N = 6$ , and  $g = 1$ .

Now consider that all actuators are locked except the first actuator in the first subchain, i.e.,  $\omega_1^{(1)} \neq 0$  and  $\omega_1^{(i)} = 0$  for  $i = 2, 3, \dots, 6$ . The instantaneous motion of the end-effector will be due solely to the input twist  $\omega_1^{(1)} \underline{\$}_1^{(1)}$ . The partial twist  $\hat{\underline{\$}}_{p1}^{(1)}$  representing this motion can be expressed as follows

$$\hat{\underline{\$}}_{p1}^{(1)} = \omega_{p1}^{(1)} \underline{\$}_{p1}^{(1)} = \omega_1^{(1)} \underline{R}_1 \quad (4.75)$$

If all actuators are locked except the actuator in the third subchain, i.e.,  $\omega_1^{(3)} \neq 0$  and  $\omega_1^{(i)} = 0$  for  $i = 1, 2, 4, 5, 6$ , the partial twist  $\hat{\underline{\$}}_{p1}^{(3)}$  representing the instantaneous motion of the end-effector in this case can be expressed as follows:

$$\hat{\underline{\$}}_{p1}^{(3)} = \omega_{p1}^{(3)} \underline{\$}_{p1}^{(3)} = \omega_1^{(3)} \underline{R}_3 \quad (4.76)$$

Therefore, equation (4.66) will be reduced, for  $m = g = 1$ , to

$$\hat{\underline{\$}}_{p1}^{(i)} = \omega_{p1}^{(i)} \underline{\$}_{p1}^{(i)} = \omega_1^{(i)} \underline{R}_i \quad (4.77)$$

for  $i = 1, 2, \dots, 6$ .

Introducing this notation, (4.74) can be expressed in the form

$$\hat{\underline{\$}} = \omega \underline{\$} = \sum_{i=1}^6 \hat{\underline{\$}}_{p1}^{(i)} = \sum_{i=1}^6 \omega_1^{(i)} \underline{R}_i \quad (4.78)$$

The twist  $\underline{\hat{S}}$  representing the instantaneous motion of the end-effector is therefore the sum of all six partial twists.

For the reverse solution, the twist  $\underline{\hat{S}}$  representing the instantaneous motion of the end-effector is specified. Using (4.72) to solve for the six unknown scalar multipliers  $\omega_1^{(i)}$  for  $i = 1, 2, \dots, 6$ , these six unknown scalars can be expressed in the form

$$\omega_1^{(i)} = \frac{\underline{\hat{S}} * \underline{\hat{S}}_{o1}^{(i)}}{\underline{\hat{S}}_1^{(i)} * \underline{\hat{S}}_{o1}^{(i)}} \quad (\text{or} = \frac{\underline{\hat{S}}_{o1} \underline{\hat{S}}_{r1}^{(i)}}{\underline{\hat{S}}_1^{(i)} \underline{\hat{S}}_{r1}^{(i)}}) \quad (4.79)$$

for  $i = 1, 2, \dots, 6$ .

#### 4.3.5.2 Three connecting subchains to platform, (N=3)

In Fig. 4.4, the end-effector is connected to the base by three connecting subchains; i.e.,  $N = 3$ . In order for the end-effector to have mobility  $M = 6$  then  $g = \frac{M}{N} = 2$ ; i.e., there are two input actuators in each subchain which are assumed to be located at the first two joints from the base of each subchain. Therefore,  $\omega_1^{(1)}$ ,  $\omega_2^{(1)}$ ,  $\omega_1^{(2)}$ ,  $\omega_2^{(2)}$ ,  $\omega_1^{(3)}$ , and  $\omega_2^{(3)}$  are the six known input scalar multipliers. The twist equation (4.56) reduces to

$$\underline{\hat{S}} = \omega \underline{\hat{S}} = \omega_1^{(1)} \underline{\hat{S}}_1^{(1)} + \omega_2^{(1)} \underline{\hat{S}}_2^{(1)} + \dots + \omega_6^{(i)} \underline{\hat{S}}_6^{(i)} \quad (4.80)$$

where  $i = 1, 2$ , or  $3$ .

For the forward solution, the six input twists are specified and it is necessary to eliminate four ( $M-g = 4$ ) unknown scalar multipliers,  $\omega_3^{(i)}$ ,  $\omega_4^{(i)}$ ,  $\omega_5^{(i)}$ , and  $\omega_6^{(i)}$  in each subchain. This is also accomplished by determining six

screws,  $\underline{s}_{o1}^{(i)}$  and  $\underline{s}_{o2}^{(i)}$  for  $i = 1, 2, 3$ , such that screw  $\underline{s}_{o1}^{(i)}$  is orthogonal to the set of screws  $\{\underline{s}_2^{(i)}, \underline{s}_3^{(i)}, \underline{s}_4^{(i)}, \underline{s}_5^{(i)}, \underline{s}_6^{(i)}\}$  and screw  $\underline{s}_{o2}^{(i)}$  is orthogonal to  $\{\underline{s}_1^{(i)}, \underline{s}_3^{(i)}, \underline{s}_4^{(i)}, \underline{s}_5^{(i)}, \underline{s}_6^{(i)}\}$ . Taking the orthogonal product of both sides of (4.80) with the orthogonal screws, the characteristic matrix equation (4.57) reduces to

$$\begin{bmatrix} \hat{\psi}_{\bar{1}}^{(1)} \\ \hat{\psi}_{\bar{1}}^{(1)} \\ \hat{\psi}_{\bar{2}}^{(1)} \\ \hat{\psi}_{\bar{1}}^{(2)} \\ \hat{\psi}_{\bar{2}}^{(2)} \\ \hat{\psi}_{\bar{1}}^{(3)} \\ \hat{\psi}_{\bar{2}}^{(3)} \end{bmatrix} = \begin{bmatrix} \hat{\psi}_{\bar{1}}^{(1)} * \hat{\psi}_{\bar{1}}^{(1)} & 0 & 0 & 0 & 0 & 0 & 0 \\ 0 & \hat{\psi}_{\bar{2}}^{(1)} * \hat{\psi}_{\bar{2}}^{(1)} & 0 & 0 & 0 & 0 & 0 \\ 0 & 0 & \hat{\psi}_{\bar{1}}^{(2)} * \hat{\psi}_{\bar{1}}^{(2)} & 0 & 0 & 0 & 0 \\ 0 & 0 & 0 & \hat{\psi}_{\bar{2}}^{(2)} * \hat{\psi}_{\bar{2}}^{(2)} & 0 & 0 & 0 \\ 0 & 0 & 0 & 0 & \hat{\psi}_{\bar{1}}^{(3)} * \hat{\psi}_{\bar{1}}^{(3)} & 0 & 0 \\ 0 & 0 & 0 & 0 & 0 & \hat{\psi}_{\bar{2}}^{(3)} * \hat{\psi}_{\bar{2}}^{(3)} & 0 \end{bmatrix} \begin{Bmatrix} \omega_{\bar{1}}^{(1)} \\ \omega_{\bar{2}}^{(1)} \\ \omega_{\bar{1}}^{(2)} \\ \omega_{\bar{2}}^{(2)} \\ \omega_{\bar{1}}^{(3)} \\ \omega_{\bar{2}}^{(3)} \end{Bmatrix} \quad (4.81)$$

Equation (4.81) can be rearranged in the form which is analogous to (4.58)

$$\left\{ \begin{array}{l} \omega_1^{(1)} \\ \omega_2^{(1)} \\ \omega_1^{(2)} \\ \omega_2^{(2)} \\ \omega_1^{(3)} \\ \omega_2^{(3)} \end{array} \right\} = \left[ \begin{array}{l} \frac{1}{\underline{\Phi}_1^{(1)} * \underline{\Phi}_{o1}^{(1)}} \underline{\Phi}_{o1}^{(1)T} \\ \frac{1}{\underline{\Phi}_2^{(1)} * \underline{\Phi}_{o2}^{(1)}} \underline{\Phi}_{o2}^{(1)T} \\ \frac{1}{\underline{\Phi}_1^{(2)} * \underline{\Phi}_{o1}^{(2)}} \underline{\Phi}_{o1}^{(2)T} \\ \frac{1}{\underline{\Phi}_2^{(2)} * \underline{\Phi}_{o2}^{(2)}} \underline{\Phi}_{o2}^{(2)T} \\ \frac{1}{\underline{\Phi}_1^{(3)} * \underline{\Phi}_{o1}^{(3)}} \underline{\Phi}_{o1}^{(3)T} \\ \frac{1}{\underline{\Phi}_2^{(3)} * \underline{\Phi}_{o2}^{(3)}} \underline{\Phi}_{o2}^{(3)T} \end{array} \right] \{\hat{\underline{\Phi}}\} \quad (4.82)$$

Since the square matrix on the right side of (4.82) is nonsingular, then (4.82) could be expressed in the form (see equation (4.59))

$$\hat{\underline{\Phi}} = [\underline{R}_1 \ \underline{R}_2 \ \underline{R}_3 \ \underline{R}_4 \ \underline{R}_5 \ \underline{R}_6] \left\{ \begin{array}{l} \omega_1^{(1)} \\ \omega_2^{(1)} \\ \omega_1^{(2)} \\ \omega_2^{(2)} \\ \omega_1^{(3)} \\ \omega_2^{(3)} \end{array} \right\} \quad (4.83)$$

From (4.83), the twist  $\hat{\underline{\$}}$  representing the instantaneous motion of the end-effector can be expressed in the form

$$\begin{aligned}\hat{\underline{\$}} = \omega \underline{\$} = & (\omega_1^{(1)} \underline{R}_1 + \omega_2^{(1)} \underline{R}_2) + (\omega_1^{(2)} \underline{R}_3 + \omega_2^{(2)} \underline{R}_4) \\ & + (\omega_1^{(3)} \underline{R}_5 + \omega_2^{(3)} \underline{R}_6)\end{aligned}\quad (4.84)$$

Equation (4.84) can be deduced from (4.62), for  $g = 2$ ,  $N = 3$  and  $M = 6$ .

Now consider that all actuators are locked except the actuator at the first base joint in the first subchain, i.e.,  $\omega_2^{(1)} = \omega_1^{(2)} = \omega_2^{(2)} = \omega_1^{(3)} = \omega_2^{(3)} = 0$  and  $\omega_1^{(1)} \neq 0$ . The instantaneous motion of the end-effector is due solely to the input twist  $\omega_1^{(1)} \hat{\underline{\$}}_1^{(1)}$ . The partial twist  $\hat{\underline{\$}}_{p1}^{(1)}$  representing the instantaneous motion could be determined from (4.84) as follows:

$$\hat{\underline{\$}}_{p1}^{(1)} = \omega_{p1}^{(1)} \hat{\underline{\$}}_{p1}^{(1)} = \omega_1^{(1)} \underline{R}_1 \quad (4.85)$$

The partial twist representing the instantaneous motion of the end-effector due solely to any one of the six input twists can be determined either by substituting the appropriate values for the various scalar multipliers in (4.84) or directly from (4.66), for  $m = 1, 2$ ,  $g = 2$ , and  $i = 1, 2, 3$ ; i.e.,

$$\hat{\underline{\$}}_{pm}^{(i)} = \omega_{pm}^{(i)} \hat{\underline{\$}}_{pm}^{(i)} = \omega_m^{(i)} \underline{R}_{[m+2(i-1)]} \quad (4.86)$$

Introducing this notation, (4.84) can be expressed in the form

$$\hat{\underline{\$}} = \omega \underline{\$} = \sum_{i=1}^3 \sum_{m=1}^2 \hat{\underline{\$}}_{pm}^{(i)} \quad (4.87)$$

Equation (4.87) can be deduced from (4.68), (for  $N=3$  and  $g=2$ ), and it also expresses that the twist  $\hat{\$}$  representing the instantaneous motion of the end-effector is the sum of all six partial twists.

For the reverse solution, the twist  $\hat{\$}$  representing the instantaneous motion of the end-effector is specified. Using (4.82) to solve for the six unknown scalar multipliers  $\omega_1^{(i)}$   $\omega_2^{(i)}$  gives

$$\omega_1^{(i)} = \frac{\hat{\$} * \hat{\$}_{o1}^{(i)}}{\hat{\$}_1^{(i)} * \hat{\$}_{o1}^{(i)}} \quad (\text{or} = \frac{\hat{\$}_{o\$_{r1}}^{(i)}}{\hat{\$}_1^{(i)} o \hat{\$}_{r1}^{(i)}}) \quad (4.88)$$

and

$$\omega_2^{(i)} = \frac{\hat{\$} * \hat{\$}_{o2}^{(i)}}{\hat{\$}_2^{(i)} * \hat{\$}_{o2}^{(i)}} \quad (\text{or} = \frac{\hat{\$}_{o\$_{r2}}^{(i)}}{\hat{\$}_2^{(i)} o \hat{\$}_{r2}^{(i)}}) \quad (4.89)$$

where  $i = 1, 2, 3$ .

#### 4.3.5.3 Two connecting subchains to platform, (N=2)

In Fig. 4.6, the end-effector platform is connected to the base by two subchains, i.e.,  $N = 2$ . In order for the end-effector to have mobility  $M = 6$  there are three input actuators, ( $g = \frac{M}{N} = 3$ ), in each subchain which also assumed to be located at the first three joints from the base, i.e.,  $\omega_1^{(i)} \hat{\$}_1^{(i)}$ ,  $\omega_2^{(i)} \hat{\$}_2^{(i)}$  and  $\omega_3^{(i)} \hat{\$}_3^{(i)}$  for  $i = 1, 2$  are the six known input twists. The twist  $\hat{\$}$ , ( $= \omega \hat{\$}$ ), representing the instantaneous motion of the end-effector can be determined from (4.56), for  $N = 2$  and  $M = 6$ , as follows:



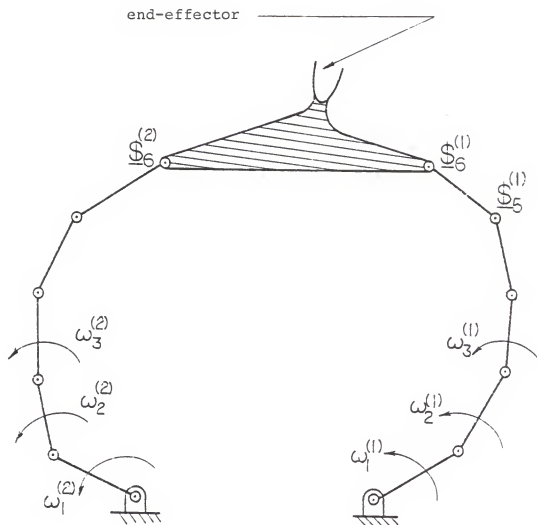


Figure 4.6. Six-Dof Fully-Parallel Symmetrical Device with Two Connecting Subchains to Platform

$$\begin{aligned}\hat{\underline{s}} &= \omega \underline{s} = \omega_1^{(1)} \underline{s}_1^{(1)} + \omega_2^{(1)} \underline{s}_2^{(1)} + \dots + \omega_6^{(1)} \underline{s}_6^{(1)} \\ &= \omega_1^{(2)} \underline{s}_1^{(2)} + \omega_2^{(2)} \underline{s}_2^{(2)} + \dots + \omega_6^{(2)} \underline{s}_6^{(2)}\end{aligned}\quad (4.90)$$

For the forward solution, where the six input scalar multipliers are specified, it is necessary to eliminate the other six unknown scalar multipliers,  $\omega_j^{(i)}$ ; three ( $M-g = 3$ ) in each subchain. This is accomplished by determining six screws  $\underline{s}_{o1}^{(i)}$ ,  $\underline{s}_{o2}^{(i)}$ , and  $\underline{s}_{o3}^{(i)}$  for  $i = 1, 2$ . For instance, screw  $\underline{s}_{o2}^{(i)}$  is orthogonal to all screws in the  $i$ th subchain except  $\underline{s}_2^{(i)}$ ; i.e., to the set of screws  $\{\underline{s}_1^{(i)}, \underline{s}_3^{(i)}, \underline{s}_4^{(i)}, \underline{s}_5^{(i)}, \underline{s}_6^{(i)}\}$  for  $i = 1$  or  $2$ . Taking the orthogonal product of each screw of these six orthogonal screws with the appropriate equation of (4.90), gives six linear equations. Therefore, the characteristic matrix equation (4.57) reduces to (for  $g=3$  and  $N=2$ )

$$\begin{bmatrix} \underline{\hat{\psi}}_{-01}^{(1)} \\ \underline{\hat{\psi}}_{-02}^{(1)} \\ \underline{\hat{\psi}}_{-03}^{(1)} \\ \underline{\hat{\psi}}_{-01}^{(2)} \\ \underline{\hat{\psi}}_{-02}^{(2)} \\ \underline{\hat{\psi}}_{-03}^{(2)} \end{bmatrix} = \begin{bmatrix} \underline{\hat{\psi}}_1^{(1)} * \underline{\hat{\psi}}_{-01}^{(1)} & 0 & 0 & 0 & 0 & 0 \\ 0 & \underline{\hat{\psi}}_2^{(1)} * \underline{\hat{\psi}}_{-02}^{(1)} & 0 & 0 & 0 & 0 \\ 0 & 0 & \underline{\hat{\psi}}_3^{(1)} * \underline{\hat{\psi}}_{-03}^{(1)} & 0 & 0 & 0 \\ 0 & 0 & 0 & \underline{\hat{\psi}}_1^{(2)} * \underline{\hat{\psi}}_{-01}^{(2)} & 0 & 0 \\ 0 & 0 & 0 & 0 & \underline{\hat{\psi}}_2^{(2)} * \underline{\hat{\psi}}_{-02}^{(2)} & 0 \\ 0 & 0 & 0 & 0 & 0 & \underline{\hat{\psi}}_3^{(2)} * \underline{\hat{\psi}}_{-03}^{(2)} \end{bmatrix} \begin{Bmatrix} \omega_1^{(1)} \\ \omega_2^{(1)} \\ \omega_3^{(1)} \\ \omega_1^{(2)} \\ \omega_2^{(2)} \\ \omega_3^{(2)} \end{Bmatrix} \quad (4.91)$$

Equation (4.91) can be rearranged in the form

$$\left\{ \begin{array}{l} \omega_1^{(1)} \\ \omega_2^{(1)} \\ \omega_3^{(1)} \\ \omega_1^{(2)} \\ \omega_2^{(2)} \\ \omega_3^{(2)} \end{array} \right\} = \left[ \begin{array}{cc} \frac{1}{\psi_1^{(1)} * \psi_{o1}^{(1)}} & \psi_{o1}^{(1)T} \\ \frac{1}{\psi_2^{(1)} * \psi_{o2}^{(1)}} & \psi_{o2}^{(1)T} \\ \frac{1}{\psi_3^{(1)} * \psi_{o3}^{(1)}} & \psi_{o3}^{(1)T} \\ \frac{1}{\psi_1^{(2)} * \psi_{o1}^{(2)}} & \psi_{o1}^{(2)T} \\ \frac{1}{\psi_2^{(2)} * \psi_{o2}^{(2)}} & \psi_{o2}^{(2)T} \\ \frac{1}{\psi_3^{(2)} * \psi_{o3}^{(2)}} & \psi_{o3}^{(2)T} \end{array} \right] \{\hat{\underline{S}}\} \quad (4.92)$$

Further, since the square matrix on the right side of (4.92) is, in general, nonsingular, then (4.92) can be expressed in the same form (see equation (4.59)),

$$\hat{\underline{\psi}} = \omega \underline{S} = \begin{bmatrix} \underline{R}_1 & \underline{R}_2 & \underline{R}_3 & \underline{R}_4 & \underline{R}_5 & \underline{R}_6 \end{bmatrix} \left\{ \begin{array}{l} \omega_1^{(1)} \\ \omega_2^{(1)} \\ \omega_3^{(1)} \\ \omega_1^{(2)} \\ \omega_2^{(2)} \\ \omega_3^{(2)} \end{array} \right\} \quad (4.93)$$

The twist  $\hat{\underline{s}}$  representing the instantaneous motion of the end-effector can be determined from (4.93) and also it can be deduced from (4.62) (for  $M = 6$ ,  $g = 3$  and  $N = 2$ ) and

$$\begin{aligned}\hat{\underline{s}} = \omega \underline{s} = & (\omega_1^{(1)} \underline{R}_1 + \omega_2^{(1)} \underline{R}_2 + \omega_3^{(1)} \underline{R}_3) \\ & + (\omega_1^{(2)} \underline{R}_4 + \omega_2^{(2)} \underline{R}_5 + \omega_3^{(2)} \underline{R}_6)\end{aligned}\quad (4.94)$$

It should be noted that for the above simple parallel device, which consists of a single-closed loop, a single screw equation can be written and solved without taking orthogonal products. The screw equation can be expressed in the form

$$\begin{aligned}(\omega_1^{(1)} \underline{s}_1^{(1)} + \omega_2^{(1)} \underline{s}_2^{(1)} + \omega_3^{(1)} \underline{s}_3^{(1)} + \dots + \omega_6^{(1)} \underline{s}_6^{(1)}) \\ - (\omega_1^{(2)} \underline{s}_1^{(2)} + \omega_2^{(2)} \underline{s}_2^{(2)} + \omega_3^{(2)} \underline{s}_3^{(2)} + \dots + \omega_6^{(2)} \underline{s}_6^{(2)}) = 0\end{aligned}\quad (4.95)$$

and further expressed in the matrix form

$$\begin{aligned}
 & \left[ \begin{matrix} \phi_1^{(1)} & \phi_2^{(1)} & \phi_3^{(1)} & \phi_1^{(2)} & \phi_2^{(2)} & \phi_3^{(2)} \end{matrix} \right] \left\{ \begin{matrix} \omega_1^{(1)} \\ \omega_2^{(1)} \\ \omega_3^{(1)} \\ -\omega_1^{(2)} \\ -\omega_2^{(2)} \\ -\omega_3^{(2)} \end{matrix} \right\} \\
 &= \left[ \begin{matrix} \phi_1^{(1)} & \phi_5^{(1)} & \phi_6^{(1)} & \phi_4^{(2)} & \phi_5^{(2)} & \phi_6^{(2)} \end{matrix} \right] \left\{ \begin{matrix} -\omega_4^{(1)} \\ -\omega_5^{(1)} \\ -\omega_6^{(1)} \\ \omega_4^{(2)} \\ \omega_5^{(2)} \\ \omega_6^{(2)} \end{matrix} \right\} \quad (4.96)
 \end{aligned}$$

Also, since the square matrix on the right side of (4.96) is nonsingular, in general, then (4.96) can be expressed in the form

$$\left\{ \begin{matrix} \omega_4^{(2)} \\ \omega_5^{(2)} \\ \omega_6^{(2)} \\ \omega_4^{(1)} \\ \omega_5^{(1)} \\ \omega_6^{(1)} \end{matrix} \right\} = \begin{bmatrix} E_{11} & E_{12} & E_{13} & E_{14} & E_{15} & E_{16} \\ E_{21} & E_{22} & E_{23} & E_{24} & E_{25} & E_{26} \\ E_{31} & E_{32} & E_{33} & E_{34} & E_{35} & E_{36} \\ E_{41} & E_{42} & E_{43} & E_{44} & E_{45} & E_{46} \\ E_{51} & E_{52} & E_{53} & E_{54} & E_{55} & E_{56} \\ E_{61} & E_{62} & E_{63} & E_{64} & E_{65} & E_{66} \end{bmatrix} \left\{ \begin{matrix} \omega_1^{(1)} \\ \omega_2^{(1)} \\ \omega_3^{(1)} \\ \omega_1^{(2)} \\ \omega_2^{(2)} \\ \omega_3^{(2)} \end{matrix} \right\} \quad (4.97)$$

Expanding (4.97), explicit expressions for the unknown scalar multipliers can be written as follows

$$\begin{aligned}\omega_j^{(1)} = & (E_{j1}\omega_1^{(1)} + E_{j2}\omega_2^{(1)} + E_{j3}\omega_3^{(1)}) \\ & + (E_{j4}\omega_1^{(2)} + E_{j5}\omega_2^{(2)} + E_{j6}\omega_3^{(2)})\end{aligned}\quad (4.98)$$

where  $j = 4, 5, 6$ . Substituting (4.98) in the first twist equation in (4.90), then  $\hat{\underline{\$}}$  can be expressed in the form

$$\begin{aligned}\hat{\underline{\$}} = \omega \underline{\$} = & \sum_{m=1}^3 \{ \omega_m^{(1)} [\underline{\$}_m^{(1)} + \sum_{j=4}^6 E_{jm} \underline{\$}_j^{(1)}] \\ & + \omega_m^{(2)} [ \sum_{j=4}^6 E_{j(m+3)} \underline{\$}_j^{(1)} ] \}\end{aligned}\quad (4.99)$$

Equation (4.99) is analogous to (4.27).

Now consider that all actuators are locked except the actuator at the third joint in the first subchain, i.e.,  $\omega_3^{(1)} \neq 0$  and  $\omega_1^{(1)} = \omega_2^{(1)} = \omega_1^{(2)} = \omega_2^{(2)} = \omega_3^{(2)} = 0$ . The instantaneous motion of the end-effector will be due solely to the input twist  $\omega_3^{(1)} \underline{\$}_3^{(1)}$ . The partial twist representing this motion can be determined from (4.95) as follows

$$\hat{\underline{\$}}_{p3}^{(1)} = \omega_{p3}^{(1)} \underline{\$}_{p3}^{(1)} = \omega_3^{(1)} \underline{\$}_3 \quad (4.100)$$

Introducing this notation, (4.94) can be expressed in the form

$$\hat{\underline{\$}} = \omega \underline{\$} = \hat{\underline{\$}}_{p1}^{(1)} + \hat{\underline{\$}}_{p2}^{(1)} + \hat{\underline{\$}}_{p3}^{(1)} + \hat{\underline{\$}}_{p1}^{(2)} + \hat{\underline{\$}}_{p2}^{(2)} + \hat{\underline{\$}}_{p3}^{(2)} \quad (4.101)$$

Therefore, (4.101) indicates that the twist  $\hat{\underline{\$}}$  representing the instantaneous motion of the end-effector is the sum of all six partial twists of the end-effector.

Finally, for the reverse solution, where the twist  $\hat{\underline{s}}$  representing the instantaneous motion of the end-effector is specified, it is required to compute the six input twists. From (4.93), expressions for the six unknown scalar multipliers can be expressed in the form

$$\omega_j^{(1)} = \frac{\hat{\underline{s}}^* \underline{s}_{oj}}{\underline{s}_j^{(1)} * \underline{s}_{oj}^{(1)}} \quad (\text{or} = \frac{\hat{\underline{s}}_o \underline{s}_{rj}^{(1)}}{\underline{s}_j^{(1)} o \underline{s}_{rj}^{(1)}}) \quad (4.102)$$

$$\omega_j^{(2)} = \frac{\hat{\underline{s}}^* \underline{s}_{oj}^{(2)}}{\underline{s}_j^{(2)} * \underline{s}_{oj}^{(2)}} \quad (\text{or} = \frac{\hat{\underline{s}}_o \underline{s}_{rj}^{(2)}}{\underline{s}_j^{(2)} o \underline{s}_{rj}^{(2)}}) \quad (4.103)$$

where  $j = 1, 2, 3$ .

#### 4.3.6 Instantaneous Kinematics of the End-Effector of a Planar Fully-Parallel Symmetrical Device

The instantaneous kinematics of the end-effector of the planar version of the spherical three-degree of freedom Florida Shoulder (see Fig. 4.7) is now investigated in detail using the procedure described in sections 4.3.1-4.3.4. The end-effector platform is connected to the base by three subchains, i.e.,  $N = 3$ . In order for the end-effector to have mobility  $M = 3$ , there is one input actuator in each subchain ( $g = \frac{M}{N} = 1$ ). It is assumed to be located at the base, i.e.,  $\omega_1^{(1)} \underline{s}_1^{(1)}$ ,  $\omega_1^{(2)} \underline{s}_1^{(2)}$ , and  $\omega_1^{(3)} \underline{s}_1^{(3)}$  are the three known input twists.

The twist  $\hat{\underline{s}}$ , ( $= \omega \underline{s}$ ), representing the instantaneous motion of the end-effector can be expressed as a linear combination of the joint twists in any subchain in the device (see equation (4.56)),



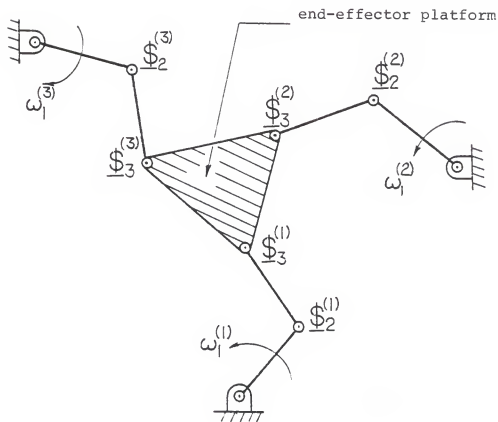


Figure 4.7. Planar Version of the Spherical Florida Shoulder

$$\hat{\underline{\$}} = \omega \underline{\$} = \omega_1^{(i)} \underline{\$}_1^{(i)} + \omega_2^{(i)} \underline{\$}_2^{(i)} + \omega_3^{(i)} \underline{\$}_3^{(i)} \quad (4.104)$$

for  $i = 1, 2, 3$ .

For the forward solution where the three input scalar multipliers are specified, it is necessary to eliminate two ( $M-g = 3-1 = 2$ ) unknown scalar multipliers  $\omega_2^{(i)}$  and  $\omega_3^{(i)}$  in each subchain. As mentioned previously in section 4.3.2, this is accomplished by determining three screws  $\underline{\$}_{o1}^{(1)}$ ,  $\underline{\$}_{o1}^{(2)}$  and  $\underline{\$}_{o1}^{(3)}$  orthogonal to the screws  $\{\underline{\$}_2^{(1)}, \underline{\$}_3^{(1)}\}$ ,  $\{\underline{\$}_2^{(2)}, \underline{\$}_3^{(2)}\}$  and  $\{\underline{\$}_2^{(3)}, \underline{\$}_3^{(3)}\}$  respectively. Taking the orthogonal product of both sides of (4.104) with the appropriate orthogonal screw, gives three ( $M = 3$ ) linear equations which can be expressed in the matrix form,

$$\begin{bmatrix} \hat{\underline{\$}} * \underline{\$}_{o1}^{(1)} \\ \hat{\underline{\$}} * \underline{\$}_{o1}^{(2)} \\ \hat{\underline{\$}} * \underline{\$}_{o1}^{(3)} \end{bmatrix} = \begin{bmatrix} \underline{\$}_1^{(1)} * \underline{\$}_{o1}^{(1)} & 0 & 0 \\ 0 & \underline{\$}_1^{(2)} * \underline{\$}_{o1}^{(2)} & 0 \\ 0 & 0 & \underline{\$}_1^{(3)} * \underline{\$}_{o1}^{(3)} \end{bmatrix} \begin{Bmatrix} \omega_1^{(1)} \\ \omega_1^{(2)} \\ \omega_1^{(3)} \end{Bmatrix} \quad (4.105)$$

When the device is not in a special configuration (see section 5.2), equation (4.105) can be rearranged in the form

$$\begin{Bmatrix} \omega_1^{(1)} \\ \omega_1^{(2)} \\ \omega_1^{(3)} \end{Bmatrix} = \begin{bmatrix} \frac{1}{\underline{\$}_1^{(1)} * \underline{\$}_{o1}^{(1)}} \underline{\$}_{o1}^{(1)T} \\ \frac{1}{\underline{\$}_1^{(2)} * \underline{\$}_{o1}^{(2)}} \underline{\$}_{o1}^{(2)T} \\ \frac{1}{\underline{\$}_1^{(3)} * \underline{\$}_{o1}^{(3)}} \underline{\$}_{o1}^{(3)T} \end{bmatrix} \{\hat{\underline{\$}}\} \quad (4.106)$$

Equation (4.106) could be derived directly from (4.58) for  $g = 1$  and  $N = 3$ .

Further, since the square matrix on the right side of (4.106) is, in general, nonsingular, then (4.106) can be expressed in the form

$$\hat{\underline{\$}} = [\underline{R}_1 \quad \underline{R}_2 \quad \underline{R}_3] \begin{Bmatrix} \omega_1^{(1)} \\ \omega_1^{(2)} \\ \omega_1^{(3)} \end{Bmatrix} \quad (4.107)$$

From (4.107), the twist  $\hat{\underline{\$}}$  representing the instantaneous motion of the end-effector can be expressed as follows:

$$\hat{\underline{\$}} = \omega_1^{(1)} \underline{R}_1 + \omega_1^{(2)} \underline{R}_2 + \omega_1^{(3)} \underline{R}_3 \quad (4.108)$$

Equation (4.108) could be derived from (4.62), for  $g = 1$  and  $N = 3$ .

Now consider that all actuators are locked except the one at the first base joint in the first subchain, i.e.,  $\omega_1^{(2)} = \omega_1^{(3)} = 0$  and  $\omega_1^{(1)} \neq 0$ . The instantaneous motion of the end-effector is due solely to the input twist  $\omega_1^{(1)} \underline{\$}_1^{(1)}$ . The partial twist representing this motion will be labelled  $\hat{\underline{\$}}_{p1}^{(1)}$ . Equation (4.108) reduces to

$$\hat{\underline{\$}}_{p1}^{(1)} = \omega_1^{(1)} \underline{\$}_{p1}^{(1)} = \omega_1^{(1)} \underline{R}_1 \quad (4.109)$$

Similarly, the partial twists  $\hat{\underline{\$}}_{p1}^{(2)}$  and  $\hat{\underline{\$}}_{p1}^{(3)}$  representing the instantaneous motion of the end-effector due to the input twists  $\omega_1^{(2)} \underline{\$}_1^{(2)}$  and  $\omega_1^{(3)} \underline{\$}_1^{(3)}$  respectively are given by

$$\hat{\$}_{p1}^{(2)} = \omega_{p1}^{(2)} \hat{\$}_{p1}^{(2)} = \omega_1^{(2)} \underline{R}_2 \quad (4.110)$$

and

$$\hat{\$}_{p1}^{(3)} = \omega_{p1}^{(3)} \hat{\$}_{p1}^{(3)} = \omega_1^{(3)} \underline{R}_3 \quad (4.111)$$

Introducing this notation, (4.108) can be expressed in the form

$$\hat{\$} = \omega \hat{\$} = \hat{\$}_{p1}^{(1)} + \hat{\$}_{p1}^{(2)} + \hat{\$}_{p1}^{(3)} \quad (4.112)$$

Therefore, (4.112) indicates that the twist  $\hat{\$}$  representing the instantaneous motion of the end-effector is the sum of the three partial twists.

For the reverse solution where the twist  $\hat{\$}$  representing the instantaneous motion of the end-effector is specified, it is required to compute the three input twists. From (4.105) the three unknown scalar multipliers can be expressed in the form

$$\omega_1^{(1)} = \frac{\hat{\$} * \hat{\$}_{o1}^{(1)}}{\hat{\$}_1^{(1)} * \hat{\$}_{o1}^{(1)}} \quad (\text{or} = \frac{\hat{\$}_o \hat{\$}_{r1}^{(1)}}{\hat{\$}_1^{(1)} \hat{\$}_{r1}^{(1)}}) \quad (4.113)$$

$$\omega_1^{(2)} = \frac{\hat{\$} * \hat{\$}_{o1}^{(2)}}{\hat{\$}_1^{(2)} * \hat{\$}_{o1}^{(2)}} \quad (\text{or} = \frac{\hat{\$}_o \hat{\$}_{r1}^{(2)}}{\hat{\$}_1^{(2)} \hat{\$}_{r1}^{(2)}}) \quad (4.114)$$

$$\text{and} \quad \omega_1^{(3)} = \frac{\hat{\$} * \hat{\$}_{o1}^{(3)}}{\hat{\$}_1^{(3)} * \hat{\$}_{o1}^{(3)}} \quad (\text{or} = \frac{\hat{\$}_o \hat{\$}_{r1}^{(3)}}{\hat{\$}_1^{(3)} \hat{\$}_{r1}^{(3)}}) \quad (4.115)$$

The above expressions for  $\omega_1^{(1)}$ ,  $\omega_1^{(2)}$ , and  $\omega_1^{(3)}$  could be derived directly from equation (4.69) for  $m = 1$  and  $i = 1, 2, 3$ .

#### 4.4 Instantaneous Kinematics of the End-Effector of Asymmetrical Fully-Parallel Devices

The general analysis procedures developed in sections 4.2 and 4.3 cannot be applied directly to asymmetrical devices. This is simply because a unified notation cannot be devised for counting the number of joints and the number and location of the actuated joints in each subchain. Therefore, each asymmetrical device will be analyzed separately.

Figure 4.8 illustrates an asymmetrical fully-parallel device in which the end-effector platform is connected to the base by three subchains, ( $N=3$ ). In order for the end-effector to have mobility  $M = 6$ , six input actuators are needed to drive the platform. They will be assumed to be located as follows: three at the first three joints from the base of the first subchain, two at the first two joints from the base of the second subchain, and one at the base joint of the third subchain, i.e.,  $\omega_1^{(1)}$ ,  $\omega_2^{(1)}$ ,  $\omega_3^{(1)}$ ,  $\omega_1^{(2)}$ ,  $\omega_2^{(2)}$ , and  $\omega_1^{(3)}$  are the known input scalar multipliers.

Procedures analogous to both procedures of sections 4.2 and 4.3 could be developed for the analysis of this asymmetrical device. However, a procedure analogous to that of section 4.3 is presented in this section.

The twist  $\hat{\$}$  representing the instantaneous motion of the end-effector platform can be expressed in the form

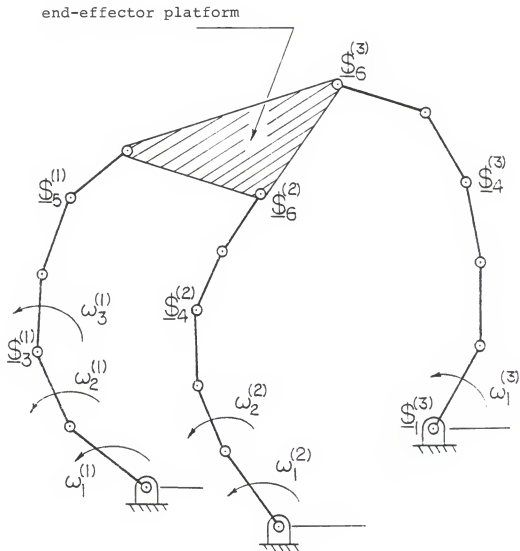


Figure 4.8. Six-Degree of Freedom Fully-Parallel Asymmetrical Device with Three Connecting Subchains to Platform

$$\begin{aligned}
\hat{\underline{\$}} &= \omega \underline{\$} = \omega_1^{(1)} \underline{\$}_1^{(1)} + \omega_2^{(1)} \underline{\$}_2^{(1)} + \omega_3^{(1)} \underline{\$}_3^{(1)} + \dots + \omega_6^{(1)} \underline{\$}_6^{(1)} \\
&= \omega_1^{(2)} \underline{\$}_1^{(2)} + \omega_2^{(2)} \underline{\$}_2^{(2)} + \omega_3^{(2)} \underline{\$}_3^{(2)} + \dots + \omega_6^{(2)} \underline{\$}_6^{(2)} \\
&= \omega_1^{(3)} \underline{\$}_1^{(3)} + \omega_2^{(3)} \underline{\$}_2^{(3)} + \omega_3^{(3)} \underline{\$}_3^{(3)} + \dots + \omega_6^{(3)} \underline{\$}_6^{(3)}
\end{aligned}
\tag{4.116}$$

In the above set of equations (4.116) there are three unknown scalar multipliers,  $\omega_4^{(1)}$ ,  $\omega_5^{(1)}$ , and  $\omega_6^{(1)}$ , in the first equation, four scalar multipliers,  $\omega_3^{(2)}$ ,  $\omega_4^{(2)}$ ,  $\omega_5^{(2)}$ , and  $\omega_6^{(2)}$ , in the second equation and five unknown scalars,  $\omega_2^{(3)}$ ,  $\omega_3^{(3)}$ ,  $\omega_4^{(3)}$ ,  $\omega_5^{(3)}$ , and  $\omega_6^{(3)}$ , in the third equation. In order to determine the twist  $\hat{\underline{\$}}$  it is necessary to determine six orthogonal screws,  $\underline{\$}_{o1}^{(1)}$ ,  $\underline{\$}_{o2}^{(1)}$ ,  $\underline{\$}_{o3}^{(1)}$ ,  $\underline{\$}_{o1}^{(2)}$ ,  $\underline{\$}_{o2}^{(2)}$ , and  $\underline{\$}_{o1}^{(3)}$ , where  $\underline{\$}_{o1}^{(i)}$  is orthogonal to the set of screws  $\{\underline{\$}_2^{(i)}, \underline{\$}_3^{(i)}, \underline{\$}_4^{(i)}, \underline{\$}_5^{(i)}, \underline{\$}_6^{(i)}\}$  for  $i = 1, 2, 3$ ;  $\underline{\$}_{o2}^{(i)}$  is orthogonal to the set of screws  $\{\underline{\$}_1^{(i)}, \underline{\$}_3^{(i)}, \underline{\$}_4^{(i)}, \underline{\$}_5^{(i)}, \underline{\$}_6^{(i)}\}$  for  $i = 1, 2$ ; and  $\underline{\$}_{o3}^{(1)}$  is orthogonal to  $\{\underline{\$}_1^{(1)}, \underline{\$}_2^{(1)}, \underline{\$}_4^{(1)}, \underline{\$}_5^{(1)}, \underline{\$}_6^{(1)}\}$ . Taking the orthogonal products of  $\underline{\$}_{o1}^{(1)}$ ,  $\underline{\$}_{o2}^{(1)}$ , and then of  $\underline{\$}_{o3}^{(1)}$  with the first equation of (4.116), of  $\underline{\$}_{o1}^{(2)}$  and  $\underline{\$}_{o2}^{(2)}$  with the second equation, and of  $\underline{\$}_{o1}^{(3)}$  with the third equation in (4.116) gives six ( $M=6$ ) equations which are linear in the six known input twists. This set of equations can be written in the matrix form

$$\begin{bmatrix} \hat{f}_{-01}^{(1)} \\ \hat{f}_{-02}^{(1)} \\ \hat{f}_{-03}^{(1)} \\ \hat{f}_{-01}^{(2)} \\ \hat{f}_{-02}^{(2)} \\ \hat{f}_{-01}^{(3)} \end{bmatrix} = \begin{bmatrix} \hat{f}_{-01}^{(1)} * \hat{f}_{-01}^{(1)} & 0 & 0 & 0 & 0 & 0 \\ 0 & \hat{f}_{-02}^{(1)} * \hat{f}_{-02}^{(1)} & 0 & 0 & 0 & 0 \\ 0 & 0 & \hat{f}_{-03}^{(1)} * \hat{f}_{-03}^{(1)} & 0 & 0 & 0 \\ 0 & 0 & 0 & \hat{f}_{-01}^{(2)} * \hat{f}_{-01}^{(2)} & 0 & 0 \\ 0 & 0 & 0 & 0 & \hat{f}_{-02}^{(2)} * \hat{f}_{-02}^{(2)} & 0 \\ 0 & 0 & 0 & 0 & 0 & \hat{f}_{-01}^{(3)} * \hat{f}_{-01}^{(3)} \end{bmatrix} \begin{pmatrix} \omega_1^{(1)} \\ \omega_2^{(1)} \\ \omega_3^{(1)} \\ \omega_1^{(2)} \\ \omega_2^{(2)} \\ \omega_1^{(3)} \end{pmatrix}$$

(4.117)



The characteristic matrix equation (4.117) can be rearranged in the form

$$\left\{ \begin{array}{l} \omega_1^{(1)} \\ \omega_2^{(1)} \\ \omega_3^{(1)} \\ \omega_1^{(2)} \\ \omega_2^{(2)} \\ \omega_1^{(3)} \end{array} \right\} = \left[ \begin{array}{l} \frac{1}{\underline{\mathbb{I}}_1^{(1)} * \underline{\mathbb{I}}_{o1}^{(1)}} \underline{\mathbb{I}}_{o1}^{(1)T} \\ \frac{1}{\underline{\mathbb{I}}_2^{(1)} * \underline{\mathbb{I}}_{o2}^{(1)}} \underline{\mathbb{I}}_{o2}^{(1)T} \\ \frac{1}{\underline{\mathbb{I}}_3^{(1)} * \underline{\mathbb{I}}_{o3}^{(1)}} \underline{\mathbb{I}}_{o3}^{(1)T} \\ \frac{1}{\underline{\mathbb{I}}_1^{(2)} * \underline{\mathbb{I}}_{o1}^{(2)}} \underline{\mathbb{I}}_{o1}^{(2)T} \\ \frac{1}{\underline{\mathbb{I}}_2^{(2)} * \underline{\mathbb{I}}_{o2}^{(2)}} \underline{\mathbb{I}}_{o2}^{(2)T} \\ \frac{1}{\underline{\mathbb{I}}_1^{(3)} * \underline{\mathbb{I}}_{o1}^{(3)}} \underline{\mathbb{I}}_{o1}^{(3)T} \end{array} \right] \{\hat{\underline{\mathbb{I}}}\} \quad (4.118)$$

Further, since the square matrix on the right side of (4.118) is, in general, nonsingular, then (4.118) can be expressed in the form

$$\hat{\underline{\mathbb{I}}} = \omega \underline{\mathbb{I}} = [\underline{R}_1 \ \underline{R}_2 \ \underline{R}_3 \ \underline{R}_4 \ \underline{R}_5 \ \underline{R}_6] \left\{ \begin{array}{l} \omega_1^{(1)} \\ \omega_2^{(1)} \\ \omega_3^{(1)} \\ \omega_1^{(2)} \\ \omega_2^{(2)} \\ \omega_1^{(3)} \end{array} \right\} \quad (4.119)$$

Expanding (4.119), the twist  $\hat{\$}$  can be expressed in the form

$$\begin{aligned}\hat{\$} = \omega \$ = & (\omega_1^{(1)} \underline{R}_1 + \omega_2^{(1)} \underline{R}_2 + \omega_3^{(1)} \underline{R}_3) \\ & + (\omega_1^{(2)} \underline{R}_4 + \omega_2^{(2)} \underline{R}_5 + \omega_3^{(2)} \underline{R}_6) \quad (4.120)\end{aligned}$$

Now consider that all actuators are locked except the actuator at the second joint in the first subchain, i.e.,  $\omega_1^{(1)}, \omega_3^{(1)}, \omega_1^{(2)}, \omega_2^{(2)}$ , and  $\omega_1^{(3)} = 0$  and  $\omega_2^{(1)} \neq 0$ . The instantaneous motion of the end-effector platform is due solely to the input twist  $\omega_2^{(1)} \hat{\$}_{p2}^{(1)}$ . The partial twist  $\hat{\$}_{p2}^{(1)}$  representing this instantaneous motion can be determined from (4.120) by substituting  $\omega_1^{(1)}, \omega_3^{(1)}, \omega_1^{(2)}, \omega_2^{(2)}$ , and  $\omega_1^{(3)} = 0$ , yielding

$$\hat{\$}_{p2}^{(1)} = \omega_{p2}^{(1)} \hat{\$}_{p2}^{(1)} = \omega_2^{(1)} \underline{R}_2 \quad (4.121)$$

In a similar fashion, the other partial twists can be expressed in the form

$$\hat{\$}_{p1}^{(1)} = \omega_{p1}^{(1)} \hat{\$}_{p1}^{(1)} = \omega_1^{(1)} \underline{R}_1 \quad (4.122)$$

$$\hat{\$}_{p3}^{(1)} = \omega_{p3}^{(1)} \hat{\$}_{p3}^{(1)} = \omega_3^{(1)} \underline{R}_3 \quad (4.123)$$

$$\hat{\$}_{p1}^{(2)} = \omega_{p1}^{(2)} \hat{\$}_{p1}^{(2)} = \omega_1^{(2)} \underline{R}_4 \quad (4.124)$$

$$\hat{\$}_{p2}^{(2)} = \omega_{p2}^{(2)} \hat{\$}_{p2}^{(2)} = \omega_2^{(2)} \underline{R}_5 \quad (4.125)$$

and 
$$\hat{\$}_{p1}^{(3)} = \omega_{p1}^{(3)} \hat{\$}_{p1}^{(3)} = \omega_1^{(3)} \underline{R}_6 \quad (4.126)$$

Introducing this notation, (4.120) can be expressed in the form

$$\begin{aligned}\hat{\$} = \omega \hat{\$} = & (\hat{\$}_{p1}^{(1)} + \hat{\$}_{p2}^{(1)} + \hat{\$}_{p3}^{(1)}) \\ & + (\hat{\$}_{p1}^{(2)} + \hat{\$}_{p2}^{(2)}) + \hat{\$}_{p1}^{(3)}\end{aligned}\quad (4.127)$$

Then the twist  $\hat{\$}$  representing the instantaneous motion of the end-effector is the sum of all six partial twists.

For the reverse solution where the twist  $\hat{\$}$  representing the instantaneous motion of the end-effector is specified, the six unknown scalar multipliers can be expressed as follows:

$$\omega_j^{(1)} = \frac{\hat{\$}_j^{(1)} * \hat{\$}_{oj}^{(1)}}{\hat{\$}_j^{(1)} * \hat{\$}_{oj}^{(1)}} \quad (\text{or} = \frac{\hat{\$}_{oj}^{(1)} \hat{\$}_{rj}^{(1)}}{\hat{\$}_j^{(1)} \hat{\$}_{rj}^{(1)}}) \quad j = 1, 2, 3 \quad (4.128)$$

$$\omega_j^{(2)} = \frac{\hat{\$}_j^{(2)} * \hat{\$}_{oj}^{(2)}}{\hat{\$}_j^{(2)} * \hat{\$}_{oj}^{(2)}} \quad (\text{or} = \frac{\hat{\$}_{oj}^{(2)} \hat{\$}_{rj}^{(2)}}{\hat{\$}_j^{(2)} \hat{\$}_{rj}^{(2)}}) \quad j = 1, 2 \quad (4.129)$$

$$\text{and} \quad \omega_1^{(3)} = \frac{\hat{\$}_1^{(3)} * \hat{\$}_{o1}^{(3)}}{\hat{\$}_1^{(3)} * \hat{\$}_{o1}^{(3)}} \quad (\text{or} = \frac{\hat{\$}_{o1}^{(3)} \hat{\$}_{r1}^{(3)}}{\hat{\$}_1^{(3)} \hat{\$}_{r1}^{(3)}}) \quad (4.130)$$

The above expressions are obtained by solving (4.117).

## CHAPTER 5 SPECIAL CONFIGURATIONS

The first section of this chapter is essentially a literature survey of special configurations of single- and multi-loop devices [3,9,40-44]. The literature on multi-loop devices is sparse and the author has included in this section an introduction to the so-called uncertainty configurations of multi-loop devices.

In the second section, special configurations of fully-parallel devices are investigated in detail using the characteristic matrix equation (4.57) derived in the previous chapter. These results are then summarized in Table 5.1. By way of example, special configurations of the planar three-dof Florida Shoulder are studied in detail and numerical results are presented.

### 5.1 Special Configurations of Single- and Multi-Loop Devices

#### 5.1.1 Introduction

The term "Special Configuration" was introduced by Hunt in [3] and is used to describe various unique geometrical phenomena which occur in the motion of planar, spherical, and spatial mechanisms. Generally, for single-loop mechanisms, these special configurations could be categorized into "Stationary Configurations" and "Uncertainty

Configurations." In addition to these two types, an arrangement of interconnected links may form an immovable structure. Examples of a stationary configuration, an uncertainty configuration, and an immovable structure using the familiar planar four-bar linkage are shown in Fig. 5.1.

### 5.1.2 Stationary Configurations

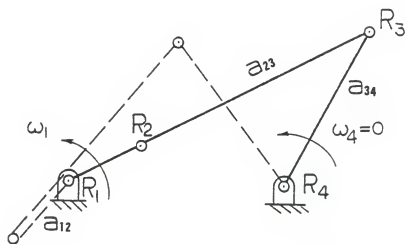
A kinematic chain is in stationary configuration when at least one joint is transitorily inactive. A joint is transitorily inactive when the scalar multiplier,  $\omega$ , of the twist of that joint is instantaneously zero no matter the values of the other multipliers.\*

A stationary configuration is referred to in the literature as an "extreme-range position," "dead center," "change point," or "limit position." However, the generality of the concept of stationary configurations is preferred as it relates to transitorily inactive freedom(s).

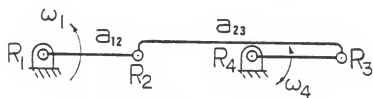
Consider the four-bar planar mechanism in Fig. 5.1(a). The revolute joint  $R_4$  is shown at its two extreme angular positions. In either case, the axes of screws  $\$1$ ,  $\$2$ , and  $\$3$  representing the relative motion of the first, second, and the third joints lie in the same plane. In this configuration the intersection of the two screw systems spanned by  $\{\$1, \$2, \$3\}$  and by  $\{\$4\}$  is the zero vector (see the parallel

---

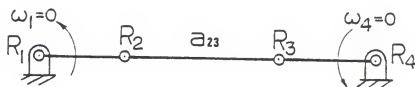
\*For kinematic chains with  $M > 1$ , a joint can be inactive if the  $M$  independent input scalar multipliers happen to have values that make the scalar multipliers associated with this joint vanish. However, it is inappropriate to call such a joint an inactive joint [40].



(a) stationary configuration



(b) uncertainty configuration



(c) immovable configuration

Figure 5.1. Special Configurations and Immovable Structure of a Planar Four-Bar

law, equation (2.30)) and therefore joint  $R_4$  is considered to be transitorily inactive (or equivalently, link  $a_{34}$  is transitorily inactive), i.e.,  $\omega_4 = 0$ .

Hunt [3] introduced a theorem which can be restated as follows:

When  $(g-p)$  screws of a single-closed loop mechanism containing  $g$  ( $= d+1$ ) single-freedom joints become linearly dependent instantaneously and none of the remaining  $p$  linearly independent\* screws are linearly dependent on these  $(g-p)$  screws, then the  $(g-p)$  screws form a configuration with mobility one, i.e., they belong to a  $((g-p)-1)$ , ( $= d-p$ ), system. The remaining  $p$  screws form a configuration which cannot move instantaneously. The mechanism is said to be in a simple, double, triple, . . . , stationary configuration respectively when  $p = 1, 2, 3, \dots, 5$ .

Figure 5.1(a) illustrates a simple stationary configuration, ( $g=4$ , and  $p=1$ ). Figure 5.2 illustrates a spatial four link RSCR mechanism in a double stationary configuration, ( $g=7$  and  $p=2$ ), for which the five screws  $\underline{\$}_1, \underline{\$}_2, \dots, \underline{\$}_5$  belong to a four-system. There are two linearly independent screws  $\underline{\$}_{r1}$  and  $\underline{\$}_{r2}$  (pure forces) which are reciprocal to the four-system. The remaining two screws,  $\underline{\$}_6$  and  $\underline{\$}_7$ , representing the translatory freedom of the C-pair and the rotary freedom of the  $R_7$  pair are instantaneously inactive.

Stationary configurations of a single-closed loop mechanism [41,42] can be detected by monitoring all the  $[dx]$  determinants of the  $[dx(d+1)]$  matrix of the screw coordinates (see equation (2.44)), or alternatively by monitoring

---

\*If these  $p$  screws are not linearly independent, then it is an uncertainty configuration which is discussed in the next section.

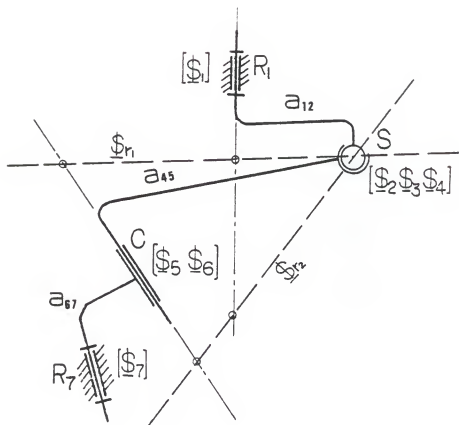


Figure 5.2. R-S-C-R Spatial Mechanism in a Double Stationary Configuration



the [dxd] Gramians of the  $g$  screws (see equation (2.45) with  $n=g$ ). A  $k$ th joint is inactive when the [dxd] determinant which does not include the  $k$ th column vector vanishes, (or when the [dxd] determinant, deduced from the Gramian, which does not include both the  $k$ th row and column, vanishes).

Equation (2.43), which was derived for a single-loop mechanism, can be easily extended to multi-loop mechanisms. Davies [38] derived such an equation for mechanism with  $v$  independent loops\* and called it the constraint equation (see equation (4.10)). The constraint equation can be transferred into the canonical form (see equation (4.11))

$$\left[ \begin{array}{c|c} I_{r,r} & A_{r,M} \\ \hline O_{6v-r,r} & O_{6v-r,M} \end{array} \right] \left\{ \begin{array}{c} \omega_{r,1} \\ \dot{q}_{M,1} \end{array} \right\} = O_{6v,1} \quad (5.1)$$

Equation (5.1) is everywhere identical to (4.11) except that the subscript  $M$  replaces the subscript  $F$ . When a unit element in the identity matrix  $I_{r,r}$  is the only non-zero element in that row of the constraint matrix  $C_{6v,e}$ , then the corresponding element of  $\omega_{r,1}$ , i.e., the corresponding scalar multiplier, must be zero and the corresponding joint is said to be transitorily inactive. Equation (5.1) can be rearranged in the following form which highlights the zero elements of  $\omega_{r,1}$ :

---

\*When  $v = 1$ , equation (2.43) and (4.10) are identical.

$$\left[ \begin{array}{c|c} I_{p,p} & O_{p,e-p} \\ \hline O_{6v-p,p} & \begin{array}{c|c} I_{r-p,r-p} & A_{r-p,M} \\ \hline & O_{6v-r,e-p} \end{array} \end{array} \right] \begin{Bmatrix} \omega_{p,1} \\ \omega_{r-p,1} \\ \dot{q}_{M,1} \end{Bmatrix} = O_{6v,1} \quad (5.2)$$

In equation (5.2),  $M$  is the degree of freedom,  $e$  is the number of joints,  $r$  is the rank of the constraint matrix  $C_{6v,e}$  (see equation (4.10), and  $\dot{q}_{M,1}$  is an  $[M \times 1]$  column vector which contains the  $M$  known input scalar multipliers (primary coordinates). The secondary coordinates  $\omega_{r,1}$  have been further subdivided into the  $p$  coordinates comprising  $\omega_{p,1}$  that have zero values, and  $(r-p)$  comprising  $\omega_{r-p,1}$  that can be expressed in terms of the primary coordinates  $\dot{q}_{M,1}$ . Further, the following result can be deduced from (5.2):

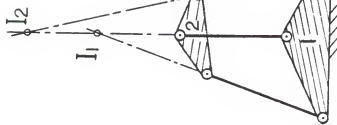
When the scalar multiplier of the twist of a joint is instantaneously zero no matter the values of the other multipliers, the mechanism is said to be in a stationary configuration. When one joint is transitorily inactive ( $p=1$ ), the mechanism is in a simple stationary configuration. When two, three, ..., etc., joints are transitorily inactive ( $p=2, 3, \dots$ ), the mechanism is in a double, triple, ..., etc. stationary configuration.

It is important to note that a stationary configuration does not affect the rank  $r$  of the constraint matrix. For instance, all seven screws in Fig. 5.2 belong to a six-system when the mechanism is not in a stationary configuration and also when the mechanism is in a simple, double, ..., etc. stationary configuration.

### 5.1.3 Uncertainty Configurations

Stationary configurations for mechanisms for which one or more joints have become transitorily inactive have been discussed. It is now appropriate to discuss the special configurations of structures for which one or more joints have become transitorily active.

As an example, consider the pin-jointed structure with zero overall mobility illustrated in Fig. 5.3(a). Here, neither of the two independent loops which when considered separately are planar four-bar mechanisms can have motion since the ternary 2 cannot rotate simultaneously about two distinct instant centers  $I_1$  and  $I_2$ . However, Figs. 5.3(b) and (c) which are topologically the same as Fig. 5.3(a) illustrate configurations which are respectively transitorily mobile and permanently mobile. For the configuration illustrated in Fig. 5.3(b),  $I_1$  and  $I_2$  coincide instantaneously at point I and therefore the ternary 2 can rotate throughout an infinitesimal angle about I. However any finite relative motion could, of course, destroy that special geometrical feature of coincidence. Buckens [43] called the configuration in Fig. 5.3(b), "Singular," Paul [44] said the configuration had an instantaneously critical form, while Hunt [3] simply said it was transitorily mobile. Whereas, for the configuration illustrated in Fig. 5.3(c),  $I_1$  and  $I_2$  coincide permanently at a point at infinity. This configuration of the double parallelogram, Fig. 5.3(c), which has complete



(a) a jointed structure

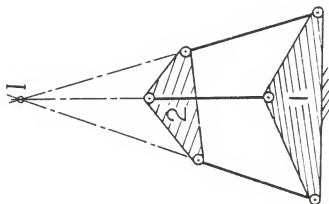
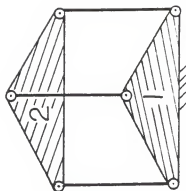
(b) a jointed structure  
with transitory  
mobility(c) a double parallelogram  
with full-cycle  
mobility

Figure 5.3. Some Planar Arrangements with the Same Topology

cycle mobility was described by Paul [44] to be in a permanently critical form.

The above discussion is illustration that a structure can gain one or more freedoms and become mobile. Analogously, a mechanism can transitorily acquire one or more extra degrees of freedom during its cycle. For example, consider the planar four-bar mechanism illustrated in Fig. 5.1(b). The axes of all four screws representing the joint motions lie in the same plane. It has a transitory mobility  $M = 2$  and therefore it can open up in two distinct ways (see Fig. 2.7, [3]). It is also important to note that when any joint in Fig. 5.1(b) is locked there still a transitorily mobile flattened triangle which is also a jointed structure with transitory mobility  $M = 1$ .

Uncertainty configurations are often referred to in the literature as "folded configurations," "flattened configurations," or "locking or cross-over positions." However, the generality of the concept of uncertainty configuration is preferred as it relates to the acquisition of one (or more) extra mobility (or reduction in constraints).

Hunt introduced a theorem in [3], which can be restated as follows:

When all the  $g$  ( $=d+1$ ) screws representing the instantaneous motion of the joints of a single-closed loop mechanism with ordinary mobility  $M = 1$  are linearly dependent and belong to a  $g-(j+1)$  screw system, then these  $g$  screws are reciprocal to  $j$  common reciprocal screw(s),  $1 \leq j \leq (d-1)$ , and the loop is said to be at a  $j$ -fold uncertainty configuration and its mobility is transitorily increased by  $j$ , i.e., increased from  $M = 1$  to  $M = j+1$ .

As an example, consider the RSCR spatial mechanism illustrated in Fig. 5.4. In this configuration, all the seven screws representing the joint motions have become linearly dependent and they instantaneously belong to a five-system, i.e., the rank of the matrix of all seven screws is reduced from six to five. There is a single screw  $\$_{\underline{r}}$  (a pure force) reciprocal to all these seven screws. Depending upon the inertial loading, when the input link  $a_{12}$  is being driven, there are two distinct modes for the motion of the remaining links. The mechanism has instantaneously mobility  $M = 2$  and is said to be in a single-fold uncertainty configuration.

Uncertainty configurations [41,42] of single-closed loop mechanisms can also be detected by monitoring the  $[dx(d+1)]$  matrix of screw coordinates (see equation (2.44)) or their Gramian (see equation (2.45)). A  $j$ -fold uncertainty configuration occurs when the rank of this matrix is  $(d-j)$ .

As discussed in the previous section, equation (2.43) can be extended to mechanisms with  $v$  independent loops (see

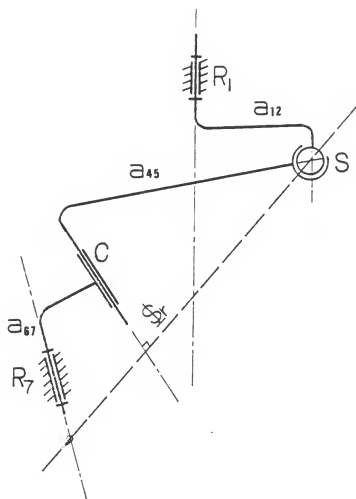


Figure 5.4. R-S-C-R Spatial Mechanism in a Single-Fold Uncertainty Configuration

equation (5.1)). Equation (5.1)\* can be used to determine uncertainty configurations for both single- and multi-loop mechanisms, and

A  $j$ -fold uncertainty configuration occurs when the rank of the constraint matrix  $C_{6v,e}$  is instantaneously reduced by  $j$  (i.e., from  $r$  to  $(r-j)$ ). This means that there exist  $j$  independent screws reciprocal to the screw system of all screws of the mechanism.

A mechanism can ordinarily be expected to have several stationary configurations in its cycle and it will pass through provided that the input actuator's freedom never become inactive. However, a mechanism will not ordinarily encounter an uncertainty configuration during its cycle unless it has special dimensions. Mechanisms which have uncertainty configurations are obviously best avoided.

However, it is sometimes difficult to distinguish between stationary and uncertainty configurations of mechanisms, especially parallel mechanisms.

## 5.2 Special Configurations of Fully-Parallel Devices

### 5.2.1 Introduction

Fully-Parallel devices may also encounter some special configurations other than those discussed in the previous

---

\*In the canonical form, equation (5.1), there are  $(6v-r)$  zero rows which represent constraints that are additional to the minimum necessary for the mechanism to perform its intended function. These additional constraints are called in [40] redundant constraints, and the number  $R = 6v-r$  is called the degree of redundancy. A mechanism with redundancy is usually called an overconstrained or overclosed mechanism.



sections. Such special configurations will not be detected in a straight-forward approach using the only existing procedure for multi-loop devices which was introduced by Davies [40] and has been reviewed in the previous sections (5.1.2, 5.1.3).

Equation (4.57), together with equation (4.58), most elegantly describes the instantaneous kinematics of fully-parallel devices and gives the geometrical conditions for special configurations. The characteristic matrix equation (4.57) can be rewritten as follows:

$$\begin{bmatrix} \underline{\$}_1^{(1)} * \underline{\$}_{o1}^{(1)} & 0 & \dots & \dots & 0 \\ 0 & \underline{\$}_2^{(1)} * \underline{\$}_{o2}^{(1)} & & \dots & 0 \\ \vdots & \vdots & & & \vdots \\ 0 & 0 & \underline{\$}_g^{(1)} * \underline{\$}_{og}^{(1)} & & 0 \\ \vdots & \vdots & \vdots & & \vdots \\ \vdots & \vdots & \vdots & & \vdots \\ 0 & 0 & \dots & 0 & \dots & \underline{\$}_g^{(N)} * \underline{\$}_{og}^{(N)} \end{bmatrix} \begin{Bmatrix} \omega_1^{(1)} \\ \omega_2^{(1)} \\ \vdots \\ \omega_g^{(1)} \\ \vdots \\ \omega_g^{(N)} \end{Bmatrix} = \begin{bmatrix} \underline{\$}_{o1}^{(1)T} \\ \underline{\$}_{o2}^{(1)T} \\ \vdots \\ \underline{\$}_{og}^{(1)T} \\ \vdots \\ \underline{\$}_{og}^{(N)T} \end{bmatrix} \{\hat{\underline{\$}}\} \quad (5.3)$$

Further, (5.3) can be expressed in the abbreviated form

$$[C]\{\underline{\omega}\} = [D]\{\hat{\underline{\$}}\} \quad (5.4)$$

where [C] is a [MxM] diagonal matrix and [D] is also a [MxM] matrix, (M = gN, see Chapter 4).

A mechanism is in special configurations at the instant that at least one of the two matrices [C] and [D] in equation (5.4) becomes singular. When matrix [C] becomes singular

there are additional constraints acting upon the end-effector platform, and when matrix [D] becomes singular there are restrictions on the input velocities. Six different cases may arise. These cases are described and investigated in detail in the following sections.

### 5.2.2 Case I

Matrix [C] becomes singular if and only if at least one of its diagonal elements becomes zero, i.e.,

$$\hat{\$}_j^{(i)} * \hat{\$}_{oj}^{(i)} = 0 \quad (5.5)$$

for  $i = 1, 2, \dots$ , or  $N$ , and  $j = 1, 2, \dots$ , or  $g$ . Equation (5.5) implies that the screw  $\hat{\$}_{oj}^{(i)}$  is orthogonal to (or, equivalently, the corresponding screw  $\hat{\$}_{rj}^{(i)}$  is reciprocal to) all  $M$  screws in the  $i$ th subchain since  $\hat{\$}_{oj}^{(i)}$  is (by definition) orthogonal to all screws in the subchain except  $\hat{\$}_j^{(i)}$ . Therefore, these  $M$  screws are not linearly independent and the screw system  $W_i$  spanned by these  $M$  screws degenerates,

$$\dim(W_i) < M \quad (5.6)$$

It can be deduced from (5.4) that when  $n$  diagonal elements of [C] vanish simultaneously, then the corresponding  $n$  orthogonal screws  $\hat{\$}_{oj}^{(i)}$  in [D] represent the unattainable motion of the end-effector platform. This is because

$$\hat{\$} * \hat{\$}_{oj}^{(i)} = 0 \quad (5.7)$$

where  $\hat{\$}$  is the twist representing the instantaneous motion of the end-effector. Therefore, the order of the screw

system representing the instantaneous motion of the platform reduces by  $n$  and there are  $n$  extra constraints acting upon the platform, provided that the set of these  $n$  orthogonal screws are themselves not linearly dependent.

It can thus be deduced that when  $[D]$  is nonsingular and that when  $[C]$  is singular, its rank being reduced by  $n$ , the platform then loses  $n$  freedoms.

It is important to notice that the value of each scalar multiplier  $\omega_j^{(i)}$  associated with a screw  $\$j^{(i)}$  that satisfies equation (5.5) is arbitrary. In other words, the values of the scalar multipliers  $\omega_j^{(i)}$  do not affect the resultant instantaneous motion of the end-effector platform.

### 5.2.3 Case II

When all the diagonal elements of matrix  $[C]$  become zero simultaneously, i.e.,

$$\$j^{(i)} \cdot \$o_j^{(i)} = 0 \quad (5.8)$$

and the screw system spanned by the  $M$  screws in each sub-chain degenerates\*,

$$\dim(W_i) < M \quad (5.9)$$

for  $i = 1, 2, \dots, N$ . This means that all the  $M$  orthogonal screws in  $[D]$  represent the unattainable motion of the end-effector platform since

---

\*The subchains considered here are those subchains that contain at least one actuated joint (for asymmetrical devices).

$$\hat{\$}_i * \hat{\$}_{oj}^{(i)} = 0$$

When matrix [D] is nonsingular, all these M orthogonal screws are linearly independent and they form an orthogonal screw system which represents the unattainable motion of the end-effector platform. Since this orthogonal screw system spans the whole space, the platform will be immovable and the device becomes an immovable structure regardless of the values of the inputs.

#### 5.2.4 Case III

Matrix [D] becomes singular when its M rows, which are the M orthogonal screws  $\hat{\$}_{oj}^{(i)}$  become linearly dependent. The rank of [D] reduces instantaneously. When matrix [C] is nonsingular, equation (5.4) can be expressed in the form (see also equation (4.58)).

$$\left\{ \begin{matrix} \omega_1^{(1)} \\ \omega_2^{(1)} \\ \vdots \\ \omega_g^{(1)} \\ \vdots \\ \omega_g^{(N)} \end{matrix} \right\} = \left[ \begin{array}{ccc} \frac{1}{\hat{\$}_1^{(1)} * \hat{\$}_{o1}^{(1)}} & \hat{\$}_{o1}^{(1)T} \\ \frac{1}{\hat{\$}_2^{(1)} * \hat{\$}_{o2}^{(1)}} & \hat{\$}_{o2}^{(1)T} \\ \vdots & \vdots \\ \frac{1}{\hat{\$}_g^{(1)} * \hat{\$}_{og}^{(1)}} & \hat{\$}_{og}^{(1)T} \\ \vdots & \vdots \\ \frac{1}{\hat{\$}_g^{(N)} * \hat{\$}_{og}^{(N)}} & \hat{\$}_{og}^{(N)T} \end{array} \right] \{\hat{\$}\} \quad (5.11)$$

Equation (5.11) can also be expressed in the abbreviated form

$$\{\underline{\omega}\} = [A] \{\hat{\underline{\$}}\} \quad (5.12)$$

where  $[A] = [C]^{-1}[D]$ .

The inverse  $[C]^{-1}$  is nonsingular and thus the rank of  $[A]$  is equal to the rank,  $r$ , of  $[D]$  which is less than  $M$ . Therefore, the column space of  $[A]$ ,  $cs[A]$ , is of order  $r$ . In order for equation (5.12) to have at least a solution, the column vector  $\{\omega\}$  has to be an element of the column space of  $[A]$ , i.e.,  $\{\omega\} \in cs[A]$ . The input scalar multipliers cannot be chosen independently, therefore, since  $\dim(cs[A]) < M$ . In this case for a specified set of inputs  $\{\omega\}$  there exists more than one solution  $\hat{\underline{\$}}$ . Therefore, it can be concluded that the  $M$  chosen inputs are dependent and are not capable of controlling\* the end-effector platform for any specified motion. In order to control the platform some other joint or joints must be actuated.

The twist  $\hat{\underline{\$}}$  representing the instantaneous motion of the end-effector platform is in the form

$$\hat{\underline{\$}} = \{\hat{\underline{\$}}_0\} + (a_1 \hat{\underline{\$}}_1 + a_2 \hat{\underline{\$}}_2 + \dots + a_v \hat{\underline{\$}}_v) \quad (5.13)$$

where  $\{\hat{\underline{\$}}_0\}$  is a solution to equation (5.12),  $a_1, a_2, \dots, a_v$  are  $v$  ( $= M-r$ ) independent scalars, and  $\{\hat{\underline{\$}}_1, \hat{\underline{\$}}_2, \dots, \hat{\underline{\$}}_v\}$  form a basis for the solution set of the corresponding

---

\*A wrench applied to the end-effector platform cannot be controlled (resisted) by these  $M$  inputs.

homogeneous system\*  $[A]\hat{\underline{\$}} = \underline{0}$ . Therefore, by locking all these  $M$  dependent chosen input actuated joints,  $\{\underline{\omega}\} = \underline{0}$ , the system will not be a structure as it should be. Such linkages were described by Buckens [43] as having a singular configuration. The remaining linkage will be in a simple, double,... etc. singular configuration if  $v = 1, 2, \dots$ , etc.

It can now be concluded that when matrix  $[C]$  is non-singular and that when  $[D]$  is singular then the input scalar multipliers cannot be chosen independently.

#### 5.2.5 Case IV

For Case I matrix  $[C]$  was singular when  $n$  diagonal elements ( $1 \leq n < M$ ) were zero simultaneously with the corresponding  $n$  orthogonal screws  $\underline{\$}_{oj}^{(i)}$  in  $[D]$  representing the unattainable motion of the end-effector platform, and matrix  $[D]$  was nonsingular.

Consider now that  $[D]$  also become singular because any one screw  $\underline{\$}_{oj}^{(i)}$  of the remaining  $(M-n)$  orthogonal screws in  $[D]$  is dependent on the  $n$  orthogonal screws. The scalar multiplier  $\omega_j^{(i)}$  associated with this  $\underline{\$}_{oj}^{(i)}$  must vanish and the joint is momentarily inactive. More generally, a subset of the  $(M-n)$  orthogonal screws can become dependent on those  $n$  screws. Each of the scalar multipliers associated with the  $(M-n)$  screws in the subset must vanish momentarily. All the

---

\* $\{\underline{\$}_1, \underline{\$}_2, \dots, \underline{\$}_v\}$  form a basis for the kernel of  $[A]$ , i.e., a basis of the null space of  $[A]$ . The dimension of the null space of  $[A]$  is called the nullity of  $[A]$  and it is equal to  $v$  ( $= M-r$ ).

(M-n) input joints associated with these screws thus are momentarily inactive. This type of configuration is analogous to the stationary configuration discussed in section (5.1.2).

It is interesting to note that when the inputs are locked, the system will not be a structure. It will have instantaneous mobility. The twist  $\hat{\$}$  representing the instantaneous motion of the end-effector platform in the system is determined by the null space of [D].

#### 5.2.6 Case V

Consider again that matrix [C] is singular because n diagonal elements ( $1 \leq n < M$ ) are zero simultaneously and therefore the corresponding n orthogonal screws  $\$_{oj}^{(i)}$  in [D] represent the unattainable motion of the end-effector platform. Consider also that [D] is singular because the n orthogonal screws have themselves become linearly dependent. The order of the screw system representing the unattainable motion is less than n and as in Case I each of the n scalar multipliers is arbitrary.

However, [D] can also become singular when the remaining (M-n) orthogonal screws become linearly dependent. Here the scalar multipliers associated with these (M-n) screws are themselves dependent whilst, as above, the n scalar multipliers are arbitrary.

In conclusion, by locking the inputs, the system will not be a structure but will have instant mobility. The twist  $\hat{\$}$

representing the motion of the end-effector platform can be determined by the null space of matrix  $[D]$ .

#### 5.2.7 Case VI

When all diagonal elements of matrix  $[C]$  become zero simultaneously, then all  $M$  orthogonal screws  $\$_{oj}^{(i)}$  in  $[D]$  represent the unattainable motion of the end-effector platform. All the  $M$  input scalar multipliers are arbitrary and their values do not affect the instantaneous motion of the end-effector platform.

When matrix  $[D]$  becomes singular, then all  $M$  orthogonal screws become linearly dependent and they form an orthogonal screw system of order  $(M-n)$  which represents the unattainable motion of the end-effector platform. Therefore, the end-effector platform has  $n$  remaining freedom(s) and these  $n$  freedom(s) cannot be controlled by the  $M$  independently chosen inputs.

This type of configuration is analogous to the uncertainty configuration, discussed earlier in section (5.1.3). A device is in a simple, double, ... uncertainty configuration when  $n = 1, 2, \dots$ .

The above six types of special configurations are listed in Table 5.1. It can be concluded that unlike single-loop devices with mobility one, special configurations of fully-parallel devices with mobility greater than one cannot be defined simply as stationary and uncertainty configurations. Whilst, Cases IV and VI can be defined respectively



Table 5.1  
Types of Special Configurations  
Of Fully-Parallel Devices\*

Case No.	Matrix [C] is Singular		Matrix [C] Is Nonsingular	Matrix [D] Is Singular	Matrix [D] Is Nonsingular
	[C] Is Zero	[C] Is Nonzero			
I					
II					
III					
IV					
V					
VI					

\*For the difference between Case IV and Case V, see sections 5.2.5 and 5.2.6.

as stationary and uncertainty configurations, Cases I, II, III, and V cannot. Admittedly, Case II which is an immovable structure perhaps should not be included.

### 5.2.8 Special Configurations of the Planar Version of the Florida Shoulder\*

#### Case I

Two distinct types of Case I special configurations can occur:

(a) Figure 5.5 illustrates the device with the first subchain in a fully extended configuration. The axes of the three revolute joints lie in the same plane and the screws  $\$1^{(1)}$ ,  $\$2^{(1)}$ , and  $\$3^{(1)}$  are therefore linearly dependent and form a two-system, i.e.,

$$\dim (W_1) = 2$$

Therefore, a screw  $\$01^{(1)}$  which is orthogonal to  $\{\$2^{(1)}, \$3^{(1)}\}$  is also orthogonal to  $\$1^{(1)}$  and,

$$\$1^{(1)} * \$01^{(1)} = 0$$

The first diagonal element of matrix [C] vanishes instantaneously and [C] become singular. Equation (5.4) reduces to

---

\*Special configurations of the planar version of the Florida Shoulder were first considered by Cox [4] in which he gave an expository account.

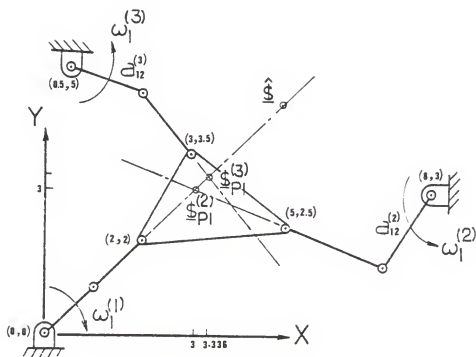


Figure 5.5. Example of Case I-(a)

$$\begin{bmatrix} 0 & 0 & 0 \\ 0 & -3.75 & 0 \\ 0 & 0 & -1.375 \end{bmatrix} \begin{Bmatrix} \omega_1^{(1)} \\ \omega_1^{(2)} \\ \omega_1^{(3)} \end{Bmatrix} = \begin{bmatrix} 0 & 1 & 1 \\ 8.25 & -2 & 0.75 \\ -7.5 & 1 & -1.25 \end{bmatrix} \{\hat{\underline{\$}}\}$$

It is clear that the three orthogonal screws  $\underline{\$}_{o1}^{(1)}$ ,  $\underline{\$}_{o1}^{(2)}$ , and  $\underline{\$}_{o1}^{(3)}$  are linearly independent and that  $\underline{\$}_{o1}^{(1)}$  represents the unattainable motion of the end-effector platform,  $\underline{\$}_{o1}^{(1)} * \hat{\underline{\$}} = 0$ . The twist  $\hat{\underline{\$}}$  representing the instantaneous motion of the end-effector must lie along that plane formed by the axes of  $\underline{\$}_1^{(1)}$ ,  $\underline{\$}_2^{(1)}$ , and  $\underline{\$}_3^{(1)}$  and also formed by the two partial twists\*  $\hat{\underline{\$}}_{p1}^{(2)}$  and  $\hat{\underline{\$}}_{p1}^{(3)}$ . Therefore the twist  $\hat{\underline{\$}}$  can be represented as the sum of these two partial twists, and

$$\begin{aligned} \hat{\underline{\$}} &= \hat{\underline{\$}}_{p1}^{(2)} + \hat{\underline{\$}}_{p1}^{(3)} \\ &= 4.0512 \omega_1^{(2)} \begin{Bmatrix} 1 \\ 3.336 \\ -3.336 \end{Bmatrix} + 1.833 \omega_1^{(3)} \begin{Bmatrix} 1 \\ 3 \\ -3 \end{Bmatrix} \end{aligned}$$

It is apparent that the end-effector platform can move only in a direction normal to that plane and therefore has only two freedoms instantaneously. The input scalar multiplier  $\omega_1^{(1)}$  can assume any value without effecting the instantaneous motion of the end-effector platform.

It is interesting to note that when the two input links  $a_{12}^{(2)}$  and  $a_{12}^{(3)}$  are locked simultaneously, the system becomes a

---

\*The point formed by the intersection of the axis of the partial twist  $\hat{\underline{\$}}_{p1}^{(i)}$ , ( $i=1,2,3$ ), and the plane of the device is identical with the planar instant center, [4].

structure and all joints become inactive, regardless of the value of  $\omega_1^{(1)}$ .

Clearly the analysis is the same when any other subchain is in a fully extended configuration or when it is in a folded configuration (see Fig. 5.6).

(b) Figure 5.7 illustrates the device with the first and second subchains in fully extended configurations. The axes of screws  $\underline{\$}_1^{(1)}$ ,  $\underline{\$}_2^{(1)}$ , and  $\underline{\$}_3^{(1)}$  lie in one plane whilst the axes of screws  $\underline{\$}_1^{(2)}$ ,  $\underline{\$}_2^{(2)}$ , and  $\underline{\$}_3^{(2)}$  lie in another plane. Equation (5.4) reduces to

$$\begin{bmatrix} 0 & 0 & 0 \\ 0 & 0 & 0 \\ 0 & 0 & -1.375 \end{bmatrix} \begin{Bmatrix} \omega_1^{(1)} \\ \omega_1^{(2)} \\ \omega_1^{(3)} \end{Bmatrix} = \begin{bmatrix} 0 & 1 & 1 \\ 8.25 & -2 & 0.75 \\ -7.5 & 1 & -1.25 \end{bmatrix} \{\hat{\underline{\$}}\}$$

The twist  $\hat{\underline{\$}}$  representing the instantaneous motion of the end-effector platform can be expressed as follows

$$\hat{\underline{\$}} = \hat{\underline{\$}}_{p1}^{(3)} = (1.833 \omega_1^{(3)}) \begin{Bmatrix} 1 \\ 3 \\ -3 \end{Bmatrix}$$

which passes through point (3,3).

The end-effector platform is capable instantaneously of rotating about the partial screw  $\underline{\$}_1^{(3)} = \begin{Bmatrix} 1 \\ 3 \\ -3 \end{Bmatrix}$  which is the line of intersection of the two planes, and therefore the end-effector platform loses two freedoms. It is important to note that the two input scalar multipliers  $\omega_1^{(1)}$  and  $\omega_1^{(2)}$  can assume any values without affecting the instantaneous

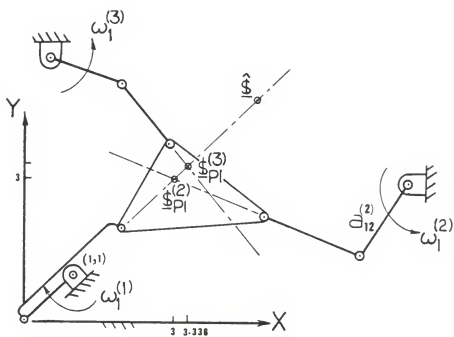


Figure 5.6. Example of Case I-(a) with Folded Subchain

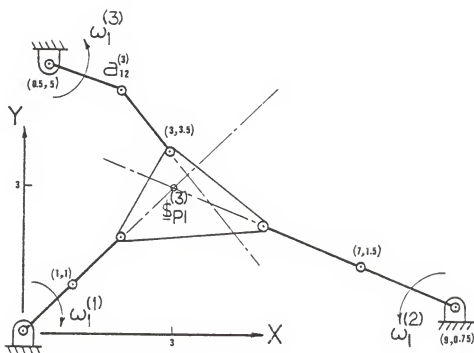


Figure 5.7. Example of Case I-(b)

motion of the platform. When the input link  $a_{12}^{(3)}$  is locked (i.e.,  $\omega_1^{(3)}$  becomes zero), the system becomes a structure.

### Case II

In this configuration all three subchains are fully extended and are not concurrent (Fig. 5.8). All three diagonal elements of matrix  $[C]$  vanish simultaneously and therefore all three input scalar multipliers can assume any value. Equation (5.4) reduces to

$$\begin{bmatrix} 0 & 0 & 0 \\ 0 & 0 & 0 \\ 0 & 0 & 0 \end{bmatrix} \begin{Bmatrix} \omega_1^{(1)} \\ \omega_1^{(2)} \\ \omega_1^{(3)} \end{Bmatrix} = \begin{bmatrix} 0 & 1 & 1 \\ 8.25 & -2 & 0.75 \\ -7.25 & 1 & -1.25 \end{bmatrix} \{\hat{\underline{x}}\}$$

Since the three fully extended subchains are not concurrent, the three orthogonal screws  $\underline{\$}_{o1}^{(1)}$ ,  $\underline{\$}_{o1}^{(2)}$ , and  $\underline{\$}_{o1}^{(3)}$  are linearly independent and form an orthogonal three-system that represents the unattainable motion of the end-effector platform. Therefore, the end-effector platform will become immovable and the device becomes a structure.

### Case III

(a) In the configuration shown in Fig. 5.9, the screws representing the relative motions of the joints in each subchain are linearly independent, i.e.,

$$\dim(W_i) = M = 3$$

for all subchains ( $i = 1, 2$ , and  $3$ ). Therefore matrix  $[C]$



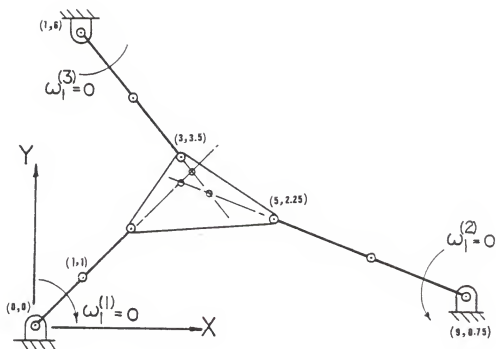


Figure 5.8. Example of Case II

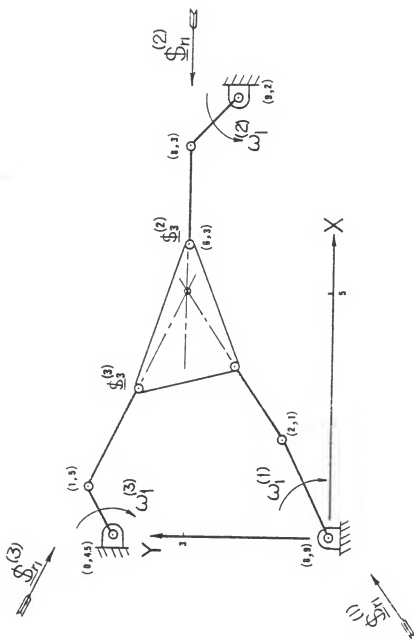


Figure 5.9. Example of Case III-(a)

in (5.4) is nonsingular and equation (5.11) becomes

$$\begin{Bmatrix} \omega_1^{(1)} \\ \omega_1^{(2)} \\ \omega_1^{(3)} \end{Bmatrix} = \begin{bmatrix} \frac{1}{0.5} & 0.5 & 1.5 & 1 \\ \frac{1}{2} & 6 & -2 & 0 \\ \frac{1}{-2} & -11 & 2 & -1 \end{bmatrix} \{\hat{\underline{s}}\}$$

The three orthogonal screws  $\underline{s}_{o1}^{(1)}$ ,  $\underline{s}_{o1}^{(2)}$ , and  $\underline{s}_{o1}^{(3)}$  are linearly dependent and form a two-system\*. Therefore, the three chosen input scalar multipliers are dependent and related as follows

$$\omega_1^{(3)} = 0.25 \omega_1^{(1)} + 1.75 \omega_1^{(2)}$$

The three chosen inputs are therefore not capable of controlling the end-effector platform. The only way for this device to exit this special configuration is by actuating some joint other than the base joints, such that  $\omega_1^{(1)}$ ,  $\omega_1^{(2)}$  and say  $\omega_3^{(3)}$  are not dependent.

The twist  $\hat{\underline{s}}$  representing the instantaneous motion of the end-effector platform can be expressed as follows

$$\hat{\underline{s}} = \begin{Bmatrix} 0.1 \omega_1^{(1)} + 0.3 \omega_1^{(2)} \\ 0.3 \omega_1^{(1)} - 0.1 \omega_1^{(2)} \\ 0 \end{Bmatrix} + a_1 \begin{Bmatrix} -0.2 \\ -0.6 \\ 1 \end{Bmatrix}$$

where  $a_1$  is a scalar.

\*The three corresponding reciprocal screws  $\underline{\$}_{r1}^{(1)}$ ,  $\underline{\$}_{r1}^{(2)}$ , and  $\underline{\$}_{r1}^{(3)}$  can be represented as three pure forces each acting along the centerline of link  $a_{23}^{(1)}$  in a subchain (i), (see Fig. 5.9). These three forces intersect in a point (5,3) and therefore the three reciprocal screws also form a two-system.

It is apparent from this expression that when the base joints of the first and second subchains are locked ( $\omega_1^{(1)} = \omega_1^{(2)} = 0$ ) the system will not be a structure. It is in a simple singular configuration ( $v=1$ ). The twist representing the instantaneous motion of the end-effector platform can now be expressed as follows

$$\hat{\underline{\$}} = -0.2 (a_1) \begin{Bmatrix} 1 \\ 3 \\ -5 \end{Bmatrix}$$

and the end-effector platform is capable of twisting about an ISA normal to the plane of the device and passing through point (5,3), see Fig. 5.10.

(b) In Fig. 5.11, none of the three subchains is stretched and therefore matrix [C] in (5.4) is nonsingular. Equation (5.11) reduces to

$$\begin{Bmatrix} \omega_1^{(1)} \\ \omega_1^{(2)} \\ \omega_1^{(3)} \end{Bmatrix} = \begin{bmatrix} \frac{1}{-3} (5.5 & -1.5 & 0.5) \\ \frac{1}{-1.5} (0.5 & -1 & -1) \\ \frac{1}{-0.5} (-0.5 & 1 & 1) \end{bmatrix} \{\hat{\underline{\$}}\}$$

The two orthogonal screws  $\underline{\$}_{o1}^{(2)}$  and  $\underline{\$}_{o1}^{(3)}$  are linearly dependent, ( $\underline{\$}_{o1}^{(3)} = -\underline{\$}_{o1}^{(2)}$ ), and therefore all three orthogonal screws  $\underline{\$}_{o1}^{(1)}$ ,  $\underline{\$}_{o1}^{(2)}$ , and  $\underline{\$}_{o1}^{(3)}$  are linearly dependent and form a two-system. Further, the two input scalar multipliers  $\omega_1^{(2)}$  and  $\omega_1^{(3)}$  are also dependent ( $\omega_1^{(3)} = -3 \omega_1^{(2)}$ ) and therefore all three chosen input scalar multipliers are dependent.

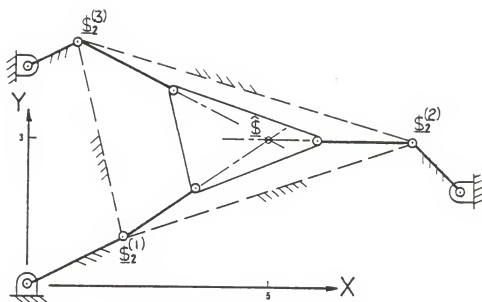


Figure 5.10. Example of Case III-(a)  
in Simple Singularity

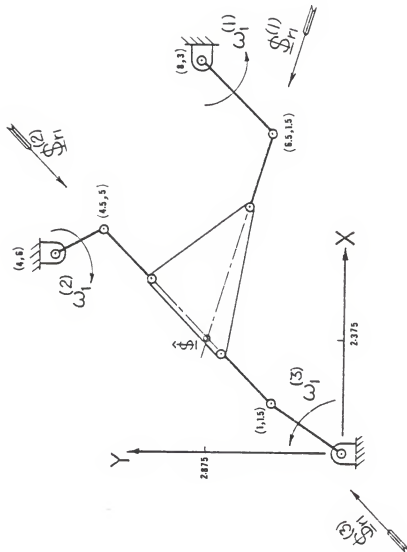


Figure 5.11. Example of Case III-(b)

The three chosen inputs are therefore not capable of controlling the end-effector platform.

The twist  $\hat{\underline{s}}$  representing the instantaneous motion of the end-effector platform can be expressed as follows

$$\hat{\underline{s}} = \begin{pmatrix} -0.6316 \omega_1^{(1)} - 0.1579 \omega_1^{(3)} \\ -0.3158 \omega_1^{(1)} - 0.5789 \omega_1^{(3)} \\ 0 \end{pmatrix} + a_1 \begin{pmatrix} -0.421 \\ -1.2105 \\ 1 \end{pmatrix}$$

where  $a_1$  is a scalar.

It is apparent from this expression that when the base joints of the first and third subchains are locked ( $\omega_1^{(1)} = \omega_1^{(3)} = 0$ ) the system will not be a structure. It is in a simple singular configuration ( $v=1$ ). The twist representing the instantaneous motion of the end-effector platform can now be expressed as follows

$$\hat{\underline{s}} = -0.421 (a_1) \begin{pmatrix} 1 \\ 2.875 \\ -2.375 \end{pmatrix}$$

and the end-effector platform is capable of twisting about ISA normal to the plane of the device and passes through point (2.375, 2.875), see Fig. 5.11.

(c) In the special configuration illustrated in Fig. 5.12, equation (5.11) reduces to

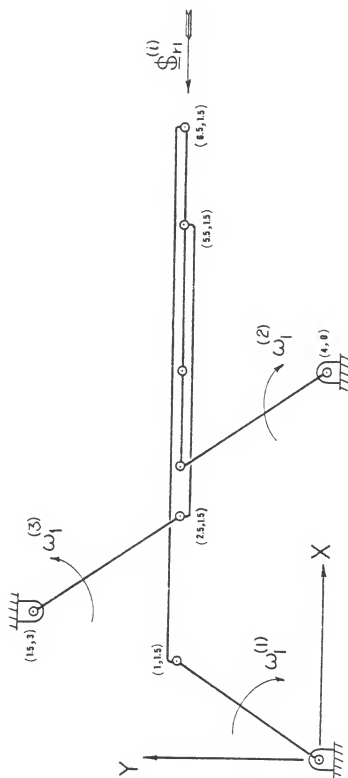


Figure 5.12. Example of Case III-(c)



$$\begin{Bmatrix} \omega_1^{(1)} \\ \omega_1^{(2)} \\ \omega_1^{(3)} \end{Bmatrix} = \begin{bmatrix} \frac{1}{-8.25} & (-8.25 & 5.5 & 0) \\ \frac{1}{-8.25} & (-8.25 & 5.5 & 0) \\ \frac{1}{8.25} & (-8.25 & 5.5 & 0) \end{bmatrix} \{ \hat{\underline{\$}} \}$$

All three orthogonal screws  $\underline{\$}_{o1}^{(1)}$ ,  $\underline{\$}_{o1}^{(2)}$ , and  $\underline{\$}_{o1}^{(3)}$  are linearly dependent, ( $\underline{\$}_{o1}^{(1)} = \underline{\$}_{o1}^{(2)} = \underline{\$}_{o1}^{(3)}$ ), and form a one-system\*.

Further, the three chosen input scalar multipliers are also dependent, ( $\omega_1^{(1)} = \omega_1^{(2)} = -\omega_1^{(3)}$ ). Therefore, the chosen three inputs are not capable of controlling the motion of the end-effector platform.

The twist  $\hat{\underline{\$}}$  representing the instantaneous motion of the end-effector platform can be expressed as follows

$$\hat{\underline{\$}} = \begin{Bmatrix} \omega_1^{(1)} \\ 1 \\ 0 \\ 0 \end{Bmatrix} + a_1 \begin{Bmatrix} 0.6667 \\ 1 \\ 0 \end{Bmatrix} + a_2 \begin{Bmatrix} 0 \\ 0 \\ 1 \end{Bmatrix}$$

where  $a_1$  and  $a_2$  are two independent scalars. It is apparent from this expression that when the base joint of the first subchain is locked the system will not be a structure. It is in a double singular configuration ( $v=2$ ). The twist representing the instantaneous motion of the end-effector platform can now be expressed in the form

---

\*A single pure force in the plane and passing through all joints of the device except the three base joints represents a one-system reciprocal to the joints in the folded configuration.

$$\hat{\mathbb{H}} = \frac{2}{3} a_1 \begin{Bmatrix} 1 \\ 1.5 \\ 0 \end{Bmatrix} + a_2 \begin{Bmatrix} 0 \\ 0 \\ 1 \end{Bmatrix}$$

The instantaneous motion is thus a combination of a pure rotation about an axis through the point (0, 1.5) and a pure translation (0 ; 0,1) parallel to the X-axis. This pure translation is equivalent to a rotation about an axis which is in the plane at infinity and which is perpendicular to the Y axis.

#### Case IV

Since the second subchain in the configuration illustrated in Fig. 5.13 is fully extended then the second diagonal element of  $[C]$ , in equation (5.4) is equal to zero, i.e.,  $n = 1$ , and

$$\hat{\mathbb{H}}_1^{(2)} * \mathbb{H}_{o1}^{(2)} = 0$$

Therefore the orthogonal screw  $\mathbb{H}_{o1}^{(2)}$  in this subchain is also orthogonal to the twist  $\hat{\mathbb{H}}$  representing the instantaneous motion of the end-effector platform, i.e., (see section 5.2.2, Case I)

$$\hat{\mathbb{H}} * \mathbb{H}_{o1}^{(2)} = 0$$

Equation (5.4) reduces to

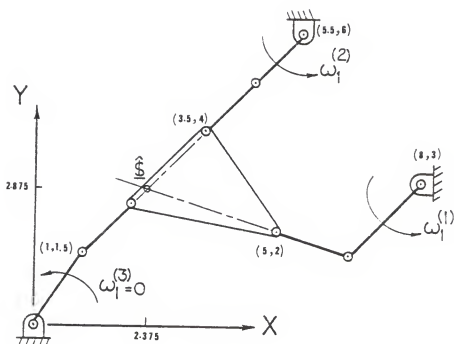


Figure 5.13. Example of Case IV

$$\begin{bmatrix} -3 & 0 & 0 \\ 0 & 0 & 0 \\ 0 & 0 & -0.5 \end{bmatrix} \begin{Bmatrix} \omega_1^{(1)} \\ \omega_1^{(2)} \\ \omega_1^{(3)} \end{Bmatrix} = \begin{bmatrix} 5.5 & -1.5 & 0.5 \\ 0.5 & -1 & -1 \\ -0.5 & 1 & 1 \end{bmatrix} \{\hat{\underline{\$}}\}$$

The orthogonal screw  $\underline{\$}_{01}^{(3)}$  is linearly dependent on  $\underline{\$}_{01}^{(2)}$ , ( $\underline{\$}_{01}^{(3)} = -\underline{\$}_{01}^{(2)}$ ). Since  $\underline{\$}_{01}^{(2)}$  is orthogonal to  $\hat{\underline{\$}}$  then  $\underline{\$}_{01}^{(3)}$  is also orthogonal to  $\hat{\underline{\$}}$  and therefore  $\underline{\$}_{01}^{(2)}$  and  $\underline{\$}_{01}^{(3)}$  form a one-system which represents the unattainable motion of the end-effector platform. Therefore, from the above matrix equation,  $\omega_1^{(2)}$  can assume any value while  $\omega_1^{(3)}$  has to equal zero, ( $-0.5 \omega_1^{(3)} = 0$ ). It is clear from Fig. 5.13 that screws  $\underline{\$}_1^{(2)}$ ,  $\underline{\$}_2^{(2)}$ ,  $\underline{\$}_3^{(2)}$ ,  $\underline{\$}_3^{(3)}$ , and  $\underline{\$}_2^{(3)}$  lie on the same plane and form a two-system while  $\underline{\$}_1^{(3)}$  is not contained in that two-system. Therefore, the base joint of the third subchain is inactive momentarily and the device is said to be in a stationary configuration.

It is apparent that when the three base joints are locked, or equivalently when just the base joint of the first subchain is locked ( $\omega_1^{(1)} = 0$ ) the system will not be a structure. It is in a simple singular configuration. The twist representing the instantaneous motion of the end-effector platform can now be expressed in the form

$$\hat{\underline{\$}} = -0.421 (a_1) \begin{Bmatrix} 1 \\ 2.875 \\ -2.375 \end{Bmatrix}$$

and therefore it is capable of twisting about an axis which is normal to the plane of the device and passes through point (2.375 , 2.875). This result is identical to that of Case III, example (b).

#### Case V

In the configuration illustrated in Fig. 5.14, only the first subchain is fully extended, i.e.,  $n = 1$ , and

$$\underline{\$}_1^{(1)} * \underline{\$}_{o1}^{(1)} = 0$$

Therefore,  $\underline{\$}_{o1}^{(1)}$  represents the unattainable motion of the end-effector platform and  $\omega_1^{(1)}$  can assume any value without affecting the instantaneous motion of the platform. In this case matrix [C] is nonzero singular matrix.

The other orthogonal screws  $\underline{\$}_{o1}^{(2)}$  and  $\underline{\$}_{o1}^{(3)}$  are linearly independent but this two-system is linearly dependent on that orthogonal screw  $\underline{\$}_{o1}^{(1)}$ , ( $\underline{\$}_{o1}^{(1)} = -\underline{\$}_{o1}^{(3)} - 1.75 \underline{\$}_{o1}^{(2)}$ ). Thus matrix [D] becomes singular. Equation (5.4) reduces to

$$\begin{bmatrix} 0 & 0 & 0 \\ 0 & 2 & 0 \\ 0 & 0 & -2 \end{bmatrix} \begin{Bmatrix} \omega_1^{(1)} \\ \omega_1^{(2)} \\ \omega_1^{(3)} \end{Bmatrix} = \begin{bmatrix} 0.5 & 1.5 & 1 \\ 6 & -2 & 0 \\ -11 & 2 & -1 \end{bmatrix} \{\hat{\underline{\$}}\}$$

The input scalar multipliers are dependent and therefore are not capable of controlling the end-effector platform.

By locking the inputs, the system will be identical to that illustrated in Fig. 5.10 (see Case III, example (a)).

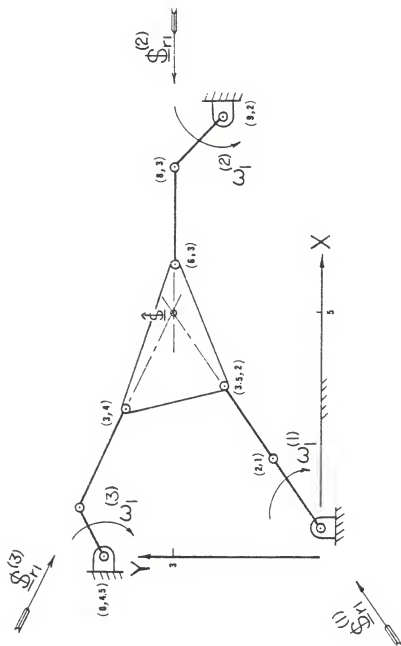


Figure 5.14. Example of Case V

Case VI

(a) In the configuration shown in Fig. 5.15 the three subchains meet at a single point (5, 3) and the three screw systems degenerate. Therefore, all diagonal elements in matrix [C] vanish simultaneously and matrix [C] becomes a zero singular matrix. Equation (5.4) reduces to

$$\begin{bmatrix} 0 & 0 & 0 \\ 0 & 0 & 0 \\ 0 & 0 & 0 \end{bmatrix} \begin{Bmatrix} \omega_1^{(1)} \\ \omega_1^{(2)} \\ \omega_1^{(3)} \end{Bmatrix} = \begin{bmatrix} 0.5 & 1.5 & 1 \\ 6 & -2 & 0 \\ -11 & 2 & -1 \end{bmatrix} \{\hat{\underline{\$}}\}$$

It is obvious from the above equation that all three input scalar multipliers  $\omega_1^{(1)}$ ,  $\omega_1^{(2)}$ , and  $\omega_1^{(3)}$  can assume any values and therefore all three independent inputs do not have any control on the instantaneous motion of the end-effector platform.

The three orthogonal screws  $\underline{\$}_{o1}^{(1)}$ ,  $\underline{\$}_{o1}^{(2)}$ , and  $\underline{\$}_{o1}^{(3)}$  are linearly dependent ( $\underline{\$}_{o1}^{(1)} + 1.75 \underline{\$}_{o1}^{(2)} = -\underline{\$}_{o1}^{(3)}$ ) and therefore form an orthogonal two-system which represents the unattainable motion of the end-effector platform. Thus the end-effector platform has one uncontrollable freedom. The twist  $\hat{\underline{\$}}$  representing this instantaneous motion of the platform can be described by the null space of matrix [D] and

$$\hat{\underline{\$}} = 0.2 (a_1) \begin{Bmatrix} 1 \\ 3 \\ -5 \end{Bmatrix}$$

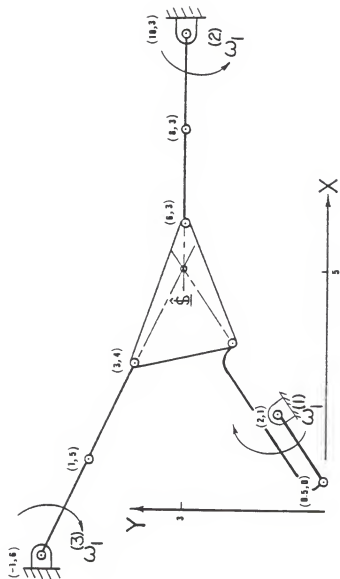


Figure 5.15. Example of Case VI-(a)



Therefore, this uncontrollable motion of the end-effector platform is a twisting motion of magnitude  $(0.2 a_1)$ , where  $a_1$  is an arbitrary scalar, about an axis normal to the plane and passing through point  $(5, 3)$  which is the point of intersection of the three subchains. The device in this configuration is said to be in a simple uncertainty configuration.

(b) For the configuration illustrated in Fig. 5.16 the three subchains meet at a single point  $(3.5, 3.5)$  which is the center of the third joint of the third subchain and the three screw systems degenerate. Equation (5.4) reduces to

$$\begin{bmatrix} 0 & 0 & 0 \\ 0 & 0 & 0 \\ 0 & 0 & 0 \end{bmatrix} \begin{Bmatrix} \omega_1^{(1)} \\ \omega_1^{(2)} \\ \omega_1^{(3)} \end{Bmatrix} = \begin{bmatrix} 0 & 1.5 & 1.5 \\ 7 & -1 & 1 \\ -5.25 & 0 & -1.5 \end{bmatrix} \{ \hat{\underline{\$}} \}$$

The analysis is similar to that of the previous example and the end-effector platform has one uncontrollable freedom which is a twist of magnitude  $(0.286 a_1)$  about an axis which coincides with the axis of  $\underline{\$}_3^{(3)}$ , i.e.,

$$\hat{\underline{\$}} = 0.286 (a_1) \begin{Bmatrix} 1 \\ 3.5 \\ -3.5 \end{Bmatrix}$$

The device is also in a simple uncertainty configuration.

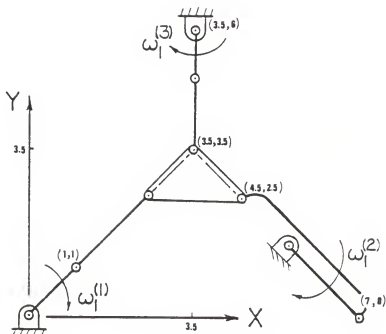


Figure 5.16. Example of Case VI-(b)

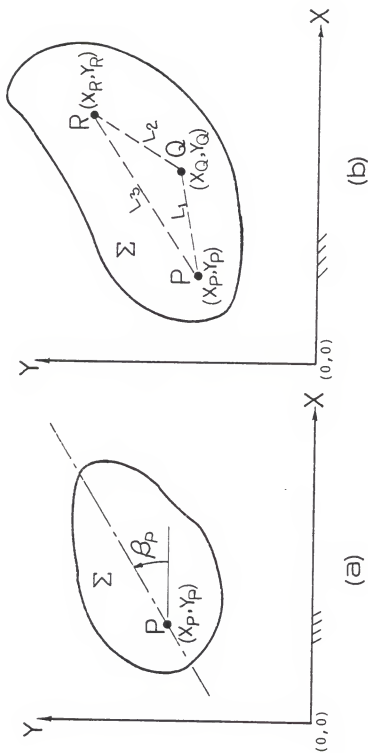
CHAPTER 6  
DISPLACEMENT ANALYSIS OF THE THREE-DoF  
PLANAR FLORIDA SHOULDER

### 6.1 Introduction

The location (position and orientation) of a rigid body (or Lamina  $\Sigma$ ), in a general co-planar motion can completely be defined with respect to the fixed plane of motion by three independent coordinates which may be chosen in a variety of ways. For example, Fig. 6.1(a), the cartesian coordinates  $(X_P, Y_P)$  of a reference point P fixed in the body and an orientation  $\beta_P$  of an arbitrary line in the plane passing through that reference point constitute three degrees of freedom which uniquely define the configuration of the body. Three distinct points P, Q, and R, Fig. 6.1(b) can be used to locate the lamina. They constitute only three independent parameters since the six parameters are related by the following three equations.

$$\begin{aligned}L_1^2 &= (X_Q - X_P)^2 + (Y_Q - Y_P)^2 \\L_2^2 &= (X_R - X_Q)^2 + (Y_R - Y_Q)^2 \\L_3^2 &= (X_R - X_P)^2 + (Y_R - Y_P)^2\end{aligned}\tag{6.1}$$

Analogous to the investigation of the instantaneous kinematics, the displacement analysis can also be categorized into two types of analyses. First it will be assumed that numerical values for the actuated joint displacements are known and

Figure 6.1.1. Lamina  $\Sigma$  in a General Planar Motion

it is required to compute the location of the end-effector lamina. This will be called the forward analysis, (analogous to the hand-location analysis-II of single-loop manipulators, [1]). Secondly it will be assumed that it is required to obtain a set of joint displacements which will locate the end-effector lamina at some prespecified position and orientation. This will be called the reverse analysis, (analogous to the hand-location analysis-I, [1]).

The notation developed in [1] for single-loop manipulators is adapted here to analyze the planar version of the Florida Shoulder illustrated by Fig. 6.2:

$a_{ij,n}$  : is the link connecting the  $i$ th and the  $j$ th joints in the  $n$ th subchain,

$a_{i,nm}$  : is the link connecting the  $i$ th joint in both the  $n$ th and the  $m$ th subchains,

$\theta_{i,j}$  : is the exterior angle measured about the  $i$ th joint axis in the  $j$ th subchain,

$\phi_{i,j}$  : is the angle that link  $a_{i(i+1),j}$  makes with the horizontal X-axis,

and

$(X_{ij}, Y_{ij})$  : are the X and Y coordinates of the center of the  $i$ th joint in the  $j$ th subchain.

The planar sine, sine-cosine, and cosine laws derived in [1] will be used throughout this analysis expressed using the above modified notation.

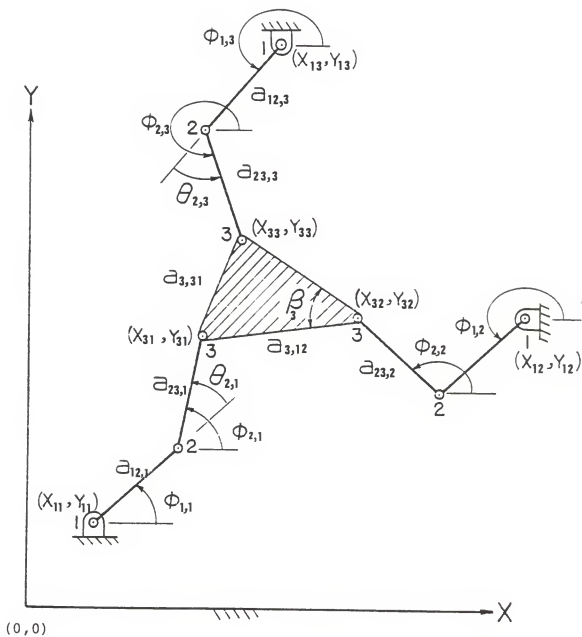


Figure 6.2. Planar Version of the Florida Shoulder

## 6.2 Forward Analysis

Here it is assumed that numerical values are known for the three input displacements ( $\phi_{1,i}$ ) and for the cartesian coordinates of the three fixed points ( $X_{1i}, Y_{1i}$ ) for  $i = 1, 2, 3$ . It is required to compute the location of the end-effector lamina, i.e., determine the coordinates of the three points ( $X_{3i}, Y_{3i}$ ) where  $i = 1, 2, 3$ . This is accomplished by computing the joint angles  $\phi_{2,1}$ ,  $\phi_{2,2}$ , and  $\phi_{2,3}$ .

Firstly the position of the second joint in each subchain is determined from the following pairs of expressions

$$\begin{aligned} X_{2i} &= X_{1i} + a_{12,i} \cos \phi_{1,i} \\ Y_{2i} &= Y_{1i} + a_{12,i} \sin \phi_{1,i} \end{aligned} \quad (6.2)$$

where  $i = 1, 2, 3$ .

Following this three hypothetical links  $a_{2,12}$ ,  $a_{2,23}$ , and  $a_{2,31}$  can be drawn which connect the second joints of the subchains (see Fig. 6.3) and,

$$\begin{aligned} a_{2,12}^2 &= (X_{21} - X_{22})^2 + (Y_{21} - Y_{22})^2 \\ a_{2,23}^2 &= (X_{22} - X_{23})^2 + (Y_{22} - Y_{23})^2 \\ a_{2,31}^2 &= (X_{23} - X_{21})^2 + (Y_{23} - Y_{21})^2 \end{aligned} \quad (6.3)$$

Further the interior angles  $\beta_2$  and  $\beta_3$  can be computed using the law of cosines and

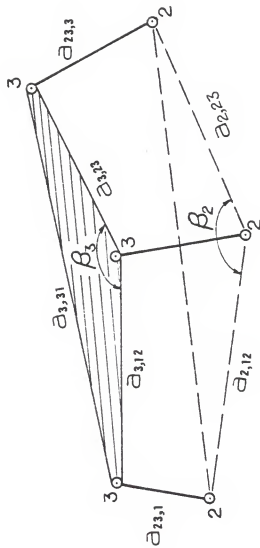


Figure 6.3. Six-Bar Structure



$$\cos \beta_2 = \frac{a_{2,12}^2 + a_{2,23}^2 - a_{2,31}^2}{2 a_{2,12} a_{2,23}}$$

$$\cos \beta_3 = \frac{a_{3,12}^2 + a_{3,23}^2 - a_{3,31}^2}{2 a_{3,12} a_{3,23}} \quad (6.4)$$

In this way the determination of the joint displacements is reduced to an analysis of the pin-jointed structure illustrated in Fig. 6.3. There are two independent loops in this structure which when considered separately are planar four-bar mechanisms. The exterior angles ( $\theta_{2,2}$ ,  $\theta_{2,2}^b$ ) and ( $\theta_{3,2}$ ,  $\theta_{3,2}^b$ ) are related by the following expressions (see Fig. 6.4),

$$\theta_{2,2}^b = (2\pi - \beta_2) - \theta_{2,2} \quad (6.5)$$

$$\theta_{3,2}^b = \beta_3 - \theta_{3,2} \quad (6.6)$$

Here the superscript 'b' used to label the exterior angle of the quadrilateral (the four-bar mechanism) illustrated in Fig. 6.4(b).

The law of cosines for the quadrilateral (Fig. 6.4(a)) can be expressed in the form

$$-a_{2,12}(\bar{x}_{3,2} s_{2,2} + \bar{y}_{3,2} c_{2,2}) + \bar{z}_{3,2} + (a_{2,12})^2/2 = (a_{23,1})^2/2 \quad (6.7)$$

where by definition

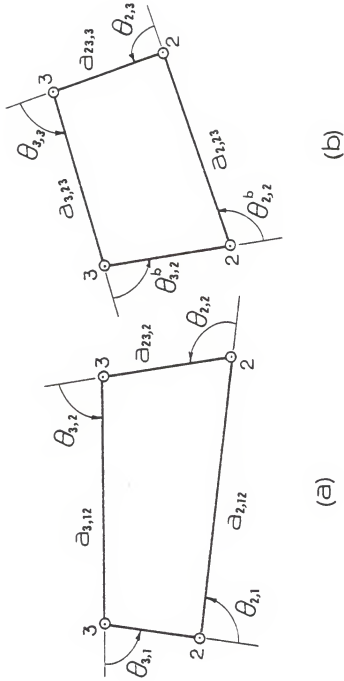


Figure 6.4. Two Independent Quadrilaterals

$$\begin{aligned}
\bar{X}_{3,2} &\equiv a_{3,12} S_{3,2} \\
\bar{Y}_{3,2} &\equiv -(a_{23,2} + a_{3,12} C_{3,2}) \\
\bar{Z}_{3,2} &\equiv (a_{3,12})^2/2 + (a_{23,2})^2/2 \\
&\quad + a_{3,12} a_{23,12} C_{3,2}
\end{aligned} \tag{6.8}$$

and  $S_{2,2}$  and  $C_{2,2}$  denote  $\sin \theta_{2,2}$  and  $\cos \theta_{2,2}$ , respectively. Substituting (6.8) in (6.7), then (6.7) can be expressed in the form

$$A_1 C_{3,2} + B_1 S_{3,2} + D_1 = 0 \tag{6.9}$$

where

$$\begin{aligned}
A_1 &= a_1 C_{2,2} + d_1 \\
B_1 &= b_2 S_{2,2} \\
D_1 &= a_3 C_{2,2} + d_3
\end{aligned} \tag{6.10}$$

and

$$\begin{aligned}
a_1 &= a_{2,12} a_{3,12} \\
d_1 &= a_{23,2} a_{3,12} \\
b_2 &= -a_{2,12} a_{3,12} = -a_1 \\
a_3 &= a_{2,12} a_{23,2} \\
d_3 &= (a_{2,12})^2/2 + (a_{23,2})^2/2 + (a_{3,12})^2/2 - (a_{23,1})^2/2
\end{aligned} \tag{6.11}$$

Similarly, the law of cosines for the quadrilateral in Fig. 6.4(b) can be expressed in the form

$$\begin{aligned}
& -a_{2,23} (x_{3,2}^b s_{2,2}^b + y_{3,2}^b c_{2,2}^b) + z_{3,2}^b \\
& + (a_{2,23})^2/2 = (a_{23,3})^2/2
\end{aligned} \tag{6.12}$$

where by definition

$$\begin{aligned}
x_{3,2}^b & \equiv a_{3,23} s_{3,2}^b \\
y_{3,2}^b & \equiv -(a_{23,2} + a_{3,23} c_{3,2}^b) \\
z_{3,2}^b & \equiv (a_{3,23})^2/2 + (a_{23,2})^2/2 \\
& + a_{3,23} a_{23,2} c_{3,2}^b
\end{aligned} \tag{6.13}$$

Substitute (6.13) in (6.12):

$$\begin{aligned}
& -a_{2,23} [a_{3,23} s_{3,2}^b s_{2,2}^b - (a_{23,2} + a_{3,23} c_{3,2}^b) c_{2,2}^b] \\
& + [(a_{3,23})^2/2 + (a_{23,2})^2/2 + a_{3,23} a_{23,2} c_{3,2}^b] \\
& + (a_{2,23})^2/2 - (a_{23,3})^2/2 = 0
\end{aligned} \tag{6.14}$$

Using (6.5) and (6.6),  $s_{3,2}^b$ ,  $c_{3,2}^b$ ,  $s_{2,2}^b$ , and  $c_{2,2}^b$  can be expressed in the form

$$\begin{aligned}
s_{3,2}^b & = \sin \beta_3 c_{3,2} - \cos \beta_3 s_{3,2} \\
c_{3,2}^b & = \cos \beta_3 c_{3,2} + \sin \beta_3 s_{3,2} \\
s_{2,2}^b & = -\sin \beta_2 c_{2,2} - \cos \beta_2 s_{2,2} \\
c_{2,2}^b & = \cos \beta_2 c_{2,2} - \sin \beta_2 s_{2,2}
\end{aligned} \tag{6.15}$$

Substituting (6.15) in (6.14) gives

$$A_2 c_{3,2} + B_2 s_{3,2} + D_2 = 0 \tag{6.16}$$

where

$$\begin{aligned} A_2 &= a_4 C_{2,2} + b_4 S_{2,2} + d_4 \\ B_2 &= a_5 C_{2,2} + b_5 S_{2,2} + d_5 \\ D_2 &= a_6 C_{2,2} + b_6 S_{2,2} + d_6 \end{aligned} \quad (6.17)$$

and

$$\begin{aligned} a_4 &= a_{2,23} a_{3,23} \cos(\beta_3 - \beta_2) \\ b_4 &= a_{2,23} a_{3,23} \sin(\beta_3 - \beta_2) \\ d_4 &= a_{23,2} a_{3,23} \cos \beta_3 \\ a_5 &= a_{2,23} a_{3,23} \sin(\beta_3 - \beta_2) = b_4 \\ b_5 &= -a_{2,23} a_{3,23} \cos(\beta_3 - \beta_2) = -a_4 \\ d_5 &= a_{23,2} a_{3,23} \sin \beta_3 \\ a_6 &= a_{2,23} a_{23,2} \cos \beta_2 \\ b_6 &= -a_{2,23} a_{23,2} \sin \beta_2 \\ d_6 &= (a_{2,23})^2/2 + (a_{23,2})^2/2 + (a_{3,23})^2/2 - (a_{23,3})^2/2 \end{aligned} \quad (6.18)$$

The two equations (6.9) and (6.16) are thus of the form

$$A_j C_{3,2} + B_j S_{3,2} + D_j = 0 \quad (6.19)$$

where  $j = 1, 2$ . Eliminating  $S_{3,2}$  and then  $C_{3,2}$  from set (6.19) yields,

$$C_{3,2} = |BD|/|AB| \quad (6.20)$$

$$S_{3,2} = -|AD|/|AB| \quad (6.21)$$

where  $|AB| = (A_1B_2 - A_2B_1)$ ,  $|BD| = (B_1D_2 - B_2D_1)$ , and  $|AD| = (A_1D_2 - A_2D_1)$ . Squaring and adding (6.20) and (6.21), and rearranging the eliminant of set (6.19) can be expressed in the form

$$|AB|^2 - |AD|^2 - |BD|^2 = 0 \quad (6.22)$$

Using (6.10), (6.11), (6.17), and (6.18),

$$\begin{aligned} |AB| &= A' C_{2,2}^2 + B' S_{2,2}^2 + C' S_{2,2} C_{2,2} + D' C_{2,2} + E' S_{2,2} + F' \\ |BD| &= A'' C_{2,2}^2 + B'' S_{2,2}^2 + C'' S_{2,2} C_{2,2} + D'' C_{2,2} + E'' S_{2,2} + F'' \\ |AD| &= A''' C_{2,2}^2 + B''' S_{2,2}^2 + C''' S_{2,2} C_{2,2} + D''' C_{2,2} + E''' S_{2,2} + F''' \end{aligned} \quad (6.23)$$

and equation (6.22) becomes

$$\begin{aligned} &AC_{2,2}^4 + BS_{2,2}^3 + CC_{2,2}^3 + DS_{2,2}^2 C_{2,2}^2 + ES_{2,2} C_{2,2}^2 \\ &+ FC_{2,2}^2 + GS_{2,2}^3 + HS_{2,2}^2 C_{2,2} + IS_{2,2} C_{2,2} + JS_{2,2}^4 \\ &+ KS_{2,2}^3 + LS_{2,2}^2 + MS_{2,2} + NC_{2,2} + Q = 0 \end{aligned} \quad (6.24)$$

where,

$$\begin{aligned}
A &= A'^2 - A''^2 - A'''^2 \\
B &= 2(A' C' - A'' C'' - A''' C''') \\
C &= 2(A' D' - A'' D'' - A''' D''') \\
D &= 2(A' B' - A'' B'' - A''' B''') + (C'^2 - C''^2 - C'''^2) \\
E &= 2(A' E' - A'' E'' - A''' E''') + 2(C' D' - C'' D'' - C''' D''') \\
F &= 2(A' F' - A'' F'' - A''' F''') + D'^2 - D''^2 - D'''^2 \\
G &= 2(B' C' - B'' C'' - B''' C''') \\
H &= 2(C' E' - C'' E'' - C''' E''') + 2(B' D' - B'' D'' - B''' D''') \\
I &= 2(C' F' - C'' F'' - C''' F''') + 2(D' E' - D'' E'' - D''' E''') \\
J &= B'^2 - B''^2 - B'''^2 \\
K &= 2(B' E' - B'' E'' - B''' E''') \\
L &= 2(B' F' - B'' F'' - B''' F''') + 2(E'^2 - E''^2 - E'''^2) \\
M &= 2(E' F' - E'' F'' - E''' F''') \\
N &= 2(D' F' - D'' F'' - D''' F''') \\
Q &= F'^2 - F''^2 - F'''^2
\end{aligned} \tag{6.25}$$

From (6.11) and (6.18),  $a_1 = -b_2$ ,  $a_4 = -b_5$ , and  $a_5 = b_4$ .

Making these substitutions, the coefficients in the right side of (6.25) can be expressed in the simple form,

$$\begin{aligned}
A' &= B' = a_1 a_5 \\
C' &= 0 \\
D' &= a_1 d_5 + a_5 d_1 \\
E' &= a_1 d_4 - a_4 d_1 \\
F' &= d_1 d_5 \\
A'' &= -a_3 a_5 \\
B'' &= -a_1 b_6 \\
C'' &= -a_1 a_6 + a_3 a_4 \\
D'' &= -d_3 a_5 - a_3 d_5 \\
E'' &= -a_1 d_6 + d_3 a_4 \\
F'' &= -d_3 d_5 \\
A''' &= -C'' \\
B''' &= 0 \\
C''' &= a_1 b_6 - a_3 a_5 \\
D''' &= a_1 d_6 + d_1 a_6 - d_3 a_4 - a_3 d_4 \\
E''' &= d_1 b_6 - d_3 a_5 \\
F''' &= d_1 d_6 - d_3 d_4
\end{aligned} \tag{6.26}$$

Substituting  $S_{2,2}^2 = 1 - C_{2,2}^2$  and  $S_{2,2}^4 = 1 - 2C_{2,2}^2 + C_{2,2}^4$  in (6.24) and rearranging yields,

$$\begin{aligned}
&\{a C_{2,2}^4 + b C_{2,2}^3 + c C_{2,2}^2 + d C_{2,2} + e\} \\
&= -S_{2,2} \{f C_{2,2}^3 + g C_{2,2}^2 + h C_{2,2} + i\}
\end{aligned} \tag{6.27}$$



where,

$$\begin{aligned}
 a &= A - D + J \\
 b &= C - H \\
 c &= D + F - L - 2J \\
 d &= H + N \\
 e &= J + L + Q \\
 f &= B - G \\
 g &= E - K \\
 h &= G + I \\
 i &= K + M
 \end{aligned} \tag{6.28}$$

Equation (6.27) can be expressed as an eighth-degree polynomial in  $C_{2,2}$ . This is accomplished by squaring (6.27) and making the substitution  $S_{2,2}^2 = 1 - C_{2,2}^2$ ,

$$\begin{aligned}
 &[a^2+f^2]C_{2,2}^8 + [2(fg+ab)]C_{2,2}^7 + [2(fh+ac) + g^2 \\
 &+ b^2-f^2]C_{2,2}^6 + [2(fi+gh+ad+bc-fg)]C_{2,2}^5 \\
 &+ [2(gi+ae+bd-fh)+h^2+c^2-g^2]C_{2,2}^4 \\
 &+ [2(hi+be+cd-fi-gh)]C_{2,2}^3 + [2(ce-gi)+i^2+d^2-h^2]C_{2,2}^2 \\
 &+ [2(de-hi)]C_{2,2} + [e^2-i^2] = 0
 \end{aligned} \tag{6.29}$$

However, the number of assembly configurations of the structure illustrated in Fig. 6.3 can be determined by disconnecting the third joint in the second subchain and by counting the number of points of intersection of the planar coupler curve traced by the four-bar with the

circle. Details are given in Appendix A where it is shown that there are a maximum of 6 real intersections. It follows that the coefficients  $a$  and  $f$  in (6.29) must be zero, i.e.,

$$a = f = 0 \quad (6.30)$$

This is demonstrated in Appendix B and (6.29) reduces to the following sixth-degree polynomial

$$\begin{aligned} c_6 C_{2,2}^6 + c_5 C_{2,2}^5 + c_4 C_{2,2}^4 + c_3 C_{2,2}^3 \\ + c_2 C_{2,2}^2 + c_1 C_{2,2} + c_0 = 0 \end{aligned} \quad (6.31)$$

where,

$$\begin{aligned} c_6 &= g^2 + b^2 \\ c_5 &= 2(gh+bc) \\ c_4 &= 2(gi+bd) + (h^2+c^2-g^2) \\ c_3 &= 2(hi+be+cd-gh) \\ c_2 &= 2(ce-gi) + (i^2+d^2-h^2) \\ c_1 &= 2(de-hi) \\ c_0 &= e^2-i^2 \end{aligned} \quad (6.32)$$

Equation (6.31) can thus be solved for any arbitrary set of mechanism dimensions which can yield a maximum of 6 real values for  $C_{2,2}$ . Corresponding values for  $S_{2,2}$  can be computed using (6.27), and in this way values for  $\Theta_{2,2}$  are computed. Following this, values for the remaining joint displacements can be computed.

First, values of the exterior angle  $\Theta_{3,2}$  can be computed using (6.20) and (6.21). Following this, values of the exterior angles  $\Theta_{2,2}^b$  and  $\Theta_{3,2}^b$  (see Fig. 6.4(b)) can be computed using (6.5) and (6.6) respectively

$$\Theta_{2,2}^b = (2\pi - \beta_2) - \Theta_{2,2}$$

$$\Theta_{3,2}^b = \beta_3 - \Theta_{3,2}$$

where the interior angles  $\beta_2$  and  $\beta_3$  are expressed in (6.4).

The sine and sine-cosine laws of the four-bar illustrated in Fig. 6.4(a) can be expressed as follows

$$X_{32,2} = a_{23,1} S_{2,1} \quad (6.33)$$

$$Y_{32,2} = a_{23,1} C_{2,1} \quad (6.34)$$

where by definition

$$\begin{aligned} X_{32,2} &\equiv \bar{X}_{3,2} C_{2,2} - \bar{Y}_{3,2} S_{2,2} \\ Y_{32,2} &\equiv \bar{X}_{3,2} S_{2,2} + \bar{Y}_{3,2} C_{2,2} - a_{2,12} \end{aligned} \quad (6.35)$$

and  $\bar{X}_{3,2}$  and  $\bar{Y}_{3,2}$  are expressed in (6.8). Values of the exterior angle  $\Theta_{2,1}$  can be computed from (6.33) and (6.34).

Similarly, the sine and sine-cosine laws of the second four-bar illustrated in Fig. 6.4(b) can be expressed as follows

$$X_{32,2}^b = a_{23,3} S_{2,3} \quad (6.36)$$

$$Y_{32,2}^b = a_{23,3} C_{2,3} \quad (6.37)$$

where by definition

$$\begin{aligned}x_{32,2}^b &\equiv x_{3,2}^b C_{2,2}^b - y_{3,2}^b S_{2,2}^b \\y_{32,2}^b &\equiv x_{3,2}^b S_{2,2}^b + y_{3,2}^b C_{2,2}^b - a_{2,23}\end{aligned}\quad (6.38)$$

and  $x_{3,2}^b$  and  $y_{3,2}^b$  are expressed in (6.13). Values of the exterior angle  $\theta_{2,3}$  can be computed from (6.36) and (6.37).

The sine and the cosine of angle  $\alpha_2$  that the hypothetical link  $a_{2,23}$  makes with the horizontal X-axis (see Fig. 6.5) can be expressed as follows:

$$\sin \alpha_2 = \frac{y_{23} - y_{22}}{a_{2,23}} \quad (6.39)$$

$$\cos \alpha_2 = \frac{x_{23} - x_{22}}{a_{2,23}} \quad (6.40)$$

where  $(x_{22}, y_{22})$  and  $(x_{23}, y_{23})$  are the known coordinates of the centers of the second joints in the second and third subchains and given in (6.2). Values of the angle  $\alpha_2$  can be computed from (6.39) and (6.40).

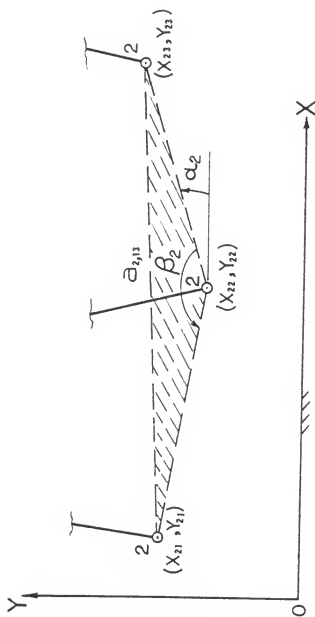
The angles  $\phi_{2,1}$ ,  $\phi_{2,2}$ , and  $\phi_{2,3}$  that links  $a_{23,1}$ ,  $a_{23,2}$  and  $a_{23,3}$ , respectively, make with the horizontal X-axis can be expressed as follows, (see Fig. 6.6):

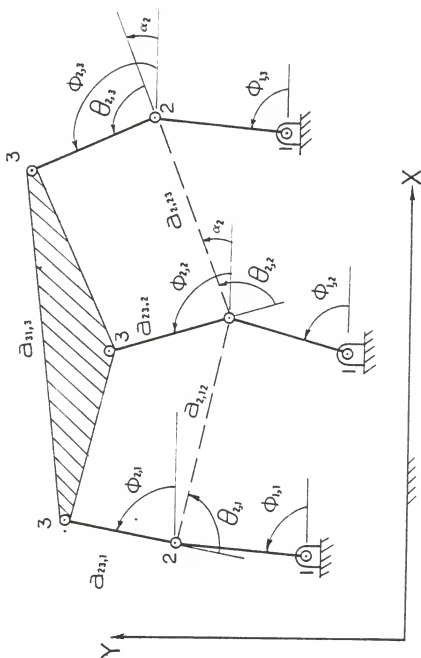
$$\begin{aligned}\phi_{2,1} &= (\pi - \theta_{2,1}) - [\pi - (\alpha_2 + \beta_3)] \\&= \alpha_2 + \beta_2 - \theta_{2,1}\end{aligned}\quad (6.41)$$

$$\phi_{2,2} = (\pi - \theta_{2,2}^b) + \alpha_2 \quad (6.42)$$

and

$$\phi_{2,3} = \theta_{2,3} + \alpha_2 \quad (6.43)$$

Figure 6.5. Determination of Angle  $\alpha_2$

Figure 6.6. Determination of Angles  $\phi_{2,i}$

Finally, the required expressions for the coordinates of the center of the third joint in each subchain can be expressed as follows:

$$\begin{aligned} X_{3i} &= X_{2i} + a_{23,i} \cos \phi_{2,i} \\ Y_{3i} &= Y_{2i} + a_{23,i} \sin \phi_{2,i} \end{aligned} \quad (6.44)$$

where  $i = 1, 2, 3$ . The coordinates  $(X_{2i}, Y_{2i})$  are given by (6.2), whilst the angles  $\phi_{2,i}$  are given by (6.44).

### 6.3 Reverse Analysis

A major problem in the operation of a robotic device (manipulator) controlled by a computer which is directing the end-effector to move from one location to another is to obtain sets of joint displacements for specified locations of the end-effector platform. The location of the platform can be specified by the coordinates of the three points  $(X_{3i}, Y_{3i})$  where  $i = 1, 2, 3$  (Fig. 6.2).

The reverse analysis for fully-parallel devices can be performed separately for each subchain. Furthermore, since the planar version of the Florida Shoulder is a symmetrical fully-parallel device, the analysis is performed only once for the  $i$ th subchain which can be any subchain in the device and the angular displacements of the joints in this  $i$ th subchain are determined.

Figure 6.7 illustrates that the  $i$ th subchain can be considered as a two-degree of freedom serial open-loop mechanism. The third joint can be connected to the housing of the first

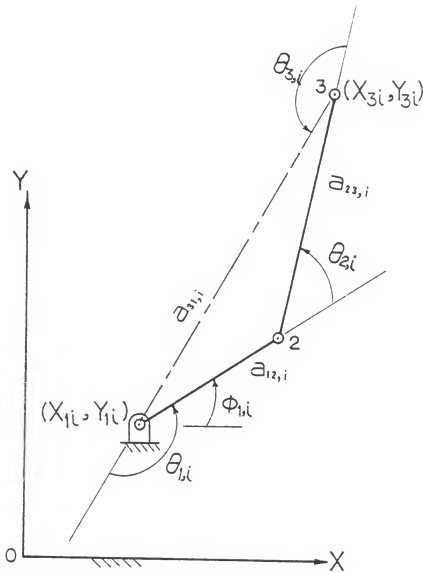


Figure 6.7. Two-Degree of Freedom Serial Arm



revolute joint by a hypothetical link  $a_{31,i}$  thus forming a closed triangle. The dimension of the closing link is given by

$$a_{31,i} = \{(X_{3i}-X_{1i})^2 + (Y_{3i}-Y_{1i})^2\}^{1/2} \quad (6.45)$$

The exterior angle  $(\theta_{1,i}-\phi_{1,i})$  can be computed from sequential solutions of

$$\begin{aligned} \sin(\theta_{1,i}-\phi_{1,i}) &= (Y_{3i}-Y_{1i})/a_{31,i} \\ \cos(\theta_{1,i}-\phi_{1,i}) &= -(X_{3i}-X_{1i})/a_{31,i} \end{aligned} \quad (6.46)$$

It is interesting to note that the transformation equations (6.45) and (6.46) are the same whether the second joint is a revolute or a prismatic.

The exterior angles  $\theta_{2,i}$  and  $\theta_{1,i}$  can be computed using the sine, sine-cosine, and cosine laws for the planar triangle illustrated in Fig. 6.7,

$$a_{23,i} S_{2,i} = a_{31,i} S_{1,i} \quad (6.47)$$

$$-(a_{12,i} + a_{23,i} C_{2,i}) = a_{31,i} C_{1,i} \quad (6.48)$$

$$(a_{23,i})^2/2 + (a_{12,i})^2/2 + a_{23,i} a_{12,i} C_{2,i} = (a_{31,i})^2/2 \quad (6.49)$$

Firstly, two values for  $\theta_{2,i}$  are computed using the cosine law (6.49). These values define two distinct closure configurations for each subchain. The geometric configurations of these two closures are illustrated in Fig. 6.8. Following this, a corresponding pair of values of  $\theta_{1,i}$  is computed using (6.47) and (6.48). Consequently, a pair of values of the required angular displacement  $\phi_{1,i}$  can be computed as follows:

$$\phi_{1,i} = \theta_{1,i} - (\theta_{1,i} - \phi_{1,i}) \quad (6.50)$$

where  $(\theta_{1,i} - \phi_{1,i})$  is computed using (6.46).

The sine and sine-cosine laws for the same planar triangle (Fig. 6.7) can also be expressed as follows

$$\bar{X}_{2,i} = a_{31,i} S_{3,i} \quad (6.51)$$

$$\bar{Y}_{2,i} = a_{31,i} C_{3,i} \quad (6.52)$$

where by definition

$$\begin{aligned} \bar{X}_{2,i} &\equiv a_{12,i} S_{2,i} \\ \bar{Y}_{2,i} &\equiv -(a_{23,i} + a_{12,i} C_{2,i}) \end{aligned} \quad (6.53)$$

which are known quantities. Therefore a corresponding pair of values of  $\theta_{3,i}$  is computed using (6.51) and (6.52).

Finally, the location of the center of the second joint in the  $i$ th subchain can be determined as follows (see Fig. 6.8),

--In the first closure:

$$X_{2i} = X_{1i} + a_{12,i} \cos \phi_{1,i}$$

$$Y_{2i} = Y_{1i} + a_{12,i} \sin \phi_{1,i}$$

--In the second closure:

$$X'_{2i} = X_{1i} + a_{12,i} \cos \phi'_{1,i}$$

$$Y'_{2i} = Y_{1i} + a_{12,i} \sin \phi'_{1,i}$$

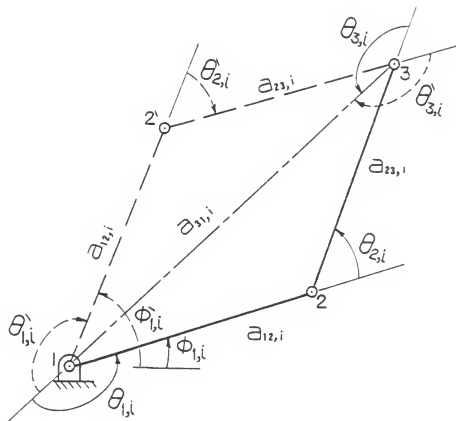


Figure 6.8. Closure Configurations

## 6.4 Numerical Examples

### Example 1

The sixth-degree polynomial (equation (6.29)) was verified by choosing a four-bar mechanism with the following dimensions

$$\begin{array}{ll} a_{23,1} = 2.46 \text{ in.} & a_{23,3} = 2.49 \text{ in.} \\ a_{2,31} = 1.253 \text{ in.} & a_{3,31} = 1.315 \text{ in.} \\ a_{3,12} = 2.98 \text{ in.} & a_{3,23} = 3.337 \text{ in.} \end{array}$$

the coupler curve for which is illustrated in Fig. 6.9. A pivot point P was chosen such that the circle with radius

$$a_{23,2} = 2.681 \text{ in.}$$

intersected the coupler curve in six real points. Following this, the three fixed pivot points were chosen

$$\begin{array}{ll} X_{11} = 0 \text{ in.} & Y_{11} = 0 \text{ in.} \\ X_{12} = 6 \text{ in.} & Y_{12} = -2.305 \text{ in.} \\ X_{13} = 5.5 \text{ in.} & Y_{13} = 2.41 \text{ in.} \end{array}$$

and three input links were also chosen

$$\begin{array}{l} a_{12,1} = 2.5 \text{ in.} \\ a_{12,2} = 3.05 \text{ in.} \\ a_{12,3} = 3.5 \text{ in.} \end{array}$$

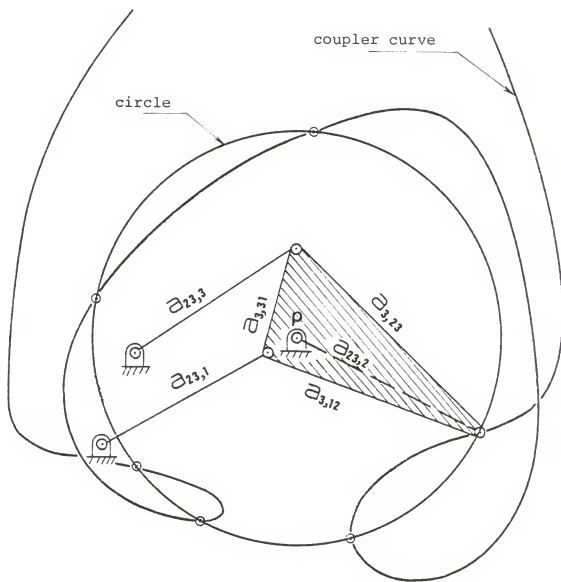


Figure 6.9. Six Real Points of Intersections of Coupler Curve and Circle, Example 6.1

The input actuated joint displacements

$$\phi_{1,1} = -20.984 \text{ deg.}$$

$$\phi_{1,2} = 112.1616 \text{ deg.}$$

$$\phi_{1,3} = -142.958 \text{ deg.}$$

were selected. Equation (6.29) yielded six real values for  $\theta_{2,2}$  and the six corresponding configurations of the lamina were determined. The six sets of coordinates of the lamina are listed in Table 6.1 and the corresponding six assembly configurations are illustrated in Figs. 6.10-6.12. In this way the sixth-degree polynomial is verified. The sixth set was used to perform a reverse analysis and eight sets of joint displacements are listed in Table 6.2. The eighth set of Table 6.2 is in exact agreement with the input for the forward analysis which verifies that both forward and reverse analyses are correct. Further, the corresponding assembly configurations are illustrated in Fig. 6.13 and the assembly configuration drawn with the broken lines is identical to the sixth configuration shown in Fig. 6.12.

### Example 2

The reverse analysis was used to determine a sequence of actuator input angles which would rotate the end-effector lamina of the device illustrated in Fig. 6.14 about an axis normal to the lamina and passing through point (4.25,7.145). Plots of one branch of the input angles ( $\phi_{1,1}$ ,  $\phi_{1,2}$ , and  $\phi_{1,3}$ ) vs. the angle of rotation ( $\gamma$ ) are shown in Figs. 6.15-6.17.

Table 6.1  
The Coordinates of the End-Effector Lamina  
and the Corresponding  $\theta_{2,2}$

Configuration No.	1	2	3	4	5	6
$X_{31}$	2.8546	4.4536	4.7683	-.019	2.5497	3.7304
$Y_{31}$	-3.2996	0.3536	-.5395	-.1783	1.5553	1.1302
$X_{32}$	5.5660	7.2523	2.2096	2.784	5.0385	3.5885
$Y_{32}$	-2.0638	-.66949	0.9877	-1.1895	3.1940	-1.8463
$X_{33}$	2.23	4.8210	4.1719	0.3431	1.7543	5.0451
$Y_{33}$	-2.1424	1.6162	-1.7114	1.0859	2.6024	1.1561
$\theta_{2,2}$	-13.723	32.296	-44.266	-56.382	31.542	-48.277

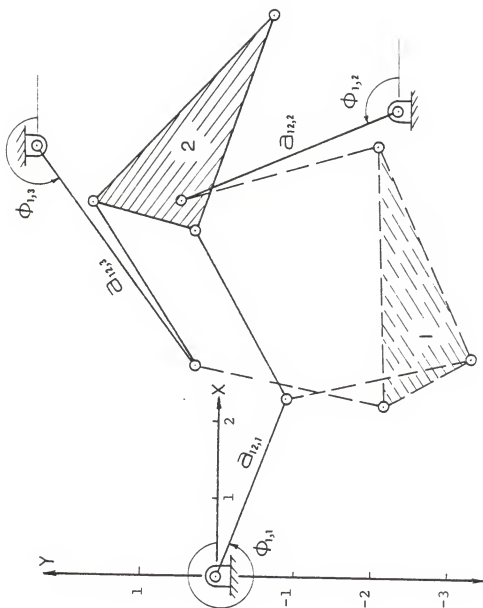


Figure 6.10. Configurations 1 and 2



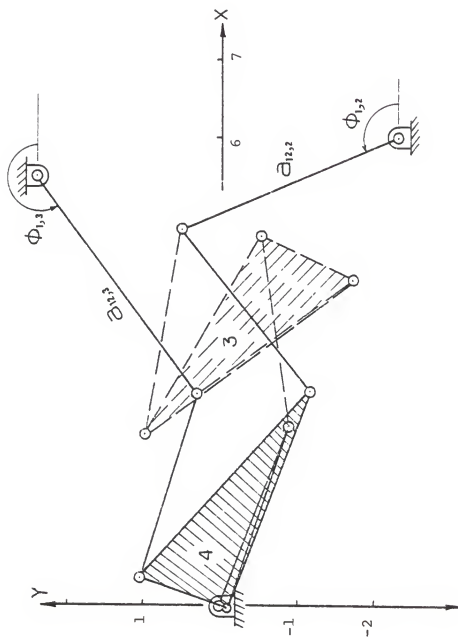


Figure 6.11. Configurations 3 and 4

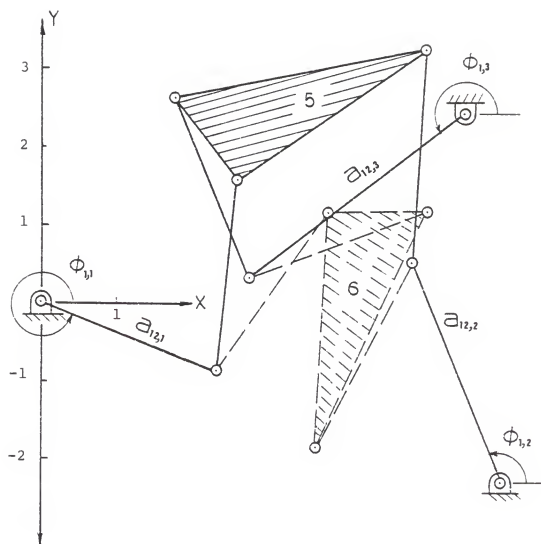


Figure 6.12. Configurations 5 and 6

Table 6.2  
The Required Sets of Joint Displacements

i		1	2	3	4	5	6	7	8
$\theta_{1,i}$	1	217.844	217.844	217.844	217.844	142.156	142.156	142.156	142.156
	2	122.936	237.064	237.064	122.936	237.064	237.064	122.936	122.936
	3	146.991	146.991	213.009	213.009	146.991	213.009	213.009	146.991
$\theta_{2,i}$	1	-76.415	-76.415	-76.415	-76.415	76.415	76.415	76.415	76.415
	2	129.77	-129.77	-129.77	129.77	-129.77	-129.77	129.77	129.77
	3	163.036	163.036	-163.036	-163.036	163.036	-163.036	-163.036	163.036
$\theta_{3,i}$	1	218.571	218.571	218.571	218.571	141.429	141.429	141.429	141.429
	2	107.294	252.706	252.706	107.294	252.706	252.706	107.294	107.294
	3	49.974	49.974	310.026	310.026	49.974	310.026	310.026	49.974
$\phi_{1,i}$	1	54.703	54.703	54.703	54.703	-20.984	-20.984	-20.984	-20.984
	2	112.162	226.289	226.289	112.162	226.289	226.289	112.162	112.162
	3	-142.958	-142.958	-76.939	-76.939	-142.958	-76.939	-76.939	-142.958

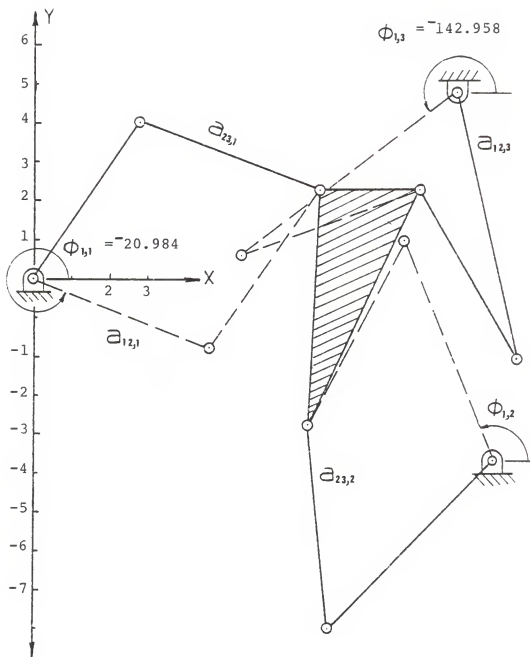


Figure 6.13 Six Assembly Configurations,  
Example 6.1

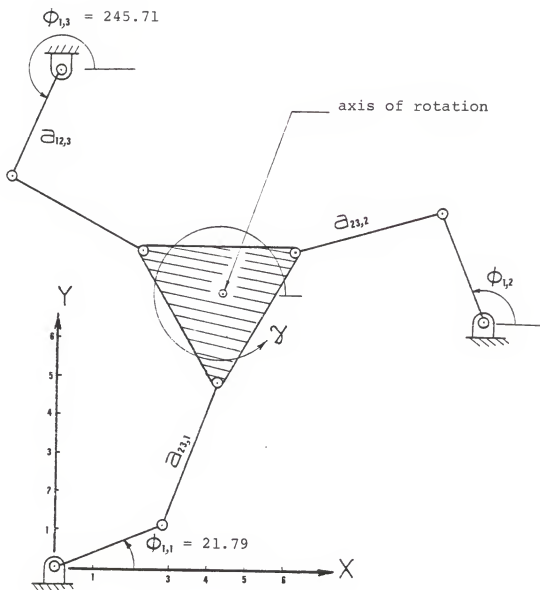


Figure 6.14. Planar Florida Shoulder,  
Example 6.2

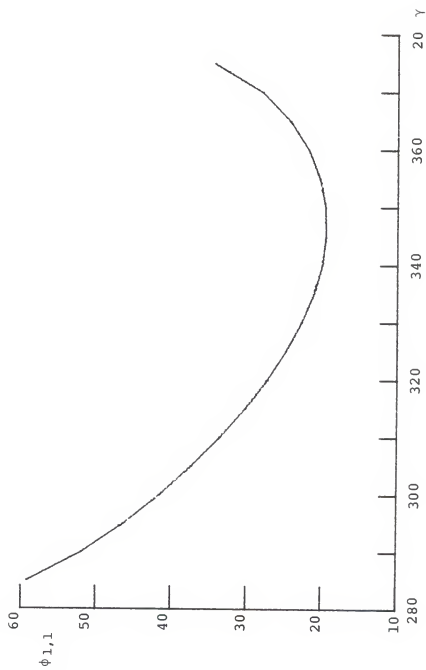


Figure 6.15. Input Angular Displacement  $\phi_{1,1}$ , Example 6.2

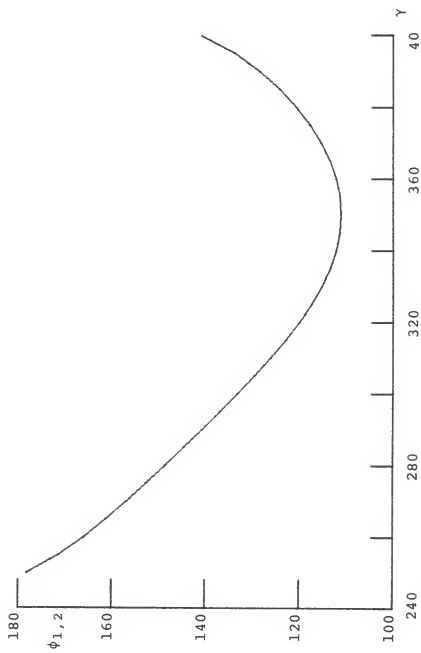


Figure 6.16. Input Angular Displacement  $\phi_{1,2}$ , Example 6.2

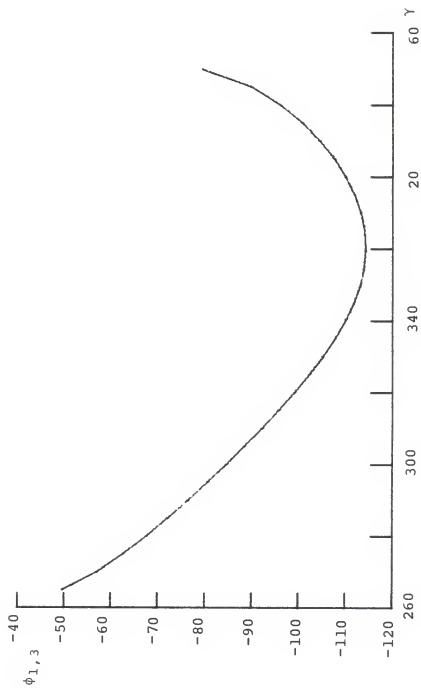


Figure 6.17. Input Angular Displacement  $\phi_{1,3}$ , Example 6.2



Computer programs and listings of the printed results of this chapter are presented in Appendix C.

CHAPTER 7  
THE REVERSE JOINT DISPLACEMENT ANALYSIS OF  
SPATIAL FULLY-PARALLEL DEVICES

7.1 Introduction

The major problem in the operation of a manipulator controlled by a computer which is directing the end-effector to move from one position to another is to obtain a set of joint displacements which will position the end-effector at a given point with a specified orientation within the working space. As mentioned in the previous chapter this analysis is called the reverse joint displacement analysis, or simply the reverse analysis. The reverse analysis of a number of some practical six-degree of freedom spatial robotic devices is presented in this chapter.

The location of the end-effector platform can be specified by a point  $q$  in the platform and by the orientation of the platform. The orientation of the platform can be conveniently specified by the direction cosines of a moving coordinate system  $(x,y,z)$  attached to the platform and expressed in terms of a reference coordinate system  $(X,Y,Z)$ . For simplicity and without losing generality let the origin of the moving coordinate system  $x, y, z$  be chosen coincident with point  $q$ .

The location of the end-effector platform can be specified by a transformation matrix  $[A]$ ,

$$[A] = \left[ \begin{array}{ccc|c} & & & x_q \\ & [T_q] & & y_q \\ & & & z_q \\ \hline 0 & 0 & 0 & 1 \end{array} \right] \quad (7.1)$$

where  $(x_q, y_q, z_q)$  are the coordinates of point  $q$  in the fixed coordinate system and  $[T_q]$  is a matrix of direction cosines of the moving coordinate system.

## 7.2 The Reverse Analysis of the R-P-SP Device with Three-Subchains (Fig. 3.27)

Figure 7.1 illustrates the skeletal form of the R-P-SP device. The centers of the base revolute joints  $O_i$ , where  $i = 1, 2, 3$ , are at the mid-points of the sides of an equilateral triangle with length 'a'. Local reference coordinate systems  $(O_i, x_i, y_i, z_i)$  are chosen for which the  $z_i$ -axis is coaxial with the revolute axis and the  $y_i$ -axis is normal to the base. Without loss of generality, a fixed reference coordinate system  $(X, Y, Z)$  is selected coincident with  $(x_1, y_1, z_1)$ . The distribution of the sliding grooves in the platform are symmetrical as illustrated in Fig. 7.1.

The location of point  $q$  can be expressed in terms of any one of the local fixed coordinate systems by

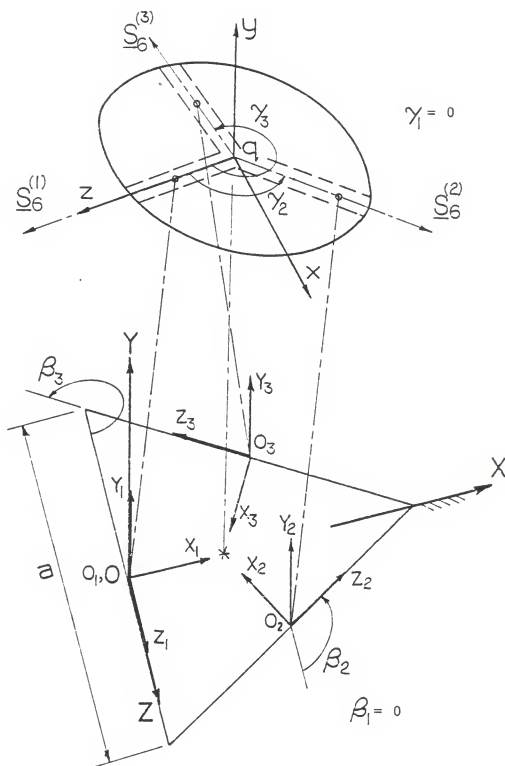


Figure 7.1. Coordinate Systems for the R-P-SP Device

$$\begin{Bmatrix} \underline{R}_1 \\ 1 \end{Bmatrix} = [B] \begin{Bmatrix} X_q \\ Y_q \\ Z_q \\ 1 \end{Bmatrix} \quad (7.2)$$

where

$$[B] = \left[ \begin{array}{ccc|ccc} \cos\beta_i & 0 & -\sin\beta_i & -X_{oi}\cos\beta_i + Z_{oi}\sin\beta_i & & \\ 0 & 1 & 0 & -Y_{oi} & & \\ \sin\beta_i & 0 & \cos\beta_i & -X_{oi}\sin\beta_i - Z_{oi}\cos\beta_i & & \\ \hline 0 & 0 & 0 & 1 & & \end{array} \right] \quad (7.3)$$

and  $(X_{oi}, Y_{oi}, Z_{oi})$  are the coordinates of the origins  $O_i$  in terms of the reference coordinate system. Angle  $\beta_i$  between the local and the reference coordinate system is illustrated in Fig. 7.1.

The direction cosines of the sliding axes  $\underline{S}_6^{(i)}$ , where  $i = 1, 2, 3$ , in the moving coordinate system  $(x, y, z)$  are

$$\underline{S}_6^{(i)} = \begin{Bmatrix} \sin \gamma_i \\ 0 \\ \cos \gamma_i \end{Bmatrix} \quad (7.4)$$

and therefore the direction cosines of  $\underline{S}_6^{(i)}$  in terms of the local fixed coordinate system  $(X_1, Y_1, Z_1)$ , for  $i = 1, 2, 3$ , can be expressed as follows:

$$\underline{S}_6^{(i)} = \begin{bmatrix} \cos\beta_i & 0 & -\sin\beta_i \\ 0 & 1 & 0 \\ \sin\beta_i & 0 & \cos\beta_i \end{bmatrix} [T_q] \begin{Bmatrix} \sin\gamma_i \\ 0 \\ \cos\gamma_i \end{Bmatrix} \quad (7.5)$$

where for the configuration illustrated in Fig. 7.1,

$$\beta_1 = 0 \text{ deg.} \quad \beta_2 = 120 \text{ deg.} \quad \beta_3 = 240 \text{ deg.}$$

$$\gamma_1 = 0 \text{ deg.} \quad \gamma_2 = 120 \text{ deg.} \quad \gamma_3 = 240 \text{ deg.}$$

$$X_{o1} = 0 \quad X_{o2} = a\sqrt{3}/4 \quad X_{o3} = a\sqrt{3}/4$$

$$Y_{o1} = 0 \quad Y_{o2} = 0 \quad Y_{o3} = 0$$

$$Z_{o1} = 0 \quad Z_{o2} = a/4 \quad Z_{o3} = -a/4$$

Each subchain can be considered to be adjustable and individually controllable. The analysis can be performed separately for each subchain. It is required to express the vectors  $\underline{R}_i$ ,  $\underline{S}_1^{(i)}$ , and  $\underline{S}_2^{(i)}$ , (see Fig. 7.2) in terms of the  $i$ th subchain fixed coordinate system  $(X_i, Y_i, Z_i)$ . Further, since the analysis can be repeated for each subchain, the superscript  $(i)$  is superfluous and will not be used. The direction cosines of the revolute and prismatic joints  $\underline{S}_1$  and  $\underline{S}_2$  can be expressed as follows

$$\underline{S}_1 = \begin{Bmatrix} 0 \\ 0 \\ 1 \end{Bmatrix} \quad (7.6)$$

and



$$\underline{S}_2 = \begin{Bmatrix} \sin\alpha_{12} \sin\phi_1 \\ -\sin\alpha_{12} \cos\phi_1 \\ \cos\alpha_{12} \end{Bmatrix} = \begin{Bmatrix} -\sin\phi_1 \\ \cos\phi_1 \\ 0 \end{Bmatrix} \quad (7.7)$$

since  $\alpha_{12}$  is the angle from  $\underline{S}_1$  to  $\underline{S}_2$  measured about the mutual perpendicular vector  $\underline{a}_{12}$ , [1], and  $\alpha_{12} = \frac{3}{2}\pi$ .

The location of point q can also be expressed in the vector form

$$\underline{R}_i = (S_{22} + s_2)\underline{S}_2 - s_6\underline{S}_6 \quad (7.8)$$

where  $\underline{R}_i$  is determined by (7.3). It is required to determine the variable slider displacements  $s_2$  and  $s_6$  together with the vector  $\underline{S}_2$ . This is accomplished by forming the inner product of (7.8) with  $\underline{S}_1$  which yields

$$\underline{R}_i \cdot \underline{S}_1 = -s_6(\underline{S}_6 \cdot \underline{S}_1) \quad (7.9)$$

$\underline{S}_1$  and  $\underline{S}_2$  are perpendicular, and therefore  $(\underline{S}_2 \cdot \underline{S}_1) = 0$ . Solving (7.9) gives

$$s_6 = \frac{-(\underline{R}_i \cdot \underline{S}_1)}{(\underline{S}_6 \cdot \underline{S}_1)} \quad (7.10)$$

where  $\underline{S}_1$  and  $\underline{S}_6$  are given by (7.6) and (7.5), respectively.

It is apparent from (7.9) that when  $\underline{S}_1$  becomes perpendicular to  $\underline{S}_6$ , it also becomes perpendicular to  $\underline{R}_i$  where  $s_6$  cannot be infinity in practice. It is also apparent from (7.10) that when this happens the order of the screw system of all joints in the subchain reduces instantaneously and the device is in a special configuration (see Cases V and



VI, Chapter 5). Neither the rotating displacement  $\phi_1$ , nor the sliding displacement  $s_2$  has any effect on the motion of the platform and therefore  $s_6$  can assume any value.

Following this, (7.8) can be rearranged in the form

$$\underline{R}_1 + s_6 \underline{S}_6 = (S_{22} + s_2) \underline{S}_2 \quad (7.11)$$

and hence  $\underline{S}_2$  can be determined by

$$\underline{S}_2 = \frac{\underline{R}_1 + s_6 \underline{S}_6}{\|\underline{R}_1 + s_6 \underline{S}_6\|} \quad (7.12)$$

where  $\|\underline{R}_1 + s_6 \underline{S}_6\|$  is the norm of the resultant vector,  $(\underline{R}_1 + s_6 \underline{S}_6)$ . The direction cosines of  $\underline{S}_2$  determined by (7.12) can now be used to compute the revolute actuator displacement,  $\phi_1$ , and from (7.7),

$$\sin \phi_1 = -(\underline{S}_2 \cdot \begin{Bmatrix} 1 \\ 0 \\ 0 \end{Bmatrix}) \quad (7.13)$$

and

$$\cos \phi_1 = \underline{S}_2 \cdot \begin{Bmatrix} 0 \\ 1 \\ 0 \end{Bmatrix} \quad (7.14)$$

Finally, sliding actuator displacement,  $s_2$ , can also be computed using (7.11) and,

$$s_2 = \|\underline{R}_1 + s_6 \underline{S}_6\| - S_{22} \quad (7.15)$$

where  $S_{22}$  is the prespecified offset associated with the prismatic (sliding) joint  $P_2$ .

### Numerical Example

The R-P-SP device illustrated in Fig. 7.1 was considered. The reverse analysis was used to determine a sequence of actuator input angles  $\phi_1$  as well as of sliding input displacements  $s_2$  which would rotate the end-effector platform about the y-axis by angle  $\alpha$ .

Substituting the values of the direction cosines of  $\underline{R}_i$ ,  $\underline{S}_1$ , and  $\underline{S}_6$  given by (7.3), (7.6), and (7.5) in (7.10) and expanding, yields

$$s_6 = \frac{-[\sin\beta_i (X_q - X_{oi}) + \cos\beta_i (Z_q - Z_{oi})]}{\cos(\alpha + \gamma_i - \beta_i)} \quad (7.16)$$

where  $\alpha$  is the angle of rotation about the y-axis. It should be noted that only the denominator of (7.16) is a function of  $\alpha$ . It follows that as  $\alpha$  varies within the range  $0 \leq \alpha \leq 2\pi$  then the sign of  $s_6$  will change. For the example chosen here  $\gamma_i = \beta_i$  and the denominator reduces to  $\cos \alpha$ . The coordinates of point q were  $X_q = 2$  in.,  $Y_q = 14$  in., and  $Z_q = 5$  in. The constant offset for each of the three subchains was  $S_{2,2} = 3$  in. and the side of the equilateral base was  $a = 15$  in.

Plots of the input angles ( $\phi_{1,1}$ ,  $\phi_{1,2}$ , and  $\phi_{1,3}$ ) as well as of the input sliding displacements ( $s_{2,1}$ ,  $s_{2,2}$ , and  $s_{2,3}$ ) vs. the angle of rotation ( $\alpha$ ) are shown in Figs. 7.3-7.8.

It is apparent from Figs. 7.3-7.9 that the device is in a special configuration when either  $\alpha = 90$  deg. or  $\alpha = 270$  deg. The sliding displacement  $s_6$  was arbitrarily chosen

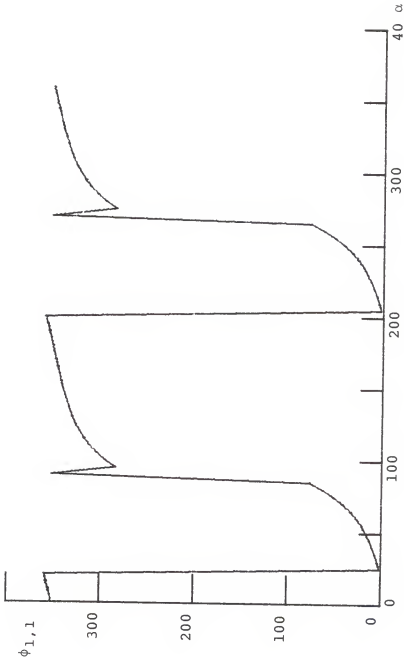


Figure 7.3. Input Angular Displacement  $\phi_{1,1}$  for the R-P-SP Device

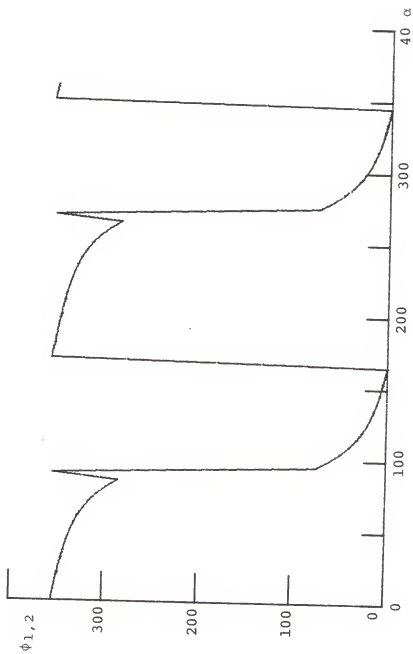


Figure 7.4. Input Angular Displacement  $\phi_{1,2}$  for the R-P-SP Device

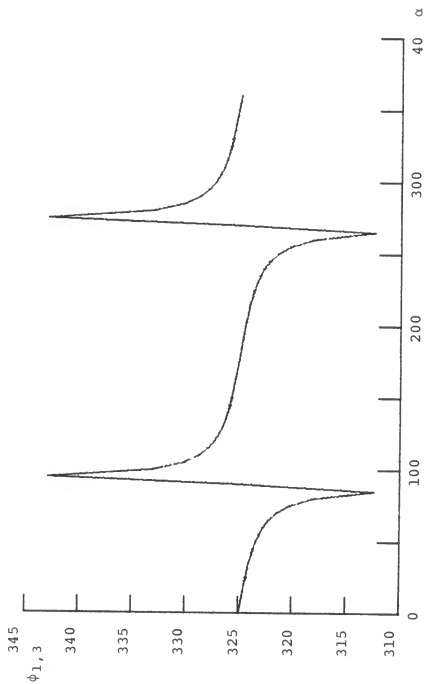


Figure 7.5. Input Angular Displacement  $\phi_{1,3}$  for the R-P-SP Device

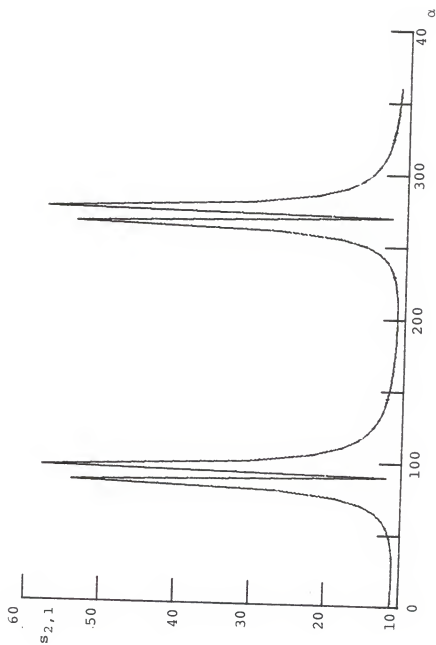


Figure 7.6. Input Sliding Displacement  $s_{2,1}$  for the R-P-SP Device

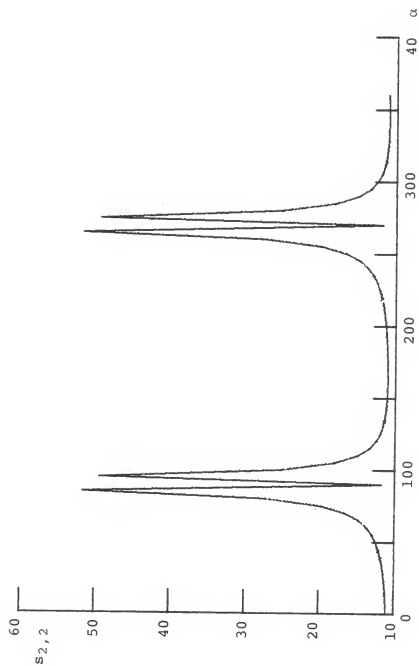


Figure 7.7. Input Sliding Displacement  $s_{2,2}$  for the R-P-SP Device

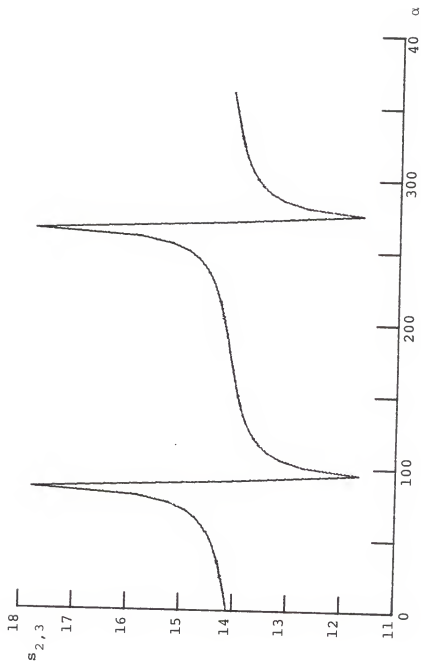


Figure 7.8. Input Sliding Displacement  $s_{2,3}$  for the R-P-SP Device



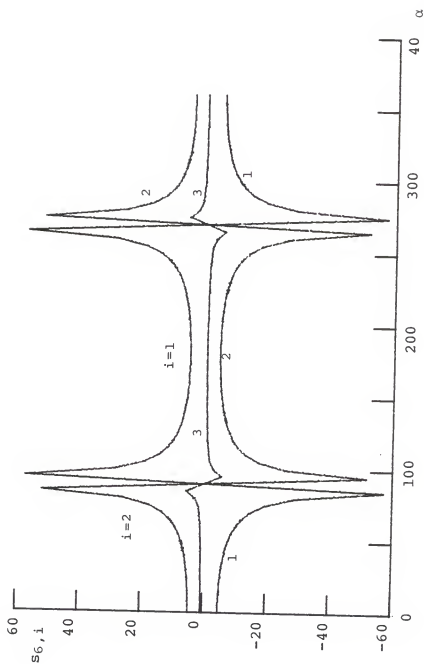


Figure 7.9. Sliding Displacement  $s_{6,i}$  for the R-P-SP Device

to be zero at these two instances. Because of the symmetry of the device ( $\gamma_i = \beta_i = 120(i-1)$ ), the order of each of the screw systems of the three subchains reduces instantaneously and the device is in an uncertainty configuration, Case VI, Chapter 5.

Figure 7.9 illustrates that any one of the three sliding displacements  $s_6$  is different in sign from the other two.

Clearly this device is not suited to perform tasks requiring  $360^\circ$ -rotations of the end-effector platform since the radius of the platform will be of the order of 5 ft.

### 7.3 The Reverse Analysis of Stewart Platform (Fig. 3.29)

For simplicity and without losing generality, both the end-effector platform and the fixed base are chosen to be circular with radii  $r_1$  and  $r_2$ , respectively (see Fig. 7.10). The distribution of the ball-and-socket joints are chosen to be symmetrical in both the platform and the base. The reference coordinate system  $X,Y,Z$  is selected such that its origin is at the center point  $O$  of the base with the  $Z$ -axis passing through the center of the first ball-and-socket joint, i.e., through point  $Q_1$ , and the  $Y$ -axis is normal to the base. The moving coordinate system  $x,y,z$  is selected with the origin at the center point  $q$  of the platform, the  $z$ -axis passing through the center point  $q_1$  of the seventh ball joint, and the  $y$ -axis normal to the end-effector platform.

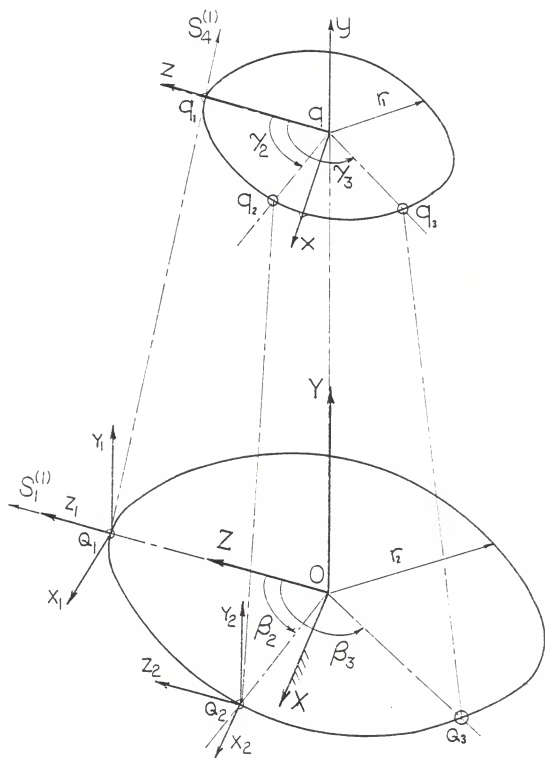


Figure 7.10. Coordinate Systems for Stewart Platform

As explained in section 7.2, since each subchain is adjustable and individually controllable, the analysis will be performed separately for each subchain. It is required to express the coordinates of both points  $q_i$  and  $Q_i$  in terms of the  $i$ th subchain fixed coordinate system  $X_i, Y_i, Z_i$ .

The location of the center point,  $q_i$ , of the ball-and-socket joint (for  $i = 1, 2, \dots, 6$ ) in terms of the moving coordinate system  $x, y, z$  can be expressed as follows

$$\begin{Bmatrix} x \\ y \\ z \end{Bmatrix}_{q_i} = \begin{Bmatrix} r_l \sin \gamma_i \\ 0 \\ r_l \cos \gamma_i \end{Bmatrix} \quad (7.17)$$

Therefore the location of  $q_i$  on the end-effector Platform can be expressed in terms of the fixed local coordinate system by

$$\begin{Bmatrix} X_i \\ Y_i \\ Z_i \\ 1 \end{Bmatrix} = [B] \left[ \begin{array}{c|c} [T_q] & \begin{Bmatrix} X_q \\ Y_q \\ Z_q \end{Bmatrix} \\ \hline 0 & 0 & 0 & 1 \end{array} \right] \begin{Bmatrix} r_l \sin \gamma_i \\ 0 \\ r_l \cos \gamma_i \\ 1 \end{Bmatrix} \quad (7.18)$$

where  $(X_q, Y_q, Z_q)$  are the prespecified coordinates of the center point  $q$  of the platform, and  $[T_q]$  is the prespecified matrix of direction cosines (see equation (7.1)).

Because of the symmetry of the distribution of the ball joints on the platform and the fixed base, then

$$\gamma_i = \beta_i = 60(i-1) \text{ deg.} \quad (7.19)$$

and the transformation matrix  $[B]$ , (7.3), reduces to

$$[B] = \left[ \begin{array}{ccc|c} \cos\beta_i & 0 & -\sin\beta_i & 0 \\ 0 & 1 & 0 & 0 \\ \sin\beta_i & 0 & \cos\beta_i & -r_2 \\ \hline 0 & 0 & 0 & 1 \end{array} \right] \quad (7.20)$$

for  $i = 1, 2, \dots, 6$ .

The direction cosines of the sliding axis  $\underline{S}_4$  in the  $i$ th subchain can be expressed in terms of the  $X_i, Y_i, Z_i$  coordinate system as follows

$$\underline{S}_4 = \left\{ \begin{array}{l} X_i / \| \underline{q}_i \| \\ Y_i / \| \underline{q}_i \| \\ Z_i / \| \underline{q}_i \| \end{array} \right\} \quad (7.21)$$

where, from (7.18)

$$\underline{q}_i = \begin{Bmatrix} x_i \\ y_i \\ z_i \end{Bmatrix} \quad (7.22)$$

and  $\|\underline{q}_i\|$  is the norm of  $\underline{q}_i$  which is the distance between points  $Q_i$  and  $q_i$ .

It is necessary to control or actuate a single joint in each of the six subchains. Two cases are now considered.

### 7.3.1 Case I--The Sliding Joint Is Actuated

For this case, (see Fig. 7.11), the required input sliding displacement  $s_4$  can directly be computed from (7.18) and (7.22) as follows

$$s_4 = \|\underline{q}_i\| - S_{44} \quad (7.23)$$

where  $S_{44}$  is the prespecified offset associated with the sliding (prismatic) joint in each subchain.

### 7.3.2 Case II--A Revolute Joint Is Actuated

The ball-and-socket joint at the base can be simulated by three co-intersecting revolute joints which are mutually perpendicular and

$$\begin{aligned} \alpha_{12} &= \alpha_{23} = 90 \text{ deg.} \\ a_{12} &= a_{23} = 0 \text{ in.} \\ S_{11} &= S_{22} = S_{33} = 0 \text{ in.} \end{aligned} \quad (7.24)$$

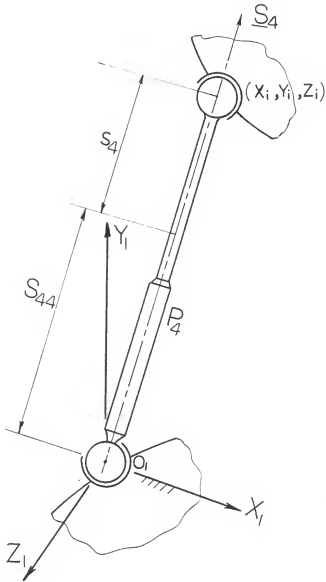


Figure 7.11. The  $i$ th Subchain of Stewart Platform with Actuated Sliding Joint

The first revolute joint is assumed to be the input-actuated joint and the angle  $\phi_1$  between  $\underline{a}_{12}$  and the local  $X_i$ -axis, measured in the right-hand sense about  $\underline{S}_1$ , is the required input angular displacement (see Fig. 7.12).

There are seven freedoms in each subchain and one of them is a spinning freedom (see Fig. 3.23(f)). Therefore, the axes of rotation  $\underline{S}_3$  and  $\underline{S}_5$  are collinear which form the spinning axis and they are parallel to the axis of translation  $\underline{S}_4$ . Therefore,

$$\alpha_{34} = 0^\circ \quad (7.25)$$

The direction cosines of  $\underline{S}_4$ , which are identical to the direction cosines of  $\underline{S}_3$ , can be expressed in terms of the local  $X_i, Y_i, Z_i$  coordinate system as follows:

$$\underline{S}_4 = \begin{Bmatrix} X_{321} \\ X_{321}^* \\ Z_{32} \end{Bmatrix} \quad (7.26)$$

Expanding  $X_{321}$ ,  $X_{321}^*$ , and  $Z_{32}$  (see Table 3.7 [1]), and making the substitutions  $\alpha_{12} = \alpha_{23} = 90^\circ$ , and  $\alpha_{34} = 0^\circ$ , yields

$$\underline{S}_4 = \begin{Bmatrix} \sin \theta_2 \cos \phi_1 \\ \sin \theta_2 \sin \phi_1 \\ -\cos \theta_2 \end{Bmatrix} \quad (7.27)$$

Equating the expressions of the direction cosines of  $\underline{S}_4$  given by (7.21) and (7.27), two values for angle  $\theta_2$  can be computed using



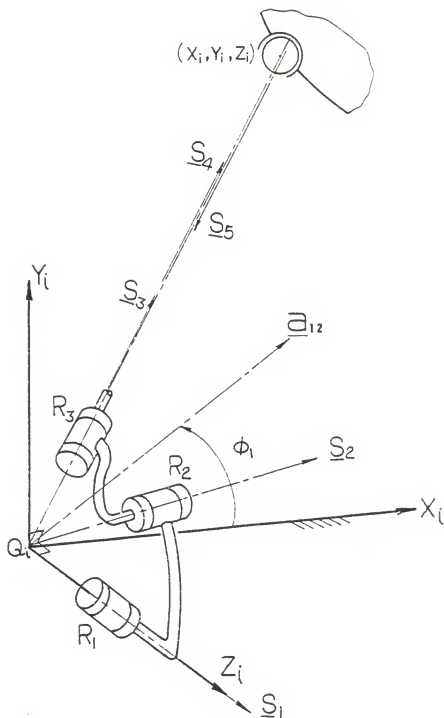


Figure 7.12 The  $i$ th Subchain of Stewart Platform with Actuated Revolute Joint

$$\cos\theta_2 = -z_i / \|q_i\| \quad (7.28)$$

These values define two distinct configurations. Following this, a corresponding pair of values of the required angular displacement  $\phi_1$  is computed using

$$\begin{aligned} \cos\phi_1 &= X_i / (\|q_i\| \times \sin\theta_2) \\ \sin\phi_1 &= Y_i / (\|q_i\| \times \sin\theta_2) \end{aligned} \quad (7.29)$$

### 7.3.3 Numerical Examples

The Stewart platform illustrated in Fig. 7.10 was considered. The reverse analysis was also used to determine a sequence of the input displacements which would rotate the end-effector platform about the y-axis continuously by angle  $\alpha$ . The radii of both the end-effector platform and the circular base were chosen;  $r_1 = 8$  in. and  $r_2 = 10$  in. The coordinates of point q were  $X_q = 3$  in.,  $Y_q = 18$  in., and  $Z_q = 6$  in. Two different cases were considered.

1. The prismatic joint,  $P_4$ , in each subchain was considered to be the input actuated joint and its constant offset was  $S_{44} = 5$  in. Plots of the input sliding displacements ( $s_{4,i}$ , for  $i = 1, 2, \dots, 6$ ) vs the angle of rotation ( $\alpha$ ) are shown in Fig. 7.13.

2. The base revolute joint,  $R_1$ , (see Fig. 7.12) in each subchain was considered to be the input actuated joint. Plots of the input angular displacements ( $\phi_{1,i}$ , for  $i = 1, 2, \dots, 6$ ) vs the angular rotation ( $\alpha$ ) are shown for the first

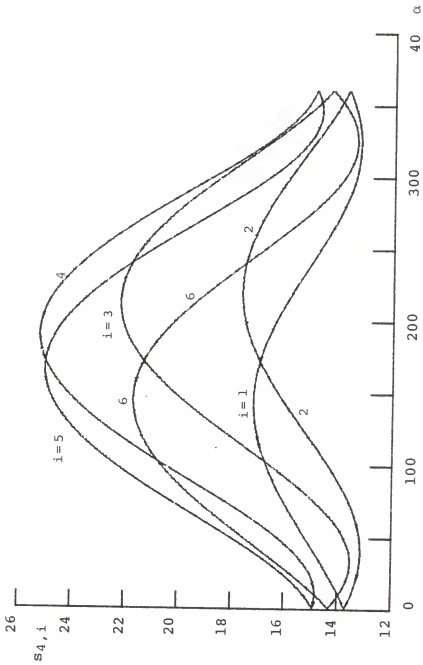


Figure 7.13. Input Sliding Displacement  $s_{4,i}$  for Stewart Platform

and the second branches of  $\phi_{1,i}$  in Figs. 7.14 and 7.15 respectively. The angular displacement  $\phi_{1,1}$  vs.  $\alpha$  is shown for both branches in Fig. 7.16.

Clearly this device is better suited to perform tasks requiring  $360^\circ$ -rotations of the end-effector platform.

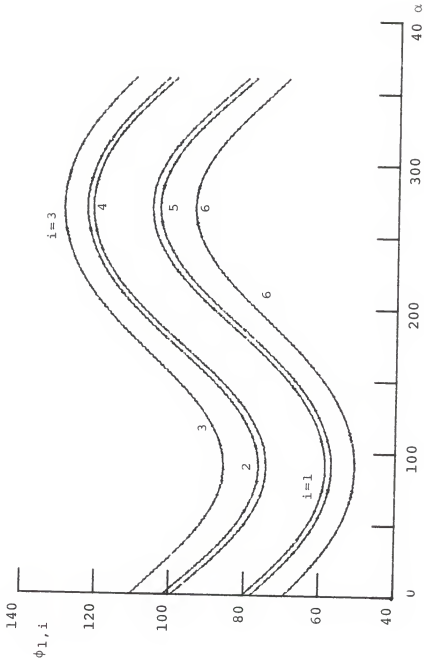


Figure 7.14. Input Angular Displacement  $\phi_{1,i}$  of the First Closure for Stewart Platform

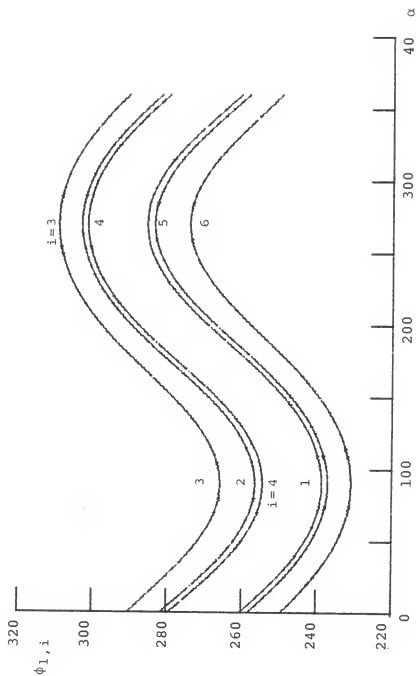


Figure 7.15. Input Angular Displacement  $\phi_{1,i}$  of the Second Closure for Stewart Platform

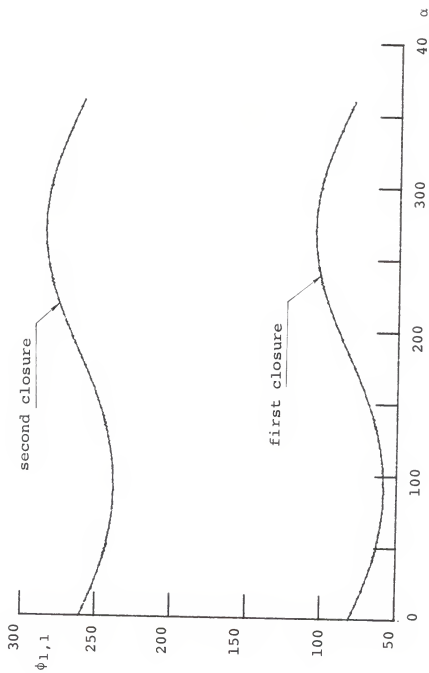


Figure 7.16. Input Angular Displacement  $\phi_{1,1}$  of the First and the Second Closures for Stewart Platform

## CHAPTER 8 SUGGESTIONS FOR FUTURE WORK

There are two distinct areas in which future work can be carried out. The first deals with the joint displacement analysis of parallel devices. The analysis performed in Chapter 7 was a reverse analysis. There is a need to investigate the forward analysis which is a more difficult task since it involves the solution of a set of highly nonlinear simultaneous equations. The forward analysis presented for the six-bar structure illustrated in Chapter 6 (Fig. 6.6) can be extended and applied to the one-degree of freedom planar Stephenson-3 linkage which is also must have a maximum of six assembly configurations. Furthermore, the joint displacement analyses of partially-parallel devices such as those illustrated in Figs. 1.5, 3.8(b), and 3.11(b), which are sometimes incorporated in earth-moving machines, are also needed.

The second area of future research is a study of the instantaneous kinematics of parallel devices. In this dissertation six different types of special configurations for fully-parallel devices were described and it was concluded that certain configurations must be avoided. The next logical step would be to implement the given strategy (analysis) in practice and to search for mechanisms with special



dimensions that may avoid such special configurations. The behavior of mechanisms close to special configurations needs to be understood.

APPENDIX A

ASSEMBLY CONFIGURATIONS OF THE  
STRUCTURE ILLUSTRATED IN FIGURE 6.3

The order of the polynomial (6.29) is determined by the maximum number of possible assembly configurations of the structure illustrated in Fig. 6.3 which has been redrawn (Fig. A.1). The structure can be disconnected at the third pin joint of the second subchain. A point C on the end-effector lamina will trace a four-bar coupler curve and the point C' on link  $a_{23,2}$  will trace a circle centered at  $(X_{22}, Y_{22})$ . The number of assembly configurations is thus determined by the number of real intersections of the coupler curve which is of order 6 with the circle which is of order 2. Using Bézout's theorem (Primrose [45] Chapter 5), one would expect that there would be a maximum of  $6 \times 2 = 12$  points of intersections. However, this is not the case because both the circle and the coupler curve contain the imaginary circular points at infinity.

The basic material of this appendix can be found in several standard texts such as Hunt [3], Primrose [45], and Salmon [46].

Briefly, the equation for the circle generated by point C' can be expressed in homogeneous coordinates in the form

$$(x-wX_{22})^2 + (y-wY_{22})^2 - (wa_{23,2})^2 = 0 \quad (\text{A.1})$$

The line  $w = 0$  is called the line at infinity. Substituting  $w = 0$  in (A.1) yields

$$x^2 + y^2 = 0 \quad (\text{A.2})$$

or

$$x = \pm iy \quad (\text{A.3})$$

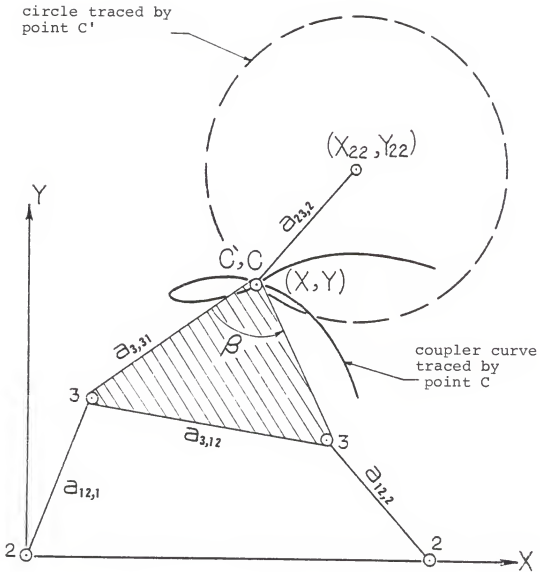


Figure A.1 Intersection of Coupler Curve with Circle

The circle thus meets the line at infinity in the two imaginary points (A.3) which are called the imaginary circular points at infinity. Since the circle contains both imaginary circular points once, the circle is said to have a circularity of one.

The equation of the coupler curve generated by point C can be expressed in the form

$$U^2 + V^2 = W^2 \quad (\text{A.4})$$

where in terms of homogeneous coordinates

$$\begin{aligned} U &= xa_{3,23}[(wa_{23,1})^2 - \{(x-wa_{2,31})^2 + y^2 \\ &\quad + (wa_{3,12})^2\}] - a_{3,12}\{y\sin\beta + (x-wa_{2,31})\cos\beta\} \\ &\quad \{(wa_{23,3})^2 - (x^2 + y^2 + (wa_{3,23})^2)\} \\ V &= a_{3,12}\{y\cos\beta - (x-wa_{2,31})\sin\beta\}\{(wa_{23,3})^2 \\ &\quad - (x^2 + y^2 + (wa_{3,23})^2)\} \\ &\quad - ya_{3,23}[(wa_{23,1})^2 - \{(x-wa_{2,31})^2 + y^2 + (wa_{3,12})^2\}] \\ W &= 2wa_{3,12}a_{3,23}[\{x(x-wa_{2,31}) + y^2\}\sin\beta \\ &\quad - yw^2a_{2,31}\cos\beta] \end{aligned} \quad (\text{A.5})$$

Substituting  $w = 0$  in (A.4) yields

$$(x^2 + y^2)^3 = 0 \quad (\text{A.6})$$

Therefore, there is a triple intersection of the coupler curve with the line at infinity in the imaginary circular points at infinity. It follows that the coupler curve and the circle must intersect three times in the two imaginary circular points at infinity. Thus they can intersect one another at no more than  $(12 - (3 \times 2)) = 6$  other points in the x-y plane and these six points themselves may be real, coincident, or complex.

It can now be concluded that the number of assembly configurations of the structure in Fig. 6.3 is of maximum six and therefore the order of the polynomial (6.29) is only six.

## APPENDIX B

REDUCTION OF COEFFICIENTS 'a' AND 'f'  
OF EQUATION (6.27)

The coefficient A in (6.24) can be expressed as follows  
(see(6.25))

$$A = A'^2 - A''^2 - A'''^2 \quad (B.1)$$

Using the expressions in (6.10), (6.18), and (6.26), the coefficient A can be expressed as follows

$$\begin{aligned} A &= (a_1 a_5)^2 - (-a_3 a_5)^2 - (a_1 a_6 - a_3 a_4)^2 \\ &= a_1^2 a_5^2 - a_3^2 a_5^2 - a_1^2 a_6^2 - a_3^2 a_4^2 + 2a_1 a_6 a_3 a_4 \\ &= a_{2,12}^2 a_{3,12}^2 a_{2,23}^2 a_{3,23}^2 \sin^2(\beta_3 - \beta_2) \\ &\quad - a_{2,12}^2 a_{23,2}^2 a_{2,23}^2 a_{3,23}^2 \sin^2(\beta_3 - \beta_2) \\ &\quad - a_{2,12}^2 a_{3,12}^2 a_{2,23}^2 a_{23,2}^2 \cos^2 \beta_2 \\ &\quad - a_{2,12}^2 a_{23,2}^2 a_{2,23}^2 a_{3,23}^2 \cos^2(\beta_3 - \beta_2) \\ &\quad + 2a_{2,12}^2 a_{3,12}^2 a_{2,23}^2 a_{23,2}^2 a_{3,23}^2 \cos \beta_2 \cos(\beta_3 - \beta_2) \end{aligned} \quad (B.2)$$

which reduces to

$$\begin{aligned} A &= -a_{2,12}^2 a_{23,2}^2 a_{2,23}^2 a_{3,23}^2 \\ &\quad - a_{2,12}^2 a_{3,12}^2 a_{2,23}^2 a_{23,2}^2 \cos^2 \beta_2 \\ &\quad + a_{2,12}^2 a_{3,12}^2 a_{2,23}^2 a_{3,23}^2 \sin^2(\beta_3 - \beta_2) \\ &\quad + 2a_{2,12}^2 a_{2,23}^2 a_{23,2}^2 a_{3,12}^2 a_{3,23}^2 \cos \beta_2 \cos(\beta_3 - \beta_2) \end{aligned} \quad (B.3)$$

Also, the coefficient D can be expressed as follows

$$D = 2(A' B' - A'' B'' - A''' B''') + (C'^2 - C''^2 - C'''^2) \quad (B.4)$$



Using equation (6.26) and the relations,  $a_1 = -b_2$ ,  $a_4 = -b_5$ , and  $a_5 = b_4$ , the expression of D can be expressed in the form

$$\begin{aligned} D = & 2\{a_1^2 a_5^2 - a_3 a_5 a_1 b_6\} \\ & + \{-a_1^2 a_6^2 - a_3^2 a_4^2 + 2a_3 a_6 a_1 a_4 - a_1^2 b_6^2 \\ & - a_3^2 a_5^2 + 2a_1 a_3 a_5 b_6\} \end{aligned} \quad (B.5)$$

Substituting the expressions in (6.10) and (6.18) in (B.5), (B.5) reduces to

$$\begin{aligned} D = & 2a_{2,12}^2 a_{3,12}^2 a_{2,23}^2 a_{3,23}^2 \sin^2(\beta_3 - \beta_2) \\ & - a_{2,12}^2 a_{3,12}^2 a_{2,23}^2 a_{23,2}^2 \\ & - a_{2,12}^2 a_{3,23}^2 a_{2,23}^2 a_{23,2}^2 \\ & + 2a_{2,12}^2 a_{2,23}^2 a_{23,2}^2 a_{3,12} a_{3,23} \cos \beta_2 \cos(\beta_3 - \beta_2) \end{aligned} \quad (B.6)$$

Following the same procedure the coefficient J can be expressed in the form

$$\begin{aligned} J = & B'^2 - B''^2 - B'''^2 \\ = & a_1^2 a_5^2 - a_1^2 b_6^2 \end{aligned} \quad (B.7)$$

and substituting the expressions in (6.10) and (6.18) in (B.7) yields

$$\begin{aligned} J = & a_{2,12}^2 a_{3,12}^2 a_{2,23}^2 a_{3,23}^2 \sin^2(\beta_3 - \beta_2) \\ & - a_{2,12}^2 a_{3,12}^2 a_{2,23}^2 a_{23,2}^2 \sin \beta_2 \end{aligned} \quad (B.8)$$

Finally, substituting the above expressions of A, D, and J, i.e., (B.3), (B.6) and (B.8), in the expression of the coefficient

$$a = A - D + J \quad (\text{B.9})$$

then (B.9) reduces to zero

$$\begin{aligned} a &= -a_{2,12}^2 a_{23,2}^2 a_{2,23}^2 a_{3,12}^2 (\sin^2 \beta_2 + \cos^2 \beta_2) \\ &\quad + a_{2,12}^2 a_{23,2}^2 a_{2,23}^2 a_{3,12}^2 \\ &= 0 \end{aligned} \quad (\text{B.10})$$

Following the same procedure, B and G can be expressed as follows

$$\begin{aligned} B &= 2(A' C' - A'' C'' - A''' C''') \\ &= 2\{-a_1 a_3 a_5 a_6 + a_3^2 a_4 a_5 - a_1^2 a_6 b_6 \\ &\quad + a_1 a_3 a_6 a_5 + a_1 a_3 a_4 b_6 - a_3^2 a_4 a_5\} \end{aligned} \quad (\text{B.11})$$

which reduces to

$$B = 2\{-a_1^2 a_6 b_6 + a_1 a_3 a_4 b_6\} \quad (\text{B.12})$$

and

$$G = 2(B' C' - B'' C'' - B''' C''') \quad (\text{B.13})$$

reduces to

$$G = 2\{-a_1^2 a_6 b_6 + a_1 a_3 a_4 b_6\} \quad (\text{B.14})$$

Therefore, from (B.12) and (B.14),

$$f = B - G = 0 \quad (\text{B.15})$$

The coefficient of  $C_{2,2}^8$ , ( $= a^2+f^2$ ), in equation (6.29) clearly vanishes. Similarly, the coefficient of  $C_{2,2}^7$ , ( $= 2fg+2ab$ ), vanishes. Since there are no further reductions in the coefficients, it can be concluded that the polynomial (6.29) is of order 6 which is in agreement with the result deduced in Appendix A.

APPENDIX C

COMPUTER PROGRAMS AND RESULTS  
OF CHAPTER 6

The programs used to perform the analysis and to generate the data for the plots of Chapter 6 are stored in the Harris computer of the CIMAR computer system under workspace 3010DT7\*PHD.

▽PREVERSE[ ] ▽

```

▽ PREVERSE; I; SA31; B; H; G; C1; S1; C2; S2; C3; S3
[1]  *****
[2]  A      REVERSE JOINT DISPLACEMENT ANALYSIS
[3]  A      PLANAR FLORIDA SHOULDER
[4]  A      I: SUBCHAIN COUNTER
[5]  A      A: 6×3 INPUT MATRIX
[6]  A      A[I;I]+ X1I Y1I X3I Y3I SA12, I SA23, I
[7]  A      THETA1+ THETA2+ THETA3+ PHI+ 2×3 MATRICES
[8]  A      THE KTH ROW IS THE KTH CLOSURE
[9]  *****
[10] 'ENTER THE INPUT MATRIX'
[11] A+[]
[12] THETA1+THETA2+THETA3+PHI+X2+Y2+2 3p0
[13] ALF+SA31+3p0
[14] I+0
[15] L0:I+I+1
[16] Y+A[4;I]-A[2;I]
[17] SA31[I;]+((X+A[3;I]-A[1;I])*2)+Y*2)*.5
[18] J+1
[19] B+(SA31[I]*2)-(A[5;I]*2)+A[6;I]*2
[20] G+(H+2×A[5;I]×A[6;I])-B
[21] THETA2[J;I]+2×30((H-B)÷G)*.5
[22] L1:S1+(A[6;I]×S2+10THETA2[J;I])÷SA31[I]
[23] C1+-(A[5;I]+A[6;I]×C2+20THETA2[J;I])÷SA31[I]
[24] S3+(A[5;I]×S2)÷SA31[I]
[25] C3+-(A[6;I]+A[5;I]×C2)÷SA31[I]
[26] THETA3[J;I]+C3 QUA S3
[27] ALF[I]+(-X+SA31[I])QUA(Y+SA31[I])
[28] PHI[J;I]+(THETA1[J;I]+C1 QUA S1)-ALF[I]
[29] X2[J;I]+A[1;I]+A[5;I]×20PHI[J;I]
[30] Y2[J;I]+A[2;I]+A[5;I]×10PHI[J;I]
[31] →L2×1((J+1)≠2)
[32] J+J+1
[33] THETA2[J;I]+-THETA2[(J-1);I]
[34] →L1
[35] L2:→L0×1(I<3)
[36] 'THETA1'
[37] (THETA1×180)÷01
[38] 'THETA2'
[39] (THETA2×180)÷01
[40] 'THETA3'
[41] (THETA3×180)÷01
[42] 'THE REQUIRED INPUT ANGLES'
[43] PHI×180÷(01)
[44] 'X2'
[45] X2
[46] 'Y2'
[47] Y2

```

▽

V PFORWARD[ ] V

```

V PFORWARD;V;A;B;C;D;E;F;G;H;I;J;K;L;M;N;Q
[1]  A*****
[2]  A FORWARD JOINT DISPLACEMENT ANALYSIS
[3]  A PLANAR FLORIDA SHOULDER 3-DOF
[4]  A*****
[5]  'ENTER THE KNOWN LINK LENGTHS;'
[6]  'SA12,I SA23,I FOR I=1,2,3 , SA3,12 SA3,23 SA3,31'
[7]  SA+
[8]  'ENTER THE COORDINATES OF THE BASE TOINTS;'
[9]  'Y+X11 Y11 X12 Y12 X13 Y13'
[10] Y+
[11] 'ENTER THE INPUT JOINT DISPLACEMENTS;'
[12] 'PHI1,1 PHI1,2 PHI1,3'
[13] PHI11+
[14] PHI12+
[15] PHI13+
[16] PDIMF
[17] POLY6
[18] JOINTD X+
[19] 'COORDINATES OF THE MOVING TERNARY;'
[20] COOR
[21] 'COORDINATES OF THE SECOND JOINT;'
[22] X21,Y21,X22,Y22,X23,Y23
V

```

V QUA[ ] V

```

V ANGL+COS QUA SIN;QU
[1] +(2<QU+(3 2 0 1=(1<COS+1)+2*1<SIN+1)/1 2 3 4)pL
[2] ANGL+(-2<COS)F-1<SINL1
[3] +L1
[4] L:-(3<QU)pL2
[5] ANGL+(01)-(-1<SIN)
[6] +L1
[7] L2:ANGL+(-1<SINF-1)+02
[8] L1:ANGL+ANGL
V

```

```

VPDINF[[]] V
V+((Y21+Y2J+SA[1]*OPHI11+PHI11*O180)-Y22+Y[4]+SA[3]*OPHI12+PHI12*O180)*2
SA2212+(((X21+Y[1]+SA[1]*OPHI11)-A22+Y[3]+SA[3]*OPHI12)*2)+V)*.5
PHI13+PHI13*O180
SA2223+(((X22-X23+Y[5]+SA[5]*2OPHI13)*2)+(Y22-Y23+Y[6]+SA[5]*OPHI13)*2)*.5
SA2231+(((X23-X21)*2)-(Y23-Y21)*2)*.5
BETA2+2O((SA212*2)+(SA2223*2)-SA2231*2)+2*SA2212*SA2223
BETA3+2O((SA[7]*2)+(SA[8]*2)-SA[9]*2)+2*SA[7]*SA[8]
AH+BH+(SA1+SA2212*SA[7])*SA5+SA2223*SA[8]*1O(BETA-BETA3-BETA2)
DH+(SA1*SD5+SA[4]*SA[8]*1OBETA3)+SA5*SD1+SA[4]*SA[7]
KH+(SA1*SD4+SA[4]*SA[8]*2OBETA3)-SD1*SA4+SA2223*SA[8]*2OBETA
CHHH+(AHH-SAS-SA3+SA2212*SA[4])-BHH-SA1*SB6+-SA2223*SA[4]*1OBETA2
AHH+-CHH-(SA3*SA4)-SA1*SA6+SA2223*SA[4]*2OBETA2
DHH-(SA4*SD5)+SA5*SD3+((SA2212*2)+(SA[4]*2)+(SA[7]*2)-SA[2]*2)+2
EHH-(SA4*SD3)-SA1*SD6+((SA2212*2)+(SA[4]*2)+(SA[8]*2)-SA[6]*2)+2
DHH+(SD1*SA6)-(SA3*SD4)+EHH
EHH+(SD1*SB6)-SD3*SA5
FHH+(SD1*SD6)-SD3*SD4
A+(AH*2)-(AHH*2)+AHH*2
B+2*(AHH*CHH)+AHHH*CHHH
C+2*(AH*DH)-(AHH*DH)+AHHH*DHH
D+(2*(AH*2)-AHH*BHH)-(CHH*2)+CHHH*2
E+2*(AH*EH)-(AHH*EHH)+AHHH*EHHH-(CHH*DHH)+CHHH*DHHH)
F+2*(AH*FH+SD1*SD5)-(AHH*FHH+-SD3*SD5)+(DHH*2)-(DHH*2)+DHHH*2
G+2*BHH*CHH
H+2*(-(CHH*EHH)+CHHH*EHHH)+(BH*DH)-BHH*DHH
I+2*(-(CHH*FHH)+CHHH*FHHH)+(DH*EH)-(DHH*EHH)+DHHH*EHHH
J+(BH*2)-BHH*2
K+2*(BH*EH)-BHH*EHH
L+(2*(BH*FH)-BHH*FHH)+(EH*2)-(EHH*2)+EHHH*2
M+2*(EH*FH)-(EHH*FHH)+EHHH*FHHH
N+2*(DH*FH)-(DHH*FHH)+DHHH*FHHH
Q+(FH*2)-(FHH*2)+FHHH*2

```



```

V JOINED[ ] V
JOINED X;W;SIN2;COS2
COOK←(7,pX)p0
COOK[1;]←1(pX)
I←0
L0:I←I+1
C22←X[I]
S22←((SB×C22×3)+(SC×C22×2)+(SD×C22×2)+(SE)÷(SG×C22×2)+(SH×C22)+(SI
ABEL←(AH×C22×2)+(BH×S22×2)+(DH×C22)+(EH×S22)+FH
EDLE←(AHH×C22×2)+(BHH×S22×2)+(CHH×S22×C22)+(DHH×C22)+(EHH×S22)+FHH
ADEL←(AHHH×C22×2)+(CHHH×S22×C22)+(DHHH×C22)+(EHHH×S22)+FHHH
S32←ADEL+ABEL
C32←BDEL+ABEL
THETA22B←((O2)-BETA2)-THETA22+C22 QUA S22
THETA22
THETA32B←BETA3-THETA32+C32 QUA S32
S21←((C22×XH32←SA[7]×S32)-S22×(YH32←-(SA[4]+C32×SA[7]))÷SA[2]
C21←((XH32×S22)+(YH32×C22)-SA2212)÷SA[2]
W←(S22B+10THETA22B)×Y32B←SA[4]+SA[8]×C32B+20THETA32B
S23←(((C22B+20THETA22B)×X32B+SA[8]×S32B+10THETA32B)-W)÷SA[6]
C23←((X32B×S22B)+(Y32B×C22B)-SA2223)×SA[6]
SIN2←(Y23-Y22)÷SA2223
COS2←(X23-X22)÷SA2223
PHI21←(ALFA2+COS2 QUA SIN2)+BELA2-THETA21+C21 QUA S21
PHI22←ALFA2+(O1)-THETA22B
PHI23←ALFA2+THETA23+C23 QUA S23
COOK[2;I]←X21+SA[2]×2OPHI21
COOK[3;I]←Y21+SA[2]×1OPHI21
COOK[4;I]←X22+SA[4]×2OPHI22
COOK[5;I]←Y22+SA[4]×1OPHI22
COOK[6;I]←X23+SA[6]×2OPHI23
COOK[7;I]←Y23+SA[6]×1OPHI23
→L0×1(I<pX)

```

V

```

V POLY6[ ] V
V Z+POLY6
[1] SAA+A+J-D
[2] SF+B-G
[3] C6+((SG+E-K)*2)+(SB+C-H)*2
[4] C5+2*(SG*SH+G+I)+SB*SC+D+F-L+2*J
[5] C4+(2*(SG*SI+K+M)+SB*SD+H+N)+(SH*2)+(SC*2)-SG*2
[6] C3+2*(SH*SI)+(SB*SE+J+L+Q)+(SC*SD)-SG*SH
[7] C2+(2*(SC*SE)-SG*SI)+(SI*2)+(SD*2)-SH*2
[8] C1+2*(SD*SE)-SH*SI
[9] C0+(SE*2)-SI*2
[10] F+C6,C5,C4,C3,C2,C1,C0
[11] Z+ROOTER F
V

```

```

V ROOTER[ ] V
V Z+ROOTER F;G;FP;IO;Δ;I;X;T
[1] Z+0 2pIO+1
[2] Z+Z,[1]((FP+-1+(pF)L(1≠1+φF)11)p0),[1.1]0
[3] +0×11=pF+(-FP)+F
[4] Z+Z,[1]((FP+-1+(pF)L(1≠1+F)11)pL/10),[1.1]0
[5] +0×11=pF+FP+F
[6] F+TRAN F+F[1]
[7] FP+DERIV F
[8] L1:X+I+0
[9] +L3×11=1+G+X1FP
[10] X+X-Δ+(X1F)÷G
[11] +((50<I+I+1),(20<|X),(1=1+Δ),1)/L3,L3,L2,L1+1
[12] L2:Z+Z,[1]T×X,0
[13] +((L1-1)×12pF+-1+(1,-X)PD F
[14] L3:FP+DERIV F+φF
[15] X+I+0
[16] +L5×11=1+G+X1FP
[17] X+X-Δ+(X1F)÷G
[18] +((50<I+I+1),(20<|X),(1=1+Δ),1)/L5,L5,L4,L3+2
[19] L4:Z+Z,[1]T×(X),0
[20] FP+DERIV F+-1+(1,-X)PD F
[21] +(L3+1)×12pF
[22] L5:Z+Z,[1]T+ROOTφF
V

```

Functions nested in ROOTER are available in Workspace  
6069GKM\*MATH

A

0	6	5.5
0	-2.305	2.41
3.73	3.588	5.045
1.1304	-1.846	1.1564
2.5	3.05	3.5
2.46	2.681	2.49

PREVERSE

ENTER THE INPUT MATRIX

U:

A

THETA1

142.1561677	122.9360488	146.9906775
217.8438323	237.0639512	213.0093225

THETA2

-76.41506656	129.7699918	163.0356789
-76.41506656	-129.7699918	-163.0356789

THETA3

141.4287657	107.2939594	49.97364364
218.5712343	252.7060406	310.0263564

THE REQUIRED INPUT ANGLES

-20.98406925	112.1615754	-142.9579259
54.70359527	226.2894777	-76.93928085

X2

2.334200081	4.849479673	2.70632323
1.444516028	3.892403726	6.290942305

Y2

-8952708981	.5196774998	.3015953655
2.040434622	-4.509662774	-999458941

A

0	11.25833	0
0	6.5	13
4.25	6.25	2.25
4.8359	8.3	8.3
3	3	3
4	4	4

XY

4.25 7.1453

V FLOG[ ] V

V FLOG

```

[1] 'ENTER THE INITIAL INPUT MATRIX;'
[2] A←[ ]
[3] 'COOR OF AXIS OF ROTATION,'
[4] XY←[ ]
[5] XX←0,(R×20(0÷6)),((R+2.3094)×20(0÷1.2))
[6] YY←(-R),(R×10(0÷6)),(R×10(0÷1.2))
[7] GAMA←((02)÷72)×(173)-1
[8] THETA1+THETA2+THETA3+PHI+X2+Y2+73 3p0
[9] J←0
[10] L1:J+J+1
[11] REVERSEP A
[12] →L1×1(J<pGAMA)
[13] 'THE REQUIRED INPUT ANGLES;'
[14] PHI×180÷(01)
[15] 'ANGLE OF ROTATION, MEASURED FROM THE X-AXIS;'
[16] GAMA×180÷(01)

```

V

```

V REVERSEP[ ] V
[1] REVERSEP A;I;X;Y;B;G;H;S1;C1;S3;C3
[2] A *****
[3] A REVERSE JOINT DISPLACEMENT ANALYSIS
[4] A PLANAR FLORIDA SHOULDER...EXAMPLE NO. 2
[5] A I: SUBCHAIN COUNTER
[6] A A: 6x3 INPUT MATRIX
[7] A A[I;I]← X1I Y1I X3I Y3I S4I2, I S4I23, I
[8] A *****
[9] ALF←SA31+3p0
[10] I←0
[11] L0: I←I+1
[12] A[3;I]←(XX[I]×2OGAMA[J])÷XY[I]-(YY[I]×1OGAMA[J])
[13] A[4;I]←(XX[I]×1OGAMA[J])÷(YY[I]×2OGAMA[J])÷XY[2]
[14] SA31[I]←((X+A[3;I]-A[1;I])×2)÷(Y+A[4;I]-A[2;I])×2*.5
[15] +((|C2÷(B÷(SA31[I]×2)-(A[5;I]×2)+H÷2×A[5;I]×A[6;I])>1) pL2
[16] +((|S2÷(1-(C2×2))×.5)>1) pL2
[17] THETA2[J;I]←C2 QUA S2
[18] S1←(A[6;I]×S2+10THETA2[J;I])÷SA31[I]
[19] C1←-(A[5;I]÷A[6;I]×C2+20THETA2[J;I])÷SA31[I]
[20] S3←(A[5;I]×S2)÷SA31[I]
[21] C3←-(A[6;I]÷A[5;I]×C2)÷SA31[I]
[22] THETA3[J;I]←C3 QUA S3
[23] PHI[J;I]←(THETA1[J;I]÷C1 QUA S1)-(ALF[I]÷(-X÷SA31[I])QUA(Y÷SA31[I]))
[24] X2[J;I]←A[1;I]÷A[5;I]×2OPHI[J;I]
[25] Y2[J;I]←A[2;I]÷A[5;I]×1OPHI[J;I]
[26] L2: →J0×1(I<3)

```

APPENDIX D

COMPUTER PROGRAMS OF CHAPTER 7

The programs used to perform the analysis and to generate the data for the plots of Chapter 7 are stored in the Harris computer of the CIMAR computer system under workspace 3010DT7\*PHD.

▽ RPSP[ ] ▽

```

V RPSP;X0;Z0;AA;BB;B;TQ;I;J;S2;S6
[1]  REVERSE ANALYSIS OF THE R-P-SP DEVICE
[2]  'ENTER THE LENGTH OF THE BASE SIDE; SA'
[3]  SA+[]
[4]  'ENTER THE OFFSET OF THE SLIDER; S221,S222,S223'
[5]  S22+[]
[6]  'ENTER THE COOR.OF THE POINT; XQ , YQ , ZQ'
[7]  XYZ+[]
[8]  RI+4p0
[9]  R+S6+S2+3 3p0
[10] PHI+SS2+SS6+73 3p0
[11] BETA+(0 120 240)*(01)+180
[12] ALFA+((02)+72)*(173)-1
[13] XO+0,(SA*(3*.5)÷4),SA*(3*.5)+4
[14] ZO+(0,SA,-SA)÷4
[15] J+0
[16] L0:J+J+1
[17] I+0
[18] L1:I+I+1
[19] AA+(ZO[I]*S+10BETA[I])-XO[I]*C+20BETA[I]
[20] BB+-(ZO[I]*C)+XO[I]*S
[21] B+4 4pC,0,(-S),AA,0,1,0,0,S,0,C,BB,0,0,0,1
[22] TQ+3 3pAC,0,AS,0,1,0,(-AS+10ALFA[J]),0,AC+20ALFA[J]
[23] R[I]+Q-1+RI+B+.xQ(XYZ,1)
[24] S6[I]+(-1-1+B)+.xCC+(TQ+.x(CS+3 1pS,0,C))
[25] +L4x1(1=S6[3;I]+1)
[26] SS6[J;I]+-R[3;I]+S6[3;I]
[27] L5:SUM+n[I]+SS6[J;I]*S6[I]
[28] S2[I]+SUM+NORM+((QSUM)+.xSUM)*.5
[29] PHI[J;I]+(S2[2;I]QUA-S2[1;I])*180÷(01)
[30] SS2[J;I]+NORM-S22[I]
[31] L2:+L1x1(I<3)
[32] +L0x1(J<pALFA)
[33] 'THE REQUIRED ANGULAR DISPLACEMENT;'
[34] PHI
[35] 'THE REQUIRED SLIDING DISPLACEMENT;'
[36] SS2
[37] 'ANGLE OF ROTATION ABOUT THE Y-AXIS;'
[38] ALFA*180÷(01)
[39] +0
[40] L4:SS6[J;I]+0
[41] +L5

```

▽

SA

15

S22

3 3 3

XYZ

2 14 5



```

V STEWART1[ ] V

V STEWART1; Q; I; J; F; B; M; N; T; S4; NOAM
[1]  Q*****
[2]  R REVERSE ANALYSIS
[3]  R STEWART PLATFORM WITH A SLIDING INPUT JOINT
[4]  R*****
[5]  'ENTER THE RADII OF THE PLATFORM AND THE BASE;'
[6]  RI+
[7]  'ENTER THE OFFSETS;'
[8]  S44+
[9]  'ENTER THE COOR. OF THE POINT; XQ,YQ,ZQ;'
[10] X+
[11] BETA+GAMA+((O2)÷6)×(16)-1
[12] ALFA+((O2)÷72)×(173)-1
[13] Q+S4÷3 6p0
[14] SS4+73 6p0
[15] J+0
[16] L0:J+J+1
[17] I+0
[18] L1:I+I+1
[19] F+(C+2OBETA[I]),(-RI[2]),0,0,0,1
[20] B+4 4pC,0,(-S),0,0,1,0,0,(S+1OBETA[I]),0,F
[21] M+1OALFA[J]
[22] N+2OALFA[J]
[23] T+4 4pN,0,M,X[1],0,1,0,X[2],(-M),0,N,X[3],0,0,0,1
[24] Q[I]+1 0+B+.×(T+.×(4 1p(RI[1]×S),0,(RI[1]×C),1))
[25] S4[I]+Q[I]÷NORM+((QQ[I])+.×Q[I])*5
[26] SS4[J;I]+NORM-S44[I]
[27] L2:→L1×1(I<6)
[28] →L0×1(J<pALFA)
[29] 'THE REQUIRED SLIDING DISPLACEMENTS;'
[30] SS4
[31] 'ANGLE OF ROTATION, ALFA'
[32] ALFA+ALFA×180÷(O1)
[33] ALFA
V

```

```

V STEWART2[ ] V

V STEWART2;Q;S4;I;J;K;F;B;N;M;U;S2;C1;S1;C2
[1]  *****
[2]  R REVERSE ANALYSIS
[3]  R STEWART PLATFORM WITH AN ACTUATED REVOLUTE JOINT
[4]  *****
[5]  'ENTER THE RADII OF THE PLATFORM AND THE BASE;'
[6]  RI←□
[7]  'ENTER THE COOR. OF THE POINT;XQ,YQ,ZQ;'
[8]  X←□
[9]  BETA+GAMA+((O2)÷6)×(16)-1
[10] ALFA+((O2)÷72)×(173)-1
[11] Q+S4+3 6p0
[12] PHI+73 6 2p0
[13] J←0
[14] L0:J+J+1
[15] I←0
[16] L1:I+I+1
[17] F+(C+2OBETA[I]),(-hI[2]),0,0,0,1
[18] B←4 4pC,0,(-S),0,0,1,0,0,(S+1OBETA[I]),0,F
[19] M←1OALFA[J]
[20] H←2OALFA[J]
[21] T←4 4pH,0,M,X[1],0,1,0,X[2],(-M),0,N,X[3],0,0,0,1
[22] Q[I]←1 0+B+.×(T+.×(4 1p(XI[1]×S),0,(RI[1]×C),1))
[23] S4[I]←Q[I]÷NORM+((QQ[I])+.×Q[I])*.5
[24] S2←(1-((C2+-S4[3;I])×2))*5
[25] K←1
[26] L4:C1+S4[1;I]÷S2
[27] S1+S4[2;I]÷S2
[28] PHI[J;I;K]←C1 QUA S1
[29] →L5×1((K+1)≠2)
[30] K←K+1
[31] S2←-S2
[32] →L4
[33] L5:→L1×1(I<6)
[34] →L0×1(J<pALFA)
[35] 'THE REQUIRED ANGULAR DISPLACEMENTS;'
[36] PHI←PHI×180÷(O1)
[37] PHI
[38] 'ANGLE OF ROTATION; ALFA'
[39] ALFA←ALFA×180÷(O1)
[40] ALFA
V

```

## REFERENCES

1. Duffy, J., Analysis of Mechanisms and Robot Manipulators, John Wiley and Sons, New York, NY, 1980.
2. Hunt, K.H., Structural Kinematics of In-Parallel-Actuated Robot-Arms, ASME Paper No. 82-DET-105, Presented at the 17th Mechanisms Conference, Arlington, VA, Sept. 12-15, 1982.
3. Hunt, K.H., Kinematic Geometry of Mechanisms, Oxford University Press, Great Britain, 1978.
- ✓ 4. Cox, D.J., The Dynamic Modeling and Command Signal Formulation for Parallel Multi-Parameter Robotic Devices, Master's Thesis, University of Florida, Gainesville, FL, 1981.
5. Roth, B., Rastegar, J., and Scheinman, V., On the Design of Computer Controlled Manipulators, Proceedings of the 1st CISM-IFTOMM Symposium on the Theory and Practice of Robots and Manipulators, Udine, Italy, 1974.
6. Roth, B., Kinematic Design for Manipulation, Proceedings of the National Science Foundation Workshop on the Research Needed to Advance the State of Knowledge in Robotics, NSF Grant ENG-79-21587, Newport, RI, April, 1980.
7. Tesar, D., Duffy, J., and Staudhammer, J., The Generalized Robotic Manipulator: Its Geometry, Dynamics, and Computer Aided Design with Graphics, Proposal to the National Science Foundation, Center of Intelligent Machines and Robotics, Gainesville, FL, June, 1981.
8. Vertut, J., and Liegeois, A., General Design Criteria of Manipulators, Proceedings of the Third CISM-IFTOMM Symposium on the Theory and Practice of Robots and Manipulators, Udine, Italy, 1978.
9. Duffy, J., Class Notes, University of Florida, Gainesville, FL, 1983.
10. Brand, L., Vector and Tensor Analysis, John Wiley and Sons, New York, NY, 1948.

11. Ball, R.S., A Treatise on the Theory of Screws, Cambridge University Press, Cambridge, 1900.
12. Rooney, J., A Comparison of Representations of General Spatial Screw Displacement, Journal of Environment and Planning, Vol. 5, pp. 45-88, 1978.
13. Lipkin, H., and Duffy, J., Analysis of Industrial Robots via the Theory of Screws, Proceedings of the 12th International Symposium on Industrial Robots, Paris, France, June, 1982.
14. Dimentberg, F.M., The Screw Calculus and Its Applications to Mechanics, Moscow, 1965, English Translation, U.S. Department of Commerce, (N.T.I.S.), No. AD 680 993, 1969.
15. Phillips, J.R., and Hunt, K.H., On the Theorem of Three Axes in the Spatial Motion of Three Bodies, Australian Journal of Applied Science, Vol. 15, pp. 267-287, 1964.
16. Waldron, K.J., The Mobility of Linkages, Ph.D. Dissertation, Stanford University, Stanford, CA, 1969.
17. Bottema, O., and Roth, B., Theoretical Kinematics, North-Holland Publishing Co., Amsterdam, Holland, 1979.
18. Woo, L., and Freudenstein, F., Application of Line Geometry to Theoretical Kinematics and the Kinematic Analysis of Mechanical Systems, Journal of Mechanisms, Vol. 5, pp. 417-460, 1970.
19. Hunt, K.H., The Screw as a Geometrical Element, Paper No. 7, Monash University, Clayton, Victoria, Australia, November, 1982.
- ✓ 20. Waldron, K.J., The Constraint Analysis of Mechanisms, Journal of Mechanisms, Vol. 1, pp. 101-114, 1966.
21. Davies, T.H., and Primrose, E.J.F., An Algebra for the Screw Systems of Pair of Bodies in a Kinematic Chain, Proceedings of the Third World Congress on the Theory of Machines and Mechanisms, Kupari, Yugoslavia, Paper D-14, pp. 199-212, 1971.
22. Nering, E.D., Linear Algebra and Matrix Theory, Second Edition, John Wiley and Sons, New York, NY, 1970.
- ✓ 23. Sugimoto, K., and Duffy, J., Applications of Linear Algebra to Screw Systems, Mechanism and Machine Theory, Vol. 17, No. 1, pp. 73-83, 1982.

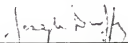
24. Friedberg, S.H., Insel, A.J., and Spence, L.E., Linear Algebra, Prentice-Hall, Englewood Cliffs, NJ, 1979.
25. Manolescu, N.I., For a United Point of View in the Study of the Structural Analysis of Kinematic Chains and Mechanisms, Journal of Mechanisms, Vol.3, pp. 149-169, 1968.
26. Davies, T.H., An Extension of Manolescu's Classification of Planar Kinematic Chains and Mechanisms of Mobility  $M > 1$ , Using Graph Theory, Journal of Mechanisms, Vol. 3, pp. 87-100, 1968.
27. Crossley, F.R.E., A Contribution to Grüebler's Theory in the Number Synthesis of Plane Mechanisms, Trans. ASME, Journal of Engineering for Industry, Vol. 86, Series B, pp. 1-8, 1964.
28. Hain, K., Discussion (of Crossley [27]), Journal of Engineering for Industry, Vol. 86, Series B, pp. 5-6, 1964.
29. Davies, T.H., and Crossley, F.R.E., Structural Analysis of Plane Linkages by Franke's Condensed Notation, Journal of Mechanisms, Vol. 1, pp. 171-183, 1966.
30. Grüebler, M., Getriebelehre, N.P., Berlin, 1917.
31. Franke, R., Vom Aufbau der Getriebe, Vol. 1, Third Edition, VDI, Verlag, 1958.
32. Rosenauer, N., and Willis, A.H., Kinematics of Mechanisms, Associated General Publications, Sydney, Australia, 1953.
33. Fichter, E.F., and McDowell, E.D., A Novel Design for a Robot Arm, Proceedings of the International Computer Technology Conference, New York, NY, 1980.
34. Orin, D.E., and Oh, S.Y., A Mathematical Approach to the Problem of Force Distribution in Locomotion and Manipulation Systems Containing Closed Kinematic Chains, Proceedings of the Third CISM-IFTOMM Symposium on the Theory and Practice of Robots and Manipulators, Udine, Italy, 1978.
35. Bejczy, A.K., Demands that Robotic Systems Place on Control Theory, Proceedings of the National Science Foundation Workshop on the Research Needed to Advance the State of Knowledge in Robotics, NSF Grant ENG-79-21587, Newport, RI, April, 1980.
36. Flatau, C.R., The Future of Generalized Robotic Manipulators, Proceedings of the National Science Foundation Workshop in the Impact of the Academic Community of Required Research Activity for Generalized Robotic Manipulators, Gainesville, FL, February, 1978.

37. Baker, J.E., On Relative Freedom between Links in Kinematic Chains with Cross-Jointing, Mechanism and Machine Theory, Vol. 15, pp. 397-413, 1980.
38. Davies, T.H., Kirchhoff's Circulation Law Applied to Multi-Loop Kinematic Chains, Mechanism and Machine Theory, Vol. 16, pp. 171-183, 1981.
39. Waldron, K.J., The Use of Motors in Spatial Kinematics, IFToMM Symposium of Linkages and Computer Design Methods, Bucharest, Romania, Paper B-41, pp. 535-545, 1973.
40. Davies, T.H., Mechanical Networks-I, Passivity and Redundancy, Mechanism and Machine Theory, Vol. 18, No. 2, pp. 95-101, 1983.
41. Sugimoto, K., and Duffy, J., Special Configurations of Industrial Robots, Proceedings of the 11th International Symposium on Industrial Robots, Tokyo, Japan, 1981.
42. Sugimoto, K., Duffy, J., and Hunt, K.H., Special Configurations of Spatial Mechanisms and Robot Arms, Mechanism and Machine Theory, Vol. 17, No. 2, pp. 119-132, 1982.
43. Buckens, F., On the Singular Configurations of Statically Determinate Structures, International Journal of Machine Sciences, Vol. 7, pp. 301-314, 1968.
44. Paul, B., Kinematics and Dynamics of Planar Machinery, Prentice-Hall, New Jersey, NJ, 1979.
45. Primrose, E.J.F., Plane Algebraic Curves, Macmillan, London, Great Britain, 1955.
46. Salmon, G., Higher Plane Curves, Third Edition, Foster and Figgis, Dublin, 1879, Reprinted, Chelsea, New York, NY, 1960.

#### BIOGRAPHICAL SKETCH

I, Maher Gaber Mohamed, was born December 30, 1951, in El-Minia, Egypt. After graduating from El-Minia High School, I began studies in mechanical engineering at El-Minia High-Industrial Institute of Technology and graduated with a Bachelor of Science in Mechanical Engineering in June, 1974. In September, 1978, I attended the Agricultural Engineering Department at Washington State University and received a Master of Science in Engineering in June 1980. In September, 1980, I began attending the University of Florida. I am married to my love, Salwa, and have a son, Kareem.

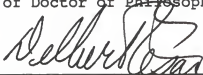
I certify that I have read this study and that in my opinion it conforms to acceptable standards of scholarly presentation and is fully adequate in scope and quality, as a dissertation for the degree of Doctor of Philosophy.



---

J. Duffy, Chairman  
Professor of Mechanical  
Engineering

I certify that I have read this study and that in my opinion it conforms to acceptable standards of scholarly presentation and is fully adequate in scope and quality, as a dissertation for the degree of Doctor of Philosophy.



---

D. Tesar  
Professor of Mechanical  
Engineering

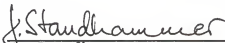
I certify that I have read this study and that in my opinion it conforms to acceptable standards of scholarly presentation and is fully adequate in scope and quality, as a dissertation for the degree of Doctor of Philosophy.



---

G.K. Matthew  
Associate Professor of  
Mechanical Engineering

I certify that I have read this study and that in my opinion it conforms to acceptable standards of scholarly presentation and is fully adequate in scope and quality, as a dissertation for the degree of Doctor of Philosophy.

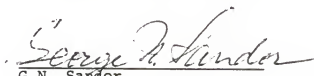


---

J. Staudhammer  
Professor of Electrical  
Engineering



I certify that I have read this study and that in my opinion it conforms to acceptable standards of scholarly presentation and is fully adequate in scope and quality, as a dissertation for the degree of Doctor of Philosophy.



G.N. Sander

Research Professor of  
Mechanical Engineering

This dissertation was submitted to the Graduate Faculty of the College of Engineering and to the Graduate School, and was accepted as partial fulfillment of the requirements for the degree of Doctor of Philosophy.

December 1983

  
Dean, College of Engineering

\_\_\_\_\_  
Dean for Graduate Studies  
and Research